

THE UNIVERSITY OF CHICAGO

DETERMINING WHETHER CERTAIN AFFINE DELIGNE-LUSZTIG SETS  
ARE EMPTY

A DISSERTATION SUBMITTED TO  
THE FACULTY OF THE DIVISION OF THE PHYSICAL SCIENCES  
IN CANDIDACY FOR THE DEGREE OF  
DOCTOR OF PHILOSOPHY

DEPARTMENT OF MATHEMATICS

BY  
DANIEL C. REUMAN

CHICAGO, ILLINOIS  
AUGUST 2002

## ABSTRACT

Let  $F$  be a non-archimedean local field, let  $L$  be the maximal unramified extension of  $F$ , and let  $\sigma$  be the Frobenius automorphism. Let  $G$  be a split connected reductive group over  $F$ , and let  $\mathcal{B}_\infty$  be the Bruhat-Tits building associated to  $G(L)$ . Let  $\mathcal{B}_1$  be the building associated to  $G(F)$ . Then  $\sigma$  acts on  $G(L)$  with fixed points  $G(F)$ . Let  $I$  be the Iwahori associated to a chamber in  $\mathcal{B}_1$ . We have the relative position map  $inv : G(L)/I \times G(L)/I \rightarrow \tilde{W}$ , where  $\tilde{W}$  is the extended affine Weyl group of  $G$ . If  $w \in \tilde{W}$  and  $b \in G(L)$ , then the affine Deligne-Lusztig set  $X_w(b\sigma)$  is  $\{x \in G(L)/I : inv(x, b\sigma(x)) = w\}$ . This dissertation answers the question of which  $X_w(b\sigma)$  are non-empty for certain  $G$  and  $b$ .

## ACKNOWLEDGEMENTS

Above all, I would like to thank my advisor, Robert Kottwitz, for being extremely helpful at every turn. Professor Kottwitz's mathematical guidance has helped with every aspect of this dissertation. His support and understanding regarding non-research issues encountered during graduate education is also remarkable. I am very grateful to have been his student. I would also like to thank Chris Degni and Sudheer Shukla for helpful discussions and lectures. Finally, I thank Moon Duchin, Kaj Gartz, Mark Behrens, and Moses Hohman for moral support.

# TABLE OF CONTENTS

ABSTRACT . . . . .	ii
ACKNOWLEDGEMENTS . . . . .	iii
LIST OF FIGURES . . . . .	vi
LIST OF TABLES . . . . .	x
1 INTRODUCTION . . . . .	1
2 GROUPS OF SEMISIMPLE RANK 1 . . . . .	5
2.1 $SL_2$ . . . . .	5
2.1.1 Identity $\sigma$ -conjugacy Class . . . . .	5
2.1.2 Non-identity $\sigma$ -conjugacy Classes . . . . .	7
2.1.3 Symmetry Under a $\mathbb{Z}/2$ -action . . . . .	8
2.1.4 Relationship Between $X_w(1\sigma)$ and $X_w(b\sigma)$ . . . . .	10
2.2 $GL_2$ and $PGL_2$ . . . . .	13
2.3 Reorganization of Results . . . . .	15
3 GROUPS OF SEMISIMPLE RANK 2 . . . . .	18
3.1 $SL_3$ . . . . .	18
3.1.1 Standard Minimal Galleries and Composite Galleries . . . . .	19
3.1.2 A Superset of the Solution Set . . . . .	21
3.1.3 Relationship Between $X_w(1\sigma)$ and $X_w(b\sigma)$ , and an Efficient Way of Computing Supersets . . . . .	50
3.1.4 A Method Suggested by Rapoport and Kottwitz . . . . .	55
3.1.5 A Subset of the Solution Set for $b = 1$ . . . . .	59
3.1.6 A Geometric Construction of a Subset of the Solution Set . . . . .	66
3.1.7 Symmetry Under a $\mathbb{Z}/3$ -action . . . . .	95
3.2 $GL_3$ and $PGL_3$ . . . . .	96
3.3 $Sp_4$ . . . . .	97
3.3.1 Standard Minimal Galleries and Composite Galleries . . . . .	98
3.3.2 A Conjectural Superset of the Solution Set . . . . .	100
3.3.3 Relationship Between $X_w(1\sigma)$ and $X_w(b\sigma)$ for $Sp_4$ , and an Ef- ficient Way of Computing Supersets . . . . .	106
3.3.4 The Method of Kottwitz and Rapoport Applied to $Sp_4$ . . . . .	106
3.3.5 A Subset of the Solution Set for $b = 1$ for $Sp_4$ . . . . .	110

3.3.6	Subsets for Other $b$ , and Symmetry under a $\mathbb{Z}/2$ -action . . . .	112
3.4	Comments on $GSp_4$ , $PSp_4$ , and $G_2$ . . . . .	119
3.5	Invariance Properties of Solution Sets . . . . .	120
REFERENCES . . . . .		125

## LIST OF FIGURES

2.1 Chamber labels . . . . .	6
2.2 Alternate chamber labels . . . . .	6
2.3 Proof of Proposition 2.1.2 . . . . .	7
2.4 Summary of $SL_2$ results . . . . .	9
2.5 Lattice labels for vertices . . . . .	10
2.6 For $w$ in the positive Weyl chamber . . . . .	11
2.7 For $w$ in the negative Weyl chamber . . . . .	12
2.8 Summary of some results for $GL_2$ . . . . .	14
2.9 Computations for some $\sigma$ -conjugacy classes for $GL_2$ . . . . .	15
2.10 Summary of some more results for $GL_2$ . . . . .	15
3.1 Primary and secondary directions . . . . .	20
3.2 Example SMG type and edge of departure . . . . .	22
3.3 Composite gallery example . . . . .	22
3.4 Results from the SMG in Figure 3.2 . . . . .	23
3.5 $\Gamma_E^1$ possibilities for $I_1$ . . . . .	24
3.6 Some composite gallery possibilities for $I_1$ . . . . .	25
3.7 Class $I_1$ , where $\Gamma_E^1$ has 3 chambers after the turning edge . . . . .	26
3.8 Class $I_1$ , where $\Gamma_E^1$ has 5 chambers after the turning edge . . . . .	27
3.9 Class $I_1$ , where $\Gamma_E^1$ has 7 chambers after the turning edge . . . . .	28
3.10 Summary of results for $I_1$ , an odd number of chambers after the turning edge . . . . .	29
3.11 More composite gallery possibilities for $I_1$ . . . . .	30
3.12 Class $I_1$ , where $\Gamma_{E_1}$ has 2 chambers after the turning edge . . . . .	31
3.13 Class $I_1$ , where $\Gamma_{E_1}$ has 4 chambers after the turning edge . . . . .	32
3.14 Class $I_1$ , where $\Gamma_{E_1}$ has 6 chambers after the turning edge . . . . .	33
3.15 Summary of results for $I_1$ , an even number of chambers after the turning edge . . . . .	34
3.16 Some composite gallery possibilities for $I_2$ . . . . .	35
3.17 More composite gallery possibilities for $I_2$ . . . . .	35
3.18 Class $I_2$ , where $\Gamma_{E_1}$ has 0, 1 or 2 chambers after the departure edge, $w = 1$ . . . . .	35
3.19 Class $I_2$ , where $\Gamma_{E_1}$ has 3 or 4 chambers after the departure edge, $w = 1$	36
3.20 Class $I_2$ , where $\Gamma_{E_1}$ has 5 or 6 chambers after the departure edge, $w = 1$	36
3.21 Summary of results for $I_2$ , $w = 1$ . . . . .	37
3.22 Summary of results for $I_2$ , $w = f$ . . . . .	38
3.23 Summary of results for $I_1$ and $I_2$ . . . . .	39

3.24	Result for $\alpha = 2, \beta = 0$ . . . . .	41
3.25	Result for $\alpha = 2, \beta = 1$ . . . . .	42
3.26	Result for $\alpha = 4, \beta = 0$ . . . . .	43
3.27	Result for $b = 1$ . . . . .	44
3.28	General shape of composite galleries for $b = 1, w = f, I_1$ . . . . .	45
3.29	General shape of composite galleries for $b = 1, w = 1, I_1$ . . . . .	45
3.30	General shapes of composite galleries for $b = 1, w = 1, I_2$ . . . . .	46
3.31	Result for $\alpha = 4, \beta = -2$ . . . . .	47
3.32	$bC_M$ for degenerate $b$ . . . . .	48
3.33	General shape of composite galleries for $b \neq 1$ with $\alpha + 2\beta = 0, w = f, I_1$ . . . . .	49
3.34	General shape of composite galleries for $b \neq 1$ with $\alpha + 2\beta = 0, w = 1, I_1$ . . . . .	49
3.35	$\Omega_1^2, \Omega_f^2, \Omega_{p,1}^1$ and $\Omega_{p,f}^1$ . . . . .	53
3.36	Choice points for a sample composite gallery . . . . .	54
3.37	Choice points for $\Omega_{p,1}^1$ and $\Gamma_x$ . . . . .	54
3.38	How to address choice points of $\Gamma_x$ that occur before the turning point of $\Gamma_E^3$ . . . . .	55
3.39	Main results of the method suggested by Rapoport and Kottwitz . . . . .	57
3.40	The $a = 1$ results of the method suggested by Rapoport and Kottwitz . . . . .	58
3.41	Results from the method suggested by Rapoport and Kottwitz under the circumstances of Lemma 3.1.5 . . . . .	58
3.42	The choice $D_1$ of $xC_M$ . . . . .	59
3.43	The resulting $\Gamma_x$ for $D_1$ and a particular choice of $aw$ . . . . .	60
3.44	The result of folding galleries of the same type as $x^{-1}\Gamma_x$ for the $\Gamma_x$ pictured in Figure 3.43 . . . . .	60
3.45	Results for $xC_M = D_1$ and $w = r^2$ or for $xC_M = D_1$ and $w = r$ . . . . .	61
3.46	The choices $D_2$ and $D_3$ of $xC_M$ . . . . .	62
3.47	Results for $xC_M = D_2$ and $w = r^2$ or for $xC_M = D_2$ and $w = r$ . . . . .	63
3.48	Results for $xC_M = D_3$ and $w = r^2$ or for $xC_M = D_3$ and $w = r$ . . . . .	64
3.49	Combination of all results referred to in Table 3.1 . . . . .	65
3.50	Some choices for $xC_M$ that are two chambers away from $C_M$ . . . . .	65
3.51	A Useful Lemma . . . . .	66
3.52	An example of $P, P_b$ and $P_\sigma$ . . . . .	68
3.53	$w_2, w_3, w_4$ and $w_5$ . . . . .	68
3.54	Multiple rows of the $w_i$ . . . . .	69
3.55	Filling in the rest of $\overline{P}$ . . . . .	69
3.56	The definition of the invariant $\gamma_2$ , part 1 . . . . .	70
3.57	The definition of the invariant $\gamma_2$ , part 2 . . . . .	71
3.58	The definition of the invariant $\gamma_2$ , part 3 . . . . .	71
3.59	$T(P) = S(P) = \infty$ . . . . .	72
3.60	The meaning of a tilde . . . . .	73

3.61	Existence of all values of $\gamma_1$ and $\gamma_2$ , case 1 . . . . .	74
3.62	Existence of all values of $\gamma_1$ and $\gamma_2$ , case 2 subcase 1 . . . . .	76
3.63	Existence of all values of $\gamma_1$ and $\gamma_2$ , case 2 subcase 2 . . . . .	77
3.64	Existence of all values of $\gamma_1$ and $\gamma_2$ , case 2 subcase 3 . . . . .	78
3.65	Existence of all values of $\gamma_1$ and $\gamma_2$ , case 2 subcase 4 . . . . .	80
3.66	Definition of negative values of $\gamma_2$ . . . . .	81
3.67	Existence of all negative values of $\gamma_2$ , case 1 . . . . .	82
3.68	Existence of all negative values of $\gamma_2$ , case 2 subcase 1 . . . . .	84
3.69	Existence of all negative values of $\gamma_2$ , case 2 subcase 1 diagram 2 . . . . .	85
3.70	Existence of all negative values of $\gamma_2$ , case 2 subcase 2 . . . . .	86
3.71	$x^{-1}(\overline{P} \cup P_\sigma)$ for $\gamma_2 > 0$ . . . . .	87
3.72	Example of how $\gamma_1$ and $\gamma_2$ determine $\rho(x^{-1}b\sigma(x)C_M)$ . . . . .	88
3.73	$x^{-1}(\overline{P} \cup P_\sigma)$ for $\gamma_2 \leq 0$ . . . . .	89
3.74	$x^{-1}(\overline{P} \cup P_\sigma)$ for $\gamma_2 \leq 0$ , folding explained . . . . .	90
3.75	$x^{-1}(\overline{P} \cup P_\sigma)$ for $\gamma_2 \leq 0$ , folding explained further . . . . .	91
3.76	Choice Points . . . . .	92
3.77	A composite gallery for $p = 1, \alpha = 2, \beta = -1$ . . . . .	93
3.78	All foldings of composite galleries with $p = 1$ occur, where $b \neq 1$ and $\alpha + 2\beta = 0$ . . . . .	94
3.79	Definition of $\gamma_3$ . . . . .	95
3.80	What happens to Figure 3.79 when $\gamma_3 = 0$ . . . . .	96
3.81	How the torus of $Sp_4$ acts on $A_M$ . . . . .	98
3.82	Primary and Secondary Directions in $Sp_4$ . . . . .	99
3.83	Result for $b = 1, Sp_4$ . . . . .	101
3.84	Result for $\alpha = 3, \beta = 1, Sp_4$ . . . . .	102
3.85	Result for $\alpha = 6, \beta = 3, Sp_4$ . . . . .	103
3.86	Result for $\alpha = 6, \beta = 5, Sp_4$ . . . . .	104
3.87	Result for $\alpha = 7, \beta = 1, Sp_4$ . . . . .	105
3.88	Half infinite galleries for $Sp_4, \alpha > \beta$ (specifically, $\alpha = 3, \beta = 1$ ) . . . . .	107
3.89	Half infinite galleries for $Sp_4, \alpha = \beta$ (specifically, $\alpha = \beta = 3$ ) . . . . .	108
3.90	Main results of the method suggested by Rapoport and Kottwitz, $Sp_4$ . . . . .	109
3.91	The $a = 1$ results of the method suggested by Rapoport and Kottwitz, $Sp_4$ . . . . .	110
3.92	Results of the method suggested by Rapoport and Kottwitz under the circumstances of Lemma 3.3.4, $Sp_4$ . . . . .	111
3.93	The choices $D_1, D_2$ and $D_3$ of $G_1$ . . . . .	112
3.94	Results for $xC_M = D_1$ and $w = r$ or for $xC_M = D_1$ and $w = r^3$ . . . . .	113
3.95	Results for $xC_M = D_2$ and $w = r$ or for $xC_M = D_2$ and $w = r^3$ . . . . .	114
3.96	Results for $xC_M = D_3$ and $w = r$ or for $xC_M = D_3$ and $w = r^3$ . . . . .	115
3.97	Results for $xC_M = D_1$ and $w = r^2$ . . . . .	116
3.98	Results for $xC_M = D_2$ and $w = r^2$ . . . . .	117
3.99	Results for $xC_M = D_3$ and $w = r^2$ . . . . .	118



3.100	The translations $\epsilon$ and $\delta$ of $A_M$ for $G_2$ . . . . .	120
3.101	Region $R$ . . . . .	123
3.102	Understood region after applying invariance properties to region $R$ .	124

## LIST OF TABLES

2.1	$D_M^{\pm i}$ intersects exactly these $\Sigma_j$ non-trivially for $i$ even . . . . .	16
2.2	$D_M^{\pm i}$ intersects exactly these $\Sigma_j$ non-trivially for $i$ odd . . . . .	16
2.3	$\sigma$ -conjugacy classes that intersect $(D_M^i, j)$ non-trivially . . . . .	17
3.1	Which figure contains which results . . . . .	62

# CHAPTER 1

## INTRODUCTION

Let  $F$  be a non-archimedean local field with ring of integers  $\mathcal{O}_F$ , and let  $G$  be a split connected reductive group over  $F$ . Let  $L$  be the completion of the maximal unramified extension of  $F$ . Let  $\sigma$  be the Frobenius automorphism of  $L$  over  $F$ . Let  $\mathcal{B}_n$  be the affine building for  $G(E)$  where  $E/F$  is the unramified extension of degree  $n$  in  $L$ , and let  $\mathcal{B}_\infty$  be the affine building for  $G(L)$ . The theory of buildings was developed by Bruhat and Tits in [1] and [2], and is reviewed by Garrett in [4]. We know that  $\sigma$  acts on  $\mathcal{B}_\infty$ , and the fixed points of  $\sigma^n$  are  $\mathcal{B}_n$ . Let  $T$  be a split torus in  $G$  and let  $I$  be an Iwahori in  $G(L)$  containing  $T(\mathcal{O}_L)$ , where  $\mathcal{O}_L$  is the ring of integers of  $L$ . Let  $A_M$  and  $C_M$  be the correspondingly specified apartment and chamber, which we assume are in  $\mathcal{B}_1$ . We will call these the *main apartment* and the *main chamber*, respectively.

If  $b \in G(L)$  then the  $\sigma$ -conjugacy class of  $b$  is  $\{x^{-1}b\sigma(x) : x \in G(L)\}$ . If  $\tilde{W}$  is the extended affine Weyl group, and  $w \in \tilde{W}$  then we define, after Rapoport and Kottwitz, the affine Deligne-Lusztig set  $X_w(b\sigma) = \{x \in G(L)/I : \text{inv}(x, b\sigma(x)) = w\}$ . Here  $\text{inv} : G(L)/I \times G(L)/I \rightarrow \tilde{W}$  is the relative position map. Note that if  $b_1$  and  $b_2$  are  $\sigma$ -conjugate then the sets  $X_w(b_1\sigma)$  and  $X_w(b_2\sigma)$  are in bijective correspondence. When  $F = \mathbb{F}_q((t))$ , the affine Deligne-Lusztig set can be given variety structure over  $\mathbb{F}_q$  (locally of finite type).

Sometimes the  $X_w(b\sigma)$  are empty. Our goal is to determine when the  $X_w(b\sigma)$  are non-empty. This paper concerns itself mainly with the question of which  $X_w(b\sigma)$  are non-empty for groups of semisimple rank 1 and 2.

The question of which  $X_w(b\sigma)$  are non-empty for  $\{x^{-1}b\sigma(x) : x \in G(L)\}$  a fixed  $\sigma$ -conjugacy class can be rephrased by saying that  $X_w(b\sigma)$  is non-empty if and only if  $\{x^{-1}b\sigma(x) : x \in G(L)\}$  intersects the double- $I$ -coset corresponding to  $w$  in a non-trivial way. Here we are using the standard correspondence between  $\tilde{W}$  and  $I \backslash G(L) / I$ . We will use this correspondence implicitly for the rest of the paper. To see that the above rephrasing is accurate, note first that  $\text{inv}(x, b\sigma(x)) = \text{inv}(1, x^{-1}b\sigma(x))$  is the relative position of 1 and  $x^{-1}b\sigma(x)$ . By definition,  $\text{inv}(1, x^{-1}b\sigma(x)) = Ix^{-1}b\sigma(x)I$ . We see that  $X_w(b\sigma)$  is non-empty if and only if there exists  $x$  such that  $Ix^{-1}b\sigma(x)I = w$ , which is what was to be proven.

If  $G$  is simply connected, then  $\tilde{W} \simeq W_a$  is in bijective correspondence with chambers in the main apartment  $A_M$ . Here  $W_a$  is the affine Weyl group of  $G$ . So for a fixed  $\sigma$ -conjugacy class  $\{x^{-1}b\sigma(x) : x \in G(L)\}$ , the set of  $w$  for which  $X_w(b\sigma)$  is non-empty can be represented geometrically as a collection of chambers in  $A_M$ . For

groups of rank 1 and 2, one can therefore draw pictures of the solution set. This is the form in which we present results in this paper.

Complete information can be obtained without difficulty for groups of semisimple rank 1. This is done in Chapter 2. The solution sets for each  $\sigma$ -conjugacy class of  $SL_2$  are pictured in Figure 2.4. The solution sets for each  $\sigma$ -conjugacy class of  $GL_2$  or  $PGL_2$  are pictured in Figures 2.8 and 2.10.

The group of semisimple rank 2 for which the most information has been obtained is  $G = SL_3$ . We have worked only with  $\sigma$ -conjugacy classes that are basic in the maximal torus. These are listed at the beginning of Section 3.1. The general approach by which we have described  $\{inv(x, b\sigma(x)) : x \in SL_3(L)\} \subseteq \tilde{W} \simeq W_a$  in these cases has two main parts. The first part, done in Sections 3.1.1, 3.1.2, and 3.1.3, seeks to produce a superset of the solution set. The general methodology here is to establish a way of choosing, for each  $x \in SL_3(L)$ , a gallery  $\Gamma_x$  between  $xC_M$  and  $b\sigma(x)C_M$ . Possible values of  $inv(x, b\sigma(x))$  can then be enumerated by listing the possible “foldings” of  $x^{-1}\Gamma_x$ . Optimizations can be implemented so that this is a finite, but still prohibitively lengthy computation. It has only been carried out to completion for two  $\sigma$ -conjugacy classes. The results are pictured in Figure 3.23 and Figure 3.27. In the process of doing these two complete computations, we observe that in fact one need only do a much smaller part of the complete computation to obtain all elements of  $W_a$  that arise in the superset. We do not have a proof that this is the case in general, but we are very strongly confident that it is. Section 3.1.3 develops an efficient way of doing the smaller, partial computation that works for any  $\sigma$ -conjugacy class. Results of the smaller computation that are (confidently) conjectured to be the results of the entire computation are listed for various  $\sigma$ -conjugacy classes in Figures 3.24, 3.25, 3.26, and 3.31.

The other half of the work for  $SL_3$  is to develop a subset of the solution set. This is done in two different ways. The first method, which is discussed in Sections 3.1.4 and 3.1.5, is simple and potentially generalizable to higher rank groups, but only applies to the case  $b = 1$ . The second method (discussed in Section 3.1.6) applies for any  $b$  in the collection of  $\sigma$ -conjugacy classes under consideration, but is very complicated and somewhat aesthetically unpleasing. Also, it probably could not be generalized to higher rank groups. In all cases, the subset results turn out to be equal to the superset results discussed above. So it is known that Figures 3.23 and 3.27 are solution sets for their respective  $\sigma$ -conjugacy classes, and we are very confident (although it is not proved) that Figures 3.24, 3.25, 3.26, and 3.31 are solution sets for their respective  $\sigma$ -conjugacy classes. It is known that these last four figures are at least subsets of their respective solution sets.

The same methods can be applied to  $Sp_4$ , although this has been carried out to a smaller extent. Again, we only consider  $\sigma$ -conjugacy classes  $b$  which are basic in the maximal torus. The complete computation of the superset of the solution set has only been done for  $b = 1$ . The result is pictured in Figure 3.83. Again, there is a partial computation which gives all results obtained from the complete computation

in this case. Carrying out the partial computation for some other  $\sigma$ -conjugacy classes (done in Section 3.3.2) yields Figures 3.84, 3.85, 3.86, and 3.87. We conjecture that these are complete supersets, but we are not completely confident of this because the chambers marked with a \* seem to be holes in the pattern.

The subset methods of Section 3.1.4 and 3.1.5 have been applied to  $Sp_4$ ,  $b = 1$  in Sections 3.3.4 and 3.3.5. The result is the same as the superset pictured in Figure 3.83, so this figure gives the solution set for  $b = 1$ . The complicated methods of Section 3.1.6 have not been adapted to  $Sp_4$ , although such an adaptation probably could be done. We conjecture that one would obtain subsets equal to the sets pictured in Figures 3.84, 3.85, 3.86, and 3.87, making these figures actual solution sets. So for  $Sp_4$  we have definite results for  $b = 1$ , and conjectural results of which we are not completely confident for other  $b$ .

The results obtained for  $SL_3$  can easily be adapted to  $GL_3$  and  $PGL_3$ . This is done in Section 3.2. Similarly, the results for  $Sp_4$  can be adapted to  $GSp_4$  and  $PSp_4$ . This is done in Section 3.4. The methods used could be applied to  $G_2$  as well. This is also discussed in Section 3.4.

We also say a few words describing the basic ideas behind the methods used. The backbone of the method by which supersets of solution sets are produced is the “folding” of galleries. If  $G$  is a gallery starting at  $C_M$ , then the *folding results* of  $G$  are the possible values of the last chamber of  $\rho(\tilde{G})$ , where  $\rho : \mathcal{B}_\infty \rightarrow A_M$  is the retraction centered at  $C_M$ , and  $\tilde{G}$  is any gallery of the same “shape” as  $G$  that starts at  $C_M$ . To produce a superset, it turns out that the folding results have to be calculated for a gallery associated to each chamber in  $\mathcal{B}_\infty$ . Perhaps the real content of the method is how these computations can be grouped so that they can be done efficiently. This will be discussed in Sections 3.1.2 and 3.1.3 for  $SL_3$ , and Sections 3.3.2 and 3.3.3 for  $Sp_4$ .

As mentioned previously, there are two methods used to produce subsets of solution sets. The first, which only applies for  $b = 1$ , is carried out in Sections 3.1.4 and 3.1.5 for  $SL_3$ , and Sections 3.3.4 and 3.3.5 for  $Sp_4$ . This method gets started using an observation of Kottwitz and Rapoport that provides, with very little work, a large and well distributed collection of chambers which must be contained in the solution set. This collection can then be enlarged as follows. If  $inv(x, \sigma(x)) = w$  is one of the chambers provided by Kottwitz’s and Rapoport’s observation, and if  $\Gamma$  is a minimal gallery between  $xC_M$  and  $\sigma(x)C_M$ , then  $\Gamma$  describes the relative position  $w$ . One can show that  $\sigma$ -conjugating  $x$  by certain very simple elements of  $G(L)$  corresponds to adding “appendages” to the ends of  $\Gamma$ . One can then understand how the addition of such appendages affects relative position. Some of the “appendage” methods used are stated in generality in Section 3.5.

The second method of producing subsets of solution sets is lengthy and unappealing, but applies for  $b \neq 1$ . The basic idea is as follows. In Section 3.1.1, we produce a gallery  $\Gamma_x$  between  $xC_M$  and  $b\sigma(x)C_M$ . We compute the folding results of  $x^{-1}\Gamma_x$  to get possible candidates for the relative position of  $x$  and  $b\sigma(x)$ . In Section 3.1.6,

we discover which of these candidates can actually occur by defining some invariants which control how  $x^{-1}\Gamma_x$  actually folds (i.e., these invariants control which of the folding results of  $x^{-1}\Gamma_x$  is the actual value of the last chamber of  $\rho(x^{-1}\Gamma_x)$ ). We then show that one can choose  $x$  such that these invariants take any pre-specified value. One of the complications of this method is that one must proceed somewhat differently for each of the three cases  $b = 1$ ,  $b$  “degenerate” but  $b \neq 1$ , and  $b$  “non-degenerate.” The “non-degenerate”  $b$  are exactly

$$b = \begin{pmatrix} \pi^\alpha & 0 & 0 \\ 0 & \pi^\beta & 0 \\ 0 & 0 & \pi^\gamma \end{pmatrix}$$

with  $\alpha + \beta + \gamma = 0$ ,  $\alpha > \beta > \gamma$ .

## CHAPTER 2

### GROUPS OF SEMISIMPLE RANK 1

If the split connected reductive group  $G$  is of semisimple rank 1, then it is possible to obtain a complete characterization of which  $X_w(b\sigma)$  are non-empty. Some of the methods which will be used on higher rank groups are similar to those used here. Considering the rank 1 case first allows one to develop a good intuition about the geometric nature of the problem before proceeding to the more complicated rank 2 and higher rank cases.

Section 2.1 of this chapter will address the specific group  $SL_2$ , and Section 2.2 will adapt the  $SL_2$  solution to other, non-simply connected groups of semisimple rank 1.

Everything in this chapter was previously known to Kottwitz and Rapoport.

#### 2.1 $SL_2$

Results from a paper of Kottwitz [6] allow us to list the following elements of  $SL_2$  as a complete collection of representatives of the  $\sigma$ -conjugacy classes of  $SL_2$ :

$$\left\{ \begin{pmatrix} \pi^n & 0 \\ 0 & \pi^{-n} \end{pmatrix} : n \in \mathbb{Z}, n \geq 0 \right\}.$$

Let  $\rho : \mathcal{B}_\infty \rightarrow A_M$  be the retraction of  $\mathcal{B}_\infty$  onto  $A_M$  relative to  $C_M$ .

In Section 2.1.1, we answer the question of which  $w$  have non-empty  $X_w(b\sigma)$  for  $b$  the identity matrix. In Section 2.1.2, we consider the cases where  $b$  is one of the above non-identity representatives. In Section 2.1.3, we prove that the results obtained in Sections 2.1.1 and 2.1.2 are invariant under a certain  $\mathbb{Z}/2$ -action. The proof is independent of the results from Sections 2.1.1 and 2.1.2. Section 2.1.4 describes the relationship between  $X_w(1\sigma)$  and  $X_w(b\sigma)$  for  $b \neq 1$ .

##### *2.1.1 Identity $\sigma$ -conjugacy Class*

As mentioned previously, to find out which  $w$  have non-empty  $X_w(b\sigma)$ , it suffices to determine the set  $\{inv(1, x^{-1}b\sigma(x)) : x \in SL_2(L)\}$ . However, it is easy to see that  $inv(1, x^{-1}b\sigma(x)) = \rho(x^{-1}b\sigma(x)C_M)$ , where again it is understood that we are making use of the correspondence between  $\tilde{W}$  and the set of chambers in  $A_M$ . So we seek to describe the set  $\{\rho(x^{-1}b\sigma(x)C_M) : x \in SL_2(L)\}$ .

Let  $D$  be any chamber in  $\mathcal{B}_\infty$ .

**Definition 2.1.1.** Let the distance  $\tilde{d}_1(D)$  between  $D$  and  $\mathcal{B}_1$  be  $n - 1$ , where  $n$  is the length of the shortest gallery containing  $D$  and some chamber  $E$  in  $\mathcal{B}_1$ .

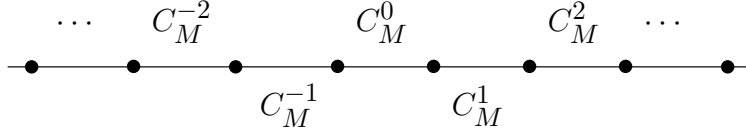


Figure 2.1: Chamber labels

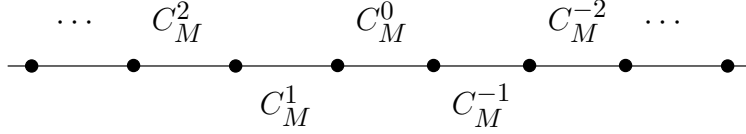


Figure 2.2: Alternate chamber labels

Note that  $D$  is in  $\mathcal{B}_1$  if and only if  $\tilde{d}_1(D) = 0$ .

**Proposition 2.1.1.** If  $\tilde{d}_1(D) > 0$  then there is a minimal gallery between  $D$  and  $\sigma(D)$  of length  $2\tilde{d}_1(D)$ .

*Proof.* Let  $G$  be a gallery of minimal length containing  $D$  and some chamber  $E$  in  $\mathcal{B}_1$ . Let  $E = G_1, G_2, G_3, \dots, G_n = D$  be the successive chambers of  $G$ . Then  $G_2$  is not contained in  $\mathcal{B}_1$ , or  $G$  would not be of minimal length. So the gallery  $G_n, G_{n-1}, \dots, G_2, \sigma(G_2), \dots, \sigma(G_{n-1}), \sigma(G_n)$  is non-stuttering and therefore minimal.  $\square$

Now let  $D = xC_M$ . By the nature of the  $SL_2$  action on the building,  $x$  can be chosen such that  $\tilde{d}_1(xC_M)$  is any non-negative integer. Therefore,  $x$  can be chosen such that the minimal gallery between  $xC_M$  and  $\sigma(xC_M) = \sigma(x)C_M$  is any even integer greater than or equal to 2. In the case where  $\tilde{d}_1(xC_M) = 0$  (i.e.,  $xC_M$  is contained in  $\mathcal{B}_1$ ), we have  $xC_M = \sigma(xC_M)$ .

We are interested in  $\rho(x^{-1}\sigma(x)C_M)$ , so the minimal gallery between  $xC_M$  and  $\sigma(x)C_M$  constructed above is useful. We will need the following terminology to describe the set  $\{\rho(x^{-1}\sigma(x)C_M) : x \in SL_2(L)\}$ .

**Definition 2.1.2.** Let  $C_M^i$  denote the chamber in  $A_M$  as described in Figure 2.1, where  $C_M^0 = C_M$ .

Note that the choice between this labeling and the one in Figure 2.2 is arbitrary, but we choose the former.

**Proposition 2.1.2.** The  $w \in \tilde{W}$  with non-empty  $X_w(1\sigma)$  are  $C_M$  and  $C_M^i$  for  $i$  odd.

*Proof.* First, note that  $C_M = \rho(x^{-1}\sigma(x)C_M)$  for  $x$  such that  $xC_M$  is contained completely in  $\mathcal{B}_1$ . Further, since  $x$  can be chosen such that the minimal gallery between  $xC_M$  and  $\sigma(xC_M)$  is of any even integral length, we see that for each odd



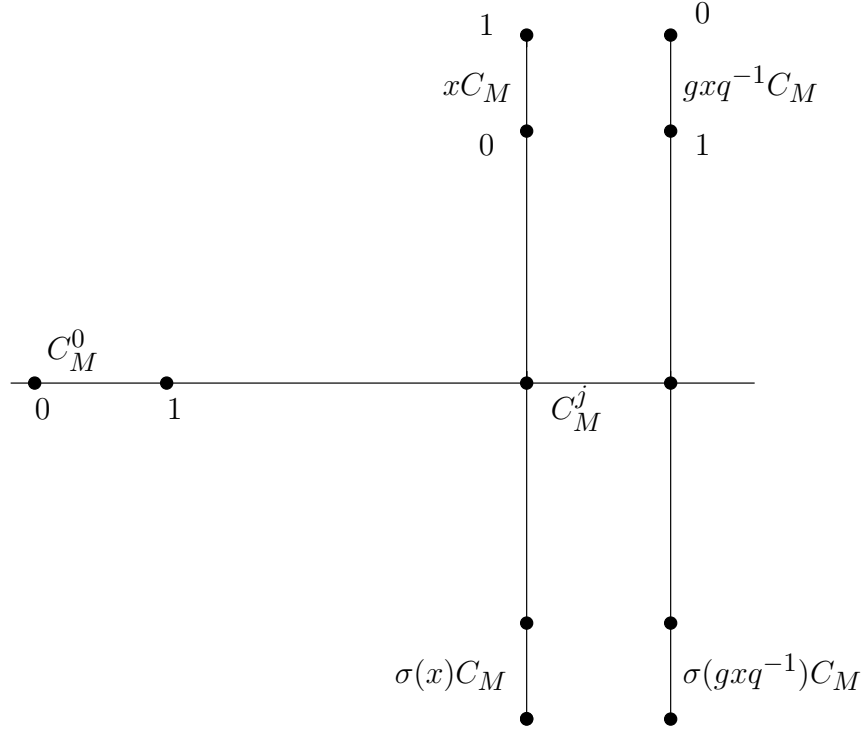


Figure 2.3: Proof of Proposition 2.1.2

$i$ , either  $C_M^i$  or  $C_M^{-i}$  is obtained. We must show that in fact both are obtained. For this, note that if  $\rho(x^{-1}\sigma(x)C_M) = C_M^i$  then  $\rho(y^{-1}\sigma(y)C_M) = C_M^{-i}$  for  $y = gxq^{-1}$  where

$$g = \begin{pmatrix} \pi & 0 \\ 0 & 1 \end{pmatrix} \quad ; \quad q = \begin{pmatrix} 0 & -\pi \\ 1 & 0 \end{pmatrix}.$$

See Figure 2.3. In this figure, the vertex types are labeled. The key point is that the vertices on the chambers  $xC_M$  are of types opposite to the corresponding vertices on  $gxq^{-1}C_M$ . Note that we still have  $\det(y) = 1$ . See Section 2.1.3 for a reminder of how  $q$  acts on  $C_M$  and  $A_M$ .  $\square$

### 2.1.2 Non-identity $\sigma$ -conjugacy Classes

Again, let  $D$  be any chamber in  $\mathcal{B}_\infty$ . Let  $b = \begin{pmatrix} \pi^s & 0 \\ 0 & \pi^{-s} \end{pmatrix}$ ,  $s > 0$ . We will enumerate the  $w$  for which  $X_w(b\sigma)$  is non-empty.

**Definition 2.1.3.** The distance  $\tilde{d}_{A_M}(D)$  between  $D$  and  $A_M$  is  $n - 1$ , where  $n$  is the length of the shortest gallery containing  $D$  and some chamber  $E$  in  $A_M$ .

Note that  $D$  is in  $A_M$  if and only if  $\tilde{d}_{A_M}(D) = 0$ .

**Proposition 2.1.3.** If  $\tilde{d}_{A_M}(D) > 0$  then there exists a minimal gallery between  $D$  and  $b\sigma(D)$  of length  $2s + 2\tilde{d}_{A_M}(D)$ .

*Proof.* Let  $G$  be a gallery of minimal length containing  $D$  and some chamber  $E$  in  $A_M$ . Let  $E = G_1, G_2, G_3, \dots, G_n = D$  be the successive chambers of  $G$ . Here  $n = \tilde{d}_{A_M}(D) + 1$ . Then  $G_2$  is not contained in  $A_M$ , or  $G$  would not be of minimal length. Let  $v$  be the vertex that  $E$  and  $G_2$  share. There is a unique minimal gallery contained in  $A_M$  between  $v$  and  $b\sigma(v) = bv$ . Call this gallery  $H$ , and its chambers  $H_1, H_2, \dots, H_{2s}$ , where  $v$  is the vertex of  $H_1$  that is not also a vertex of  $H_2$ . Consider the gallery  $G_n, G_{n-1}, \dots, G_2, H_1, H_2, \dots, H_{2s}, b\sigma(G_2), b\sigma(G_3), \dots, b\sigma(G_n)$ . This is non-stuttering and therefore minimal. It has the desired length.  $\square$

Now consider  $D = xC_M$ . Clearly,  $x$  can be chosen such that  $\tilde{d}_{A_M}(xC_M)$  is any non-negative integer. Therefore,  $x$  can be chosen such that the minimal gallery between  $xC_M$  and  $b\sigma(xC_M)$  is of length  $2s + 2n$  for any  $n \geq 1$ . If  $xC_M$  is contained in  $A_M$  then the minimal gallery between  $xC_M$  and  $b\sigma(xC_M)$  is of length  $2s + 1$ .

**Proposition 2.1.4.** The  $w \in \tilde{W}$  with non-empty  $X_w(b\sigma)$  are  $C_M^{2s}, C_M^{-2s}, C_M^{2s+i}$  and  $C_M^{-2s-i}$  for  $i \geq 1$  any odd integer.

*Proof.* Similar to Proposition 2.1.2 in Section 2.1.1.  $\square$

Figure 2.4 summarizes results from this and the previous section.

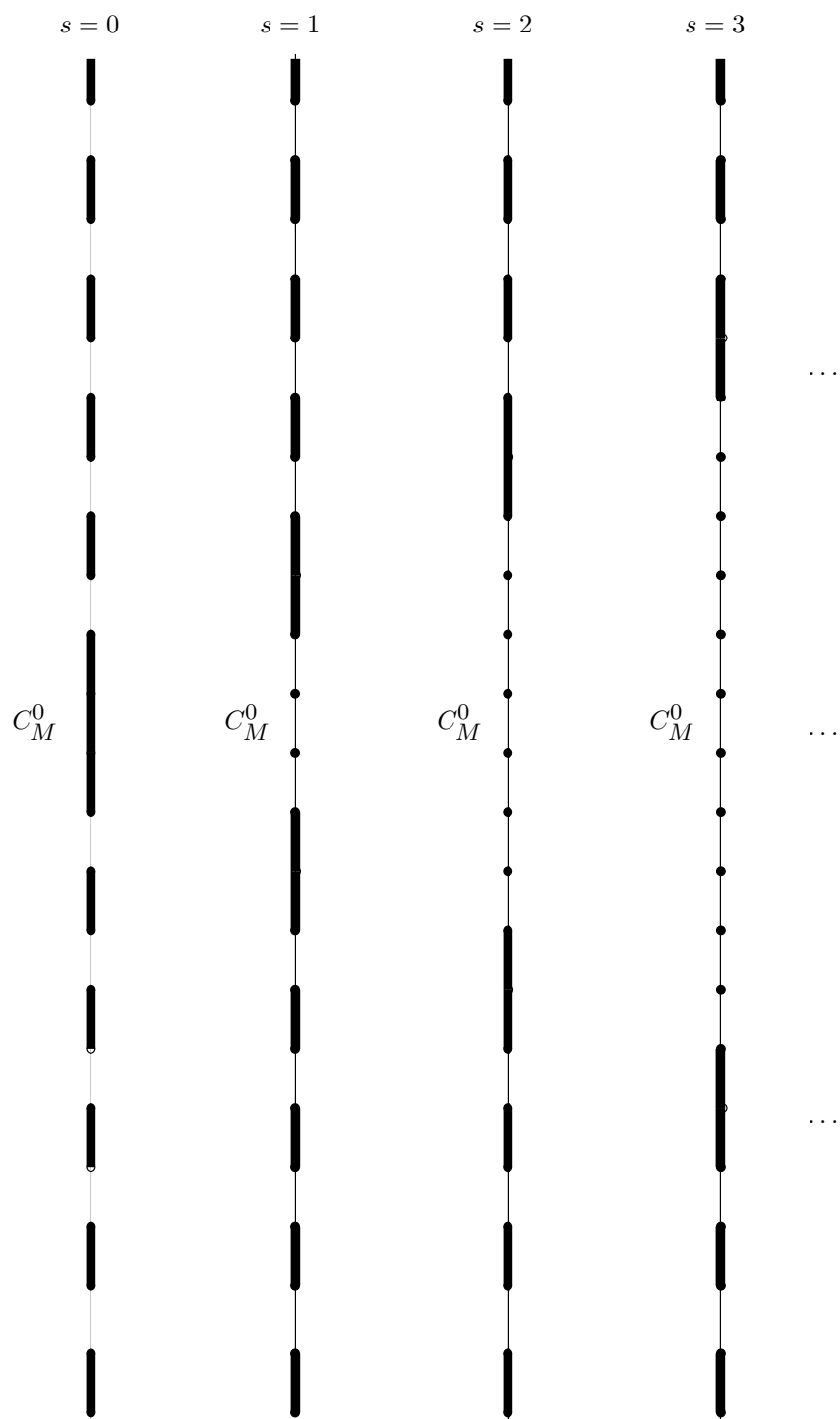
### 2.1.3 Symmetry Under a $\mathbb{Z}/2$ -action

Let  $q = \begin{pmatrix} 0 & -\pi \\ 1 & 0 \end{pmatrix} \in GL_2(L)$ . Since  $\mathcal{B}_\infty$  is also the building for  $GL_2(L)$ , we can ask how  $q$  acts on  $A_M$ . The main apartment can be represented using lattice classes as in Figure 2.5. The matrix  $q$  takes

$$\begin{aligned} \mathcal{O} \oplus \mathcal{O} &\rightarrow \pi\mathcal{O} \oplus \mathcal{O} \\ \pi\mathcal{O} \oplus \mathcal{O} &\rightarrow \mathcal{O} \oplus \mathcal{O} \\ \pi^{-1}\mathcal{O} \oplus \mathcal{O} &\rightarrow \pi^2\mathcal{O} \oplus \mathcal{O} \\ \pi^2\mathcal{O} \oplus \mathcal{O} &\rightarrow \pi^{-1}\mathcal{O} \oplus \mathcal{O} \end{aligned}$$

and therefore represents a flip about the midpoint of  $C_M$ . One can see by looking at the results of the previous two sections that  $\{w \in \tilde{W} : X_w(b\sigma) \neq \emptyset\}$  is invariant under this  $q$  action. It is instructive to develop a proof of this fact that is independent of the previous sections.

Since  $inv$  is a map from  $SL_2(L)/I \times SL_2(L)/I \rightarrow \tilde{W}$ , and since  $SL_2(L)/I$  is in one-to-one correspondence with elements of the set of chambers in  $\mathcal{B}_\infty$ , we can view  $inv$  as a map that takes two chambers in  $\mathcal{B}_\infty$  as arguments. We will use both this and the standard method of referring to  $inv$  throughout the rest of the paper.

Figure 2.4: Summary of  $SL_2$  results

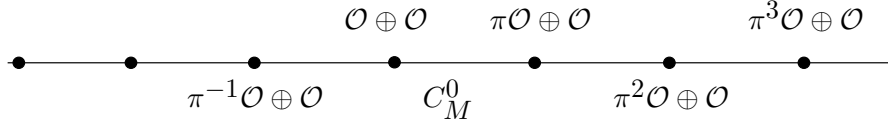


Figure 2.5: Lattice labels for vertices

We know that  $\text{inv}(xC_M, b\sigma(x)C_M) = \text{inv}(gxC_M, gb\sigma(x)C_M)$  for any  $g \in SL_2(L)$ . If  $g \in SL_2(F)$  is diagonal then  $\text{inv}(xC_M, b\sigma(x)C_M) = \text{inv}(gxC_M, gb\sigma(x)C_M) = \text{inv}(gxC_M, b\sigma(gx)C_M)$ . In the case that  $g \in GL_2(F)$  is diagonal,  $\text{inv}(xC_M, b\sigma(x)C_M)$  is not necessarily equal to  $\text{inv}(gxC_M, gb\sigma(x)C_M)$ , but  $\text{inv}(gxC_M, gb\sigma(x)C_M) = \text{inv}(gxC_M, b\sigma(gx)C_M)$ . If  $y$  is such that  $yC_M = gxC_M$ , and  $y \in SL_2(L)$ , then  $\text{inv}(gxC_M, b\sigma(gx)C_M) = \text{inv}(yC_M, b\sigma(y)C_M)$  is a new  $w \in \tilde{W}$  such that  $X_w(b\sigma) \neq \emptyset$ . We used the fact that if  $yC_M = gxC_M$  then  $b\sigma(gx)C_M = b\sigma(gxC_M) = b\sigma(yC_M) = b\sigma(y)C_M$ .

**Proposition 2.1.5.** We can choose  $g$  a diagonal element of  $GL_2(F)$  such that if  $\text{inv}(xC_M, b\sigma(x)C_M) = C_M^i$ , then  $\text{inv}(gxC_M, b\sigma(gx)C_M) = C_M^{-i}$ .

*Proof.* Let  $g = \begin{pmatrix} \pi & 0 \\ 0 & 1 \end{pmatrix}$ . We see that  $\text{inv}(gxC_M, b\sigma(gx)C_M) = \rho(s^{-1}b\sigma(gx)C_M)$ , where  $s \in SL_2(L)$  is chosen such that  $s^{-1}gxC_M = C_M$ . We may choose  $s$  such that  $s^{-1} = qx^{-1}g^{-1}$ . So  $\rho(s^{-1}b\sigma(gx)C_M) = \rho(qx^{-1}g^{-1}bg\sigma(x)C_M) = \rho(qx^{-1}b\sigma(x)C_M)$ , and if  $\text{inv}(xC_M, b\sigma(x)C_M) = C_M^i$ , then  $\rho(qx^{-1}b\sigma(x)C_M) = C_M^{-i}$ .  $\square$

We will later adapt this proof to give a similar result for some groups of higher rank.

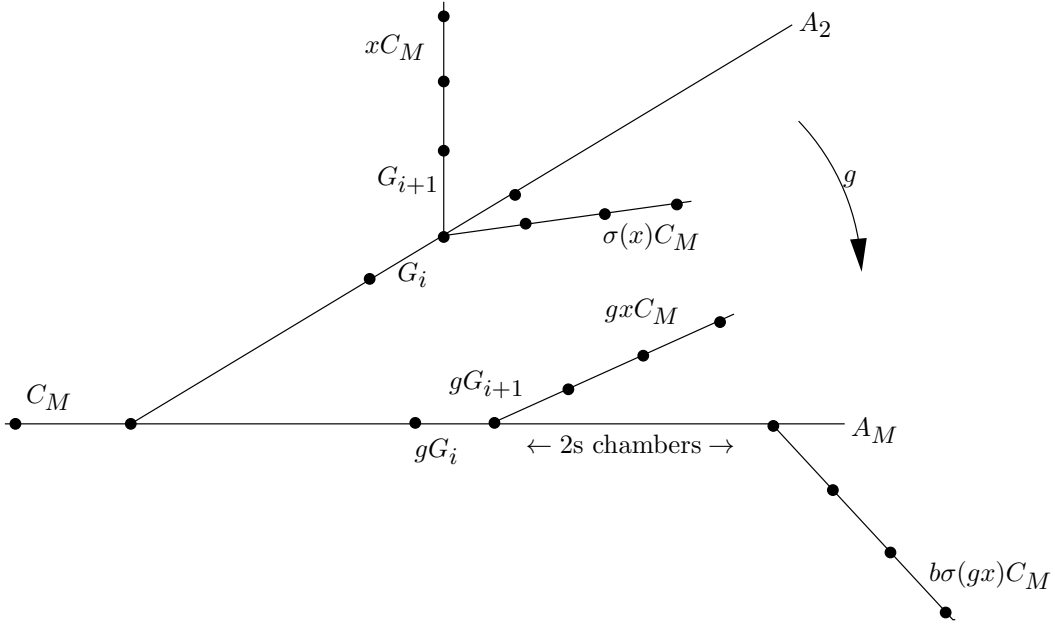
### 2.1.4 Relationship Between $X_w(1\sigma)$ and $X_w(b\sigma)$

In this section we explore the relationship between the set of  $w$  such that  $X_w(1\sigma)$  is non-empty and the set of  $w$  such that  $X_w(b\sigma)$  is non-empty, for some  $b \neq 1$ .

**Proposition 2.1.6.** If  $w$  is in the positive Weyl chamber (i.e.,  $w = C_M^i$  for  $i \geq 0$ ), then  $X_w(1\sigma)$  is non-empty if and only if  $X_{bw}(b\sigma)$  is non-empty. If  $w$  is in the negative Weyl chamber (i.e.,  $w = C_M^i$  for  $i < 0$ ), then  $X_w(1\sigma)$  is non-empty if and only if  $X_{b^{-1}w}(b\sigma)$  is non-empty.

*Proof.* We start by remarking that this is clear from the results of Section 2.1.1 and Section 2.1.2. But we produce an *a priori* proof that may be generalizable in some respects to higher rank groups.

Assume that  $w$  is in the positive Weyl chamber. If  $X_w(1\sigma)$  is non-empty then let  $x$  be such that  $\text{inv}(x, \sigma(x)) = w$ . Let  $A_1$  be an apartment containing  $xC_M$  and  $C_M$ . Let  $G$  be the minimal gallery (in  $A_1$ ) between  $C_M$  and  $xC_M$ , and let

Figure 2.6: For  $w$  in the positive Weyl chamber

$C_M = G_1, G_2, \dots, G_s = xC_M$  be the chambers of  $G$ . Let  $i$  be maximal such that  $G_i$  is contained in  $\mathcal{B}_1$ . We could have  $G_i = xC_M$  in the case that  $w = C_M$ . Let  $A_2$  be an apartment containing  $C_M$  and  $G_i$ . If  $i \neq s$  then we also require that  $A_2$  not contain  $G_{i+1}$ . Let  $g \in SL_2(L)$  be such that  $gC_M = C_M$  and  $g$  sends  $A_2$  to  $A_M$ . To see that  $\text{inv}(gx C_M, b\sigma(gx)C_M) = bw$ , consider Figure 2.6 in which  $b = \begin{pmatrix} \pi^s & 0 \\ 0 & \pi^{-s} \end{pmatrix}$ .

The minimal gallery  $E_2$  between  $gx C_M$  and  $b\sigma(gx)C_M$  is  $2s$  chambers longer than the minimal gallery  $E_1$  between  $xC_M$  and  $\sigma(x)C_M$ , and the types of the vertices on the chamber  $gx C_M$  are the same as those of the corresponding vertices of  $xC_M$ . So if  $\rho(x^{-1}E_1)$  is the minimal gallery in  $A_M$  between  $C_M$  and  $w$  then  $\rho((gx)^{-1}E_2)$  is the minimal gallery in  $A_M$  between  $C_M$  and  $bw$ . To get the other implication, use  $g^{-1}$ .

Now assume that  $w$  is in the negative Weyl chamber. Let  $G, G_i, A_2$  and  $g$  be as before. In this situation, Figure 2.6 becomes Figure 2.7. As before, the gallery  $E_2$  between  $gx C_M$  and  $b\sigma(gx)C_M$  is  $2s$  chambers longer than the minimal gallery  $E_1$  between  $xC_M$  and  $\sigma(x)C_M$ , and the types of the vertices on the chamber  $gx C_M$  are the same as those of the corresponding vertices of  $xC_M$ . So if  $\rho(x^{-1}E_1)$  is the minimal gallery in  $A_M$  between  $C_M$  and  $w$  then  $\rho((gx)^{-1}E_2)$  is the minimal gallery in  $A_M$  that begins at  $C_M$  and goes in the same direction as  $\rho(x^{-1}E_1)$ , but that is  $2s$  chambers longer. In the current case, the final chamber of this gallery is  $\tilde{b}w$ .

As before, to get the other implication, use  $g^{-1}$ . □

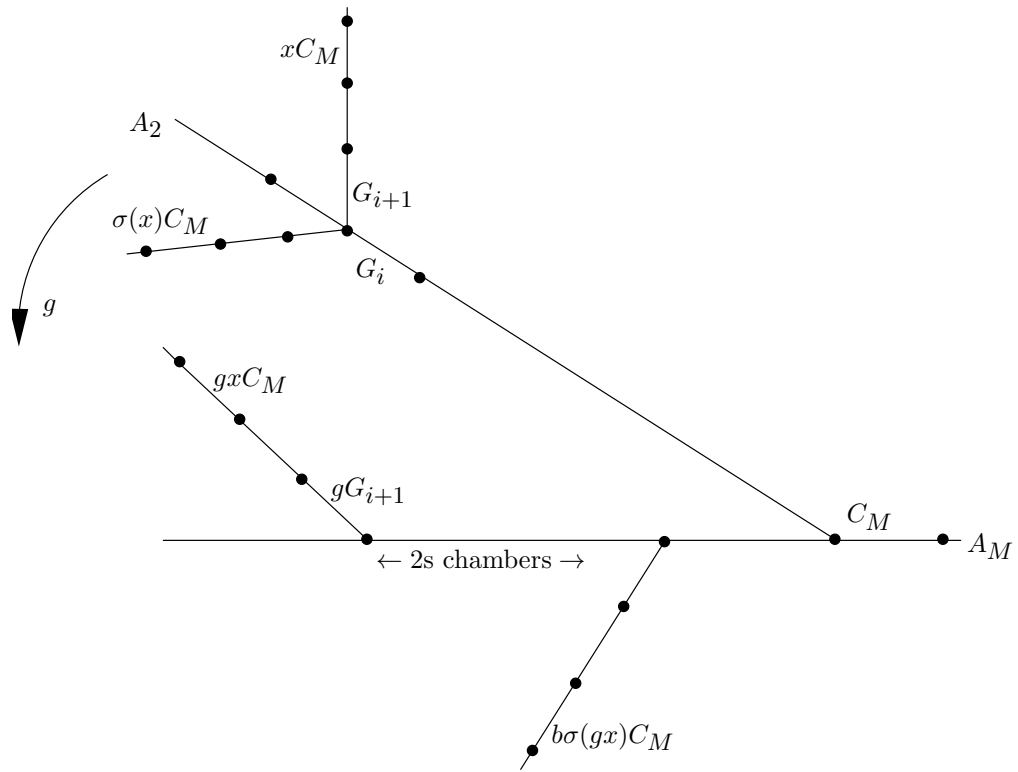


Figure 2.7: For  $w$  in the negative Weyl chamber

## 2.2 $GL_2$ and $PGL_2$

The situation is slightly different for  $GL_2$ . First, we must understand differences in setup. For  $GL_2(L)$  it is possible to send  $C_M$  to itself without fixing it pointwise. The matrix  $m = \begin{pmatrix} 0 & \pi \\ 1 & 0 \end{pmatrix}$  does this, for example. Another way of saying this is that contrary to the  $SL_2$  situation, the Iwahori associated to  $C_M$  is no longer the set  $\{g : gC_M = C_M\}$ .

We still have  $inv : GL_2(L)/I \times GL_2(L)/I \rightarrow I \backslash GL_2(L)/I \simeq \tilde{W}$ , but now  $\tilde{W} \simeq W_a \rtimes \mathbb{Z}$ , where  $W_a$ , the affine Weyl group, is in one-to-one correspondence with the chambers of  $A_M$  (recall that for  $SL_2$ , we had  $W_a \simeq \tilde{W}$ ). We therefore have  $inv : GL_2(L)/I \times GL_2(L)/I \rightarrow W_a \rtimes \mathbb{Z}$ . This map is given by  $inv(x, y) = (\rho(x^{-1}yC_M), v(\det(x^{-1}y)))$ , where  $v$  is the valuation.

The  $\sigma$ -conjugacy classes of  $GL_2(L)$  are

$$\left\{ \begin{pmatrix} \pi^\alpha & 0 \\ 0 & \pi^\beta \end{pmatrix} : \alpha \geq \beta \right\} \cup \left\{ \begin{pmatrix} 0 & \pi \\ 1 & 0 \end{pmatrix}^\alpha : \alpha \in \mathbb{Z}, \alpha \text{ odd} \right\} = R.$$

This follows from a result of Kottwitz [6].

For a given  $\sigma$ -conjugacy class  $\{x^{-1}b\sigma(x) : x \in GL_2(L)\}$ , where  $b \in R$ , we are interested in which  $(w, n) \in W_a \rtimes \mathbb{Z}$  have non-empty  $X_{(w,n)}(b\sigma)$ . To solve this, we will describe the set  $\{(\rho(x^{-1}b\sigma(x)C_M), v(\det(x^{-1}b\sigma(x)))) \in W_a \rtimes \mathbb{Z} : x \in GL_2(L)\}$  for any fixed  $b$  in the above set  $R$ .

First, note that  $v(\det(x^{-1}b\sigma(x))) = v(\det(b))$ , so the second component is fixed for fixed  $b$ . The possible values of the first component can be determined using a process that is similar to that in Sections 2.1.1 and 2.1.2. The difference is that  $b$  can now take on more values. Also, it is *a priori* possible (although we will see that it does not occur) for  $\{\rho(x^{-1}b\sigma(x)C_M) : x \in GL_2(L)\}$  to be bigger than  $\{\rho(x^{-1}b\sigma(x)C_M) : x \in SL_2(L)\}$ , since  $GL_2(L)$  acts on  $\mathcal{B}_\infty$  in ways that  $SL_2(L)$  does not.

If  $b = \begin{pmatrix} \pi^\alpha & 0 \\ 0 & \pi^\beta \end{pmatrix}$  then  $b$  shifts  $A_M$  to the right by  $\alpha - \beta$  units. Using reasoning similar to that in Section 2.1.2, for these  $b$  we see that  $\rho(x^{-1}b\sigma(x)C_M)$  could be any of the chambers  $C_M^{\pm(\alpha-\beta)}$  or  $C_M^{\pm(\alpha-\beta+i)}$ , for all  $i$  odd,  $i \geq 1$ . Figure 2.8 summarizes these results.

Now we consider  $b = \begin{pmatrix} 0 & \pi \\ 1 & 0 \end{pmatrix}^\alpha$ ,  $\alpha \in \mathbb{Z}, \alpha$  odd. The matrix  $m = \begin{pmatrix} 0 & \pi \\ 1 & 0 \end{pmatrix}$  flips  $A_M$  about the center of  $C_M$ . Therefore so does the matrix  $b$ . Let  $G$  be the minimal gallery between  $C_M$  and  $xC_M$ . Then  $b\sigma(G)$  is the minimal gallery between  $C_M$  and  $b\sigma(x)C_M$ . Let  $C_M = G_1, G_2, \dots, G_s = xC_M$  be the chambers of  $G$ . Then  $G_s, G_{s-1}, \dots, G_1, b\sigma(G_2), b\sigma(G_3), \dots, b\sigma(G_s)$  is the unique minimal gallery between  $xC_M$  and  $b\sigma(x)C_M$ . Call this gallery  $\Gamma_x$ . It has length  $2s - 1$ .

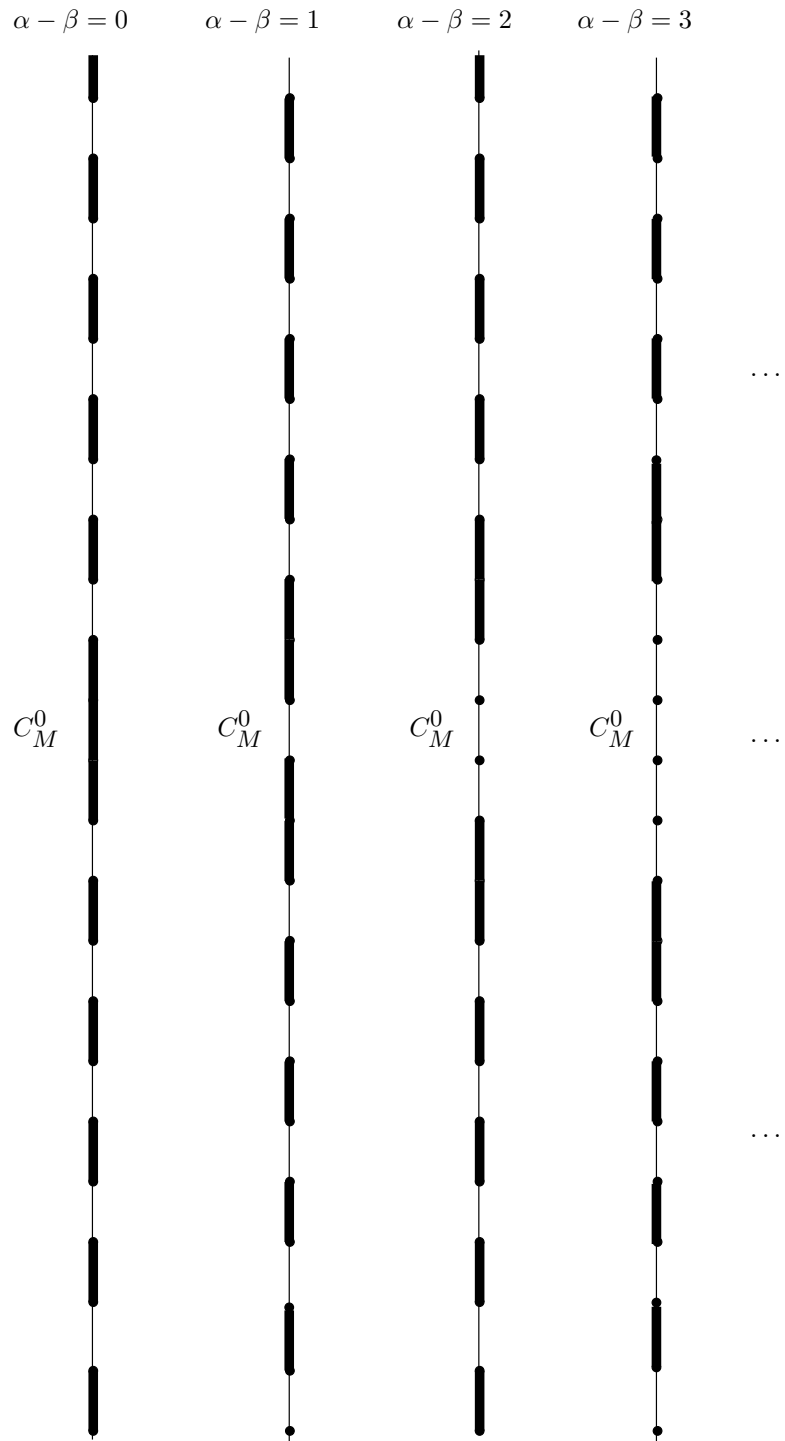


Figure 2.8: Summary of some results for  $GL_2$



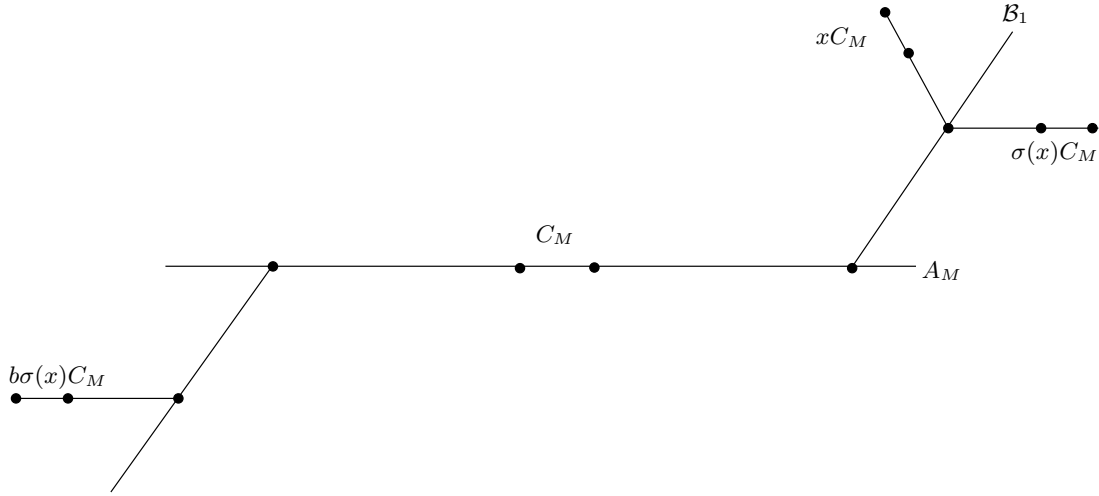


Figure 2.9: Computations for some  $\sigma$ -conjugacy classes for  $GL_2$

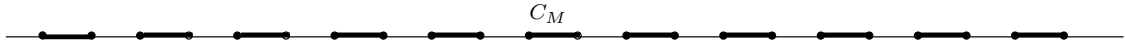


Figure 2.10: Summary of some more results for  $GL_2$

By choosing  $x$  appropriately, we can arrange for  $s$  to be any integer  $\geq 1$ . Further, if  $\rho(x^{-1}\Gamma_x)$  has final chamber  $C_M^i$ , then  $\rho(y^{-1}\Gamma_y)$  has final chamber  $C_M^{-i}$ , where  $y = xm$ . Therefore, the possible values for  $\rho(x^{-1}b\sigma(x)C_M)$  are  $C_M^i$  for any  $i$  even. This is independent of which odd  $\alpha \in \mathbb{Z}$  we have chosen. Figure 2.9 makes the calculations more clear, and Figure 2.10 summarizes the possible values of the first component of  $inv$ . The second component is always  $v(\det(x^{-1}b\sigma(x))) = v(\det(b))$ .

For  $PGL_2$ ,  $\tilde{W} \cong W_a \times \mathbb{Z}/2$ , and  $inv(x, y) = (\rho(x^{-1}yC_M), v(\det(x^{-1}y)))$ , where in  $PGL_2$ ,  $v(\det(x^{-1}y))$  is only determined mod 2. The results for  $PGL_2$  are the same as those for  $GL_2$ , but second-component values are computed mod 2.

### 2.3 Reorganization of Results

So far, we have stated all results by specifying, for each  $b$ , which  $w$  have non-empty  $X_w(b\sigma)$ , or which  $(w, n)$  have non-empty  $X_{(w,n)}(b\sigma)$ . We reword these results by saying, for each  $w$ , which  $b$  have non-empty  $X_w(b\sigma)$ , and for each  $(w, n)$ , which  $b$  have non-empty  $X_{(w,n)}(b\sigma)$ .

We first reword results for  $SL_2$ . If  $b = \begin{pmatrix} \pi^s & 0 \\ 0 & \pi^{-s} \end{pmatrix}$ , then let  $\Sigma_s$  be the  $\sigma$ -conjugacy class of  $b$ . Let  $D_M^i$  denote the double- $I$ -coset corresponding to the chamber  $C_M^i$ . Then one can see that  $D_M^{\pm 2n} \subseteq \Sigma_n$  for  $n \in \mathbb{Z}$ ,  $n \geq 0$ . One can also see that for  $n \geq 0$ ,

i	j
0	0
2	1
4	2
6	3
⋮	⋮

Table 2.1:  $D_M^{\pm i}$  intersects exactly these  $\Sigma_j$  non-trivially for  $i$  even

$i$	$j$
1	0
3	0, 1
5	0, 1, 2
7	0, 1, 2, 3
⋮	⋮

Table 2.2:  $D_M^{\pm i}$  intersects exactly these  $\Sigma_j$  non-trivially for  $i$  odd

$n \in \mathbb{Z}$ ,  $D_M^{\pm(2n+1)}$  intersects the  $\sigma$ -conjugacy classes  $\Sigma_0, \Sigma_1, \dots, \Sigma_n$ , and no others. These results are summarized in Tables 2.1 and 2.2.

In particular,  $D_M^{2n}$  for  $n \in \mathbb{Z}$  and  $D_M^{\pm 1}$  are each completely contained in some  $\sigma$ -conjugacy class. The cosets  $D_M^{\pm(2n+1)}$  for  $n \in \mathbb{Z}$ ,  $n \geq 0$  are spread over increasingly many  $\sigma$ -conjugacy classes as  $n$  gets larger.

We now reword results for  $GL_2$ . Let  $\Sigma_{\alpha, \beta}$  be the  $\sigma$ -conjugacy class of  $\begin{pmatrix} \pi^\alpha & 0 \\ 0 & \pi^\beta \end{pmatrix}$ , and let  $\Sigma_\alpha$  be the  $\sigma$ -conjugacy class of  $\begin{pmatrix} 0 & \pi \\ 1 & 0 \end{pmatrix}^\alpha$ . Let  $D_M^i$  denote the element of  $W_a$  corresponding to the chamber  $C_M^i$  in  $A_M$ , and let  $(D_M^i, j)$  be an element of  $\tilde{W} \cong W_a \times \mathbb{Z}$ . We also denote the corresponding double- $I$ -coset by  $(D_M^i, j)$ . Then one can see that  $(D_M^i, j) \subseteq \Sigma_{\frac{j+i}{2}, \frac{j-i}{2}}$  if  $i \equiv j \pmod{2}$ . If  $i$  is even and  $j$  is odd, then  $(D_M^i, j)$  intersects  $\Sigma_j$  and  $\Sigma_{\frac{j+k}{2}, \frac{j-k}{2}}$  for  $1 \leq k \leq i-1$  an odd integer. It does not intersect non-trivially with any other  $\sigma$ -conjugacy classes. Finally, if  $i$  is odd and  $j$  is even, then  $(D_M^i, j)$  intersects  $\Sigma_{\frac{j+k}{2}, \frac{j-k}{2}}$  for  $0 \leq k \leq i-1$  an even integer. It does not intersect non-trivially with any other  $\sigma$ -conjugacy classes. These results are summarized in Table 2.3.

$i$	$j$ odd	$j$ even
0	$\Sigma_j$	$\Sigma_{\frac{j}{2}, \frac{j}{2}}$
$\pm 1$	$\Sigma_{\frac{j+1}{2}, \frac{j-1}{2}}$	$\Sigma_{\frac{j}{2}, \frac{j}{2}}$
$\pm 2$	$\Sigma_j ; \Sigma_{\frac{j+1}{2}, \frac{j-1}{2}}$	$\Sigma_{\frac{j+2}{2}, \frac{j-2}{2}}$
$\pm 3$	$\Sigma_{\frac{j+3}{2}, \frac{j-3}{2}}$	$\Sigma_{\frac{j}{2}, \frac{j}{2}} ; \Sigma_{\frac{j+2}{2}, \frac{j-2}{2}}$
$\pm 4$	$\Sigma_j ; \Sigma_{\frac{j+1}{2}, \frac{j-1}{2}} ; \Sigma_{\frac{j+3}{2}, \frac{j-3}{2}}$	$\Sigma_{\frac{j+4}{2}, \frac{j-4}{2}}$
$\pm 5$	$\Sigma_{\frac{j+5}{2}, \frac{j-5}{2}}$	$\Sigma_{\frac{j}{2}, \frac{j}{2}} ; \Sigma_{\frac{j+2}{2}, \frac{j-2}{2}} ; \Sigma_{\frac{j+4}{2}, \frac{j-4}{2}}$
$\pm 6$	$\Sigma_j ; \Sigma_{\frac{j+1}{2}, \frac{j-1}{2}} ; \Sigma_{\frac{j+3}{2}, \frac{j-3}{2}} ; \Sigma_{\frac{j+5}{2}, \frac{j-5}{2}}$	$\Sigma_{\frac{j+6}{2}, \frac{j-6}{2}}$
$\vdots$	$\vdots$	$\vdots$

Table 2.3:  $\sigma$ -conjugacy classes that intersect  $(D_M^i, j)$  non-trivially

## CHAPTER 3

### GROUPS OF SEMISIMPLE RANK 2

In Section 3.1 we will show for  $b$  an element of a certain collection of  $\sigma$ -conjugacy class representatives of  $SL_3(L)$ , exactly which double- $I$ -cosets intersect  $\{x^{-1}b\sigma(x) : x \in SL_3(L)\}$  non-trivially. In Section 3.2, we will show that these results can also be made to give complete information of the same kind for certain  $\sigma$ -conjugacy classes of  $GL_3(L)$  and  $PGL_3(L)$ . Section 3.3 attempts to apply the same methods to  $Sp_4$ . Certain results are conjectural in this setting because some of the lengthy computations done for  $SL_3$  have not been done in entirety for  $Sp_4$ . Section 3.4 discusses how the methods of Section 3.1 could be applied to other rank 2 groups. Section 3.5 gives some invariance properties of the set  $\{inv(x, b\sigma(x)) : x \in G(L)\}$  that hold for any simply-connected group  $G$ , and any  $\sigma$ -conjugacy class  $b$ . These could be applied to higher rank groups, for instance. Some of the methods of Section 3.1 could also be applied to  $SL_n$  or  $Sp_{2n}$ . A comment to this effect is made when this is the case.

### 3.1 $SL_3$

In this section we enumerate the non-empty  $X_w(b\sigma)$  for  $SL_3$ , where the letter  $b$  will always refer to an element of  $SL_3(L)$  of the form

$$\begin{pmatrix} \pi^\alpha & 0 & 0 \\ 0 & \pi^\beta & 0 \\ 0 & 0 & \pi^{-\alpha-\beta} \end{pmatrix},$$

with  $\alpha \geq \beta \geq \alpha - \beta$ . These are representatives of distinct  $\sigma$ -conjugacy classes of  $SL_3(L)$ . However, not every  $\sigma$ -conjugacy class is represented by one of these elements [6].

The collection of chambers in  $A_M$  that correspond to  $w$  with non-empty  $X_w(b\sigma)$  is computed in the following way. In Section 3.1.1, we give some necessary definitions. In Section 3.1.2, we use geometric methods to produce a superset of the desired collection of chambers. In Section 3.1.4 we use algebraic methods that produce a subset of the desired collection for  $b = 1$ . We enlarge this subset in Section 3.1.5. This enlargement will be equal to the superset from Section 3.1.2, and therefore is the solution set of chambers. In Section 3.1.6 we give a geometric method of arriving at the subset of Section 3.1.5 that also applies for  $b \neq 1$ . In Section 3.1.7, we prove a symmetry result analogous to that done for  $SL_2$  in Section 2.1.3. In Section 3.1.3, we develop a relationship between the collection of  $w$  with non-empty  $X_w(1\sigma)$  and

the collection of  $w$  with non-empty  $X_w(b\sigma)$ . This is done by illuminating an efficient method of computing  $\{inv(x, b\sigma(x)) : x \in SL_3(L)\}$  that works for any of the  $b$  listed above.

### 3.1.1 Standard Minimal Galleries and Composite Galleries

Our goal is to determine which  $X_w(b\sigma)$  are non-empty. The technique that led to success in the rank 1 case involved considering, for every chamber  $E \subseteq \mathcal{B}_\infty$ , a gallery  $\Gamma_E$  connecting  $E$  to  $b\sigma(E)$ . We used the unique minimal gallery between these two chambers. We will use a similar process for  $SL_3$ . However, there is no longer a unique minimal gallery  $\Gamma_E$  connecting  $E$  and  $b\sigma(E)$ . In this section we will specify a choice of gallery, which we will call the *composite gallery*. The composite gallery is usually not minimal.

First define the three *primary directions*  $D_1, D_2, D_3$  and the three *secondary directions*  $d_1, d_2, d_3$  in the main apartment  $A_M$  for  $SL_3$  as marked by arrows in Figure 3.1. Given a chamber  $E \subseteq A_M$ , we define the *standard minimal gallery* (SMG) between  $C_M$  and  $E$  as follows. If  $E$  is in one of the corridors marked  $c_1, \dots, c_6$  in Figure 3.1, then the SMG is the unique minimal gallery from  $C_M$  to  $E$ . If  $E$  is in region  $R_i$ , proceed first in the direction  $D_i$ , then in the direction  $d_i$ . If  $E$  is in region  $r_i$ , proceed first in direction  $D_i$ , then in direction  $d_j$ , where  $j \equiv i - 1 \pmod{3}$ .

The following lemma allows us to define the SMG between  $C_M$  and  $E$  for any chamber  $E \subseteq \mathcal{B}_\infty$  in a natural way. As in Chapter 2,  $\rho$  is the retraction from  $\mathcal{B}_\infty$  to  $A_M$  centered at  $C_M$ .

**Lemma 3.1.1.** There is a unique gallery  $G_E$  between  $C_M$  and  $E$  which is minimal, and such that  $\rho(G_E)$  is the SMG between  $C_M$  and  $\rho(E)$ .

*Proof.* Let  $A_1$  be an apartment containing  $C_M$  and  $E$ . Let  $g_1 \in SL_3(L)$  be such that  $g_1A_1 = A_M$  and  $g_1C_M = C_M$ . If  $G_{\rho(E)}$  is the SMG between  $C_M$  and  $\rho(E)$ , then let  $G_E = g_1^{-1}G_{\rho(E)}$ . This proves existence.

To prove uniqueness, note that if  $\tilde{G}_E$  is another minimal gallery from  $C_M$  to  $E$ , then  $\tilde{G}_E \subseteq A_1$  (see Definition 3.1.6 and Theorem 3.1.6 in Section 3.1.6). If  $\rho(\tilde{G}_E) = G_{\rho(E)}$  then  $g_1^{-1}G_{\rho(E)} = \tilde{G}_E$ . But  $g_1^{-1}G_{\rho(E)} = G_E$ .  $\square$

To obtain a composite gallery,  $\Gamma_E$ , from the SMG between  $C_M$  and  $E$ , proceed as follows.

*Case 1:  $b = 1$ .* Let  $\Gamma_E^1$  be the gallery composed of the chambers of the SMG between  $C_M$  and  $E$  that are not in  $\mathcal{B}_1$ . Let  $\Gamma_E^3 = \sigma(\Gamma_E^1)$ . Then  $\Gamma_E = \Gamma_E^1 \cup \Gamma_E^3$ . We will call the edge  $e$  between  $\Gamma_E^1$  and  $\Gamma_E^3$  the *edge of departure of the SMG between  $C_M$  and  $E$  from  $\mathcal{B}_1$* .

*Case 2:  $b \neq 1$ .* Let  $\Gamma_E^1$  be the gallery composed of the chambers of the SMG between  $C_M$  and  $E$  that are not in  $A_M$ . Let  $\Gamma_E^3 = b\sigma(\Gamma_E^1)$ . Let  $e$  be the unique edge in  $\Gamma_E^1$

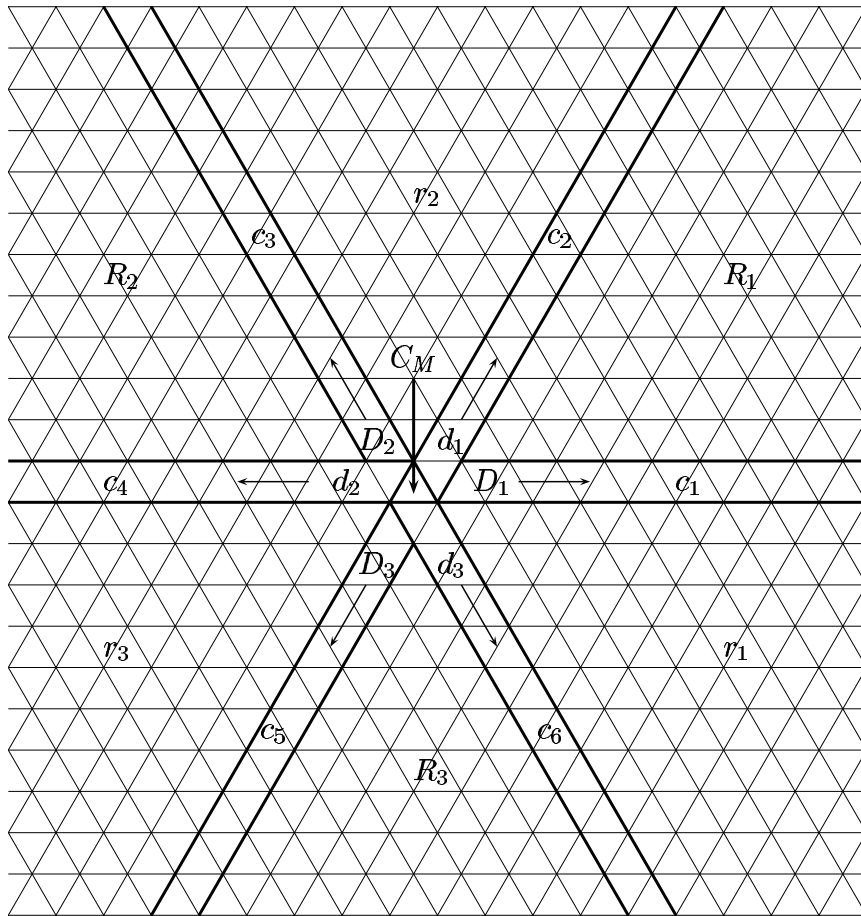


Figure 3.1: Primary and secondary directions

that is contained in  $A_M$ . Let  $\Gamma_E^2$  be any minimal gallery connecting  $e$  and  $b\sigma(e) = be$ . Then  $\Gamma_E = \Gamma_E^1 \cup \Gamma_E^2 \cup \Gamma_E^3$ . We call  $e$  the *edge of departure of the SMG between  $C_M$  and  $D$  from  $A_M$* . The term *edge of departure* without further modification will be used to refer either to an edge of departure from  $A_M$  or to an edge of departure from  $\mathcal{B}_1$ .

We will also need the following definitions.

**Definition 3.1.1.** If  $E_1$  and  $E_2$  are two chambers in  $\mathcal{B}_\infty$  that share an edge  $e$ , then we say the *transition type* from  $E_1$  to  $E_2$  is the type of the two vertices not in  $e$ .

**Definition 3.1.2.** If  $G$  is a non-stuttering gallery in  $\mathcal{B}_\infty$  consisting of  $G_0, \dots, G_s$ , and if the transition type from  $G_{i-1}$  to  $G_i$  is  $t_i$  for  $1 \leq i \leq s$ , then we say that  $G$  has *type*  $t_1, \dots, t_s$ .

Note that if  $G \subseteq A_M$ , then  $G_0$  and  $t_1, \dots, t_s$  determine  $G$ . It is also possible to specify a gallery type by giving a picture of a non-stuttering gallery in  $A_M$ .

### 3.1.2 A Superset of the Solution Set

Just as in the  $SL_2$  case,  $SL_3$  is simply connected. So given  $b$ , an answer to the question of which  $w \in \tilde{W}$  have non-empty  $X_w(b\sigma)$  can be given by specifying the corresponding chambers in  $A_M$ . As such, the answer we are looking for is the set of chambers  $S = \{\rho(x^{-1}b\sigma(x)C_M) : x \in SL_3(L)\}$ . In the  $SL_2$  case, for every  $x \in SL_2(L)$ , we had a unique minimal gallery  $\Gamma_x$  connecting  $xC_M$  and  $\sigma(x)C_M$ . Since this gallery was minimal, we were able to determine  $\rho(x^{-1}b\sigma(x)C_M)$  just by folding  $x^{-1}\Gamma_x$  from  $C_M$  down into  $A_M$  in the unique possible way. In the  $SL_3$  case, we let  $\Gamma_x$  instead be the composite gallery  $\Gamma_E$  (for  $E = xC_M$ ) constructed in the previous section. Since this composite gallery is not necessarily minimal, one can not determine  $\rho(x^{-1}b\sigma(x)C_M)$  from its type and starting point alone. One can, however, get a set of possible chambers  $S_x$  for  $\rho(x^{-1}b\sigma(x)C_M)$  by enumerating all the possible foldings of a gallery of the same type as  $x^{-1}\Gamma_x$ , and putting the final chamber of each into  $S_x$ . The set  $S_1 = \cup_{x \in SL_3(L)} S_x$  contains the set  $S$  in which we are interested.

We include an example of this computational process. Let

$$b = \begin{pmatrix} \pi^3 & 0 & 0 \\ 0 & \pi^{-1} & 0 \\ 0 & 0 & \pi^{-2} \end{pmatrix},$$

and let  $x$  be such that the SMG connecting  $C_M$  to  $xC_M$  has type and edge of departure from  $A_M$  as indicated in Figure 3.2. Then the resulting composite gallery  $\Gamma_x$  has the same type as the gallery pictured in Figure 3.3. Therefore,  $\rho(x^{-1}b\sigma(x)C_M)$  must be one of the chambers marked on Figure 3.4. These results are achieved by computing all possible values of  $\rho(E)$ , where  $E$  is the last chamber of some gallery that begins at  $C_M$  and that has the same type as  $\Gamma_x$  (pictured in Figure 3.3).

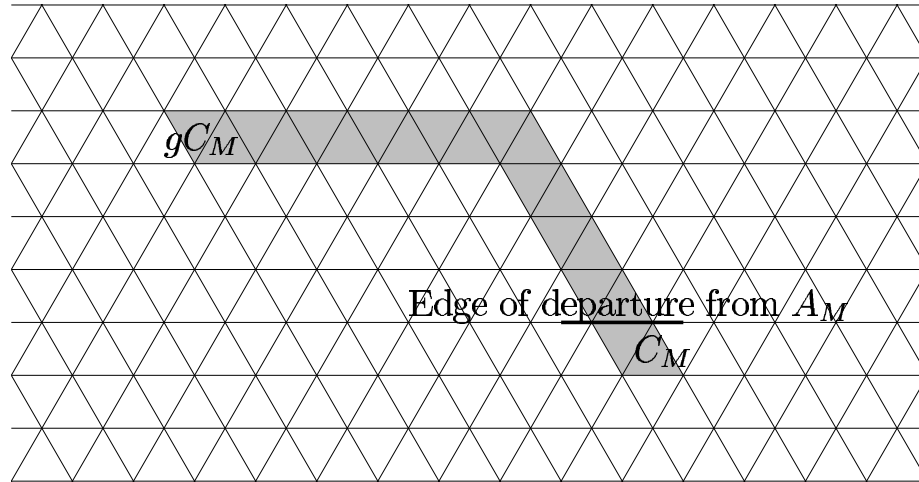


Figure 3.2: Example SMG type and edge of departure

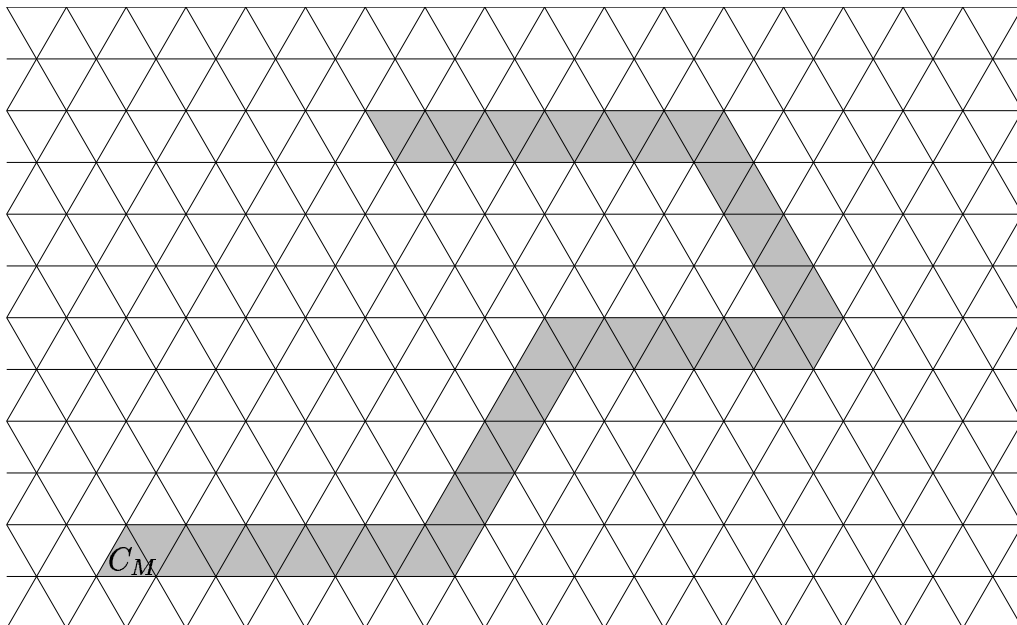


Figure 3.3: Composite gallery example



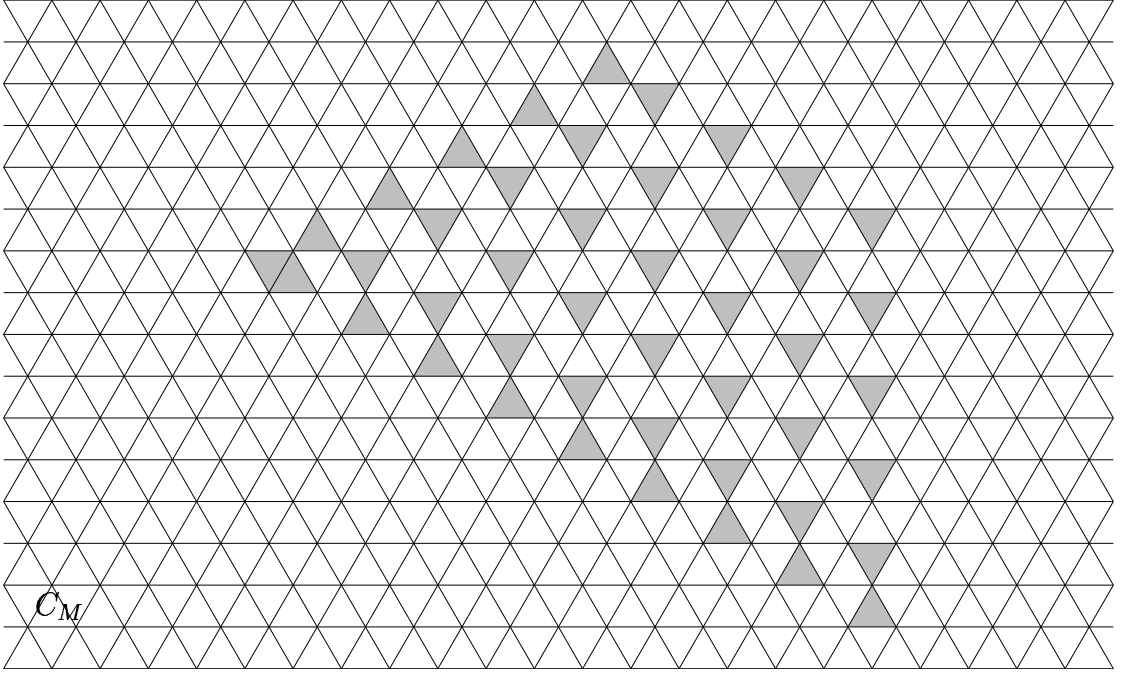


Figure 3.4: Results from the SMG in Figure 3.2

The apparent problem with this process is that it seems to be an infinite computation. The set  $S_1$  is a union of the  $S_x$ , where  $x \in SL_3(L)$  is arbitrary. Of course, we need only consider one representative  $x$  from each coset  $SL_3(L)/I$ , but there are still infinitely many such cosets. We can further optimize using the fact that only the *type* of  $x^{-1}\Gamma_x$  is important for computing  $S_x$ . This type is determined by the type of the SMG between  $C_M$  and  $xC_M$ , and the departure edge of this SMG from  $A_M$  (or from  $\mathcal{B}_1$  if  $b = 1$ ). We call a pair consisting of an SMG type and a departure edge a *type-edge pair*. The set we are trying to compute is  $S_1 = \cup S_{(t,e)}$ , where the union is over all type-edge pairs  $(t,e)$ , and where  $S_{(t,e)} = S_x$  for some  $x \in SL_3(L)$  such that the SMG from  $C_M$  to  $xC_M$  has type  $t$  and departure edge  $e$ .

The benefit of this point of view is that the  $S_{(t,e)}$  can be separated into finitely many infinite classes, each of which can be computed all at once. We give an example of two of these infinite classes,  $I_1$  and  $I_2$ , for  $b$  as above. The SMG types in  $I_1$  are those represented by the SMGs of the chambers in the region  $R_2$  in Figure 3.1. The edges of departure from  $A_M$  that we will consider are the horizontal ones. The SMG types in  $I_2$  are those represented by the SMGs of the chambers in corridor  $c_4$ . The pairs  $(t,e) \in I_2$  will have arbitrary  $e$ .

We consider  $I_1$  first. As in Case 2 of the definition of the composite gallery, let  $\Gamma_E^1$  be the gallery composed of the chambers of the SMG in question that are not in  $A_M$  (i.e., those after the edge of departure). So  $I_1$  gives rise to the  $\Gamma_E^1$  in Figure 3.5.

Let  $W$  be the finite Weyl group, and let  $w \in W$ ,  $a \in T(F)$  be such that  $awC_M =$

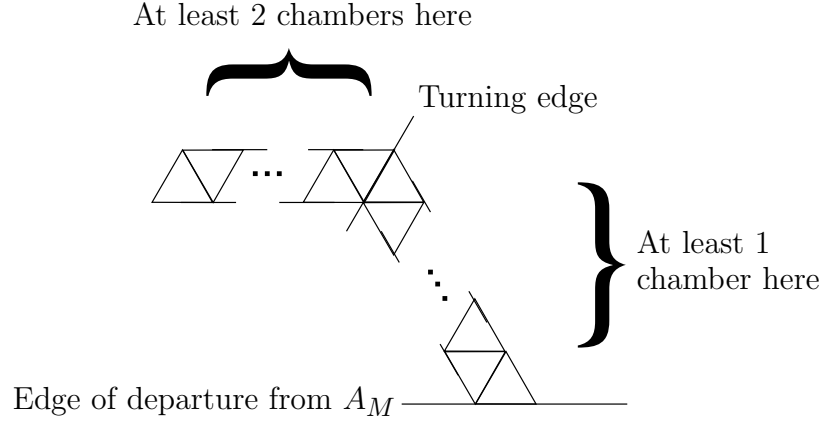


Figure 3.5:  $\Gamma_E^1$  possibilities for  $I_1$

$\rho(E)$ . We break  $I_1$  into six sub-classes according to  $w$ . Let

$$f = \begin{pmatrix} -1 & 0 & 0 \\ 0 & 0 & 1 \\ 0 & 1 & 0 \end{pmatrix}.$$

*Case 1:*  $w = f$ . We get a composite gallery of the type shown in Figure 3.6. If the *turning edge* is labeled in Figure 3.5, then we consider in Figure 3.7 the instances where  $\Gamma_E^1$  has 3 chambers after the turning edge. We consider in Figure 3.8 the instances where  $\Gamma_E^1$  has 5 chambers after the turning edge. We consider on Figure 3.9 the instances where  $\Gamma_E^1$  has 7 chambers after the turning edge. After doing these computations, it is easy to see what the situation is for the instances where  $\Gamma_E^1$  has  $2n + 1$  chambers after the turning edge, for  $n \geq 1$ . The results for these  $n$  are put together in Figure 3.10.

*Case 2:*  $w = 1$ . We get a composite gallery of the type shown in Figure 3.11. Figures 3.12 , 3.13, and 3.14 have instances where  $\Gamma_E^1$  has 2, 4, and 6 chambers after the turning edge, respectively. Figure 3.15 has the amalgamated results for  $2n$  chambers after the turning edge for all  $n \geq 1$ .

It is easy to see that the results for the cases in which  $w$  is some other order 2 element of  $W$  are just rotations of the results for case 1 by  $120^\circ$  and  $240^\circ$  about the center point of the chamber  $C_M$ . The results for the cases in which  $w$  is some other order 3 element of  $W$  are rotations of the case 2 results by  $120^\circ$  and  $240^\circ$  about the center point of  $C_M$ .

We break  $I_2$  into the same six sub-classes.

*Case 1:*  $w = 1$ . We get a composite gallery of one of the two types shown in Figures 3.16 and 3.17, where  $D$  is the last chamber in the SMG from  $C_M$  to  $x C_M$  that is contained in  $A_M$ . We consider in Figure 3.18 the instances where  $\Gamma_E^1$  has 0, 1 or 2 chambers after the departure edge, in Figure 3.19 the instances where it has

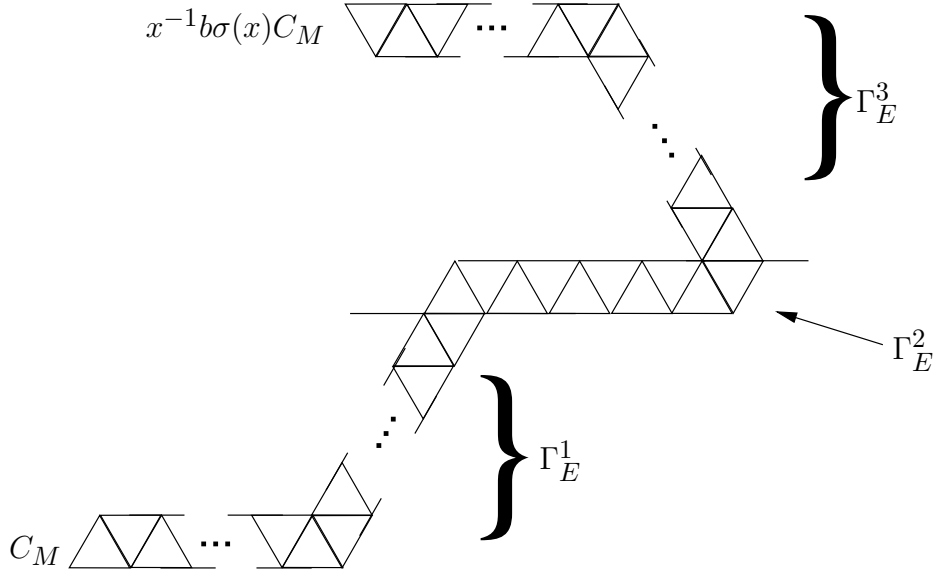


Figure 3.6: Some composite gallery possibilities for  $I_1$

3 or 4, and Figure 3.20 the instances where it has 5 or 6. Figure 3.21 is the combined results for  $n$  chambers after the departure edge, for  $n \geq 0$ .

*Case 2:  $w = f$ .* The combined results for this case are in Figure 3.22.

Again, if  $w$  is some other element of  $W$ , then the results are rotations of one of the above cases by  $120^\circ$  and  $240^\circ$  about the center of  $C_M$ . Conglomerating all results from  $I_1$  and  $I_2$  gives the results pictured in Figure 3.23. The chambers which are shaded more darkly in this figure are the chambers  $w^{-1}bwC_M$  for  $w \in W$ .

We will not compute other infinite classes of type-edge pairs here, but we will describe how the collection of type-edge pairs can be divided into infinite classes. For each corridor  $c_i$ , we get two infinite classes,  $I_{c_i}^1$  and  $I_{c_i}^2$ . The SMG types in each of these classes are those corresponding to SMGs whose terminus is in  $c_i$ . If  $\eta_1$  and  $\eta_2$  are the two possible angles of edges of departure of these SMGs, then  $I_{c_i}^j$  has type-edge pairs whose edge of departure component has angle  $\eta_j$ . Note that  $I_2$  is the union of two infinite classes of this kind, namely  $I_{c_4}^1$  and  $I_{c_4}^2$ .

If  $G$  is an SMG type corresponding to an SMG whose final chamber is in one of the regions  $R_i$  or  $r_i$ , then  $G$  has a turning point. The edge of departure for  $G$  could be before, after, or at the turning point. However, we need not consider type-edge pairs for which the edge of departure is after or at the turning point, because  $\Gamma_E^1$  for these type-edge pairs is the same as that arising from some type-edge pair in some  $I_{c_i}^j$ .

So for each  $i$  we have  $I_{R_i}^1$  and  $I_{R_i}^2$  with SMG types corresponding to an SMG whose final chamber is in  $R_i$ . The allowed edges of departure are those before the

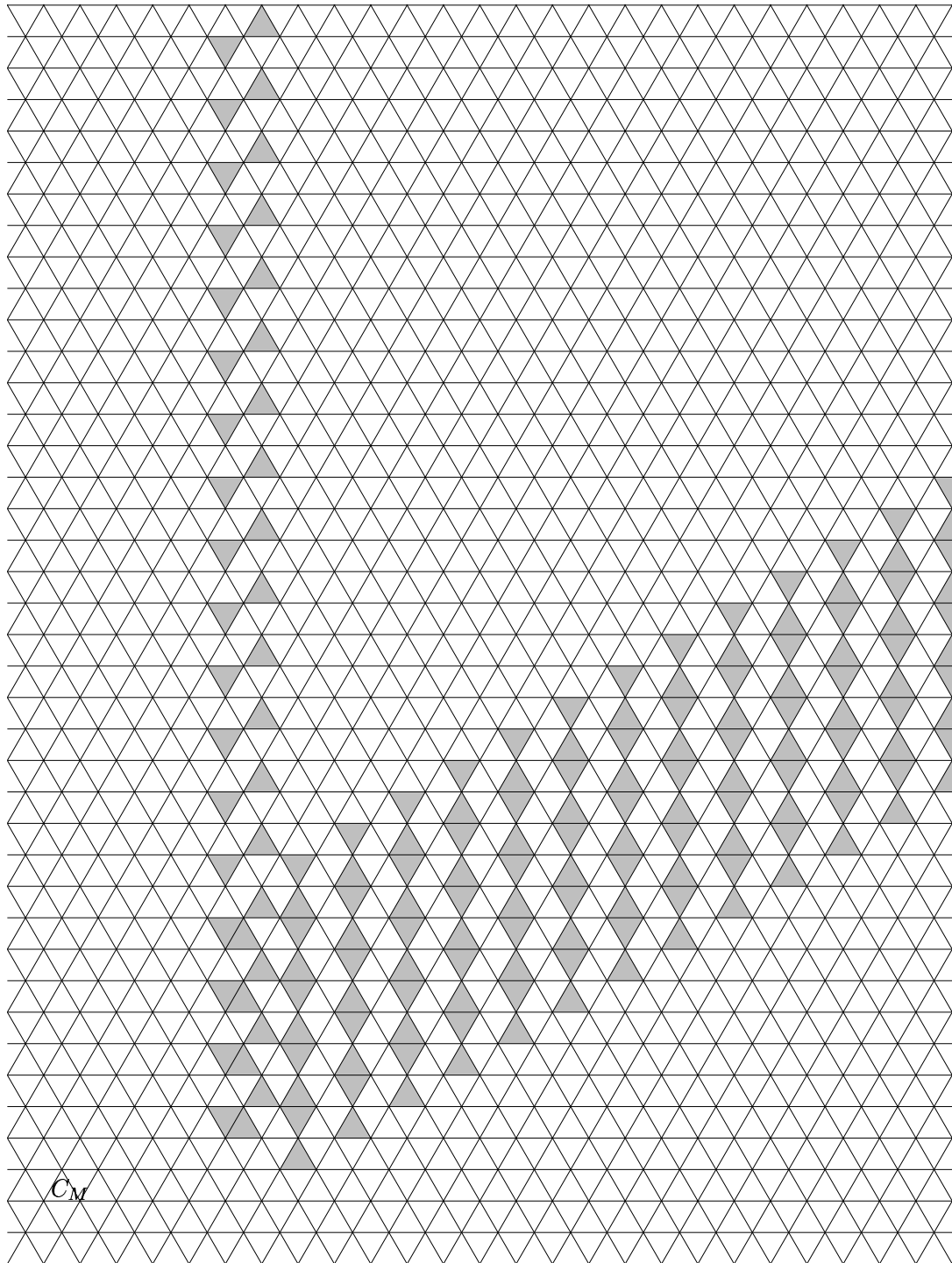


Figure 3.7: Class  $I_1$ , where  $\Gamma_E^1$  has 3 chambers after the turning edge

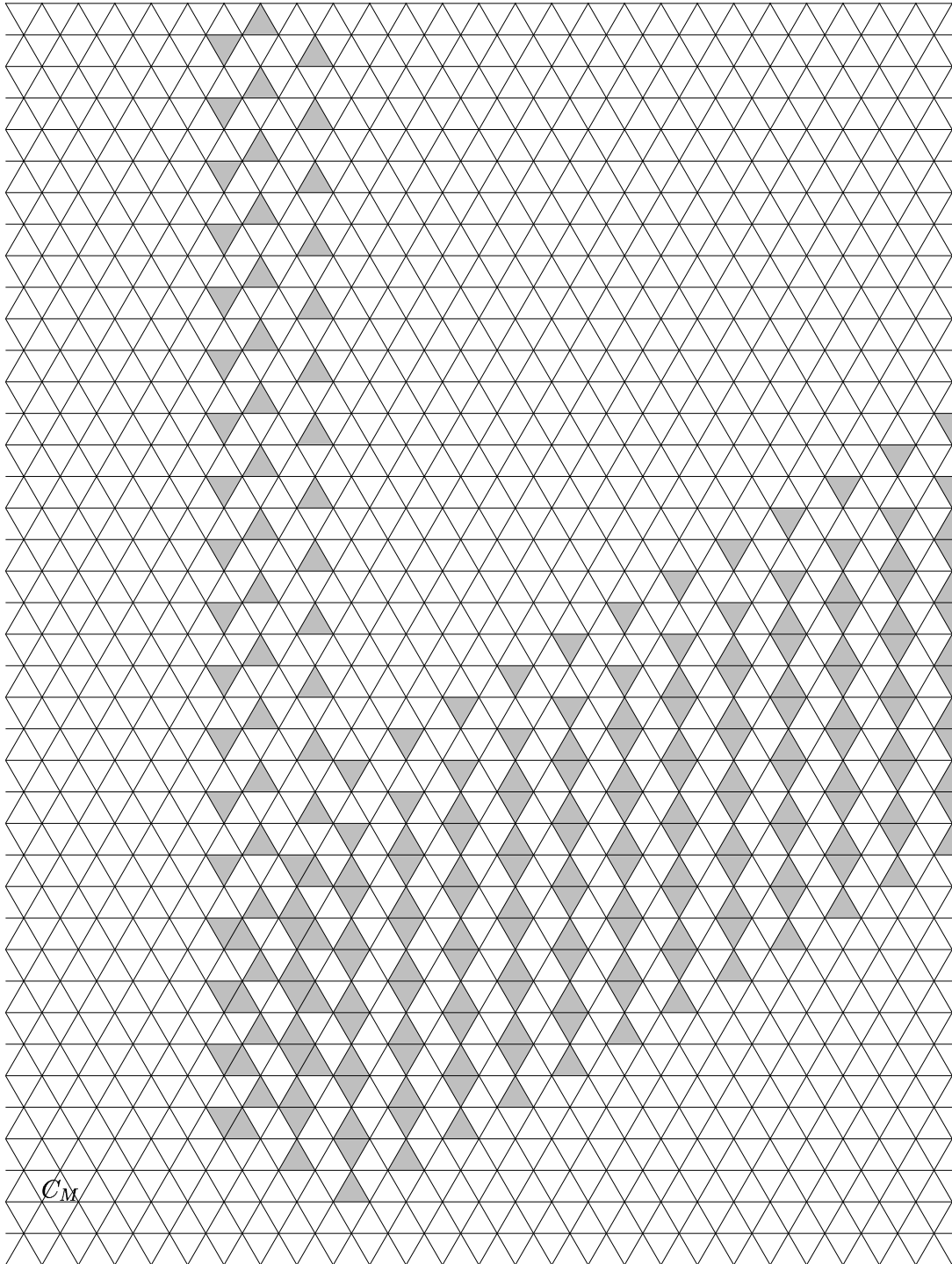


Figure 3.8: Class  $I_1$ , where  $\Gamma_E^1$  has 5 chambers after the turning edge

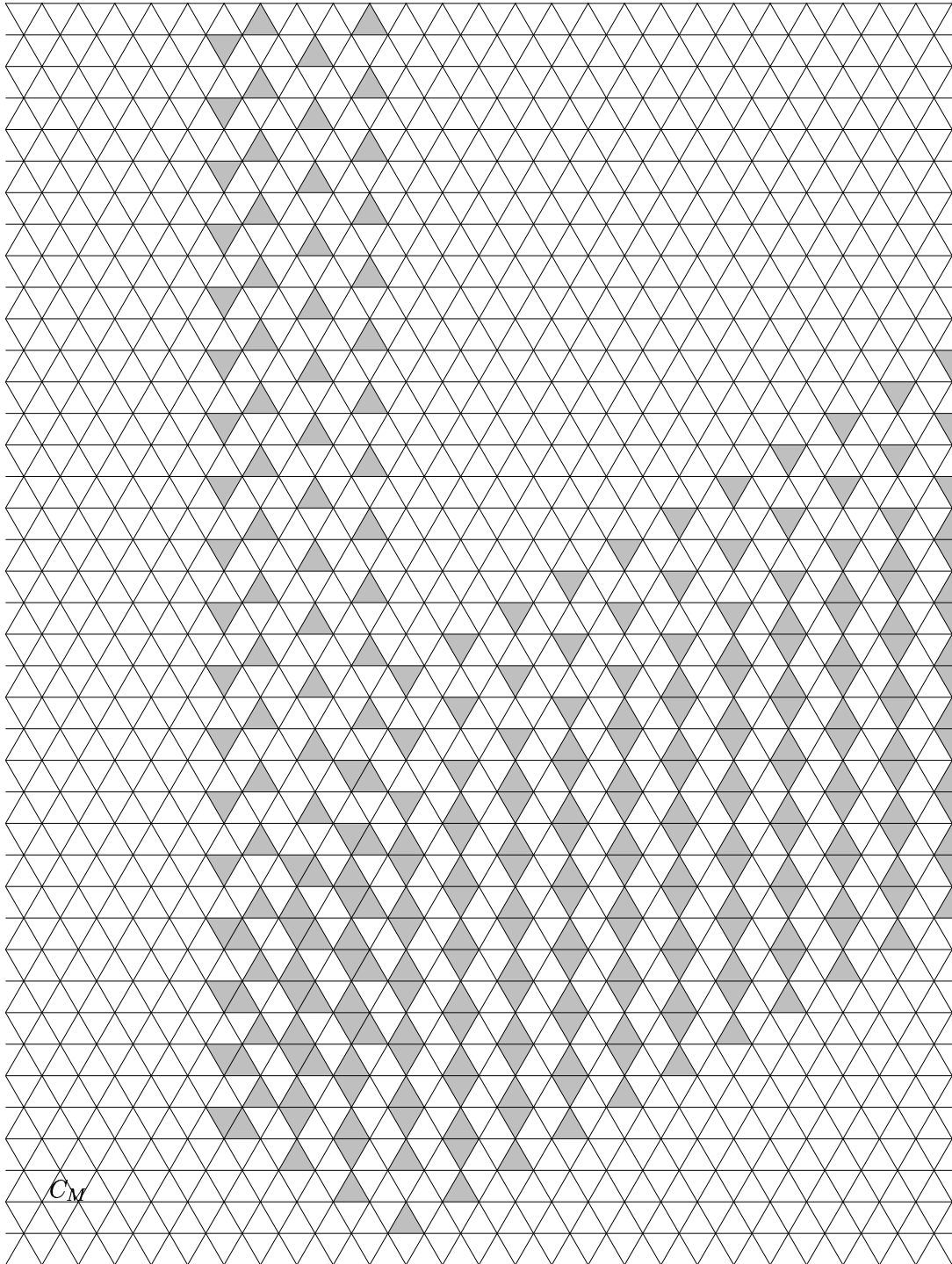


Figure 3.9: Class  $I_1$ , where  $\Gamma_E^1$  has 7 chambers after the turning edge



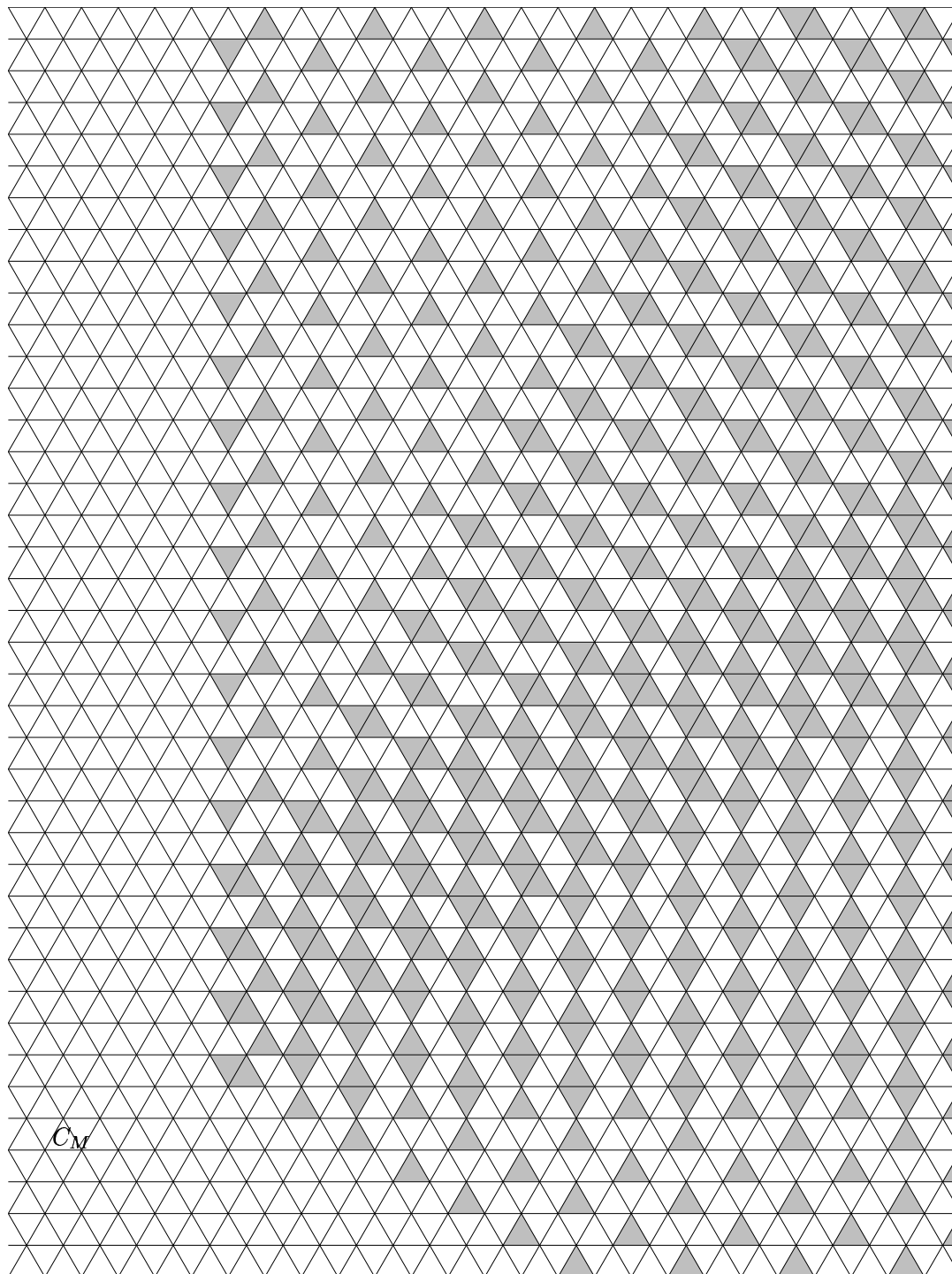


Figure 3.10: Summary of results for  $I_1$ , an odd number of chambers after the turning edge

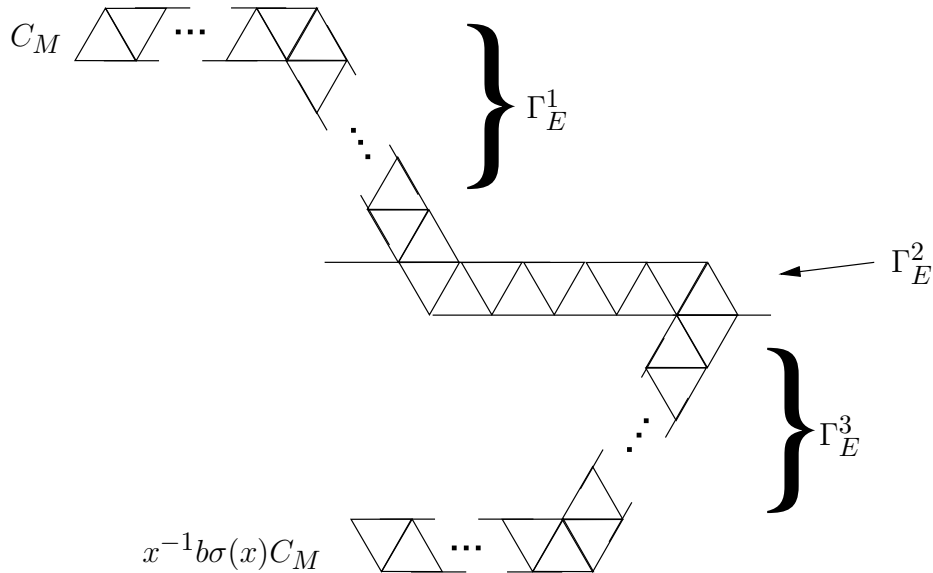


Figure 3.11: More composite gallery possibilities for  $I_1$

turning edge, with angle specified by the superscript. Note that  $I_1$  is of this type. We define  $I_{r_i}^1$  and  $I_{r_i}^2$  analogously for  $i = 1, 2, 3$ .

When one conglomerates the results from all infinite classes of composite galleries for

$$b = \begin{pmatrix} \pi^3 & 0 & 0 \\ 0 & \pi^{-1} & 0 \\ 0 & 0 & \pi^{-2} \end{pmatrix},$$

one gets an upper bound set  $S_1$ . It turns out that infinite classes other than those subsumed by  $I_1$  and  $I_2$  do not contribute any chambers beyond those contributed by  $I_1$  and  $I_2$ . So Figure 3.23 is the complete superset for  $b$  with  $\alpha = 3$  and  $\beta = -1$ .

When one conglomerates the results of the classes  $I_1$  and  $I_2$  for

$$b = \begin{pmatrix} \pi^2 & 0 & 0 \\ 0 & \pi^0 & 0 \\ 0 & 0 & \pi^{-2} \end{pmatrix},$$

one gets the chambers pictured in Figure 3.24. The results of other infinite classes have not been computed in this case, but it is reasonable to expect that they would not contribute any chambers additional to those contributed by  $I_1$  and  $I_2$ . This will be discussed further later.





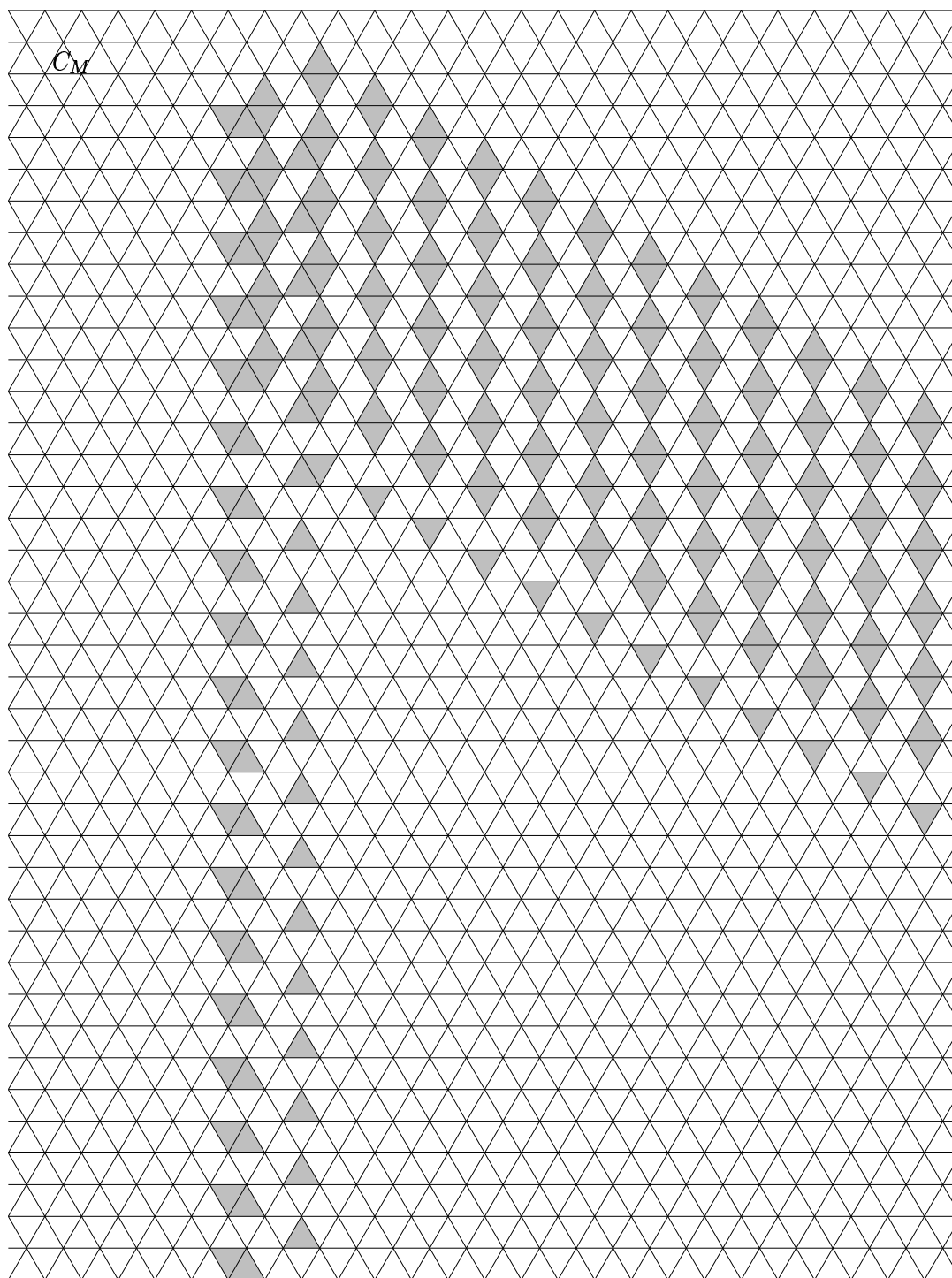


Figure 3.13: Class  $I_1$ , where  $\Gamma_{E_1}$  has 4 chambers after the turning edge

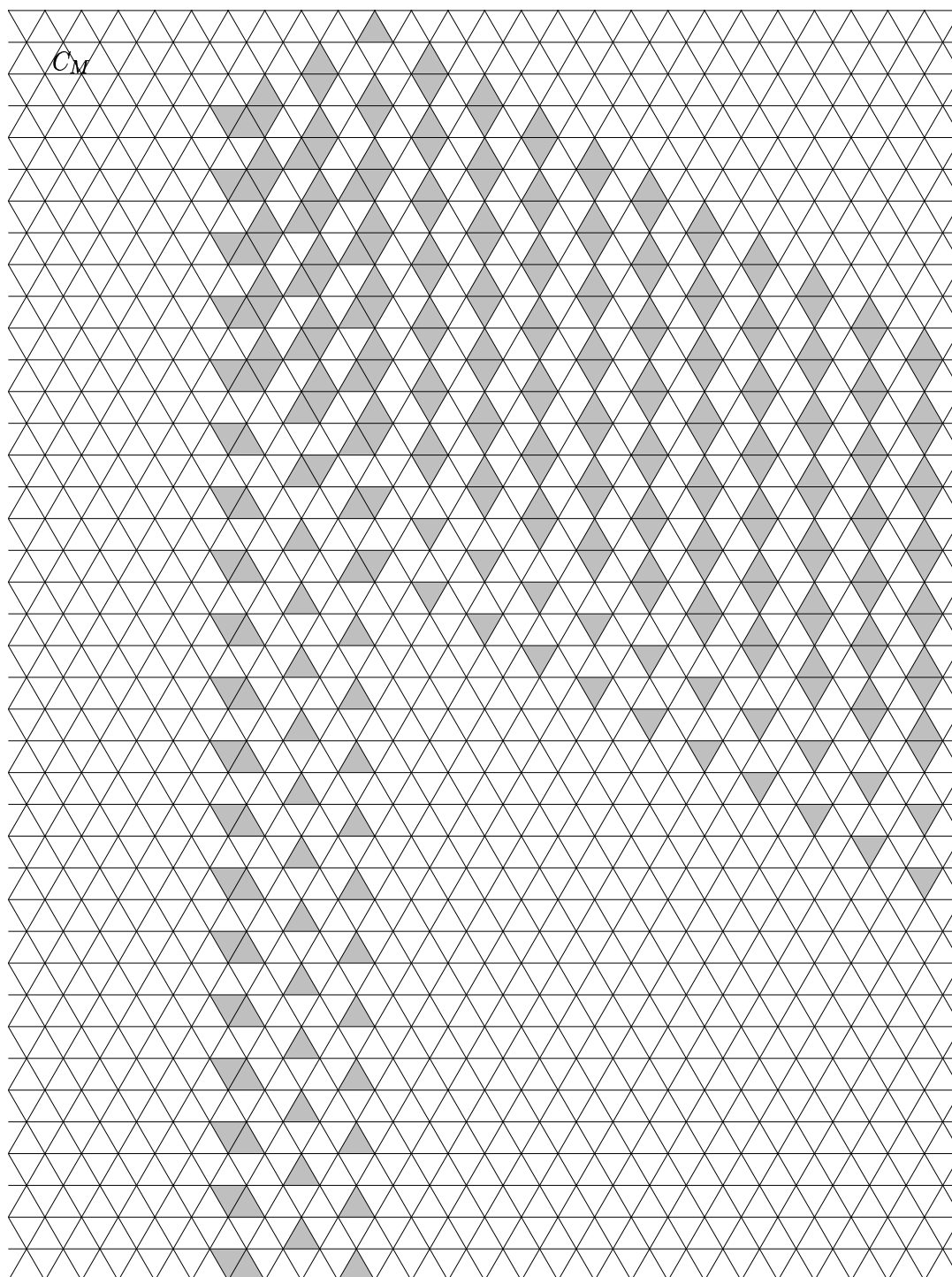


Figure 3.14: Class  $I_1$ , where  $\Gamma_{E_1}$  has 6 chambers after the turning edge

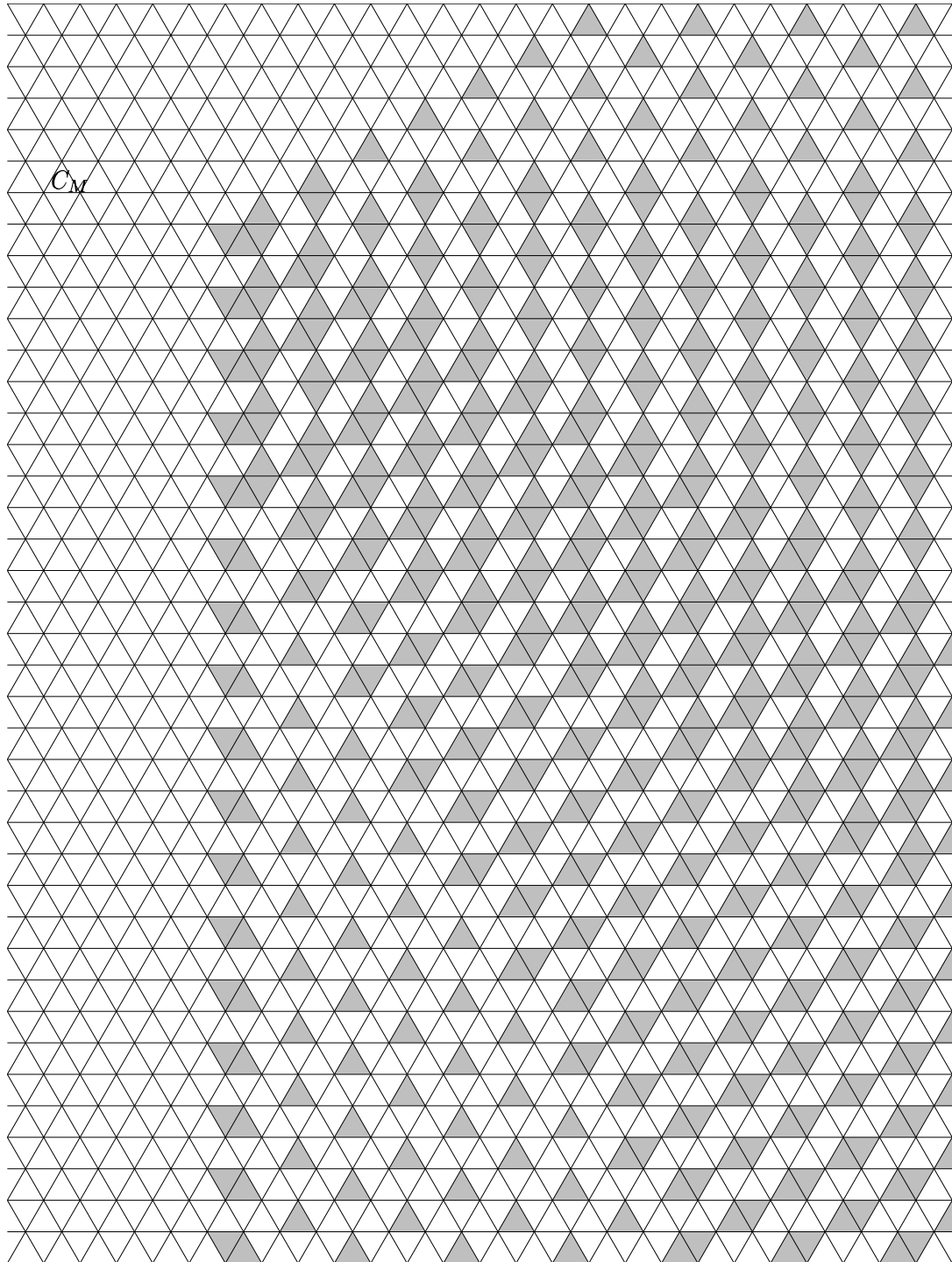


Figure 3.15: Summary of results for  $I_1$ , an even number of chambers after the turning edge

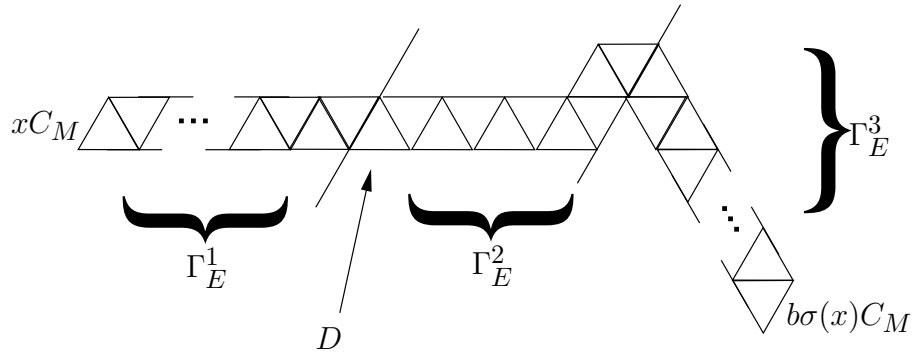


Figure 3.16: Some composite gallery possibilities for  $I_2$

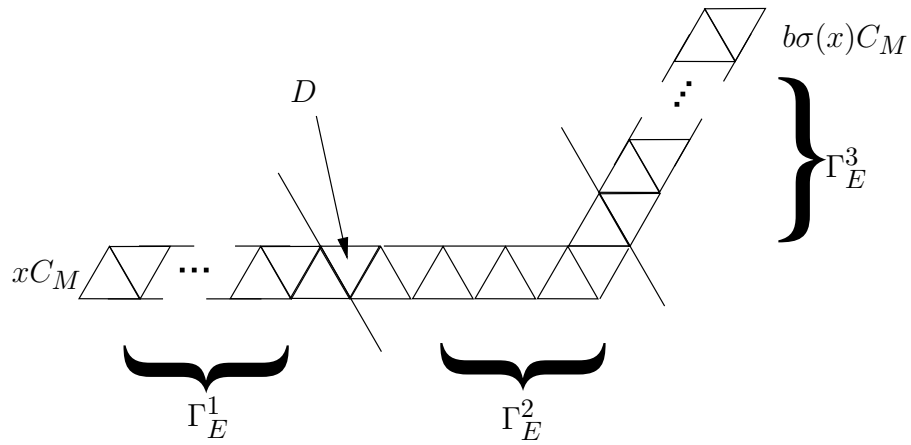


Figure 3.17: More composite gallery possibilities for  $I_2$

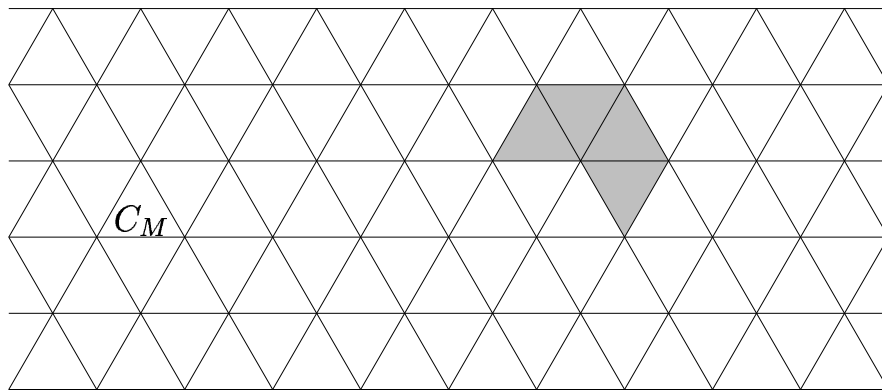


Figure 3.18: Class  $I_2$ , where  $\Gamma_{E_1}$  has 0, 1 or 2 chambers after the departure edge,  $w = 1$

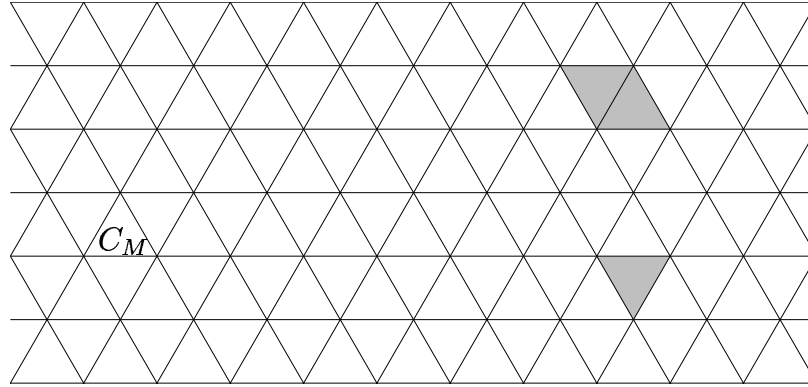


Figure 3.19: Class  $I_2$ , where  $\Gamma_{E_1}$  has 3 or 4 chambers after the departure edge,  $w = 1$

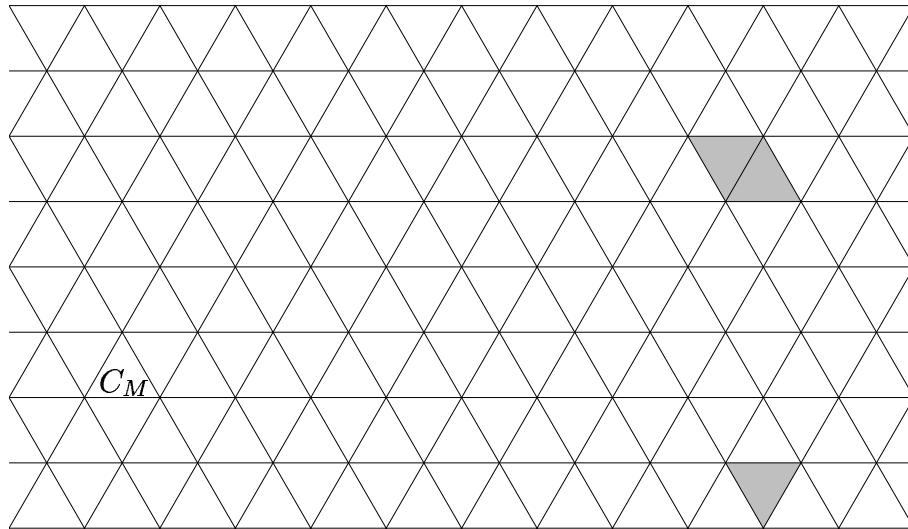


Figure 3.20: Class  $I_2$ , where  $\Gamma_{E_1}$  has 5 or 6 chambers after the departure edge,  $w = 1$

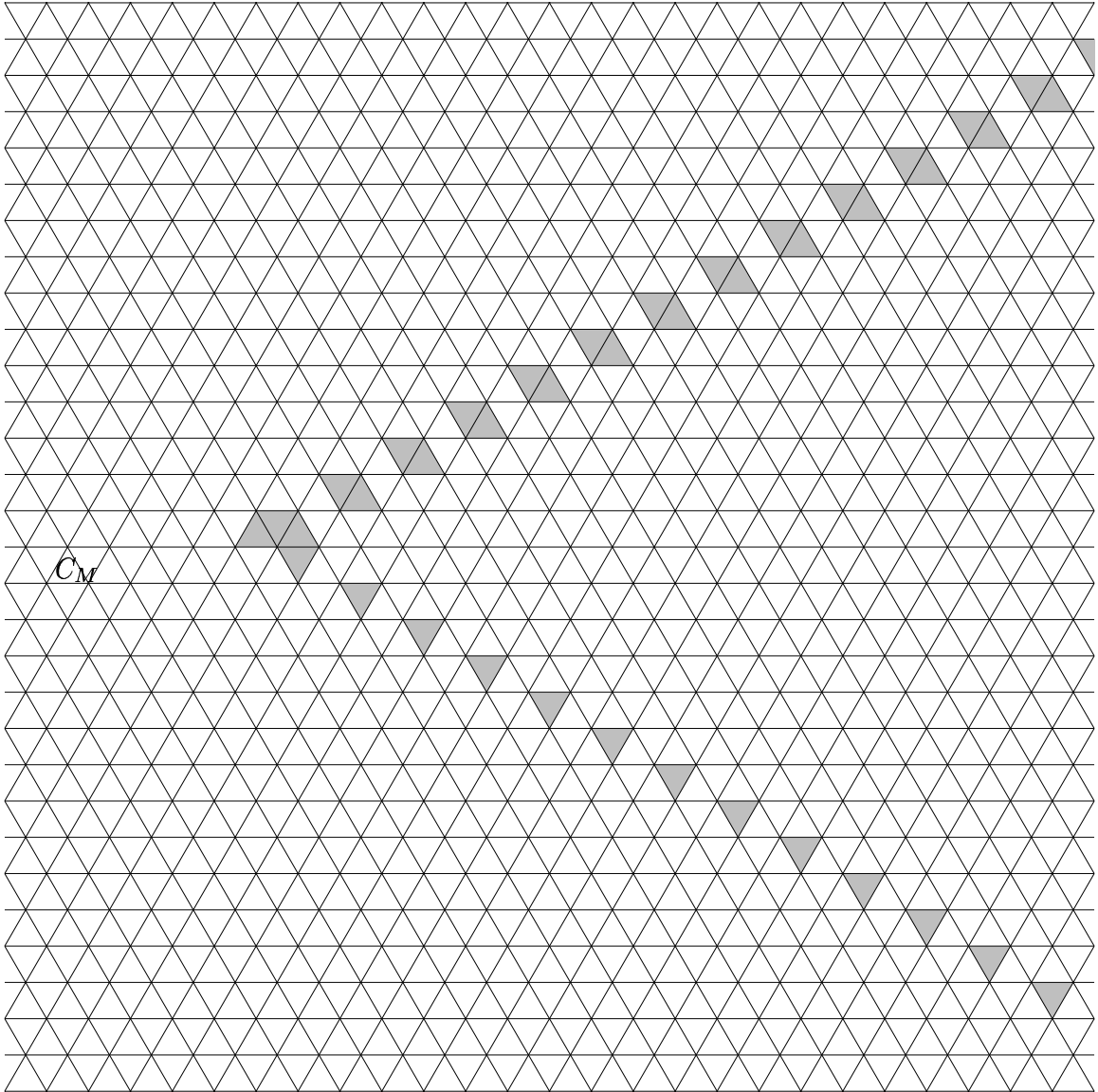


Figure 3.21: Summary of results for  $I_2$ ,  $w = 1$

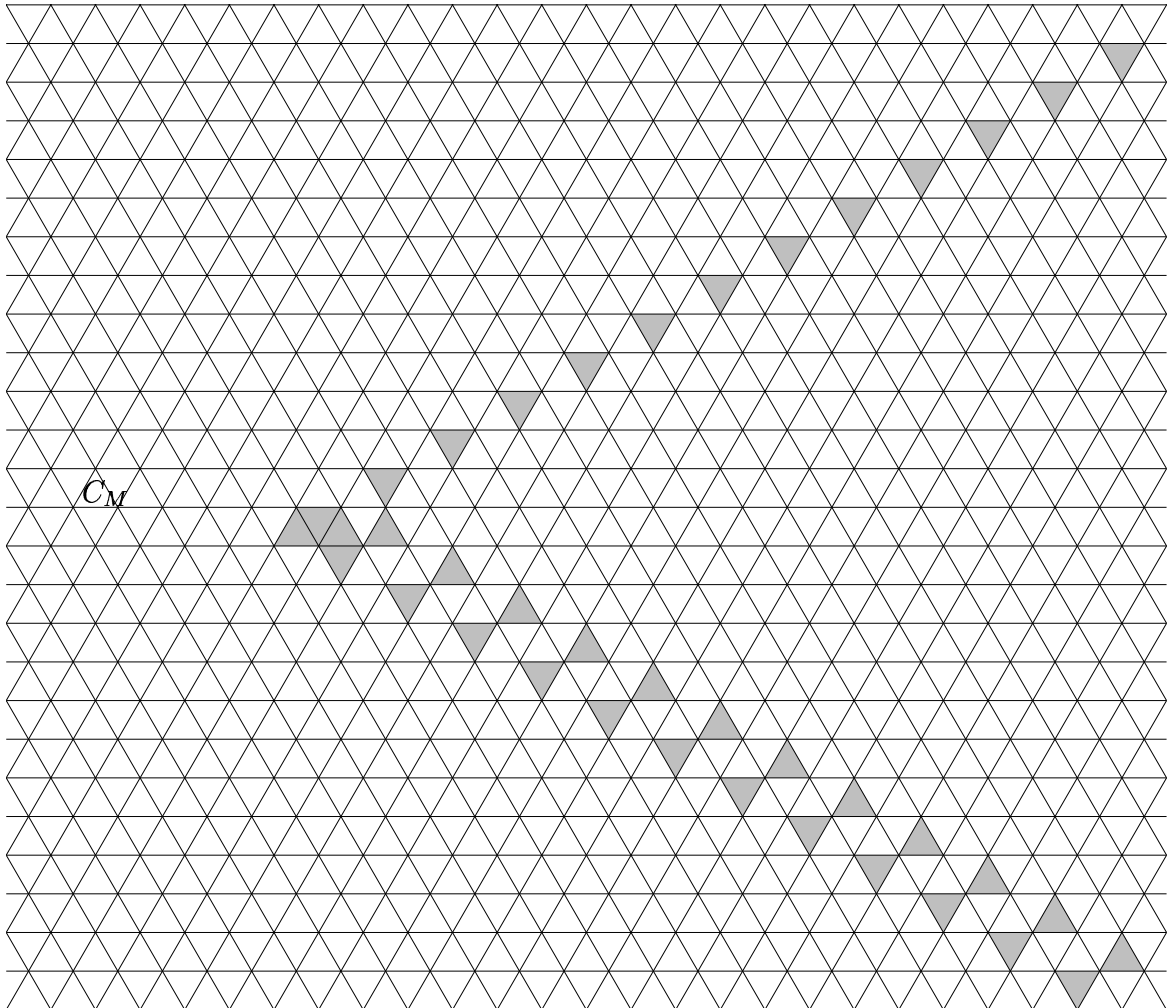


Figure 3.22: Summary of results for  $I_2$ ,  $w = f$



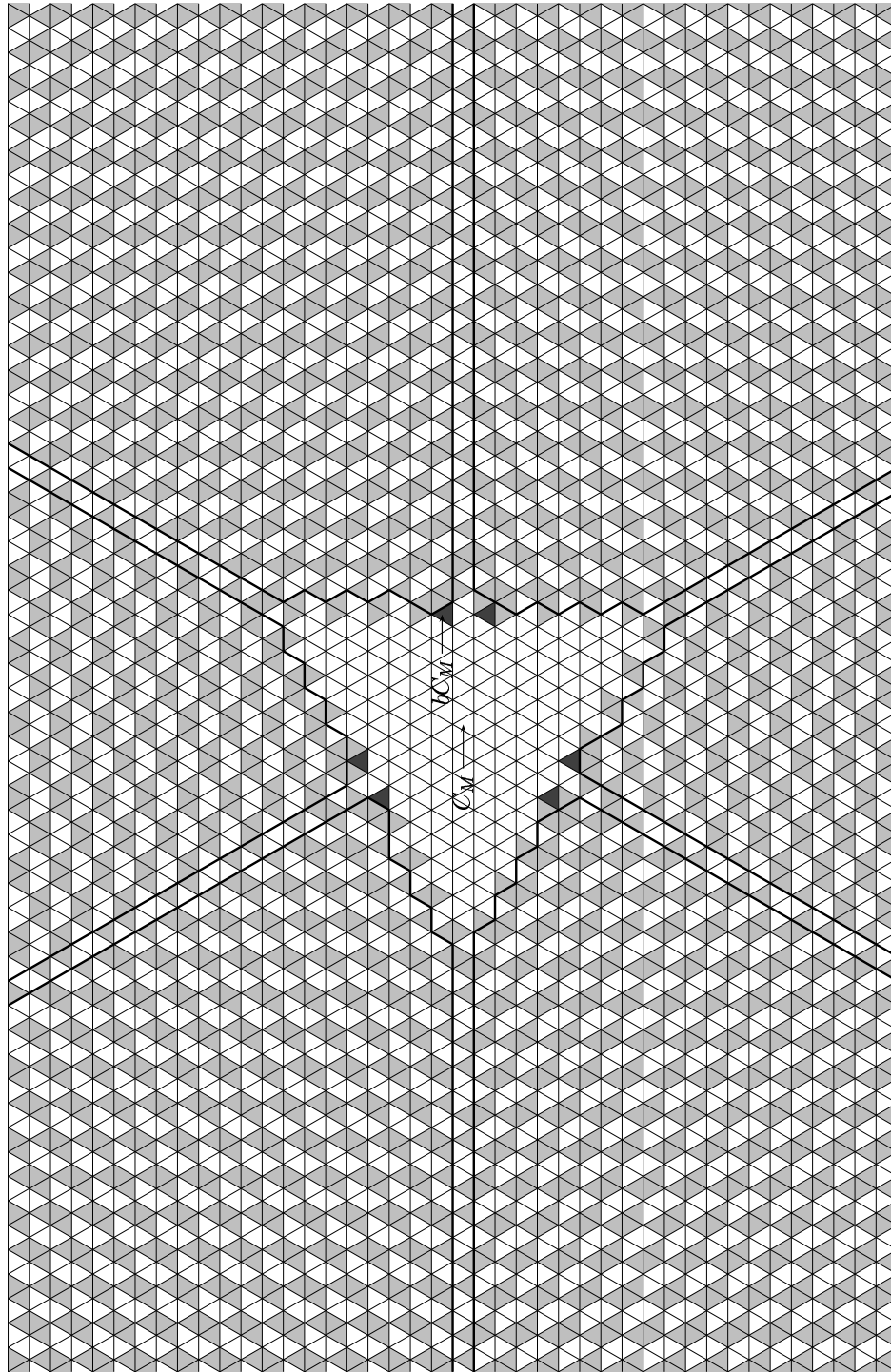


Figure 3.23: Summary of results for  $I_1$  and  $I_2$

When one conglomerates the results of the classes  $I_1$  and  $I_2$  for

$$b = \begin{pmatrix} \pi^2 & 0 & 0 \\ 0 & \pi^1 & 0 \\ 0 & 0 & \pi^{-3} \end{pmatrix},$$

one gets the chambers pictured in Figure 3.25. Again, other infinite classes have not been computed, but it is reasonable not to, as will be discussed later.

When one conglomerates the results of the classes  $I_1$  and  $I_2$  for

$$b = \begin{pmatrix} \pi^4 & 0 & 0 \\ 0 & \pi^0 & 0 \\ 0 & 0 & \pi^{-4} \end{pmatrix},$$

one gets the chambers pictured in Figure 3.26. Again, other infinite classes have not been computed, but it is reasonable not to.

When one conglomerates the results of the classes  $I_1$  and  $I_2$  for  $b = 1$ , one gets the chambers pictured in Figure 3.27. We have also computed the results of all other infinite classes of composite galleries in the  $b = 1$  case, as we did for the  $\alpha = 3$ ,  $\beta = -1$  case. Again, one can see (after the fact) that the infinite classes beyond those subsumed by  $I_1$  and  $I_2$  do not contribute any additional chambers.

The computation of the results of  $I_1$  and  $I_2$  for  $b = 1$  is a little different from the cases done thus far, all of which are similar to the example  $\alpha = 3$ ,  $\beta = -1$  that was done in detail. The general shapes for composite galleries for  $b = 1$  with  $(t, e) \in I_1$  are shown in Figure 3.28 for  $w = f$  and Figure 3.29 for  $w = 1$ . The general shapes for  $b = 1$  with  $(t, e) \in I_2$  are shown in Figure 3.30 for  $w = 1$ . The  $w = f$  for  $I_2$  galleries would be similar. All these galleries are different in general shape from their  $\alpha = 3$ ,  $\beta = -1$  counterparts. Note that the  $I_2$  galleries are minimal, and therefore would be easy to fold.

When one conglomerates the results of the classes  $I_1$  and  $I_2$  for

$$b = \begin{pmatrix} \pi^4 & 0 & 0 \\ 0 & \pi^{-2} & 0 \\ 0 & 0 & \pi^{-2} \end{pmatrix},$$

one gets the chambers pictured in Figure 3.31.

The computation of the results of  $I_1$  and  $I_2$  for this last value of  $b$  is also a little different from the cases done thus far because  $b \neq 1$ , but  $\alpha + 2\beta = 0$ . This is to say that  $bC_M$  sits along the bottom edge of the positive Weyl chamber. We will call any  $b$  with  $\alpha + 2\beta = 0$  or  $\alpha + 2\beta = 2\alpha + \beta$  *degenerate*. The values of  $bC_M$  for degenerate  $b$  are pictured in Figure 3.32. Note that the condition  $\alpha + 2\beta = 2\alpha + \beta$  corresponds to the  $bC_M$  along the top-left boundary of the positive Weyl chamber.

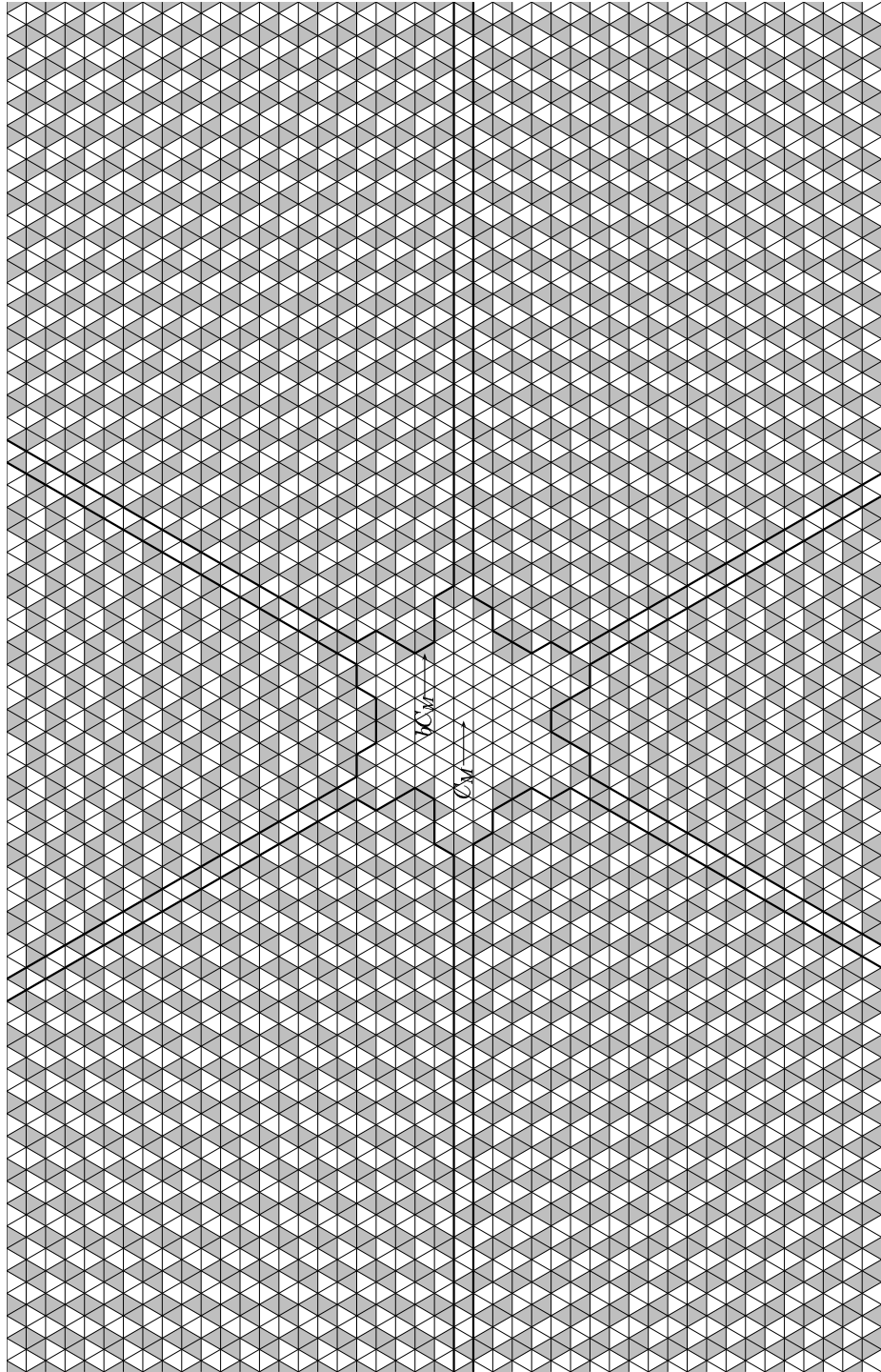


Figure 3.24: Result for  $\alpha = 2, \beta = 0$

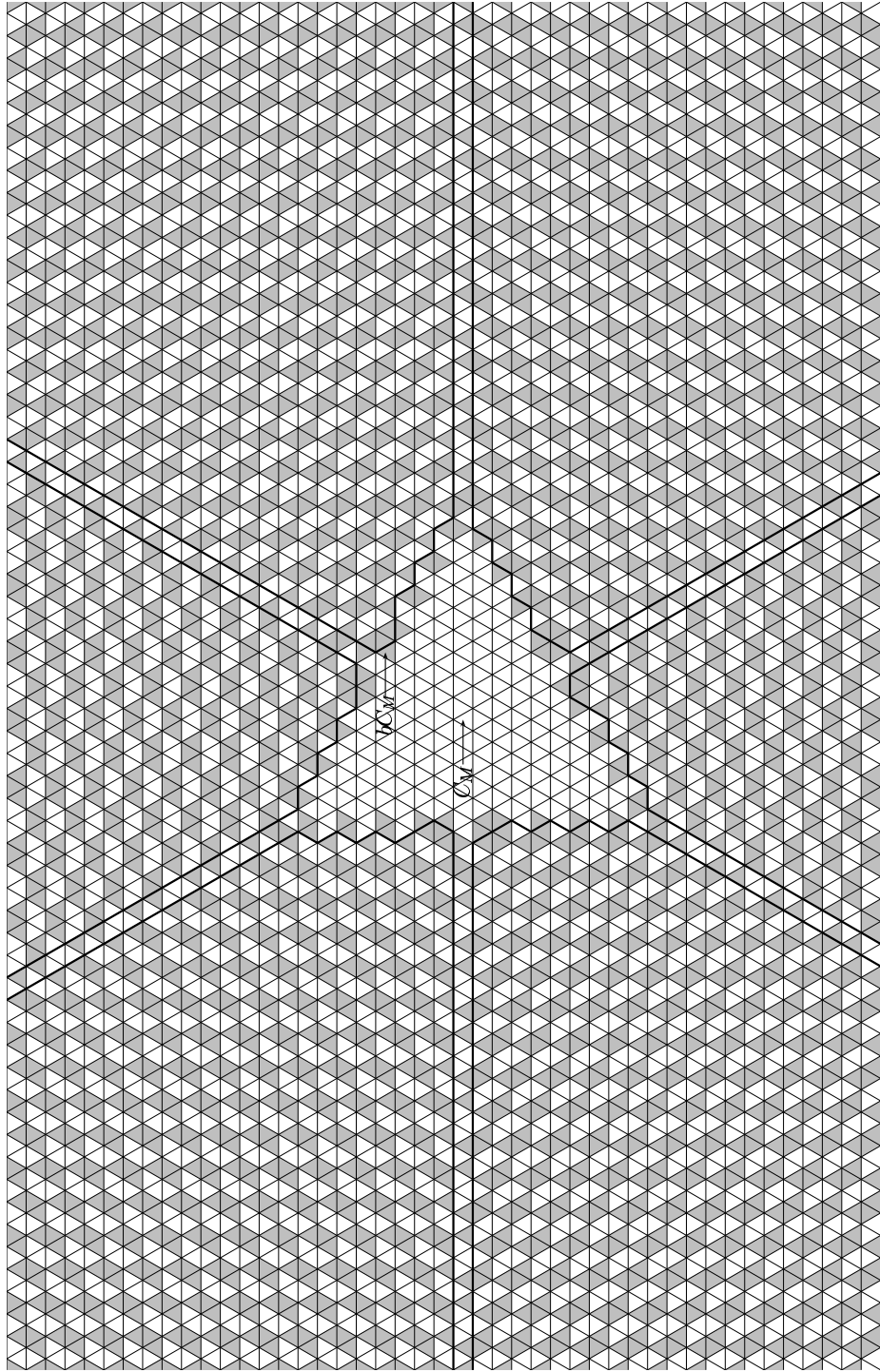


Figure 3.25: Result for  $\alpha = 2, \beta = 1$



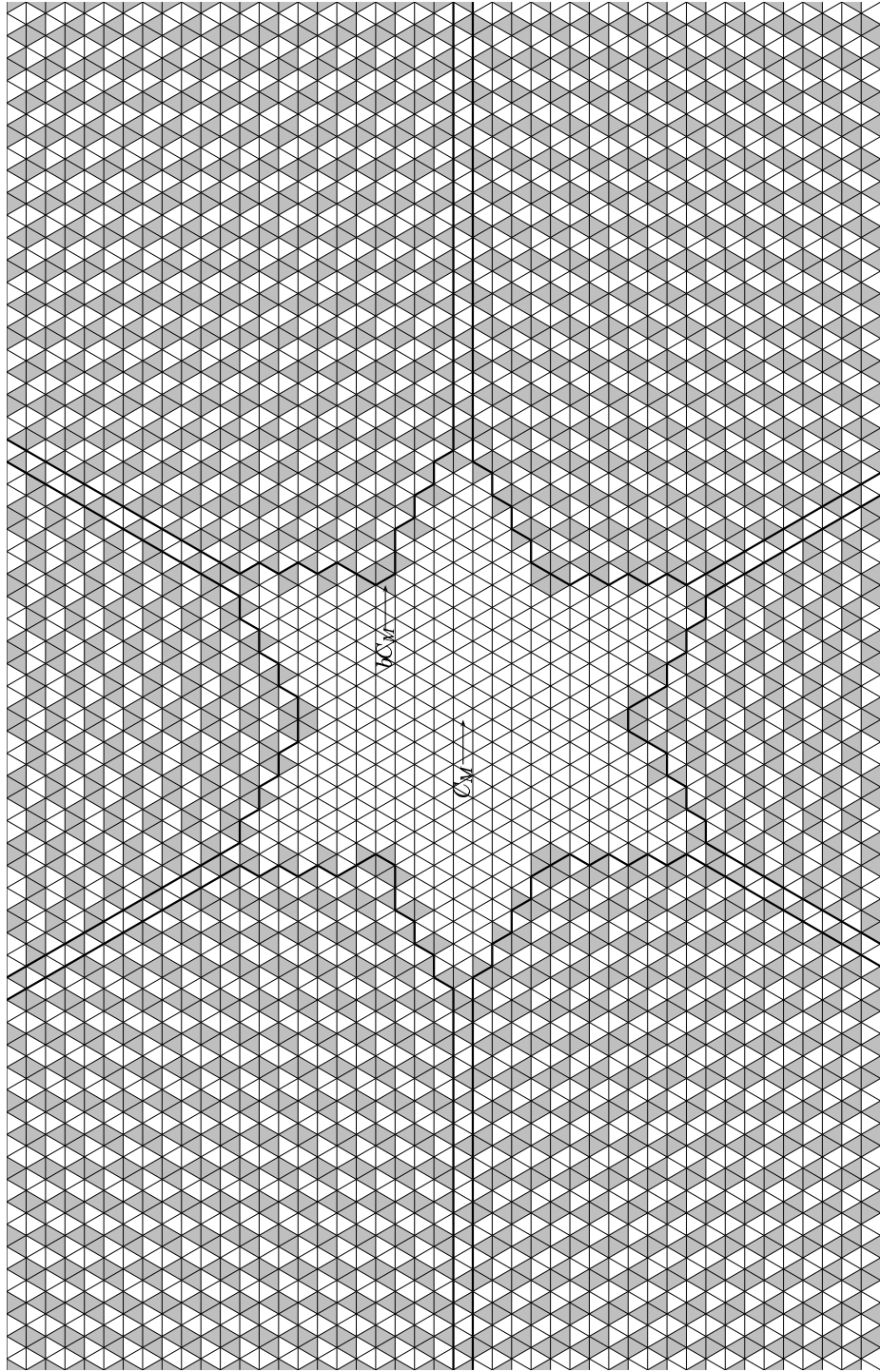


Figure 3.26: Result for  $\alpha = 4, \beta = 0$

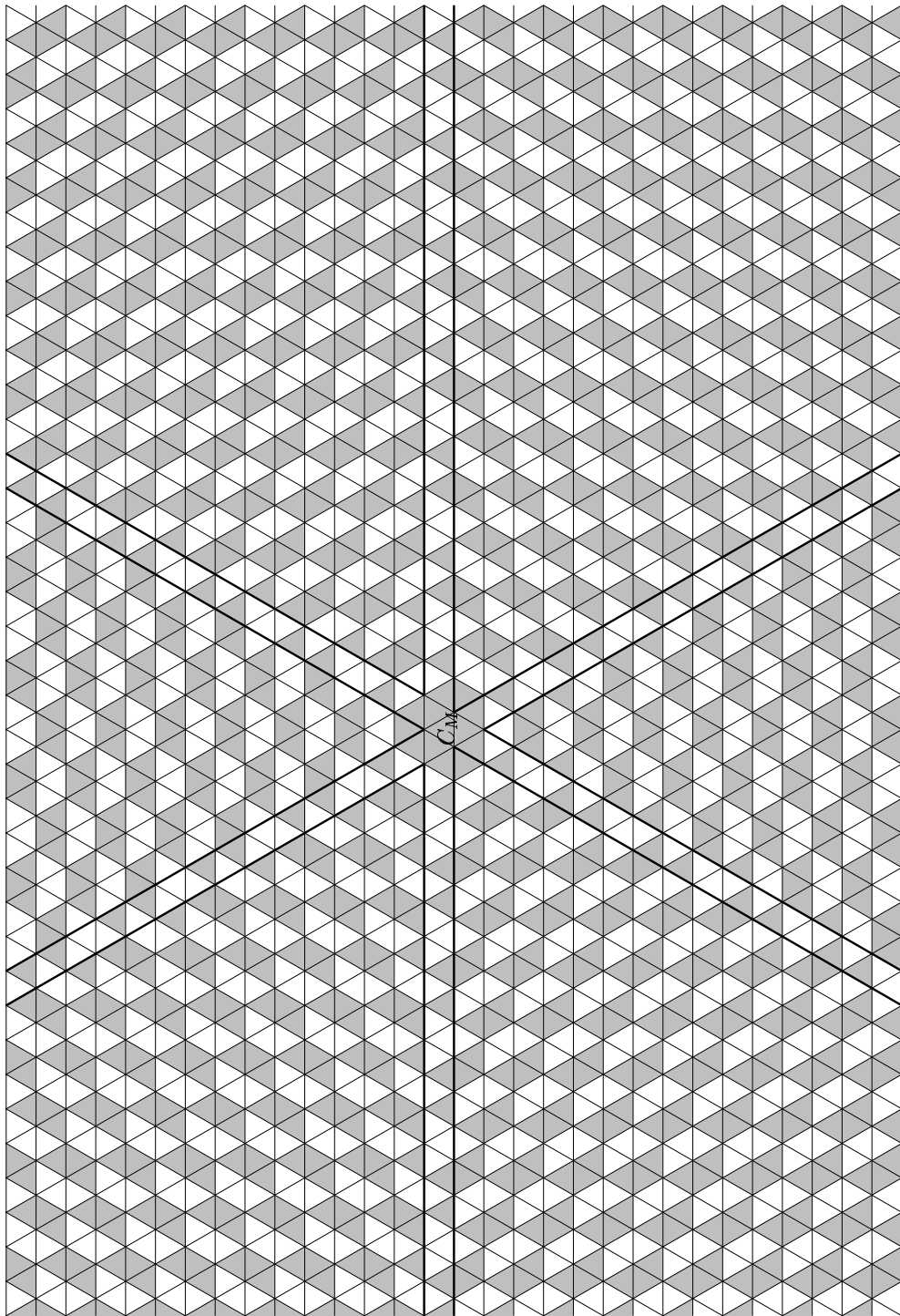


Figure 3.27: Result for  $b = 1$

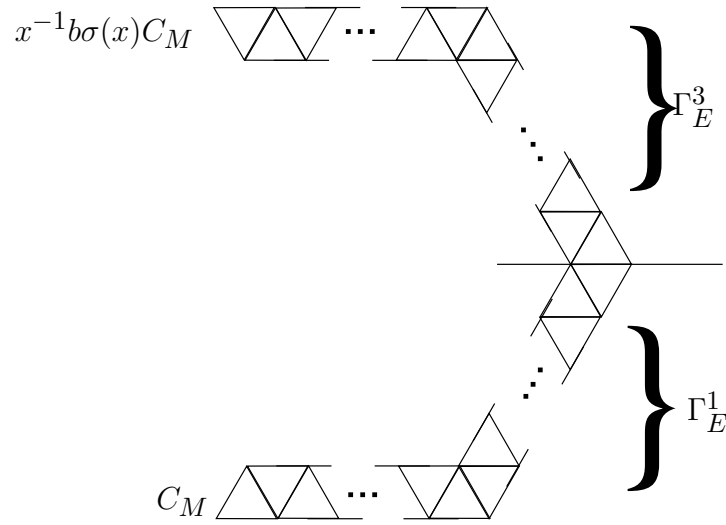


Figure 3.28: General shape of composite galleries for  $b = 1, w = f, I_1$

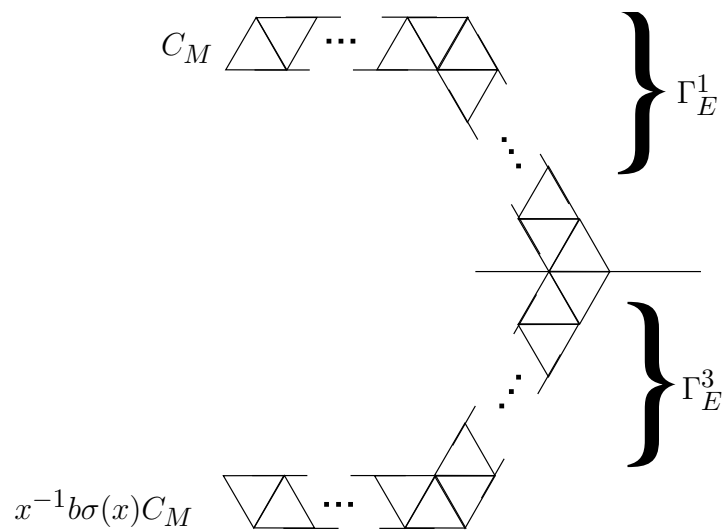


Figure 3.29: General shape of composite galleries for  $b = 1, w = 1, I_1$

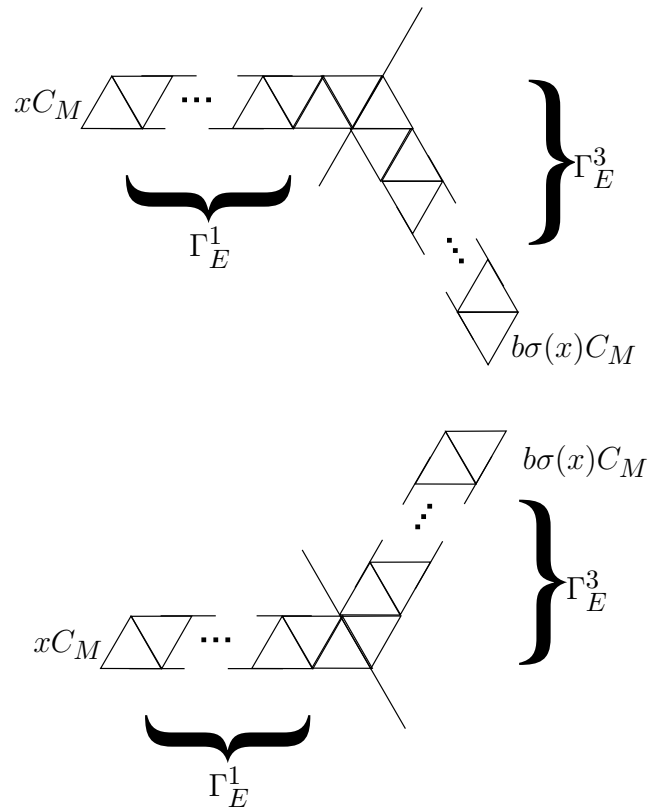


Figure 3.30: General shapes of composite galleries for  $b = 1$ ,  $w = 1$ ,  $I_2$



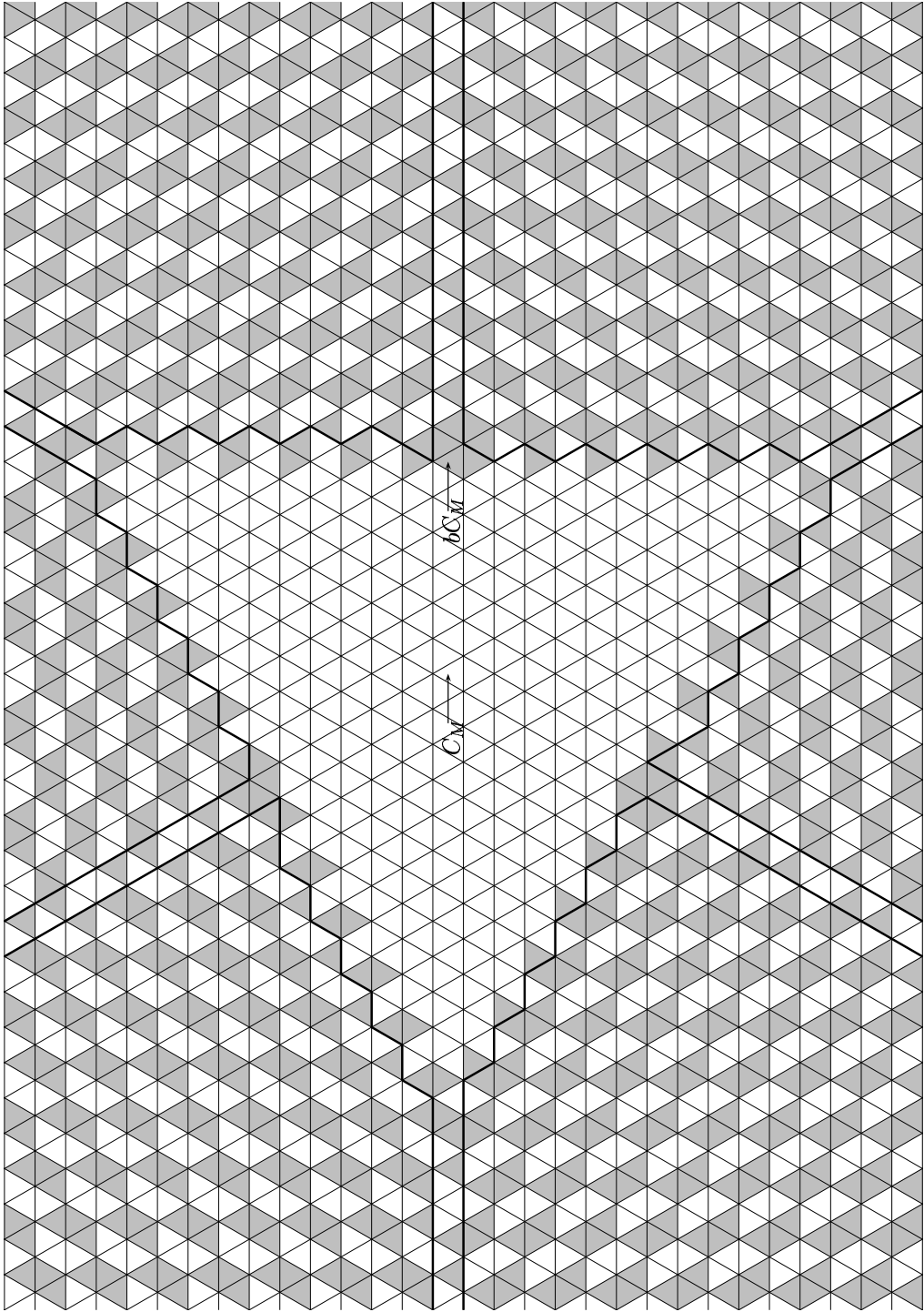
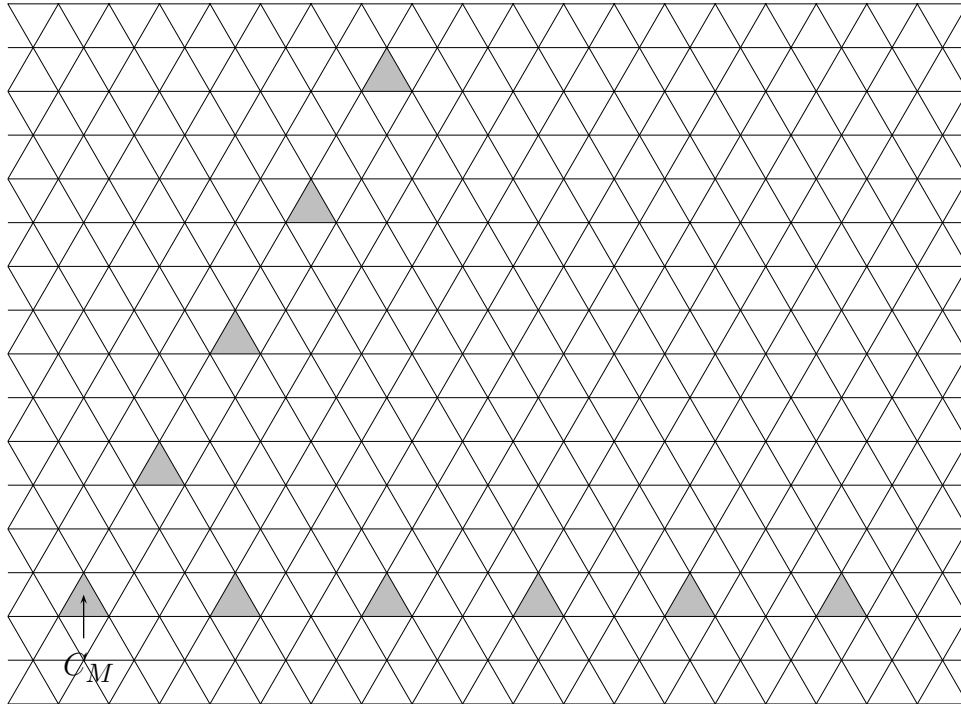


Figure 3.31: Result for  $\alpha = 4$ ,  $\beta = -2$

Figure 3.32:  $bC_M$  for degenerate  $b$ 

The general shapes of composite galleries for  $b \neq 1$ ,  $\alpha + 2\beta = 0$ ,  $(t, e) \in I_1$  are pictured in Figure 3.33 for  $w = f$  and Figure 3.34 for  $w = 1$ . The composite galleries for  $I_2$  in these cases are similar enough in general shape to those of non-degenerate  $b$  that folding considerations are essentially the same.

In the case that  $\alpha + 2\beta = 2\alpha + \beta$ ,  $b \neq 1$ , the composite galleries for  $I_2$  become different in general shape from those of non-degenerate  $b$ , but those for  $I_1$  are similar.

Even though the general shape of composite galleries is different in each of the four categories:  $b$  non-degenerate,  $b = 1$ ,  $\alpha + 2\beta = 0$  but  $b \neq 1$ ,  $\alpha + 2\beta = 2\alpha + \beta$  but  $b \neq 1$ , there is an efficient way of computing the folding results of these galleries that turns out to be very similar in all four cases. This efficient method is somewhat different from that used previously to compute the  $\alpha = 3$ ,  $\beta = -1$  example (although the efficient method will also apply to that example), and will be described in Section 3.1.3.

The lines superimposed on the patterns in Figures 3.23, 3.24, 3.25, 3.26, 3.27, and 3.31 are only there to make the patterns easier to view and to compare. The chambers which are shaded more darkly in Figure 3.23 are the chambers  $w^{-1}bwC_M$  for  $w \in W$ . These are not shaded on the other figures because one can tell where they are by analogy (or by an easy computation). Note that for Figure 3.27 and Figure 3.31, some of the  $w^{-1}bwC_M$  are equal to each other. These are degenerate cases, and will be discussed further in Section 3.1.3.

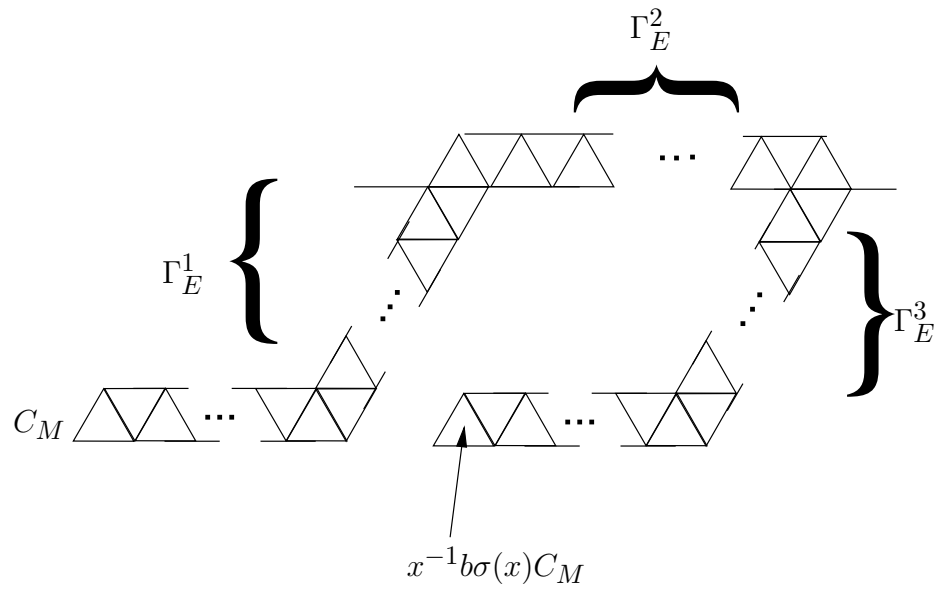


Figure 3.33: General shape of composite galleries for  $b \neq 1$  with  $\alpha + 2\beta = 0$ ,  $w = f$ ,  $I_1$

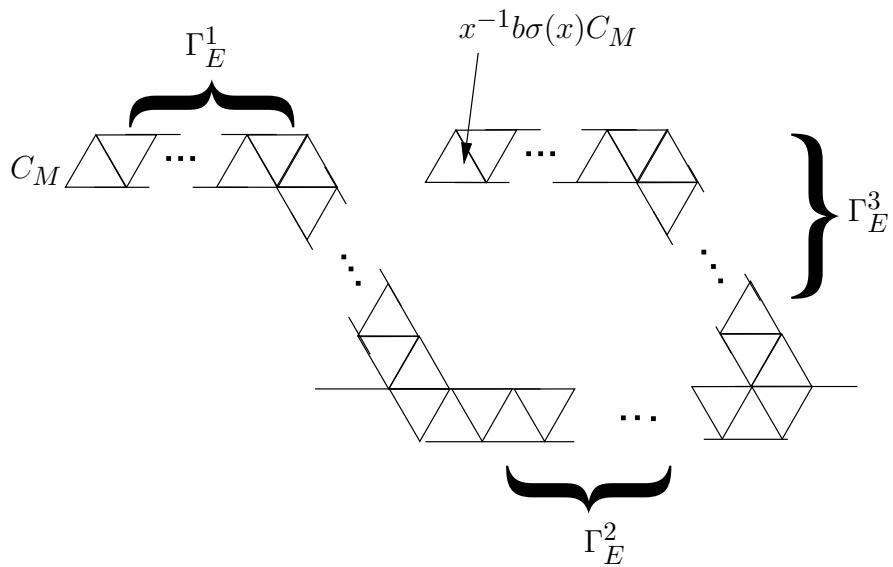


Figure 3.34: General shape of composite galleries for  $b \neq 1$  with  $\alpha + 2\beta = 0$ ,  $w = 1$ ,  $I_1$

It is reasonable to expect that other infinite classes would not contribute further to the results in Figures 3.24, 3.25, or 3.26, and 3.31 as they do not contribute further to the results in Figures 3.23 and 3.27.

It is easy to generalize what the results of classes  $I_1$  and  $I_2$  would be for any of the  $b$  we are working with (listed in the beginning of Section 3.1). This will also be done in detail in Section 3.1.3. Since the computations involved in discovering the total result of all infinite classes of type-edge pairs are very lengthy for any given  $b$ , no computation general to all  $b$  has been done. It seems very reasonable that in any case the total results would be the same as the  $I_1$  and  $I_2$  results together, as mentioned previously.

### 3.1.3 Relationship Between $X_w(1\sigma)$ and $X_w(b\sigma)$ , and an Efficient Way of Computing Supersets

In this section we try to illuminate the cause of some of the similarities among the supersets  $S_1$  for different values of  $b$ . We do this by discussing a more efficient method of computing the infinite classes  $I_1$  and  $I_2$  that were computed in Section 3.1.2. The basic idea is as follows. Let  $\Gamma_{E_1}$  and  $\Gamma_{E_2}$  be two composite galleries (constructed in Section 3.1.1) that need to be folded in order to compute one of the supersets of Section 3.1.2. Let  $p_i$  for  $i = 1, 2$  be the number of chambers appearing in  $\Gamma_{E_i}^1$  between the edge of departure and the turning edge, let  $q_i$  for  $i = 1, 2$  be the number of chambers appearing in  $\Gamma_{E_i}^1$  after the turning edge, and let  $w_i$  for  $i = 1, 2$  be elements of  $W$  such that  $a_i w_i C_M = \rho(E_i)$  for some  $a_i \in T(F)$ . If  $p_1 = p_2$  and  $w_1 = w_2$ , then the folding results of  $\Gamma_{E_1}$  and  $\Gamma_{E_2}$  can be computed in very similar ways. In fact, for most fixed values of  $p_1 = p_2$ , for any fixed values of  $w_1 = w_2$ , and for most  $b$ , one can compute folding results for arbitrary  $q_i$  all at once. This is done by replacing all the composite galleries with the given  $p$  and  $w$  with a single “half-infinite gallery” which one can show in advance will have the same folding results as all these composite galleries together. The folding results of the “half-infinite gallery” are easy to compute.

At the end of Section 3.1.1 we defined the *transition type* between two chambers that share an edge, and the *type* of a non-stuttering gallery  $G$  in  $\mathcal{B}_\infty$ . We also need the following definitions.

**Definition 3.1.3.** A *finite gallery type* is, equivalently,

- 1) An initial chamber  $C_0 \subseteq A_M$  and a finite sequence of transition types, which we will call  $\{t_1, t_2, \dots, n\}$
- 2) A non-stuttering finite gallery in  $A_M$ .

**Definition 3.1.4.** A *left-infinite gallery type* is, equivalently,

- 1) A terminal chamber  $C_0 \subseteq A_M$  and a left-infinite sequence  $\{\dots, t_{-3}, t_{-2}, t_{-1}, t_0\}$  of transition types.
- 2) A left-infinite non-stuttering gallery in  $A_M$ .

Let  $\{C_M; t_1, t_2, \dots, t_n\}$  be a finite gallery type whose initial gallery is  $C_M$ . Let  $C_M = C_0, C_1, \dots, C_n$  be the corresponding non-stuttering gallery in  $A_M$ . We call this the *standard folding* of the gallery type  $\{C_M; t_1, t_2, \dots, t_n\}$ . There are *non-standard foldings* of  $\{C_M; t_1, t_2, \dots, t_n\}$  determined as follows. We first assume inductively that  $C_i$  is determined. Note that the base case,  $C_0 = C_M$  actually is determined. Then let  $L_{i+1}$  be the wall containing the edge of  $C_i$  that does not contain the vertex of type  $t_{i+1}$ . If  $C_M$  and  $C_i$  are on the same side of  $L_{i+1}$ , then let  $C_{i+1}$  be the reflection of  $C_i$  about  $L_{i+1}$ . If  $C_M$  and  $C_i$  are on opposite sides of  $L_{i+1}$ , then let  $C_{i+1}$  be either  $C_i$  itself, or the reflection of  $C_i$  about  $L_{i+1}$ . The choices that arise in this process may lead to many different non-standard foldings of  $\{C_M; t_1, t_2, \dots, t_n\}$ .

**Definition 3.1.5.** The *folding results* of  $\{C_M; t_1, t_2, \dots, t_n\}$  are the collection of possible final chambers  $C_n$  that can arise from all possible (standard and non-standard) foldings of  $\{C_M; t_1, \dots, t_n\}$ .

We now let  $\{\dots, t_{-3}, t_{-2}, t_{-1}, t_0; C_0\}$  be a left-infinite gallery type, and we let  $\{\dots, C_{-3}, C_{-2}, C_{-1}, C_0\}$  be the corresponding non-stuttering gallery in  $A_M$ . Then it is easy to see that for any  $n$ ,  $\{C_{-n}; t_{-n+1}, t_{-n+2}, \dots, t_0\}$  is a finite gallery type. Let  $R_n$  be the folding results of this finite gallery type. Let  $R = \cup_{n=1}^{\infty} R_n$ . We call  $R$  the *folding results* of  $\{\dots, t_{-3}, t_{-2}, t_{-1}, t_0; C_0\}$ .

Each type-edge pair  $(t, e) \in I_1 \cup I_2$  gives  $\Gamma_x$  a composite gallery, and the folding results of that type-edge pair,  $S_{(t,e)}$  are the folding results of the finite gallery type that  $\Gamma_x$  represents. In fact, we frequently have  $S_{(t_1, e_1)} = S_{(t_2, e_2)}$  for  $(t_1, e_1) \neq (t_2, e_2)$ . If  $(t, e) \in I_1$ , then there are three characteristics of  $(t, e)$  that are clearly relevant to the type of  $x^{-1}\Gamma_x$ , and therefore relevant to  $S_{(t,e)}$ . First, the number  $p$  of chambers between  $e$  and the turning edge of  $t$  will have significance. Second, the number  $q$  of chambers after the turning edge of  $t$  will have significance. And third, the Weyl group element  $w \in W$  such that  $awC_M = C_n$  will have significance, where  $a$  is a diagonal matrix, and  $C_n$  is the last chamber of  $t$ . It is easy to see that if  $p_{(t_1, e_1)} = p_{(t_2, e_2)}$ ,  $q_{(t_1, e_1)} = q_{(t_2, e_2)}$ , and  $w_{(t_1, e_1)} = w_{(t_2, e_2)}$  then  $S_{(t_1, e_1)} = S_{(t_2, e_2)}$ , for  $(t_i, e_i) \in I_1$ . Let  $R_{p,q,w}^1$  be this set.

For  $(t, e) \in I_2$ , we only have  $q$ , the number of chambers after  $e$  in  $t$ ; and  $w$ . If  $q_{(t_1, e_1)} = q_{(t_2, e_2)}$ , and  $w_{(t_1, e_1)} = w_{(t_2, e_2)}$  for  $(t_i, e_i) \in I_2$ , then  $S_{(t_1, e_1)} = S_{(t_2, e_2)}$ . Let  $R_{q,w}^2$  be this set.

For fixed  $p, w$ , let  $R_{p,w}^1 = \cup_q R_{p,q,w}^1$ , and for fixed  $w$  let  $R_w^2 = \cup_q R_{q,w}^2$ . We will show that  $R_{p,w}^1$  and  $R_w^2$  can usually be computed as the folding results of some half-infinite gallery type. Let  $r \in W$  be rotation by  $120^\circ$  counterclockwise, and let  $f \in W$  be the reflection about the horizontal line through  $v_M$ . For  $b$  with  $\alpha + 2\beta > 0$ , and given  $p \geq 1$  odd, we define  $\Omega_1^2, \Omega_f^2, \Omega_{p,1}^1$  and  $\Omega_{p,f}^1$  to be the half-infinite galleries shown in Figure 3.35 (This figure shows the specified half-infinite galleries for a particular choice of  $b$ , namely  $\alpha = 4$  and  $\beta = -1$ . But it is clear how the definition would

work for other  $b$  with  $\alpha + 2\beta > 0$ .) The half-infinite galleries  $\Omega_r^2$ ,  $\Omega_{rf}^2$ ,  $\Omega_{p,r}^1$  and  $\Omega_{p,rf}^1$  are rotations of those in Figure 3.35 by  $240^\circ$  counterclockwise about the center point of  $C_M$ , and  $\Omega_{r^2}^2$ ,  $\Omega_{r^2f}^2$ ,  $\Omega_{p,r^2}^1$  and  $\Omega_{p,r^2f}^1$  are rotations of those in Figure 3.35 by  $120^\circ$  counterclockwise about the center point of  $C_M$ . If  $\alpha + 2\beta = 0$  then  $\Omega_r^2 = \Omega_{rf}^2$ ,  $\Omega_r^2 = \Omega_{rf}^2$ , and  $\Omega_{r^2}^2 = \Omega_{r^2f}^2$  (the picture would be a degenerate version of Figure 3.35).

**Proposition 3.1.2.** If  $\alpha + 2\beta > 0$  or  $b = 1$ , then  $R_{p,w}^1$  is the folding results of  $\Omega_{p,w}^1$ , and  $R_w^2$  is the folding results of  $\Omega_w^2$ . If  $\alpha + 2\beta = 0$  and  $b \neq 1$ , then  $(\cup_p R_{p,w}^1) \cup R_w^2$  is the union of the folding results of the  $\Omega_{p,w}^1$  for all  $p$ , and the folding results of  $\Omega_w^2$ . It is still true that  $R_w^2$  is the folding results of  $\Omega_w^2$ .

Before we prove this proposition, we establish some more terminology. We first let  $\{C_M; t_1, t_2, \dots, t_n\}$  be a finite gallery type. Let  $C_0 = C_M, C_1, \dots, C_m$  be a (standard or non-standard) folding of the sub-gallery type  $\{C_M; t_1, t_2, \dots, t_m\}$ , where  $m < n$ . Consider the finite gallery type  $\{C_m; t_{m+1}, \dots, t_n\}$ , and let  $C_m = D_m, D_{m+1}, D_{m+2}, \dots, D_n$  be the standard folding. If  $D_{m+j}$ , for  $1 \leq j \leq n - m$  is on the same side of the edge between  $D_{m+j}$  and  $D_{m+j-1}$  as  $C_M$ , then we say  $m + j$  is a *choice point given the history*  $C_M, C_1, \dots, C_m$ . Note that this all applies even if  $m = 0$ . Also note that if  $1 \leq k \leq n$ , then  $k$  could be a choice point given some histories, but not given others. We now prove the proposition.

*Proof.* It suffices to consider  $w = 1$  and  $w = f$ . In fact, we will only consider  $w = 1$ , since the  $w = f$  case is similar. We first assume that  $\alpha + 2\beta > 0$  or  $b = 1$ , and that  $(t, e) \in I_1$ . Suppose  $x \in SL_3(L)$  has SMG with type  $t$  and edge of departure  $e$ . Also suppose  $(t, e)$  has characteristics  $p, q$ , and  $w = 1$ . Let  $\Gamma_x$  be the composite gallery. So in the notation of Section 3.1.1,  $\Gamma_x = \Gamma_E^1 \cup \Gamma_E^2 \cup \Gamma_E^3$ , where  $E = xC_M$ . Consider the choice points given history  $C_M = C_0$ . These all lie in  $\Gamma_E^3$ , because of the shape of  $\Gamma_x$  (illustrated for  $\alpha = 3, \beta = -1, q = 11$  and  $p = 7$  in Figure 3.3). The choice points given history  $C_M = C_0$  for the same  $b$  and  $x$  that were used in Figure 3.3 are illustrated in Figure 3.36. Note that  $\Omega_{p,1}^1$  ends at the same chamber that the standard folding of  $\Gamma_x$  ends at, and note that the choice points in  $\Gamma_x$  that are after or at the turning edge of  $\Gamma_E^3$  are also choice points in  $\Omega_{p,1}^1$ . This is illustrated for the example  $\alpha = 3, \beta = -1, w = 1, p = 7$  and  $q = 11$  in Figure 3.37. Note also that if  $i$  is a choice point in  $\Gamma_E^3$  that occurs before the turning edge of  $\Gamma_E^3$ , and if  $L_i$  is the wall containing the edge corresponding to  $i$ , then  $L_i$  also passes through  $\Omega_{p,1}^1$ . Reflecting the section of  $\Gamma_E^3$  that occurs after  $i$  about  $L_i$  gives rise to a finite gallery type with no choice edges additional to those obtained by reflecting the portion of  $\Omega_{p,1}^1$  that occurs after  $L_i$  about  $L_i$ . This is illustrated in Figure 3.38. Therefore, the folding results of  $\Omega_{p,1}^1$  contain  $R_{p,1}^1$ .

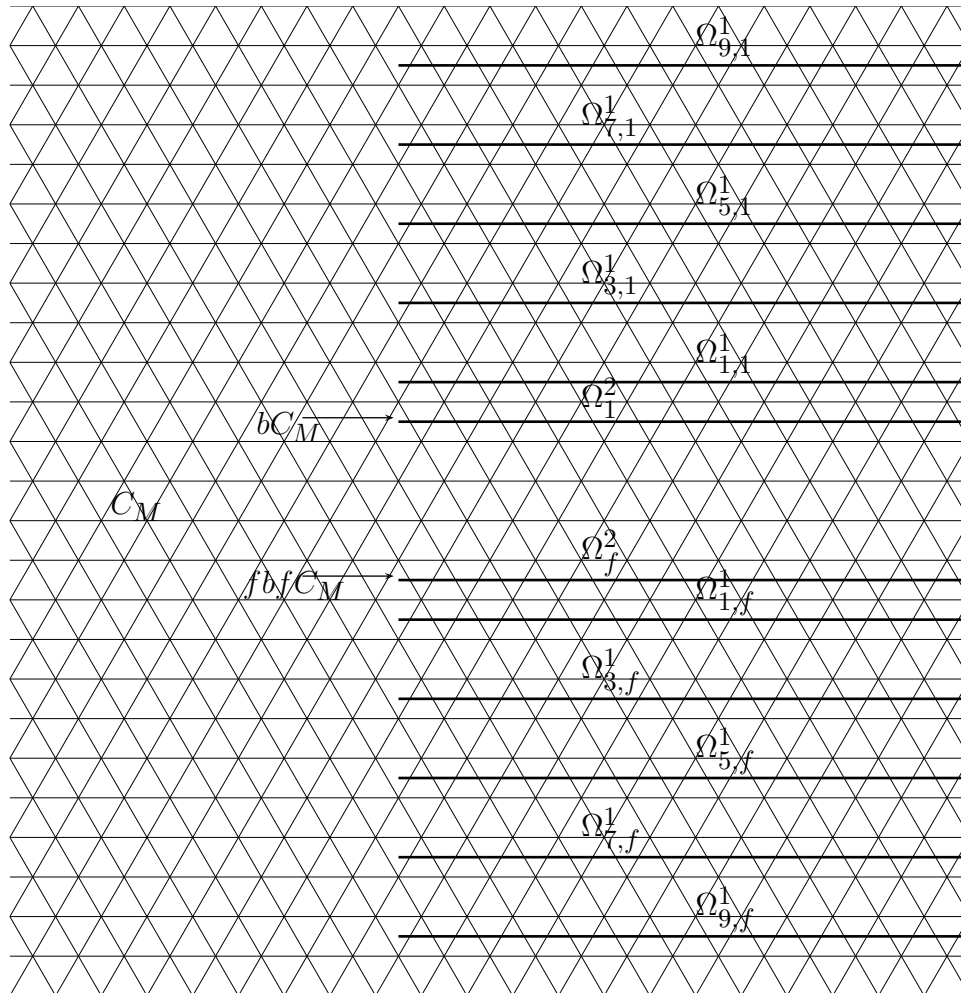


Figure 3.35:  $\Omega_1^2$ ,  $\Omega_f^2$ ,  $\Omega_{p,1}^1$  and  $\Omega_{p,f}^1$

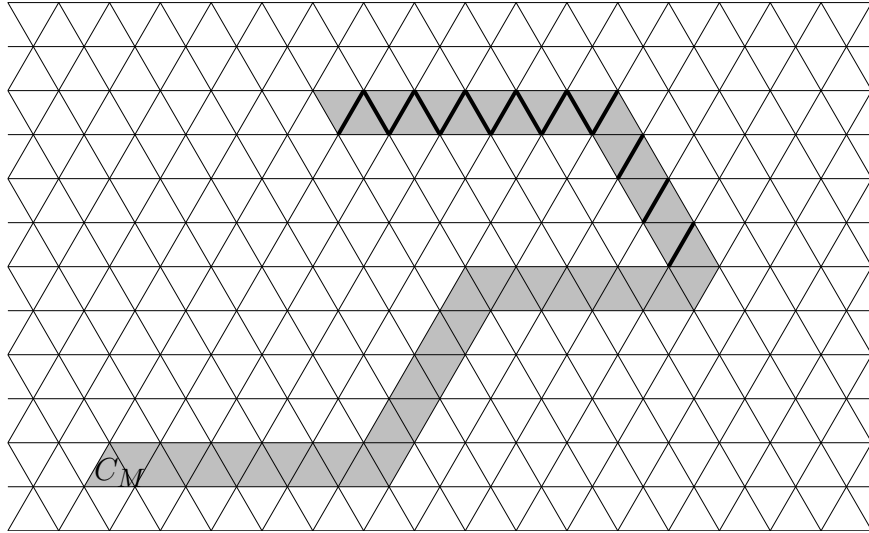


Figure 3.36: Choice points for a sample composite gallery

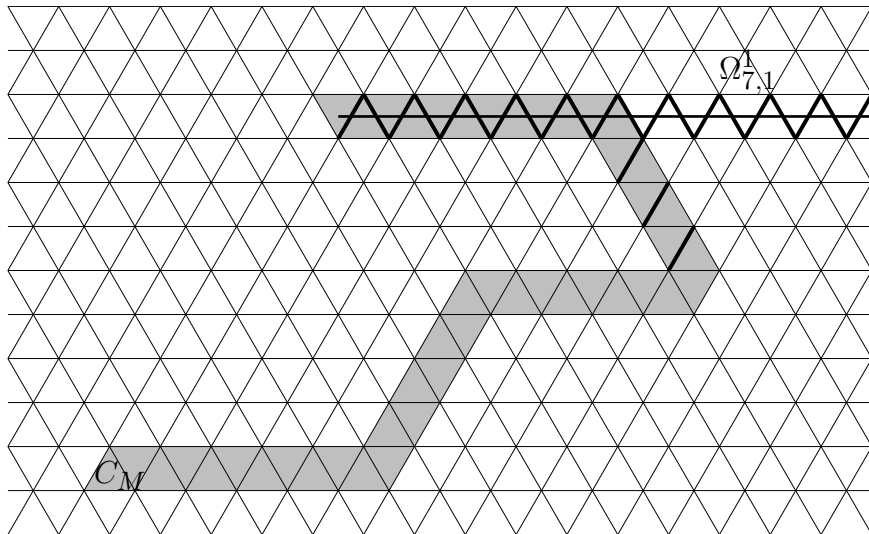


Figure 3.37: Choice points for  $\Omega_{p,1}^1$  and  $\Gamma_x$



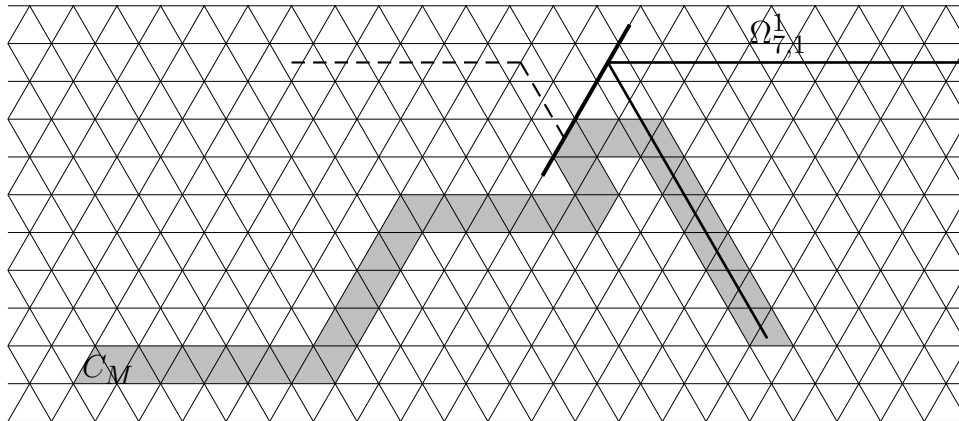


Figure 3.38: How to address choice points of  $\Gamma_x$  that occur before the turning point of  $\Gamma_E^3$

We must now show that  $R_{p,1}^1$  contains the folding results of  $\Omega_{p,1}^1$ . It suffices to show that every choice point in  $\Omega_{p,1}^1$  is also a choice point in some  $\Gamma_x$  for some  $x C_M$  with type-edge pair having characteristics  $p$ ,  $w = 1$ , and some  $q$ . But this can be accomplished by letting  $q$  get arbitrarily large.

To see that  $R_1^2$  is the folding result of  $\Omega_1^2$  for  $\alpha + 2\beta \neq 2\alpha + \beta$  or for  $b = 1$ , proceed as follows. First note that  $\Gamma_x$  for  $x$  with  $p = 0$  is minimal, and the final gallery of  $\rho(x^{-1}\Gamma_x)$  is  $b C_M$ . This is also the final gallery of the standard folding of  $\Omega_1^2$ . Then let the chambers in the standard folding of  $\Omega_1^2$  be called  $\{\dots, D_3, D_2, D_1\}$ , where  $D_1 = b C_M$ . Let the wall between  $D_i$  and  $D_{i+1}$  be called  $L_i$ . Let  $G_i$  be the left-infinite gallery in  $A_M$  that one gets by reflecting the chambers  $D_j$  for  $j \leq i$  across  $L_i$ . Note that if  $p \geq 1$ , the only choice points in  $\Gamma_x$  are duplicated in  $G_p$ . This shows that  $R_1^2$  is equal to the set of folding results of  $\Omega_1^2$ .

The  $\alpha + 2\beta = 0$  for  $b \neq 1$ ,  $(t, e) \in I_1$  case is more complicated, but makes use of the same ideas, and is therefore omitted. The  $2\alpha + \beta = \alpha + 2\beta$  case for  $b \neq 1$ ,  $(t, e) \in I_2$  is omitted for the same reason.  $\square$

This gives a more efficient way to compute the folding results of all the type-edge pairs in  $I_1 \cup I_2$  for any fixed  $b$ , and also illustrates, to some extent, the source of the similarity between the sets  $S_1$  for different values of  $b$ .

### 3.1.4 A Method Suggested by Rapoport and Kottwitz

The set  $S_1$  of chambers in  $A_M$  is, *a priori*, only a superset of the solution set  $S$  that we are seeking. In this section we give the results of a methodology suggested by Rapoport and Kottwitz for producing a subset  $S_2 \subseteq S$ . In other words, this method will show that certain chambers in  $A_M$  must be contained in  $S$ .

The method in this section is only effective in the case  $b = 1$ . In this case, techniques that will be described in the next section will serve to enlarge  $S_2$  to the point that it becomes equal to  $S_1$ , and therefore to  $S$ . In the  $b \neq 1$  cases, we will use other methods to arrive at a subset  $S_2$  (see Section 3.1.6).

Let  $a \in SL_3(F)$  be of the form

$$a = \begin{pmatrix} \pi^m & 0 & 0 \\ 0 & \pi^n & 0 \\ 0 & 0 & \pi^{-m-n} \end{pmatrix},$$

where there are no conditions on  $m$  and  $n$ . Let  $w$  be one of the following matrices:

$$r = \begin{pmatrix} 0 & 0 & 1 \\ 1 & 0 & 0 \\ 0 & 1 & 0 \end{pmatrix} \quad ; \quad r^2 = \begin{pmatrix} 0 & 1 & 0 \\ 0 & 0 & 1 \\ 1 & 0 & 0 \end{pmatrix}.$$

Therefore,  $w$  represents a 3-cycle in  $W$ , the finite Weyl group. According to a result of Kottwitz, the matrix  $aw$  belongs to a *basic*  $\sigma$ -conjugacy class if there is some  $l$  such that  $aw\sigma(aw)\sigma^2(aw)\dots\sigma^{l-1}(aw)$  is central in  $SL_3(L)$  [6], [7]. See [6] and [7] for a definition of *basic*, but for the present considerations, one only needs to know that the  $\sigma$ -conjugacy class containing  $b = 1$  is the only basic  $\sigma$ -conjugacy class of  $SL_3(L)$ .

**Lemma 3.1.3.** There exists an  $l$  such that  $aw\sigma(aw)\sigma^2(aw)\dots\sigma^{l-1}(aw)$  is central for any choice of  $m, n$ .

*Proof.* First we note that  $\sigma(aw) = aw$ , since  $aw \in SL_3(F)$ . So we want to show that  $(aw)^l$  is central for some  $l$ . But

$$\begin{aligned} (aw)^l &= awaw(aw)^{l-2} \\ &= awaw^{-1}w^2(aw)^{l-2} \\ &= aa^w w^2(aw)^{l-2}, \end{aligned}$$

where the superscript  $w$  denotes  $w$  acting on  $a$  by conjugation. Proceeding, we have

$$\begin{aligned} aa^w w^2(aw)^{l-2} &= aa^w w^2 aw(aw)^{l-3} \\ &= aa^w w^2 aw^{-2} w^3(aw)^{l-3} \\ &= aa^w a^{w^2} w^3(aw)^{l-3} \\ &= \dots \\ &= aa^w a^{w^2} a^{w^3} \dots a^{w^{l-1}} w^l. \end{aligned}$$

Choosing  $l = 3$ , we get  $aa^w a^{w^2} w^3 = 1$ , which is central.

Since  $w$  is a 3-cycle, conjugating by  $w$  serves to permute the diagonal entries of  $a$  in a cyclic way. This is why  $aa^w a^{w^2} w^3$  is central.  $\square$

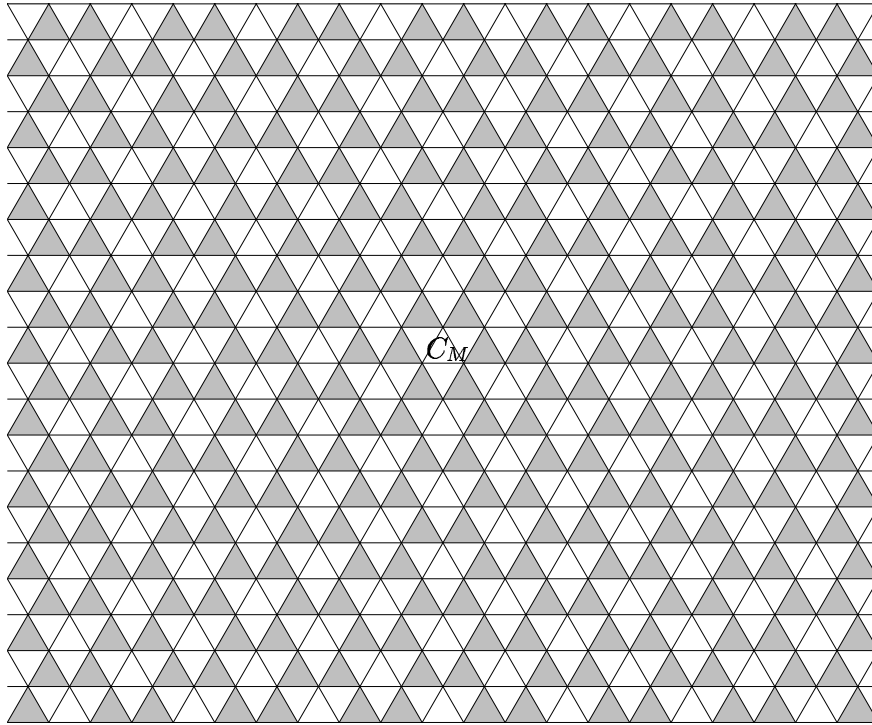


Figure 3.39: Main results of the method suggested by Rapoport and Kottwitz

So the matrices  $aw$  are in the  $\sigma$ -conjugacy class of 1 for any choice of  $m, n$ . Therefore, the double- $I$ -cosets  $\{IawI : m, n \in \mathbb{Z}\}$  all meet the identity  $\sigma$ -conjugacy class non-trivially. These double- $I$ -cosets are pictured in Figure 3.39.

With certain conditions on  $m$  and  $n$ , it is also possible for  $(aw)^l$  to be central for some  $l$  if  $w$  is not a 3-cycle in  $W$ :

**Lemma 3.1.4.** If  $a = 1$  then there exists  $l$  such that  $(aw)^l$  is central for any  $w \in W$ .

*Proof.* Take  $l = 6$ . □

The implication of this is that the double- $I$ -cosets corresponding to the chambers in Figure 3.40 all intersect the  $\sigma$ -conjugacy class of 1. Let  $f$  be as in Section 3.1.2.

**Lemma 3.1.5.** If  $m = 0$  then  $aa^w = 1$  for  $w = f$ . If  $m = -n$  then  $aa^w = 1$  for  $w = rf$ . If  $n = 0$  then  $aa^w = 1$  for  $w = r^2f$ .

*Proof.* Just compute the relevant matrix products. □

The implication of this lemma is that the double- $I$ -cosets corresponding to the chambers in Figure 3.41 all intersect the  $\sigma$ -conjugacy class of 1. Note, in addition, that we have a concrete element of the intersection of each of these double- $I$ -cosets with  $\{x^{-1}\sigma(x) : x \in SL_3(L)\}$ .

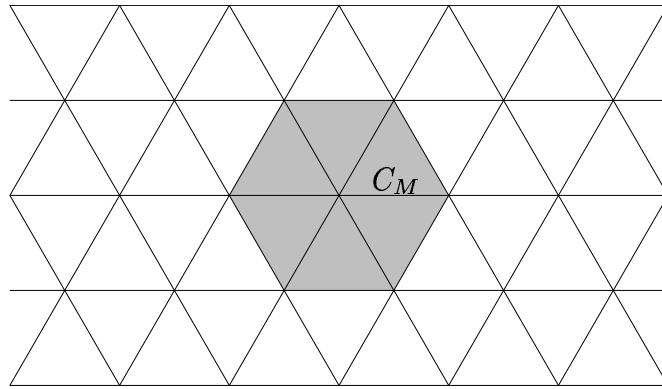


Figure 3.40: The  $a = 1$  results of the method suggested by Rapoport and Kottwitz

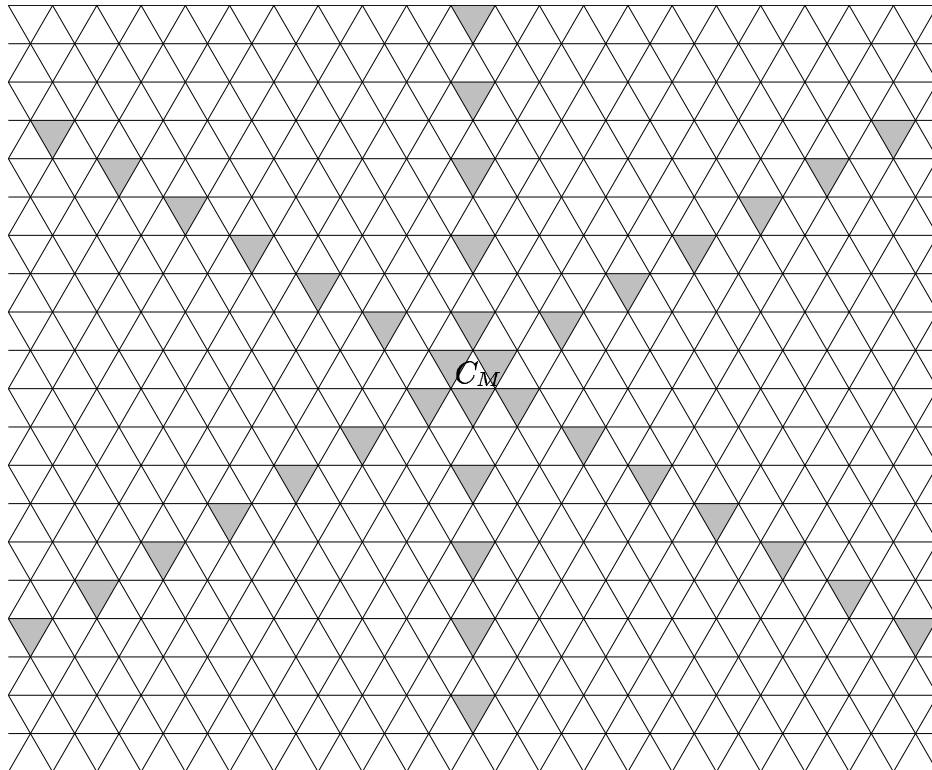
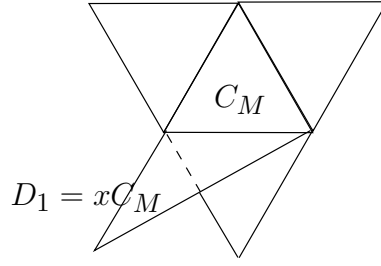


Figure 3.41: Results from the method suggested by Rapoport and Kottwitz under the circumstances of Lemma 3.1.5

Figure 3.42: The choice  $D_1$  of  $xC_M$ 

It is easy to see that  $(aw)^l$  is not central for any  $l$ , unless we are in one of the cases enumerated above.

It is clear how one would go about formulating and proving the lemmas of this section for  $SL_n$ . One would get results for every possible cycle decomposition in  $W = S_n$ , and the “most” result chambers ( $\mathbb{Z}^{n-1}$  worth of them) would arise from the  $n$ -cycles, since then  $a$  is allowed to be arbitrary. At the other end of the spectrum, the finitely many Weyl group images of the main chamber arise from  $a = 1$ . In subsequent sections, the results from this section will also be generalized to  $Sp_{2n}$  and  $G_2$ .

### 3.1.5 A Subset of the Solution Set for $b = 1$

Let  $S_2$  be the collection of all double- $I$ -cosets shown in the previous section to meet  $\{x^{-1}\sigma(x) : x \in SL_3(L)\}$ . So  $S_2$  is the union of the chambers pictured in Figures 3.39, 3.40, and 3.41. We know that  $S_2 \subseteq S \subseteq S_1$ , and in this section we enlarge  $S_2$  in such a way that it remains a subset of  $S$ . The enlarged  $S_2$  will turn out to be equal to  $S_1$ . Note that this section concerns itself only with  $b = 1$ .

Let  $w \in SL_3(L)$  be one of the matrices  $r, r^2$  from the previous section. Let  $a$  be as in the previous section. Then we know  $\tilde{b} = aw$  is  $\sigma$ -conjugate to  $b = 1$ , so  $\{x^{-1}\sigma(x) : x \in SL_3(L)\} = \{x^{-1}\tilde{b}\sigma(x) : x \in SL_3(L)\}$ , and also  $\{Ix^{-1}\sigma(x)I : x \in SL_3(L)\} = \{Ix^{-1}\tilde{b}\sigma(x)I : x \in SL_3(L)\}$ . But we know that the chamber in  $A_M$  corresponding to  $Ix^{-1}\tilde{b}\sigma(x)I$  is  $\rho(x^{-1}\tilde{b}\sigma(x)C_M)$ . Just as in Section 3.1.1, let  $\Gamma_x^1$  be the part of the SMG from  $C_M$  to  $xC_M$  that is not in  $A_M$ , let  $\Gamma_x^3 = \tilde{b}\sigma(\Gamma_x^1)$ , and, if  $e$  is the only edge of  $\Gamma_x^1$  in  $A_M$ , let  $\Gamma_x^2$  be a minimal gallery from  $e$  to  $\tilde{b}\sigma(e) = \tilde{b}e$ . If  $\Gamma_x = \Gamma_x^1 \cup \Gamma_x^2 \cup \Gamma_x^3$ , then the possible foldings of galleries of the same type as  $x^{-1}\Gamma_x$  give possible candidates for additions to the set  $S_2$ . For some choices of  $xC_M$  there is only one possible folding of galleries of the same type as  $x^{-1}\Gamma_x$ , and the final chamber of this folding is not already in  $S_2$ . Such a situation would give an additional chamber to add to  $S_2$ .

For instance, we can choose  $xC_M$  to be the chamber in Figure 3.42 that is adjacent to  $C_M$ , but not in  $A_M$ . If  $w = r^2$  and

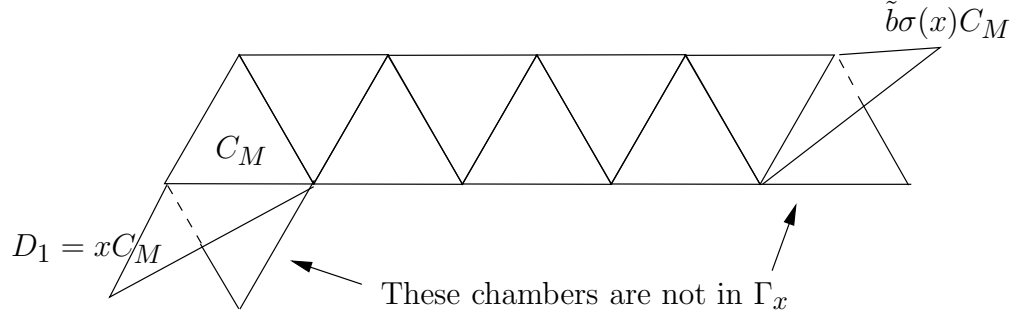


Figure 3.43: The resulting  $\Gamma_x$  for  $D_1$  and a particular choice of  $aw$

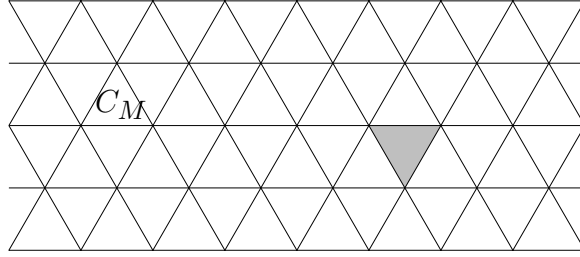


Figure 3.44: The result of folding galleries of the same type as  $x^{-1}\Gamma_x$  for the  $\Gamma_x$  pictured in Figure 3.43

$$a = \begin{pmatrix} \pi^3 & 0 & 0 \\ 0 & \pi^{-1} & 0 \\ 0 & 0 & \pi^{-2} \end{pmatrix},$$

then  $\Gamma_x$  is shown in Figure 3.43. Any gallery of the same type as  $x^{-1}\Gamma_x$  folds down into  $A_M$  in the same way, so we know that  $Ix^{-1}\tilde{b}\sigma(x)I$  corresponds to the chamber shown in Figure 3.44, which was not obtained by the methods of the previous section.

We now keep  $w$  as above, but let  $a$  take the general form

$$a = \begin{pmatrix} \pi^m & 0 & 0 \\ 0 & \pi^n & 0 \\ 0 & 0 & \pi^{-m-n} \end{pmatrix}.$$

For these  $\tilde{b} = aw$  we can compute the possible ways that galleries of the same type as  $x^{-1}\Gamma_x$  can fold into  $A_M$ , where, as before,  $x$  is chosen so that  $xC_M$  is the chamber  $D_1$  pictured in Figure 3.42. One can easily see that for each  $m, n$ , there is only one way that such galleries can fold down. The chambers obtained through this process are marked in Figure 3.45. Many of these did not arise from the methods of the previous section.

We could also choose  $x$  such that  $xC_M$  is one of the chambers  $D_2, D_3$  in Fig-

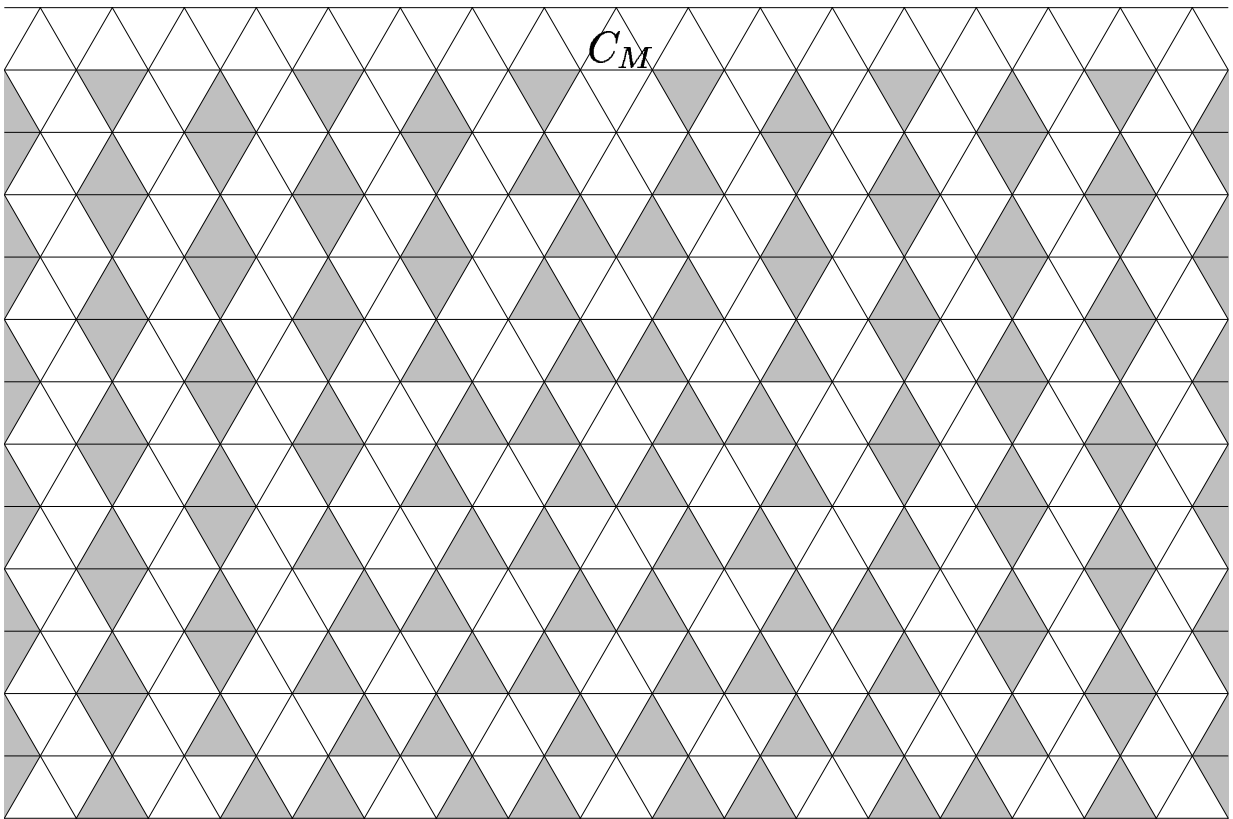
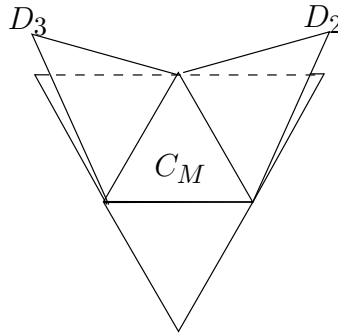


Figure 3.45: Results for  $x C_M = D_1$  and  $w = r^2$  or for  $x C_M = D_1$  and  $w = r$

Figure 3.46: The choices  $D_2$  and  $D_3$  of  $xC_M$ 

$w$	$xC_M$	Figure containing results
$r^2$	$D_1$	Figure 3.45
$r^2$	$D_2$	Figure 3.47
$r^2$	$D_3$	Figure 3.48
$r$	$D_1$	Figure 3.45
$r$	$D_2$	Figure 3.47
$r$	$D_3$	Figure 3.48

Table 3.1: Which figure contains which results

ure 3.46, and we could choose  $w = r$ . For each of these possible choices, we could make considerations similar to the above. The results of this process are pictured in subsequent figures according to Table 3.1.

If we combine all these results with those of the previous section, we get the chambers pictured in Figure 3.49. Note that this combined set of chambers is still not equal to  $S_1$ .

If  $\tilde{D}_4$ ,  $\tilde{D}_5$ , and  $\tilde{D}_6$  are the chambers in  $A_M$  labeled in Figure 3.50, and if  $g_4, g_5, g_6 \in I$  are chosen such that  $g_i E_i \neq E_i$ , then we can choose  $x$  such that  $xC_M$  is any of the  $D_i = g_i \tilde{D}_i$ . For each of these  $xC_M$ , we could make considerations similar to the above for  $w = r, r^2$ . The results of this process include all the chambers in Figure 3.27 that are not present in Figure 3.49. This proves that the chambers in Figure 3.27 represent the exact collection of double- $I$ -cosets that intersect non-trivially with the  $\sigma$ -conjugacy class of 1.

Rather than using  $xC_M$  a distance of two chambers from  $C_M$ , it is also possible to obtain the chambers in Figure 3.27 that are not in Figure 3.49 in the following way. Let  $\tilde{b}$  now be such that  $\tilde{b}C_M$  is one of the chambers in Figure 3.49 that was not obtained using the methods of the previous section. Let  $xC_M \notin A_M$  be  $D_1, D_2$  or  $D_3$ , and compute as previously. This gives rise to the chambers in Figure 3.27 that are not in Figure 3.49. Note that this constitutes an iteration of our “length



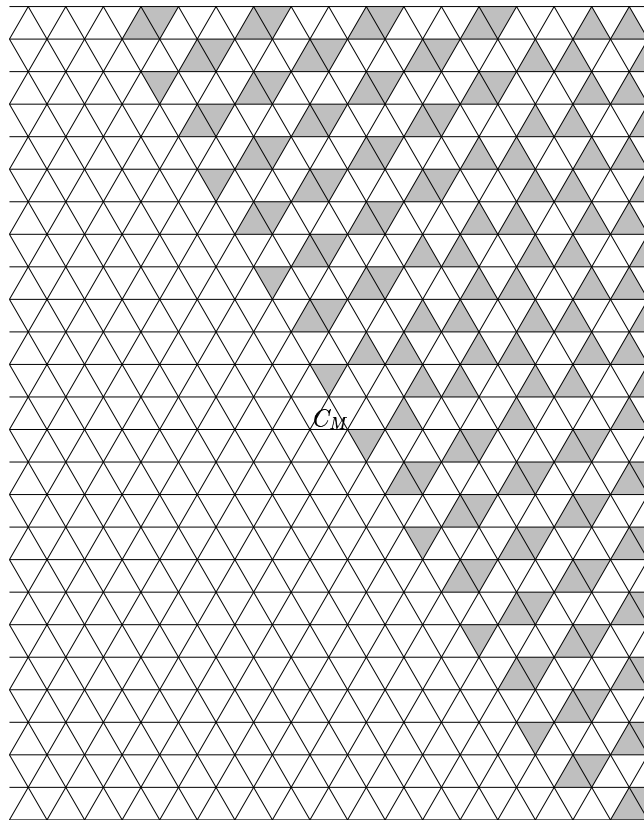


Figure 3.47: Results for  $xC_M = D_2$  and  $w = r^2$  or for  $xC_M = D_2$  and  $w = r$

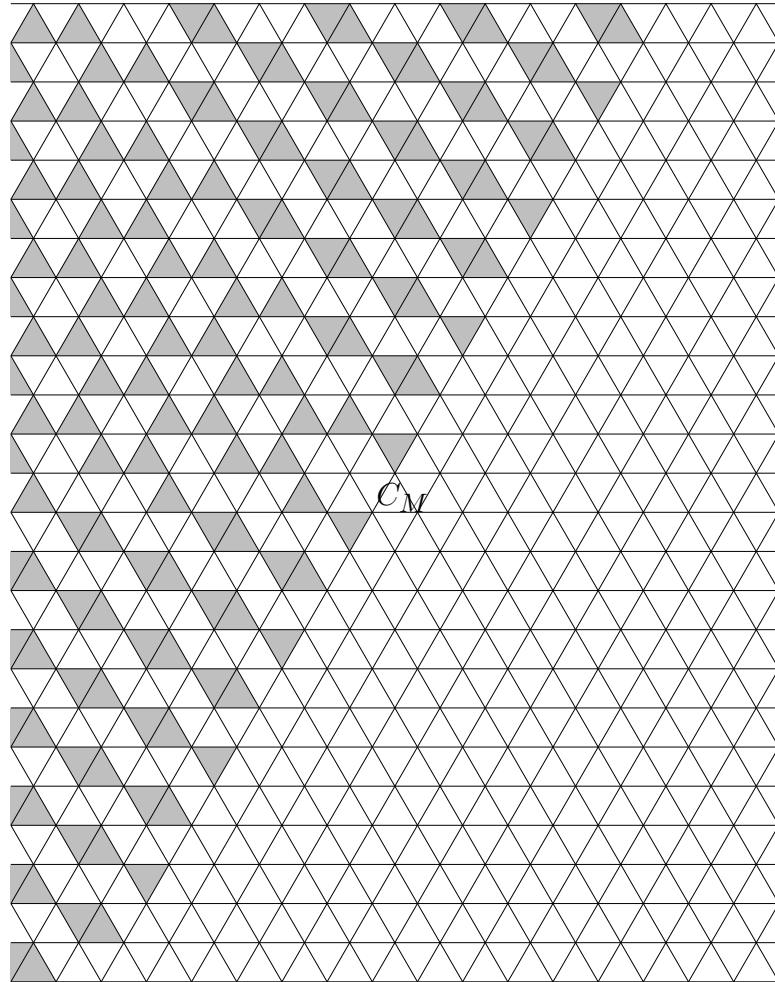


Figure 3.48: Results for  $x_{C_M} = D_3$  and  $w = r^2$  or for  $x_{C_M} = D_3$  and  $w = r$

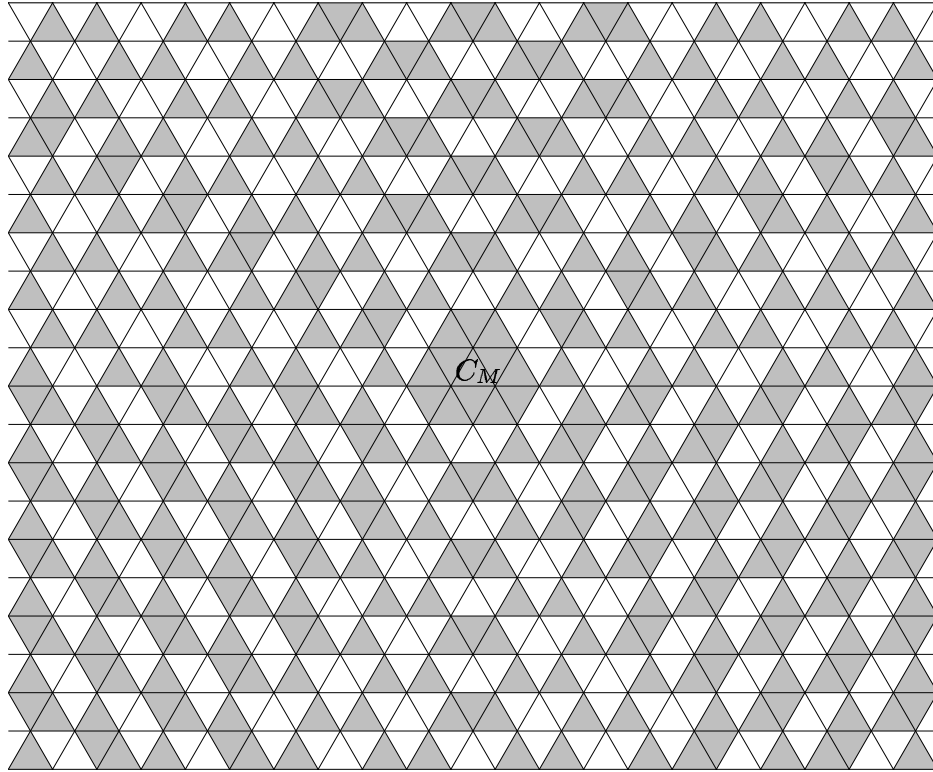


Figure 3.49: Combination of all results referred to in Table 3.1

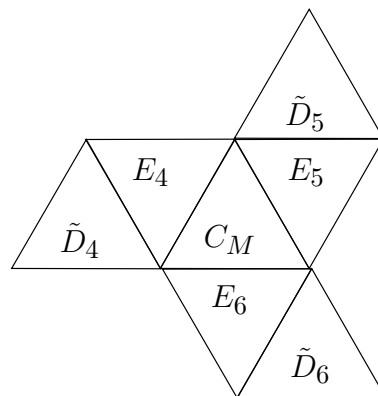


Figure 3.50: Some choices for  $x C_M$  that are two chambers away from  $C_M$

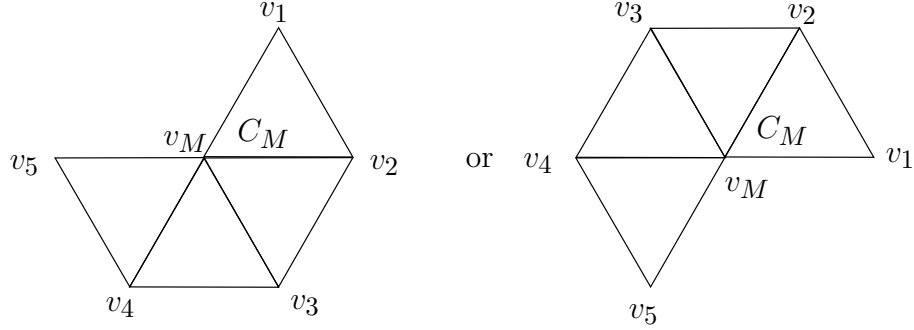


Figure 3.51: A Useful Lemma

one appendage” methods, and gives rise to the same additional chambers that our “length two appendage” methods did.

The methods in this section assume the existence of a large and well-distributed set  $S_2$ . If one has a smaller  $S_2$ , the enlargement effort will be less effective. One could apply the methods of this section to  $\sigma$ -conjugacy classes other than  $b = 1$ , but one would have to somehow come up with a reasonably large  $S_2$  first.

### 3.1.6 A Geometric Construction of a Subset of the Solution Set

In this section, we prove using geometric methods that the chambers in the superset  $S_1$  produced in Section 3.1.2 that arise from the infinite classes  $I_1$  and  $I_2$  are all actually contained in the solution set  $S$ . Since the classes  $I_1$  and  $I_2$  seemed to give rise to all chambers in  $S_1$ , this proves that  $S_1 = S$ .

We begin with the following very useful lemma.

**Lemma 3.1.6.** Let  $G$  be one of the galleries pictured in Figure 3.51. Let  $\tilde{G} = gG$ , where  $g \in GL_3(L)$  is arbitrary. There exists a unique vertex  $\tilde{v}$  such that  $\tilde{v}$  is adjacent to each of  $gv_5$ ,  $gv_1$ , and  $gv_M$ . Here,  $v_M$  is the main vertex in the building.

*Proof.* It suffices to work with  $g = 1$ . The vertices adjacent to  $v_M$  correspond to non-trivial proper subspaces of  $(\overline{\mathbb{F}}_q)^3$ , where  $\mathbb{F}_q$  is the residue field of  $F$  (so  $\overline{\mathbb{F}}_q$  is the residue field of  $L$ ). For such a vertex  $v$ , let  $v$  also denote the corresponding subspace of  $(\overline{\mathbb{F}}_q)^3$ . If  $v$  and  $w$  are two vertices adjacent to  $v_M$ , then  $v$  and  $w$  are adjacent to each other if and only if  $v \subseteq w$  or  $w \subseteq v$  as subspaces. We therefore have the following cases:

*Case 1:*  $\dim(v_1) = 1$ . Then  $\dim(v_2) = 2$ ,  $\dim(v_3) = 1$ ,  $\dim(v_4) = 2$ ,  $\dim(v_5) = 1$ , and we can and must choose  $\tilde{v} = \langle v_1, v_5 \rangle$ .

*Case 2:*  $\dim(v_1) = 2$ . Then  $\dim(v_2) = 1$ ,  $\dim(v_3) = 2$ ,  $\dim(v_4) = 1$ ,  $\dim(v_5) = 2$ , and we can and must choose  $\tilde{v} = v_1 \cap v_5$ .  $\square$

The idea of this lemma is that whenever we see an arrangement of chambers shaped like one of those in Figure 3.51, we can fill it in uniquely with two more chambers to create a hexagon.

We also need the following definition:

**Definition 3.1.6.** Given a minimal gallery  $G$ , the *parallelogram*,  $P(G)$  associated with  $G$  is  $P(G) = \cap A$ , where the intersection is over all apartments  $A$  containing  $G$ .

**Theorem 3.1.7.**  $P(G) = \cup \tilde{G}$ , where the union is over all minimal galleries  $\tilde{G}$  that stretch from the first chamber of  $G$  to the last chamber of  $G$ .

*Proof.* See [8]. □

Note that  $P(G)$  is not necessarily actually a parallelogram. It is a parallelogram with possibly a single chamber removed from either or both of the acute angle corners.

We now discuss the the program that we will follow in the rest of this section. We will begin by restricting our attention to the collection of  $\sigma$ -conjugacy classes consisting of those  $b$  with  $\alpha + 2\beta \neq 0$ , and  $b = 1$ . We also restrict our attention to type-edge pairs in  $I_1$ . If  $x \in SL_3(L)$  gives rise to a type-edge pair  $(t, e) \in I_1$ , and if  $b$  is restricted as specified, then we will define two invariants  $\gamma_1$  and  $\gamma_2$  of  $x$ . It will turn out that  $\gamma_1$  and  $\gamma_2$  determine  $\rho(x^{-1}\Gamma_x)$ . We will also show that given any  $\gamma_1$  and  $\gamma_2$ , we can choose  $x$  such that  $x$  and  $b$  give rise to  $(t, e)$ ,  $\gamma_1$ , and  $\gamma_2$ . This proves that for  $b = 1$  or  $b$  with  $\alpha + 2\beta \neq 0$ , all the results in  $S_1$  which come from  $I_1$  are in fact in  $S$ . We then use similar methods, with a few added complications, to address  $b \neq 1$  with  $\alpha + 2\beta = 0$ , still focusing our attention on  $(t, e) \in I_1$ . We then turn to  $(t, e) \in I_2$ , and we consider separately the cases  $b = 1$  or  $\alpha + 2\beta \neq 2\alpha + \beta$ , and  $b \neq 1$  with  $\alpha + 2\beta = 2\alpha + \beta$ .

As we just mentioned, we start by assuming  $(t, e) \in I_1$  and either  $b = 1$  or  $\alpha + 2\beta \neq 0$ . Recall that the associated composite gallery  $\Gamma_x$  is  $\Gamma_E^1 \cup \Gamma_E^2 \cup \Gamma_E^3$ , where each  $\Gamma_E^i$  is minimal (if  $b = 1$  then  $\Gamma_E^2 = \emptyset$ ). Let  $P = P(\Gamma_E^1)$ , let  $P_b = P(\Gamma_E^2)$ , and let  $P_\sigma = P(\Gamma_E^3)$ . It is worth noting that although we never made a specific choice of  $\Gamma_E^2$ ,  $P(\Gamma_E^2)$  is well defined (this relies on the fact that we have either  $b = 1$  or  $b$  with  $\alpha + 2\beta \neq 0$ ). Figure 3.52 has a picture of  $P$ ,  $P_b$ , and  $P_\sigma$  for

$$b = \begin{pmatrix} \pi^3 & 0 & 0 \\ 0 & \pi^{-1} & 0 \\ 0 & 0 & \pi^{-2} \end{pmatrix},$$

and the example type-edge pair pictured in Figure 3.2. By Lemma 3.1.6, we can choose a vertex  $w_1$  adjacent to  $u_2$ ,  $u_3$ , and  $u_4$ . This vertex is not necessarily  $v_1$ , although it may be. By repeated application of Lemma 3.1.6, we can choose the vertices  $w_2$ ,  $w_3$ ,  $w_4$  and  $w_5$ , labeled on Figure 3.53.

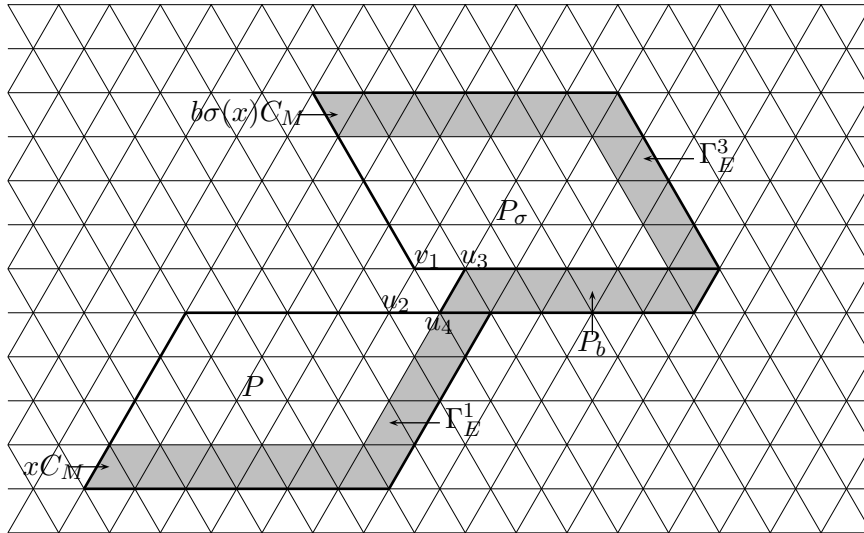


Figure 3.52: An example of  $P$ ,  $P_b$  and  $P_\sigma$

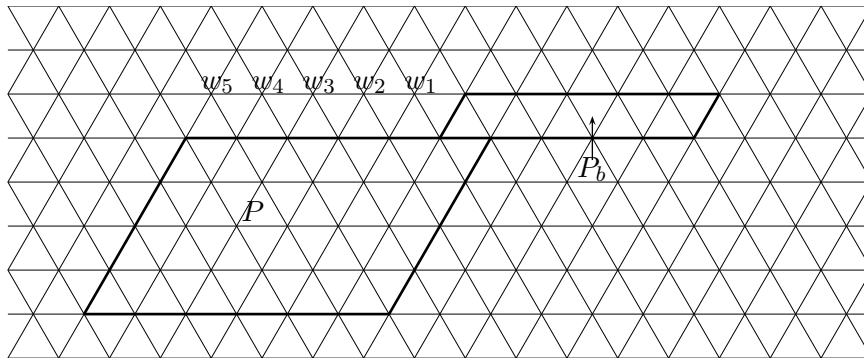
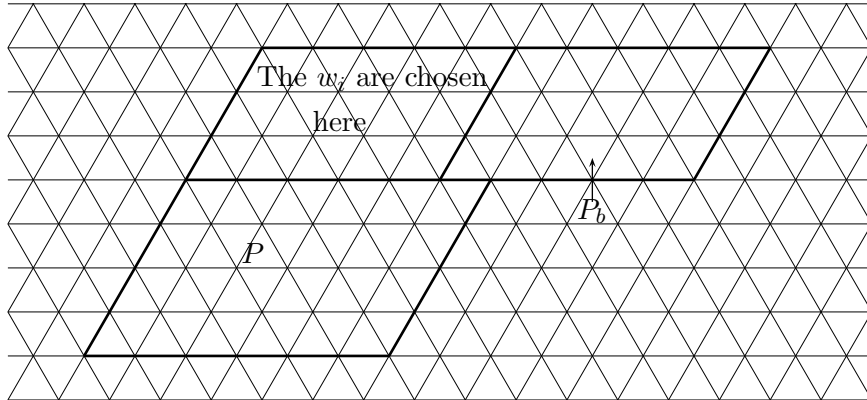
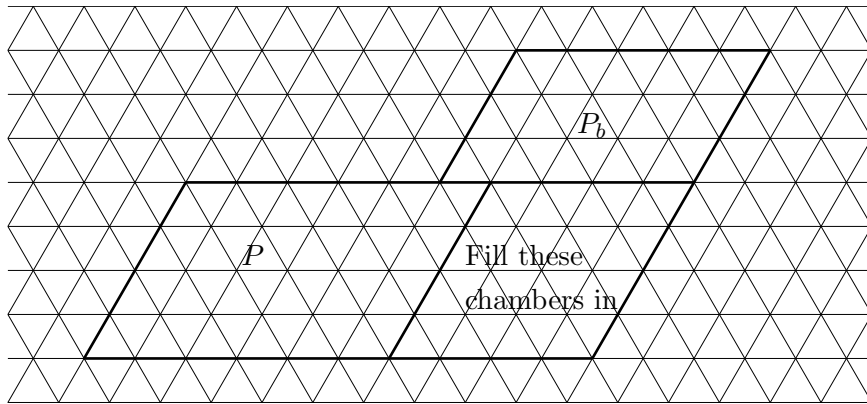


Figure 3.53:  $w_2$ ,  $w_3$ ,  $w_4$  and  $w_5$

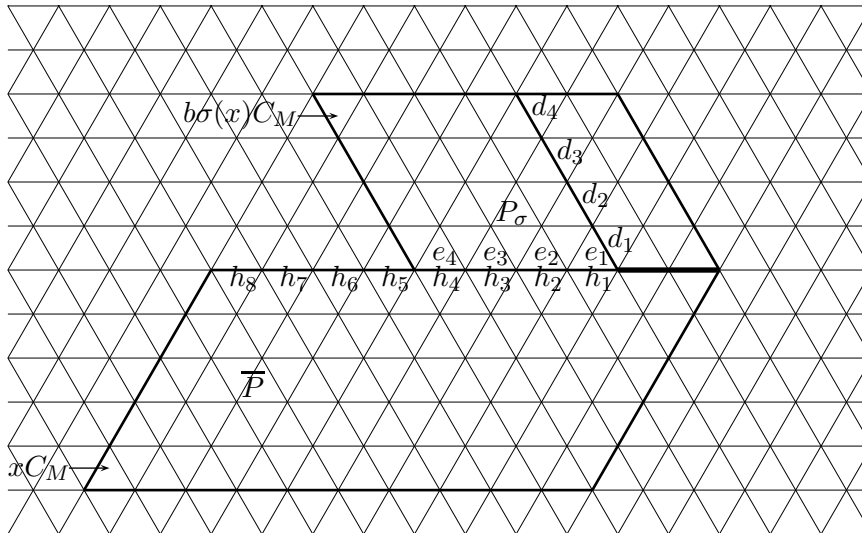
Figure 3.54: Multiple rows of the  $w_i$ Figure 3.55: Filling in the rest of  $\bar{P}$ 

For an arbitrary  $b \neq 1$  with  $\alpha + 2\beta \neq 0$ , and for any type-edge pair in  $I_1$ , we can choose vertices analogous to the  $w_i$  by repeated application of Lemma 3.1.6. Note that if  $P_b$  has more than one row of chambers, then we must choose correspondingly many rows of the  $w_i$ , one row at a time, from the bottom up. See Figure 3.54. We can also use Lemma 3.1.6 repeatedly to fill in chambers as labeled in Figure 3.55. We refer to the resulting unique construction consisting of  $P$ ,  $P_b$ , and the chambers added in the two above processes as  $\bar{P}$ . Note that  $\bar{P}$  is the intersection of all apartments containing  $P$  and  $P_b$ , and is also the union of all minimal galleries from the first chamber of  $\Gamma_E^1$  to the last chamber in  $\Gamma_E^2$ .

We now define two invariants which describe the way in which  $\bar{P}$  is connected to  $P_\sigma$ .

**Definition 3.1.7.** Let  $\gamma_1$  denote the number of edges that  $\bar{P}$  and  $P_\sigma$  have in common.

So  $\gamma_1 \geq 1$ , and in the case pictured in Figure 3.52,  $1 \leq \gamma_1 \leq 6$ .

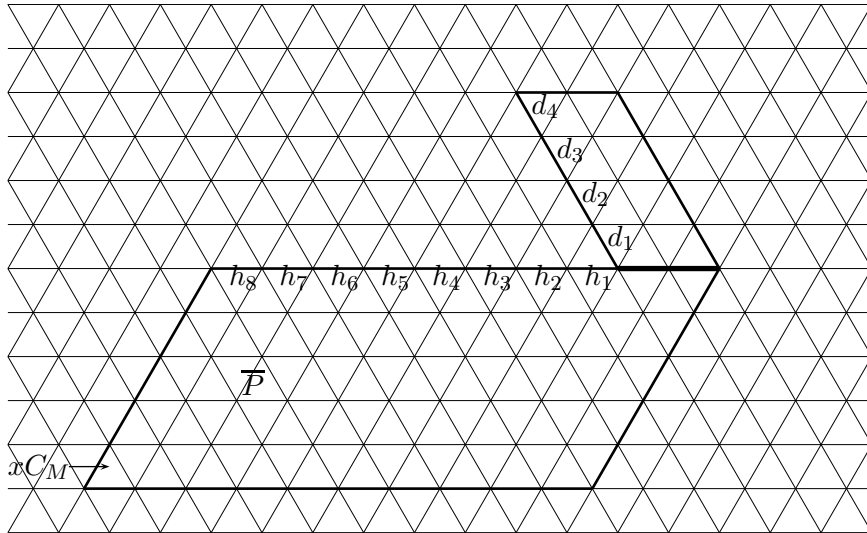
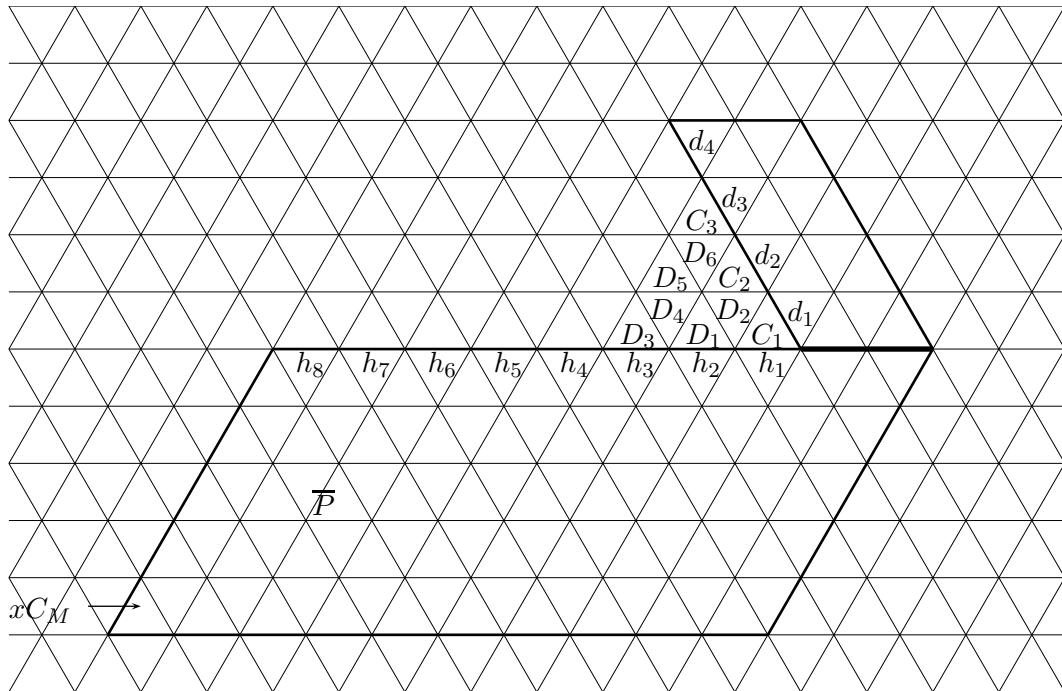
Figure 3.56: The definition of the invariant  $\gamma_2$ , part 1

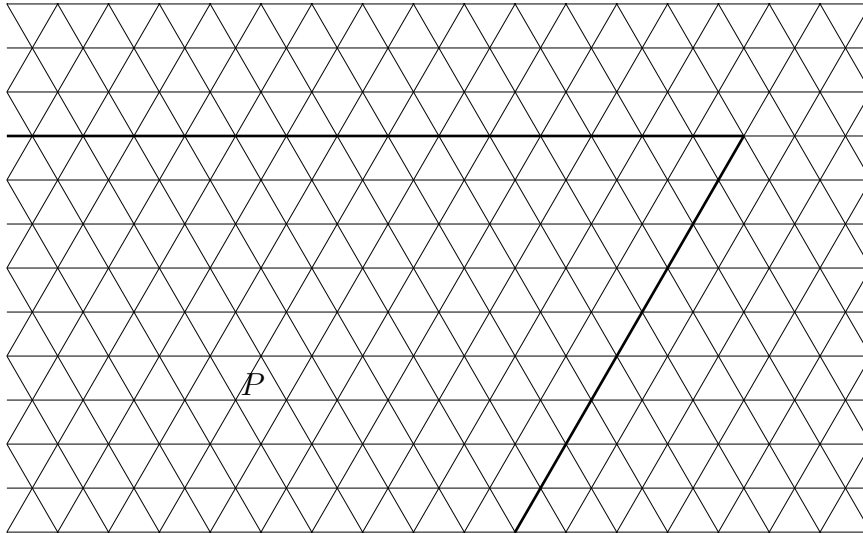
We define the second invariant  $\gamma_2$  using Figure 3.56, which shows a situation with  $\gamma_1 = 2$ . Note that for each  $i = 1, 2, 3, 4$ , the edges  $e_i$  of  $P_\sigma$  and  $h_i$  of  $\overline{P}$  are different, although they look the same in the figure. We pass to Figure 3.57, which is the same as Figure 3.56, only part of  $P_\sigma$  is not shown for clarity. We now define  $\gamma_2$  for our example situation. It will be clear from this example how  $\gamma_2$  is defined in general. If there is a chamber  $C_1$  (pictured in Figure 3.58) having  $h_1$  and  $d_1$  as edges, then it is unique, and not contained in  $P_\sigma$ . In this case we require  $\gamma_2 \geq 1$ , and we get  $D_1$  and  $D_2$  as pictured (in Figure 3.58) by using Lemma 3.1.6. If there is no  $C_1$  as described then we say  $\gamma_2 = 0$ . Given  $C_1$ , if there is a chamber  $C_2$  connecting  $D_2$  to  $d_2$ , then it is unique. In this case we require  $\gamma_2 \geq 2$ , and we get  $D_3, D_4$ , and  $D_5, D_6$  by using Lemma 3.1.6 twice. If there is no  $C_2$  as described then we say  $\gamma_2 = 1$ . Given  $C_2$ , we look for  $C_3$  as labeled. We continue in this manner, with the restriction that  $\gamma_2$  cannot be bigger than either the number of the  $h_i$  or the number of the  $d_i$ . If  $\gamma_2$  is equal to the lesser of these numbers, then we say  $\gamma_2$  is maximal.

For any parallelogram  $P$ , let  $T(P)$  be the number of edges along the top of  $P$ . Let  $S(P)$  be the number of edges along the right side of  $P$ . Recall that this could be different from the number of edges along the left side of  $P$ . Similarly,  $T(P)$  could be different from the number of edges along the bottom of  $P$ . This is because the “parallelograms” with which we are working are not true parallelograms in the traditional sense. They are parallelograms that may have one chamber removed from either or both of the acute angle corners. Although note that the upper right acute angle of  $P$  (and therefore  $\overline{P}$ ) never has a chamber removed;  $P_b$  will always be a parallelogram in the traditional sense of the word; and the lower right acute angle of  $P_\sigma$  never has a chamber removed.

Fixing  $b$  and a type-edge pair  $(t, e) \in I_1$ , let  $\gamma_1^{\max} = T(P)$ . Choose  $\gamma_1$  such that



Figure 3.57: The definition of the invariant  $\gamma_2$ , part 2Figure 3.58: The definition of the invariant  $\gamma_2$ , part 3

Figure 3.59:  $T(P) = S(P) = \infty$ 

$1 \leq \gamma_1 \leq \gamma_1^{\max}$ , and choose  $\gamma_2$  such that  $0 \leq \gamma_2 \leq \min\{S(P), T(\bar{P}) - \gamma_1\} = \gamma_2^{\max}(\gamma_1)$ . We will show that one can find  $x$  such that  $xC_M$  gives the type-edge pair  $(t, e)$ , and the invariants  $\gamma_1$  and  $\gamma_2$ . We begin by making a simplification.

If  $b$  is still fixed;  $(t_1, e_1)$  and  $(t_2, e_2)$  are two type-edge pairs in  $I_1$ ;  $P_1$  and  $P_2$  are the corresponding parallelograms  $P(\Gamma_{E_1}^1)$  and  $P(\Gamma_{E_2}^2)$ ; and if  $T(P_1) \leq T(P_2)$  and  $S(P_1) \leq S(P_2)$ , then  $\gamma_1^{\max}(P_1) \leq \gamma_1^{\max}(P_2)$ . Given  $\gamma_1 \leq \gamma_1^{\max}(P_1)$ , we also have  $\gamma_2^{\max}(P_1, \gamma_1) \leq \gamma_2^{\max}(P_2, \gamma_1)$ . To construct  $P_1$  with invariants  $\gamma_1(P_1) \leq \gamma_1^{\max}(P_1)$  and  $\gamma_2(P_1) \leq \gamma_2^{\max}(P_1, \gamma_1(P_1))$ , it would suffice to construct  $P_2$  with the same invariants. One could then chop off part of  $P_2$  to get the desired  $P_1$ . Therefore it suffices to demonstrate the construction of an “infinite parallelogram”  $P$  with  $T(P) = S(P) = \infty$  with any fixed (and still finite) invariants  $\gamma_1$  and  $\gamma_2$ . The equation  $T(P) = S(P) = \infty$  is meant to imply a parallelogram that is half-infinite along the top and along the right side as in Figure 3.59

We now discuss notation to be used in constructions to come. Regions of an apartment of the building will always be denoted using Roman letters with subscript. Single chambers will be labeled using Roman letters with subscript, or just using numbers. At several points we will have to graphically represent structures in the building that cannot be embedded into a Euclidean plane. For instance, we will discuss the main apartment  $A_M$ , together with a half apartment  $A_1^{\frac{1}{2}}$  coming out of a wall  $K$  in  $A_M$ . We would picture this example as in Figure 3.60, where  $R_1$  is a region in  $A_M$ ,  $R_2$  is also in  $A_M$ , and  $\tilde{R}_2 = A_1^{\frac{1}{2}}$ . Thus  $R_2$  and  $\tilde{R}_2$  are the same region graphically, but different regions in the construction we are describing. The chamber shaded in Figure 3.60 could be denoted 1 if in  $R_2$  or  $\tilde{1}$  if in  $\tilde{R}_2$ . The tilde will be used generally in this way, with constructions marked with a tilde understood to not be in

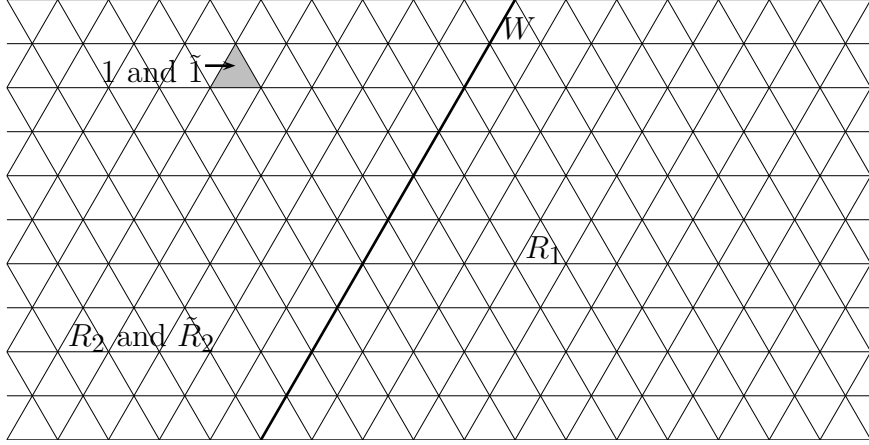


Figure 3.60: The meaning of a tilde

$\overline{P}$ ,  $P_b$ , or  $P_\sigma$ , unless specifically included.

We now proceed to demonstrate that one can find  $x$  such that  $x C_M$  gives  $(t, e)$ ,  $\gamma_1$ , and  $\gamma_2$ . We work with two cases.

*Case 1:  $b = 1$ .* Let  $A_1$  be an apartment in  $\mathcal{B}_1$ , and let  $K$  be a wall in  $A_1$  (see Figure 3.61). Let  $A_1^{\frac{1}{2}}$  be a half-apartment coming out of  $K$  that lies in  $\mathcal{B}_2$ . If  $\gamma_1$  is as labeled in Figure 3.61, choose region  $R_1$  in  $A_1^{\frac{1}{2}}$ . Choose region  $R_2$  from  $\mathcal{B}_6 \setminus \mathcal{B}_2$ . Let  $Q_1 = \sigma(R_1)$  and  $Q_2 = \sigma(R_2)$ . This determines the regions  $N_1$  and  $\tilde{r}_1$  by repeated application of Lemma 3.1.6, and therefore determines  $r_1 := \sigma(N_1)$ . So  $\tilde{r}_1$  is attached to  $N_1$ . We must check that the bottom boundaries of  $r_1$  and  $\tilde{r}_1$  have no edges in common to ensure that  $\gamma_1$  is no bigger than intended. But such commonality would imply that for some edge  $e$  along the upper boundary of  $N_1$ , we have  $\sigma(e) = e$ , i.e.,  $e \in \mathcal{B}_1$ . But let  $G$  be a minimal gallery through  $Q_2$  from  $e$  to some chamber  $D$  in  $Q_1 \subseteq \mathcal{B}_2$ . The galleries  $G$  and  $\sigma^2(G)$  are both galleries of the same type from  $e$  to  $D$ , so therefore  $G = \sigma^2(G)$ . But  $G$  passes through  $Q_2 \subseteq \mathcal{B}_6 \setminus \mathcal{B}_2$ , so  $G \neq \sigma^2(G)$ , and we have a contradiction.

We now choose  $R_3$  arbitrarily. This determines  $Q_3 = \sigma(R_3)$ , and  $\tilde{r}_2$ ,  $N_2$ ,  $\tilde{C}_2$ ,  $\tilde{E}_2$  by Lemma 3.1.6. The region  $\tilde{r}_2$  is attached on its right hand side to  $\tilde{r}_1$ . Choose  $C_2 \neq \tilde{C}_2$  to ensure that  $\gamma_2$  is no bigger than intended. Fill out the rest of  $P$  arbitrarily.

*Case 2:  $b \neq 1$ .* We break this case into subcases:

*Subcase 1:  $\gamma_1 + T(P_b) - 1 \geq \gamma_1 + \gamma_2$ ,* and if equality holds then  $\gamma_2 \neq 0$ . This situation is pictured in Figure 3.62. The inequality implies that  $c$  is at least as far left as  $a$  in that figure, and if  $a = c$  then  $\gamma_2 \neq 0$ . Let  $K$  be a wall in  $A_M$ , and let  $A_1^{\frac{1}{2}}$  be a half apartment coming out of  $K$ . Then  $b\sigma(A_1^{\frac{1}{2}})$  is a half apartment coming out of  $b\sigma(K) = bK$ . Choose  $Q_1$  and  $\tilde{r}_1$  from  $b\sigma(A_1^{\frac{1}{2}})$ . Let  $R_1 = \sigma^{-1}b^{-1}Q_1$ . Then

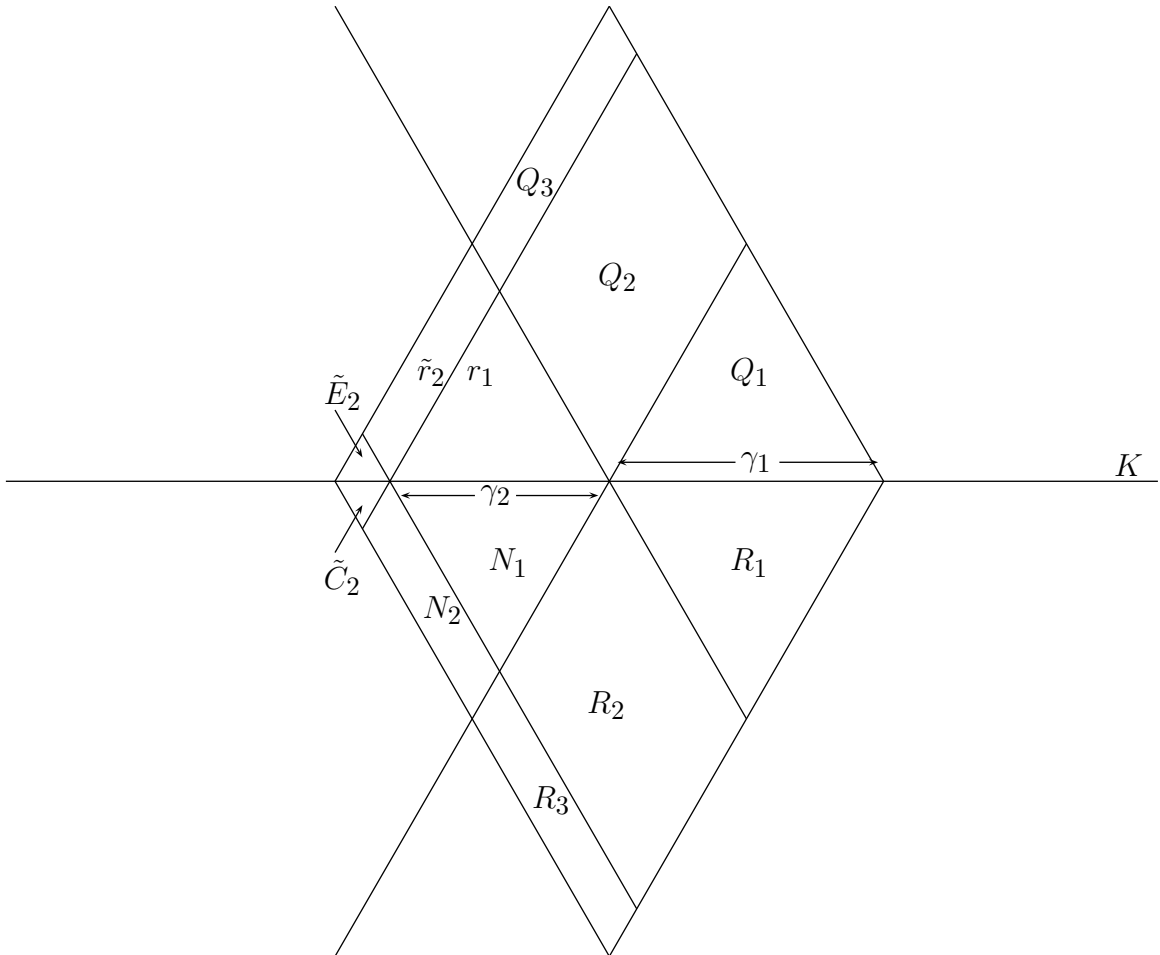


Figure 3.61: Existence of all values of  $\gamma_1$  and  $\gamma_2$ , case 1

$R_1$  is in  $A_1^{\frac{1}{2}}$ , so  $L_1 \subseteq \overline{P}$  is in  $A_M$ , and  $Q_1$  and  $\tilde{r}_1$  are attached to  $\overline{P}$  along  $b\sigma(K)$ . Choose  $r_1$  the same shape as  $\tilde{r}_1$ , and attached to  $Q_1$  along the line between  $Q_1$  and  $\tilde{r}_1$ , but sharing no chambers in common with  $\tilde{r}_1$ . This ensures that none of the chambers in  $r_1$  is attached to  $L_1$ , and therefore that  $\gamma_1$  is no bigger than intended. Let  $N_1 = \sigma^{-1}b^{-1}(r_1)$ . We can fill in  $L_2$  by repeated application of Lemma 3.1.6. Note that  $L_2$  may be empty if  $\gamma_2 = 0$ . In this case,  $r_1$ ,  $\tilde{r}_1$  and  $\tilde{r}_2$  would also be empty. If  $\gamma_2 > 0$ , choose  $\tilde{r}_2$  attached to  $L_1$ , or attached to  $L_2$  if  $c = a$  (and in this case we have  $L_2 \neq \emptyset$ , since  $\gamma_2 \neq 0$ ). This is done by repeated application of Lemma 3.1.6. Choose  $Q_2$  such that there is no chamber attaching it to  $\tilde{r}_2$  (we know this can be done by the uniqueness statement in Lemma 3.1.6). Now let  $R_2 = \sigma^{-1}b^{-1}Q_2$ . This ensures that  $\gamma_2$  is no bigger than desired. We now choose the rest of  $P$  arbitrarily.

*Subcase 2:*  $\gamma_1 + T(P_b) - 1 = \gamma_1 + \gamma_2$  and  $\gamma_2 = 0$ . In this case,  $T(P_b) = 1$ . The situation is pictured in Figure 3.63. Let  $A_1^{\frac{1}{2}}$  be a half apartment coming out of  $K$ , as before. Choose  $R_1$  in  $A_1^{\frac{1}{2}}$ , and let  $Q_1 = b\sigma(R_1)$ . We see that  $L_1 \subseteq A_M$ . Choose  $R_2$  attached to  $R_1$ . This determines  $Q_2 = b\sigma(R_2)$ , which in turn determines  $\tilde{D}_2$ ,  $\tilde{L}_2$ ,  $\tilde{E}_2$ , and  $\tilde{C}_2$  by repeated application of Lemma 3.1.6. For  $C_2$ , choose any chamber attached to  $R_2$  other than  $\tilde{C}_2$ . This ensures that  $\gamma_1$  is no bigger than intended, and that  $\gamma_2 = 0$ . Choose the rest of  $P$  arbitrarily.

*Subcase 3:*  $\gamma_1 + T(P_b) - 1 < \gamma_1 + \gamma_2$ , and point  $a$  in Figure 3.64 is at least as far right as point  $d$  (the alternative is Figure 3.65, which we will consider in subcase 4). Point  $a$  is a distance of  $\gamma_1 + \gamma_2 - T(P_b) + 1$  edge lengths from the right boundary of  $P$ , and point  $d$  is a distance of  $\gamma_1 + T(P_b) - 1$  edge lengths from the same boundary. So our condition on  $a$  and  $d$  is the same as saying  $\gamma_1 + \gamma_2 - T(P_b) + 1 \leq \gamma_1 + T(P_b) - 1$ , i.e.,  $\gamma_2 + 2 \leq 2T(P_b)$ . Choose  $Q_1$  and  $\tilde{r}_1$  from  $b\sigma(A_1^{\frac{1}{2}})$ . Let  $R_1 = \sigma^{-1}b^{-1}Q_1$ . Then  $R_1 \subseteq A_1^{\frac{1}{2}}$ , so  $L_1$  is in  $A_M$ , and  $Q_1$  and  $\tilde{r}_1$  are attached to  $\overline{P}$  along  $b\sigma(K)$ . Now consider the apartment made up of  $A_1^{\frac{1}{2}}$ ,  $b\sigma(A_1^{\frac{1}{2}})$ , and the strip in  $A_M$  between  $K$  and  $b\sigma(K)$ . Extend the line  $l$  in Figure 3.64 to a wall in this apartment, and take  $A_2^{\frac{1}{2}}$  to be a half apartment coming out of this wall. Choose  $Q_2$ ,  $\tilde{r}_2$ ,  $L_2$  and  $N_1$  from  $A_2^{\frac{1}{2}}$ . This determines  $R_2$ . Choose  $Q_3$  arbitrarily. This determines  $\tilde{r}_3$ ,  $\tilde{L}_3$  and  $\tilde{N}_3$ , none of which will be part of the final construction. Choose  $N_2$  using Lemma 3.1.6. Let  $\tilde{C}$  and  $\tilde{D}$  be the unique chambers attached to  $\tilde{N}_3$  and  $N_2$ , given by Lemma 3.1.6. Choose  $C \neq \tilde{C}$ . This assures that  $\gamma_2$  is no bigger than desired. Construct the rest of  $P$  arbitrarily.

*Subcase 4:*  $\gamma_1 + T(P_b) - 1 < \gamma_1 + \gamma_2$ , and point  $a$  in Figure 3.65 is strictly to the left of point  $d$  (so  $\gamma_2 + 2 > 2T(P_b)$  and the condition  $\gamma_1 + T(P_b) - 1 < \gamma_1 + \gamma_2$  become redundant). Construct  $R_1$ ,  $L_1$ ,  $Q_1$  and  $\tilde{r}_1$  exactly as in subcases 3 and 1. Construct  $N_1$ ,  $L_2$ ,  $\tilde{r}_2$ , and  $Q_2$  exactly as in subcase 3. This determines  $R_2$  and  $r_1$ . Choose  $Q_3$

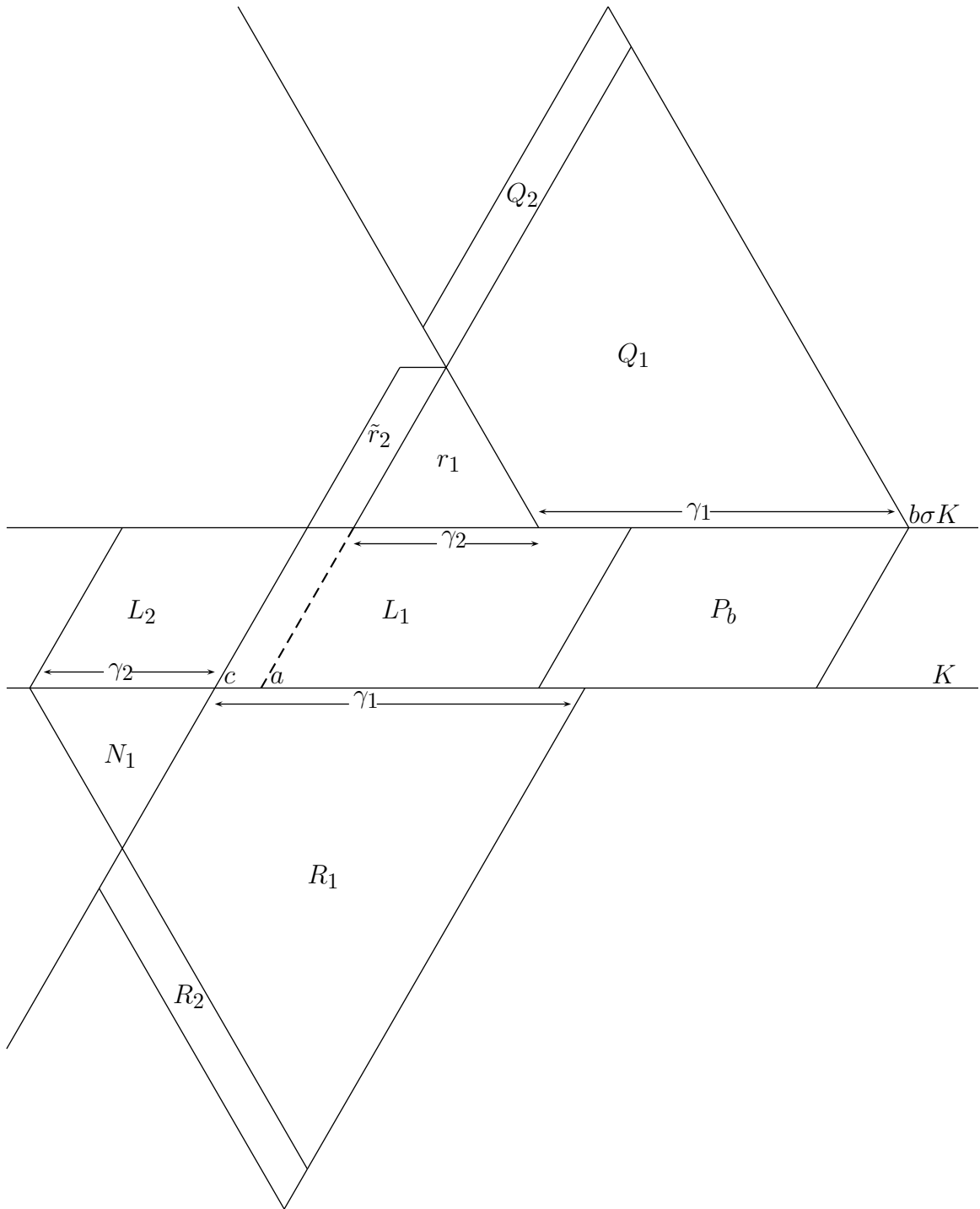


Figure 3.62: Existence of all values of  $\gamma_1$  and  $\gamma_2$ , case 2 subcase 1

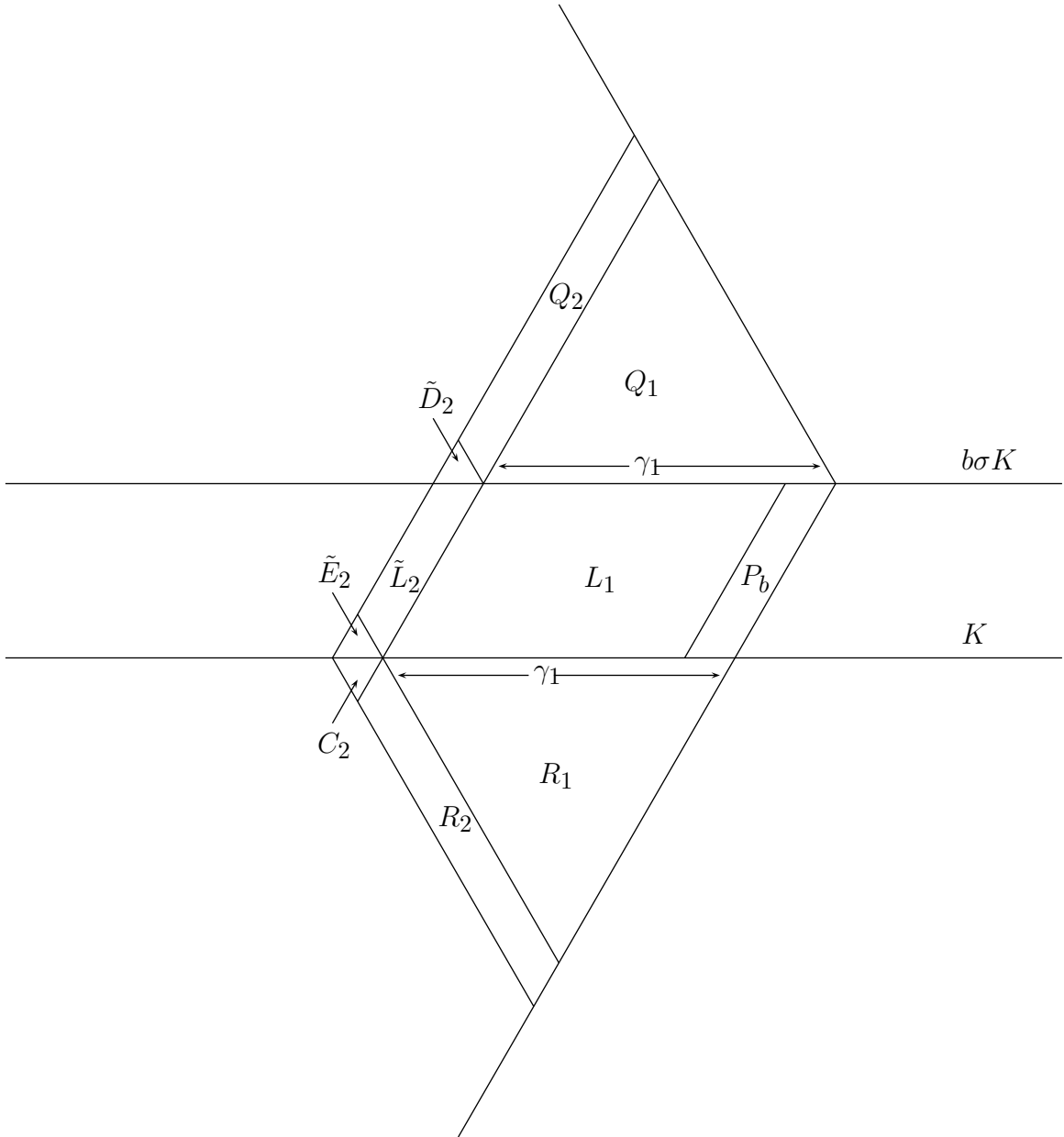


Figure 3.63: Existence of all values of  $\gamma_1$  and  $\gamma_2$ , case 2 subcase 2

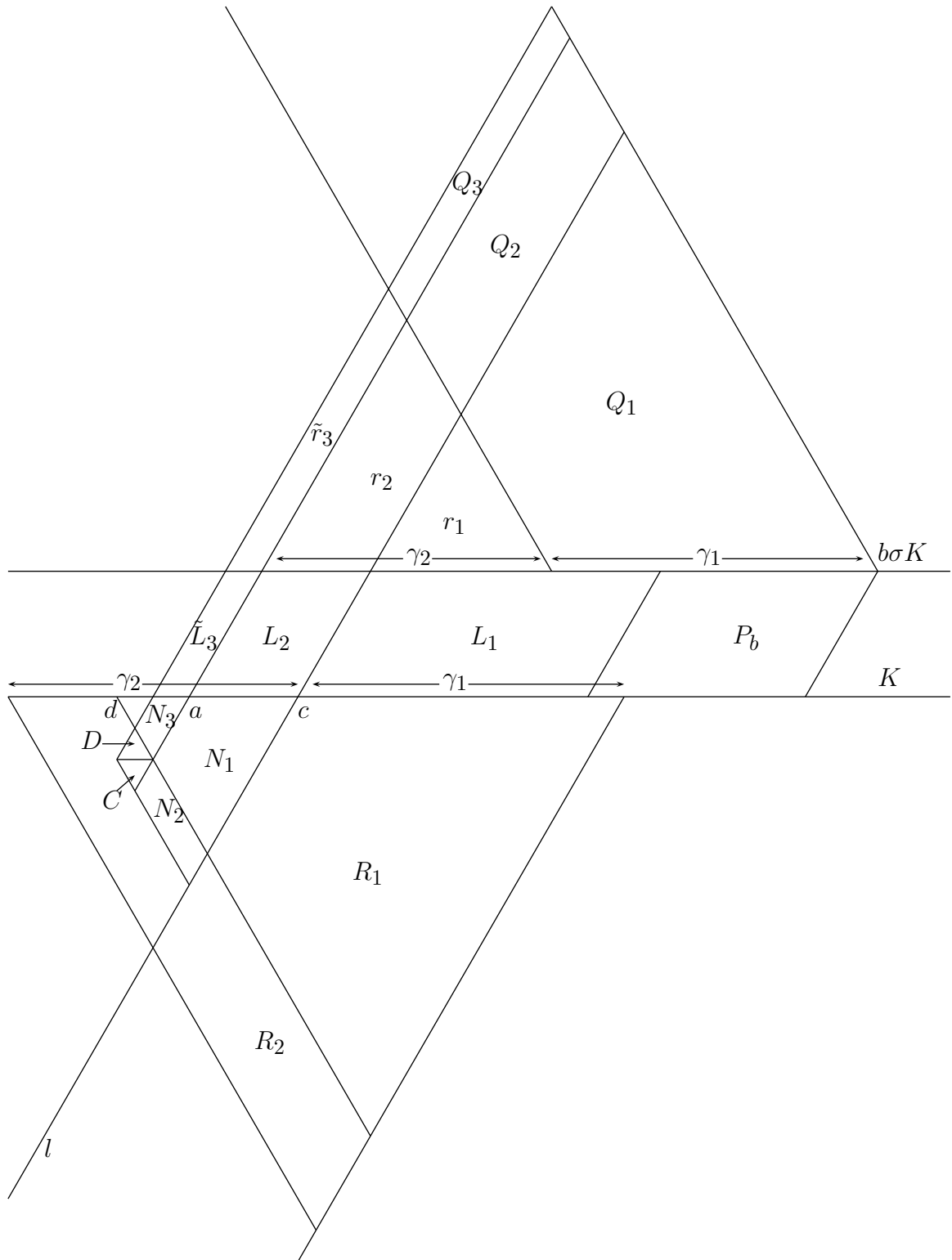


Figure 3.64: Existence of all values of  $\gamma_1$  and  $\gamma_2$ , case 2 subcase 3



arbitrarily. This determines  $R_3$ . Use Lemma 3.1.6 repeatedly to fill in  $\tilde{r}_3$ ,  $L_3$  and  $N_2$ . Choose the unique possible  $C_3$  and  $D_3$  to connect  $N_2$  and  $L_3$ . Repeat this process to point  $a$ , then, at the next step choose for  $C_i$  any chamber other than the unique one that connects to  $L_i$ . This ensures  $\gamma_2$  is no bigger than desired. Choose the rest of  $P$  arbitrarily.

Up to this point, we have defined  $\overline{P}$ ,  $P_\sigma$ , and the invariants  $\gamma_1$  and  $\gamma_2$  for  $b = 1$  or  $b$  with  $\alpha + 2\beta \neq 0$ , and  $(t, e) \in I_1$ . We have also shown that if  $1 \leq \gamma_1 \leq \gamma_1^{\max}$ ,  $0 \leq \gamma_2 \leq \gamma_2^{\max}(\gamma_1)$ , then there is some  $x \in SL_3(L)$  such that  $xC_M$  gives rise to  $(t, e)$ ,  $\gamma_1$  and  $\gamma_2$ . We now broaden the definition of  $\gamma_2$  to include negative values. We will then have to re-address the issue of whether all possible  $\gamma_2$  actually occur. Consider Figure 3.66. If there is no chamber connecting chamber 7 to chamber 5, we say  $\gamma_2 \leq 0$  (previously we just said  $\gamma_2 = 0$ ). In this case we ask if there is a chamber connecting 4 to 8. If not, then  $\gamma_2 = 0$ . If so, then  $\gamma_2 \leq -1$ , and we call the connecting chamber  $\tilde{7}$ . In this case, we fill in chambers  $\tilde{6}$  and  $\tilde{9}$  using chambers  $\tilde{7}, 8, 11, 10$  and Lemma 3.1.6. We now ask if there is a chamber connecting  $\tilde{6}$  to 2. If not, then  $\gamma_2 = -1$ , and if so then  $\gamma_2 \leq -2$ . We proceed in this way to determine the value of  $\gamma_2$ . Note that if  $\gamma_2^{\min}(\gamma_1) = -\min\{S(\overline{P}), T(P) - \gamma_1\}$ , then  $\gamma_2 \geq \gamma_2^{\min}$  automatically.

We now show that given any  $b$  such that  $b = 1$  or  $\alpha + 2\beta \neq 0$ , given  $(t, e) \in I_1$ , and given  $\gamma_1$  and  $\gamma_2$  such that  $1 \leq \gamma_1 \leq \gamma_1^{\max}$  and  $\gamma_2^{\min}(\gamma_1) \leq \gamma_2 \leq \gamma_2^{\max}(\gamma_1)$ , there exists an  $x$  such that  $x$  and  $b$  give rise to  $(t, e)$ ,  $\gamma_1$  and  $\gamma_2$ . Given what we have already done, we may assume that  $\gamma_2 \leq 0$ . As usual we proceed in cases.

*Case 1:  $b = 1$ .* See Figure 3.67. Let  $L$  be a wall in  $A_M$ , and let  $A_1^{\frac{1}{2}}$  be a half apartment in  $\mathcal{B}_2$  coming out of  $L$ . Choose  $Q_1$  in  $A_1^{\frac{1}{2}}$ . Choose chamber 4 in  $\mathcal{B}_6 \setminus \mathcal{B}_2$ . This determines 8, and therefore by Lemma 3.1.6 also determines  $\tilde{3}$  and  $\tilde{7}$  connecting 4 and 8. To arrange  $\gamma_2 = 0$ , choose 7 such that  $7 \neq \tilde{7}$  and  $\sigma(7) \neq \tilde{3}$ , and construct the rest of  $P$  arbitrarily. To arrange  $\gamma_2 \leq -1$ , choose  $7 = \sigma^{-1}(\tilde{3})$ . Since  $4, 8 \in \mathcal{B}_6 \setminus \mathcal{B}_2$ ,  $\sigma(\tilde{7}) \neq \tilde{3}$ , so  $\tilde{7} \neq 7$ , so  $\gamma_2 \leq 0$  still holds. On the other hand  $3 = \sigma(7) = \tilde{3}$ , so 3 can be connected to 8 (via  $\tilde{7}$ ), ensuring  $\gamma_2 \leq -1$ . Choose  $\tilde{6}$  and  $\tilde{9}$  to fit between  $\tilde{7}$  and 10 using Lemma 3.1.6. Choose  $\tilde{1}$  and  $\tilde{5}$  to fit between 2 and  $\tilde{6}$ . To arrange  $\gamma_2 = -1$  choose  $1 \neq \tilde{1}$  and construct the rest of  $P$  arbitrarily. To arrange  $\gamma_2 \leq -2$ , choose  $1 = \tilde{1}$ . Continue in this manner.

*Case 2:  $b \neq 1$ .* We break this case into subcases.

*Subcase 1:  $T(P_b) = 1$ .* See Figure 3.68. We let  $K$  and  $K_1$  be walls in  $A_M$ ,  $K$  a horizontal wall, and  $K_1$  a wall such that  $bK_1 = K_1$ . Let  $\tilde{T}$  be the first row of chambers in a half apartment  $A_1^{\frac{1}{2}}$  coming out of  $K_1$  to the left. Choose  $A_1^{\frac{1}{2}}$  such that  $b\sigma(\tilde{T}) \neq \tilde{T}$ . This implies that  $b\sigma(\tilde{T})$  has no chambers in common with  $\tilde{T}$ . Let  $A$  be the apartment made up of  $A_M$  on the right of  $K_1$  and  $A_1^{\frac{1}{2}}$  on the left. Then half of  $K$  is in  $A$ , and we can extend this half to  $\tilde{K}$ , a wall in  $A$ . Let  $A_2^{\frac{1}{2}}$  be a half



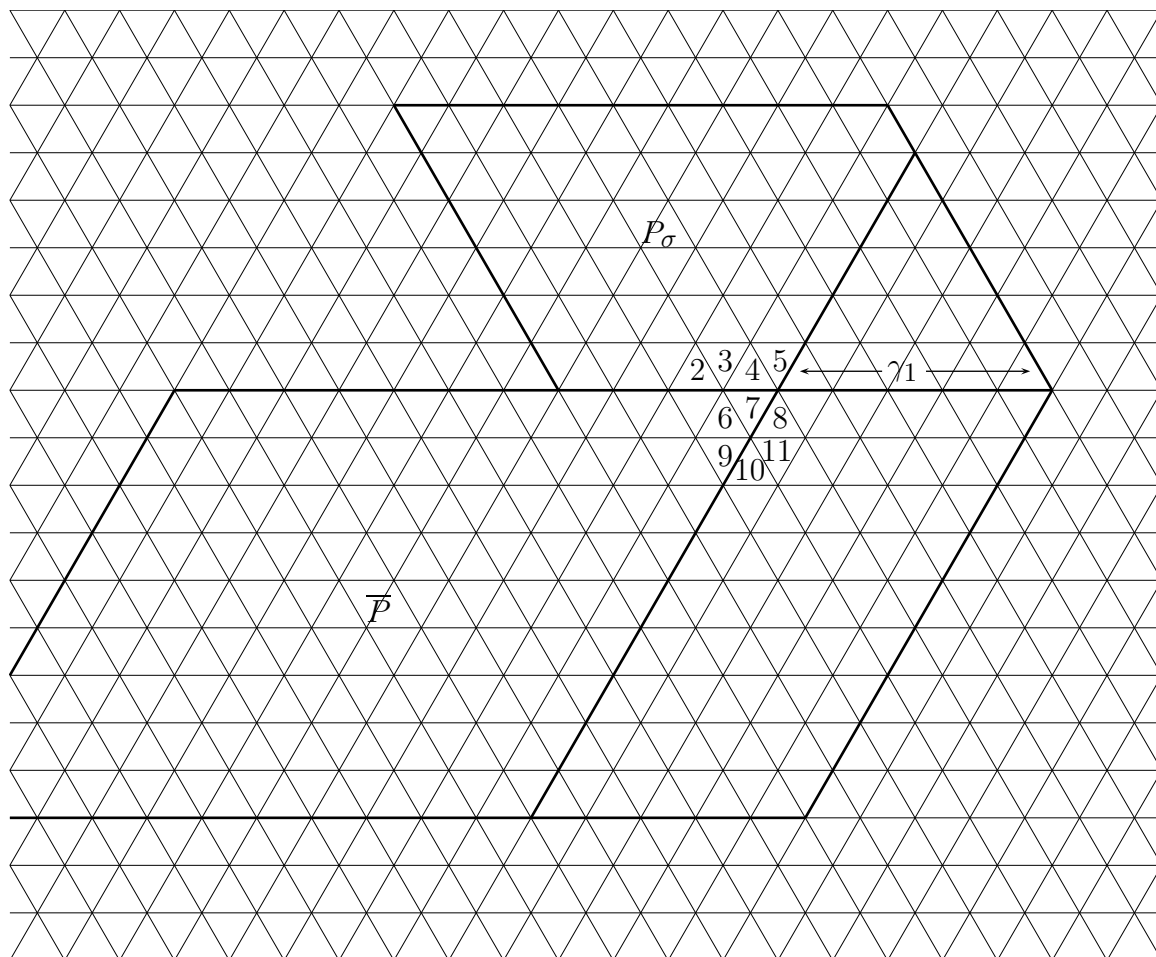


Figure 3.66: Definition of negative values of  $\gamma_2$

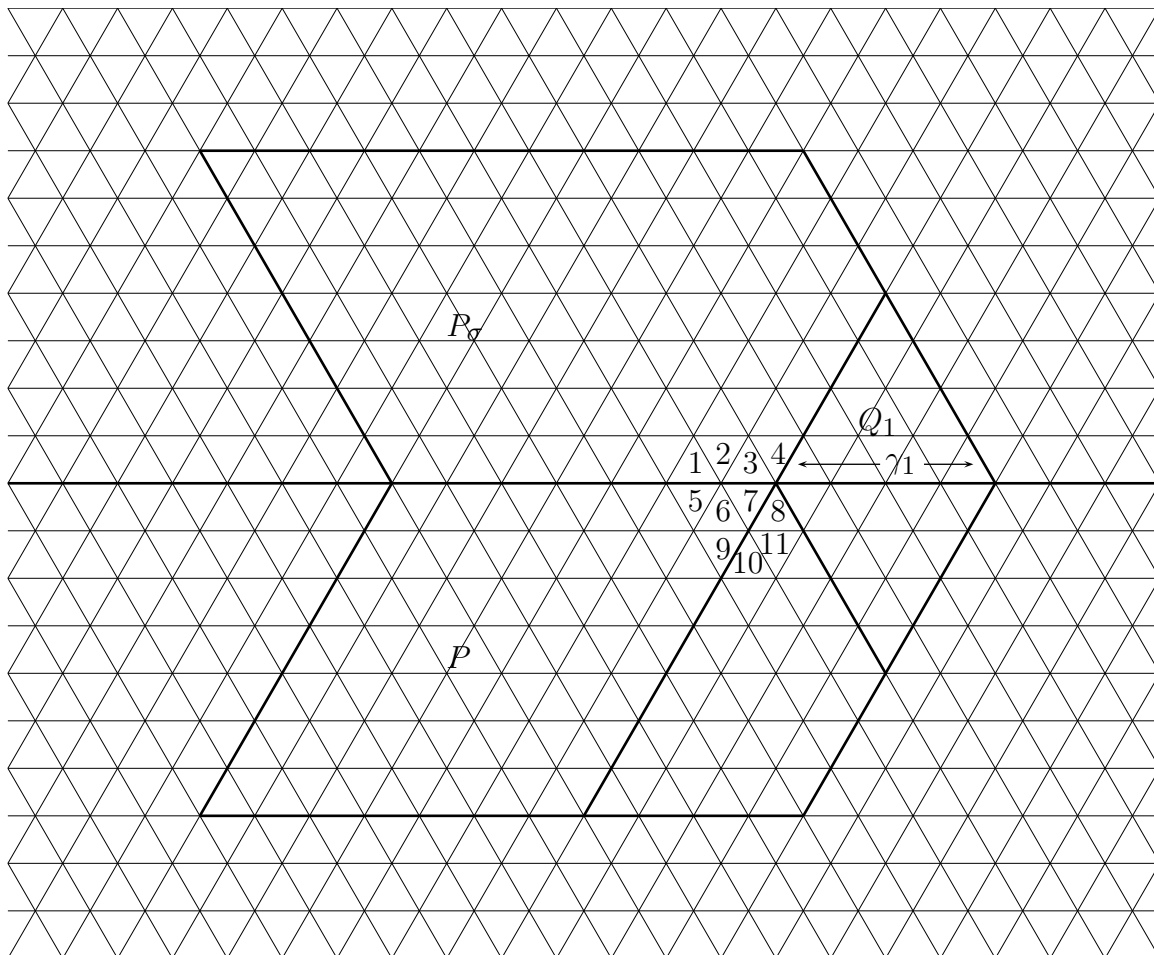


Figure 3.67: Existence of all negative values of  $\gamma_2$ , case 1

apartment coming out of  $\tilde{K}$ , and choose  $R_1, R_2$  and  $\tilde{C}_2$  from  $A_2^{\frac{1}{2}}$ . We can now throw away all of  $A_1^{\frac{1}{2}}$  except  $\tilde{T}$ . We get  $Q_1 = b\sigma(R_1)$ ,  $Q_2 = b\sigma(R_2)$ ,  $P_b$ , and  $L_1 \subseteq A_M$ . Note that  $b\sigma(\tilde{T})$  is another row of chambers coming out of  $L$ , and note that we have  $\tilde{D}_2 = b\sigma(\tilde{C}_2)$  attaching  $Q_2$  to  $b\sigma(\tilde{T})$ , as drawn in the figure. We have  $\tilde{F}_2 \subseteq b\sigma(\tilde{T})$  which connects  $\tilde{D}_2$  to  $L_1$ , and by Lemma 3.1.6, we have  $\tilde{E}_2$  and  $\tilde{C}_2$  attaching  $b\sigma(\tilde{T})$  to  $R_2$  as drawn. Note that  $\tilde{\tilde{C}}_2 \neq \tilde{C}_2$ . If these chambers were equal, we could create a contradiction to the uniqueness part of Lemma 3.1.6 by producing two galleries of length two from the edge between  $\tilde{\tilde{C}}_2 = \tilde{C}_2$  and  $\tilde{E}_2$ , down through  $\tilde{T}$  and  $b\sigma(\tilde{T})$  respectively, to  $L_1$ . To make sure  $\gamma_2 \leq 0$ , choose  $C_2 \neq \tilde{\tilde{C}}_2$ . To make sure  $\gamma_2 \leq -1$ , choose  $C_2 = \tilde{\tilde{C}}_2$ . For  $\gamma_2 = 0$ , choose any other  $C_2$ . If we chose  $\gamma_2 = 0$ , fill out the rest of  $P$  arbitrarily. If we chose  $\gamma_2 \leq -1$ , then what we have done becomes the base case of an induction.

Let  $D_2 = b\sigma(C_2)$ , and see Figure 3.69. The region made up of  $\tilde{L}_2, \tilde{S}_2$  is taken from  $b\sigma(\tilde{T})$ . We assume by induction that the  $Q_j, D_j, \tilde{L}_j$  and  $\tilde{S}_j$  for  $2 \leq j \leq i$  are all contained in a single half apartment, and that  $\gamma_2 \leq -i + 1$ . We choose  $Q_{i+1}$  arbitrarily. If we want  $\gamma_2 = -i + 1$ , we choose  $D_{i+1}$  such that there is no chamber attaching it to  $\tilde{L}_i$ . If we want  $\gamma_2 \leq -i$ , we choose a chamber  $D_{i+1}$  that can be attached to  $\tilde{L}_i$ . This enables us to fill in an  $\tilde{L}_{i+1}$  and an  $\tilde{S}_{i+1}$  uniquely using Lemma 3.1.6. We can continue thus until we either reach the desired value for  $\gamma_2$ , or until we are stopped by  $\gamma_2^{\min}(\gamma_1)$ .

*Subcase 2:  $T(P_b) > 1$ .* See Figure 3.70. Construct  $R_1$  and  $Q_1$  in the standard way. Choose  $Q_2$  such that there is no chamber connecting it to  $L_1$  (to ensure  $\gamma_2 \leq 0$ ). If we want  $\gamma_2 = 0$ , we choose  $D_2$  such that there is no chamber connecting it to the line  $l$  (which is in  $L_1$  and  $P$ ). If we want  $\gamma_2 \leq -1$ , we choose  $D_2$  such that there is a chamber  $\tilde{E}_2$  connecting it to the line  $l$ . Note that  $\tilde{E}_2 \not\subseteq L_1$ . Construct  $\tilde{S}_2$  using Lemma 3.1.6. The region  $\tilde{S}_2$  does not have any chambers in common with  $L_1$  or with  $P$ . We then choose  $Q_3$  arbitrarily, and if we want  $\gamma_2 = -1$ , we choose  $D_3$  such that there is no chamber connecting it to  $S_2$ . If we want  $\gamma_2 \leq -2$ , we choose  $D_3$  such that there is such a chamber. Proceed in this way.

We have now shown that given a  $\sigma$ -conjugacy class  $b$  such that either  $b = 1$  or  $\alpha + 2\beta \neq 0$ , and given a type edge pair  $(t, e) \in I_1$ , one can find  $x \in SL_3(L)$  such that  $x C_M$  has SMG of type  $t$  and departure edge  $e$ , and such that the invariants  $\gamma_1, \gamma_2$  associated with the composite gallery  $\Gamma_x$  are as desired (within the limitations  $1 \leq \gamma_1 \leq \gamma_1^{\max}$  and  $\gamma_2^{\min}(\gamma_1) \leq \gamma_2 \leq \gamma_2^{\max}(\gamma_1)$ ). This is useful because we will now prove that  $\rho(x^{-1}b\sigma(x)C_M)$  is determined by  $b, t, e, \gamma_1$ , and  $\gamma_2$ . Again, we consider cases.

*Case 1:  $\gamma_2 > 0$ .* See Figure 3.71, which represents the structure  $\overline{P} \cup P_\sigma$  transported back to  $C_M$  (in other words,  $x^{-1}(\overline{P} \cup P_\sigma)$ ). We can find  $g \in I$  that sends the shaded part of this picture to  $A_M$ . This is because one can find an apartment containing the shaded part of the figure but not containing the unshaded part. Therefore  $g$  does

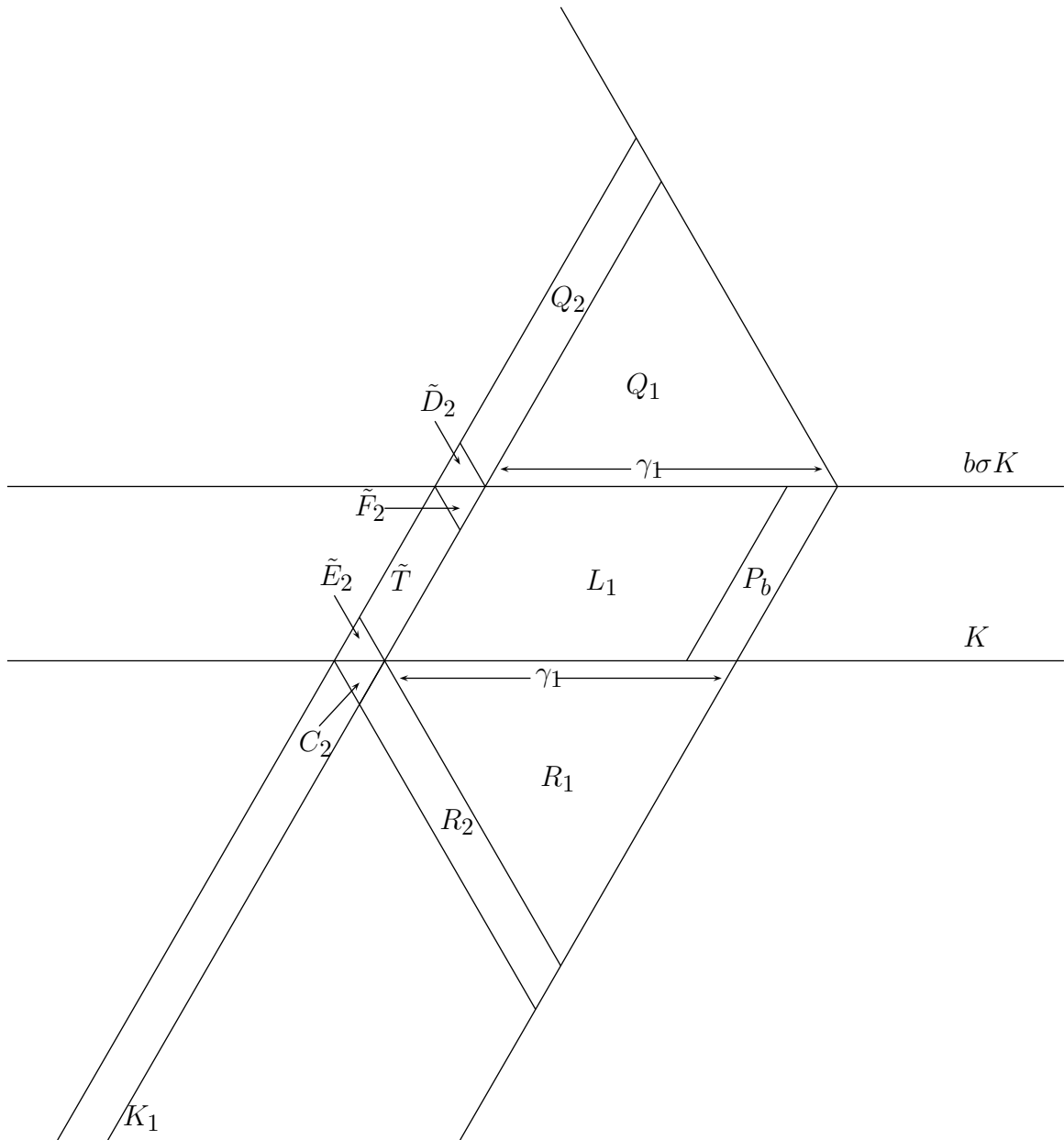


Figure 3.68: Existence of all negative values of  $\gamma_2$ , case 2 subcase 1

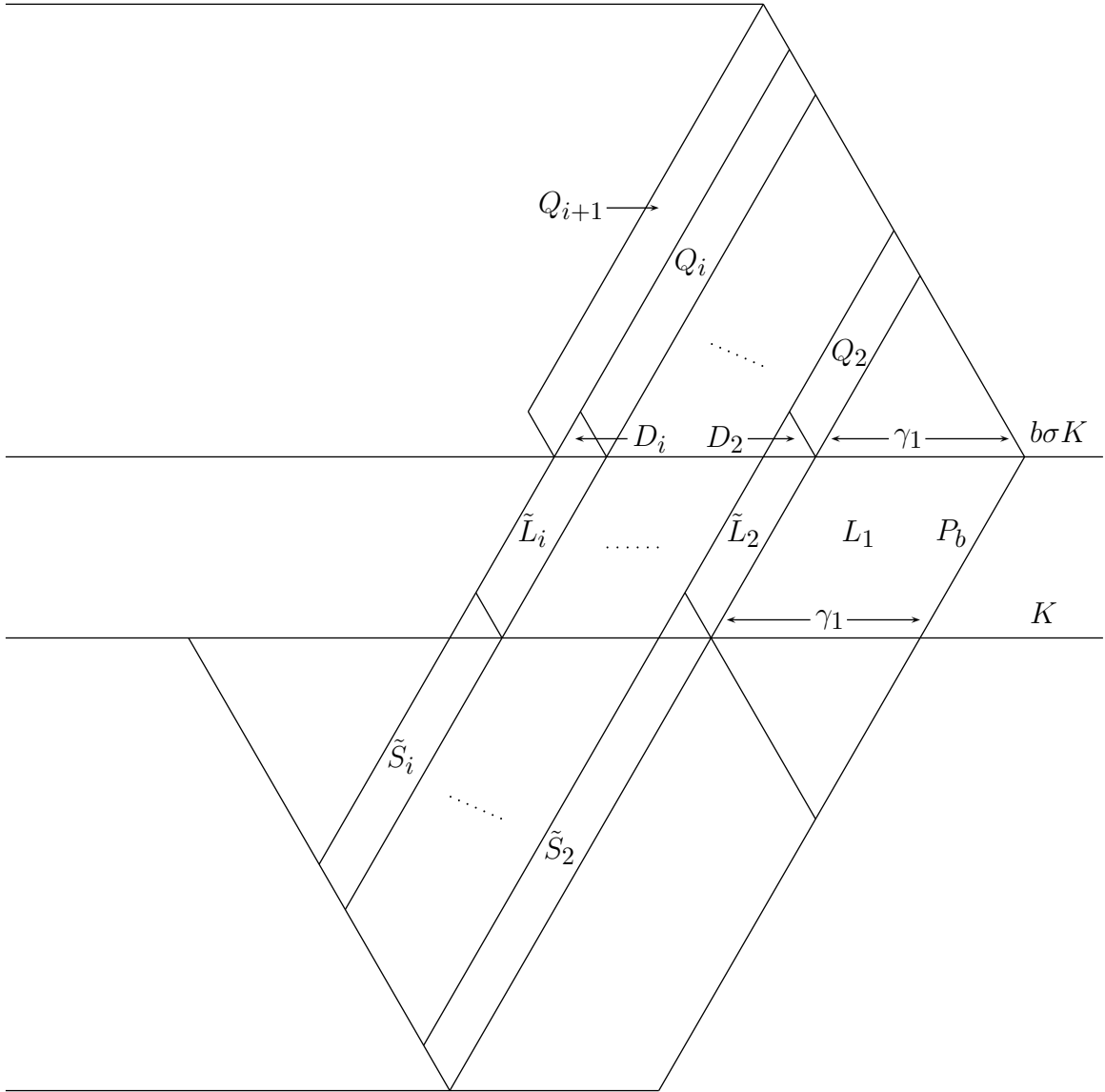


Figure 3.69: Existence of all negative values of  $\gamma_2$ , case 2 subcase 1 diagram 2

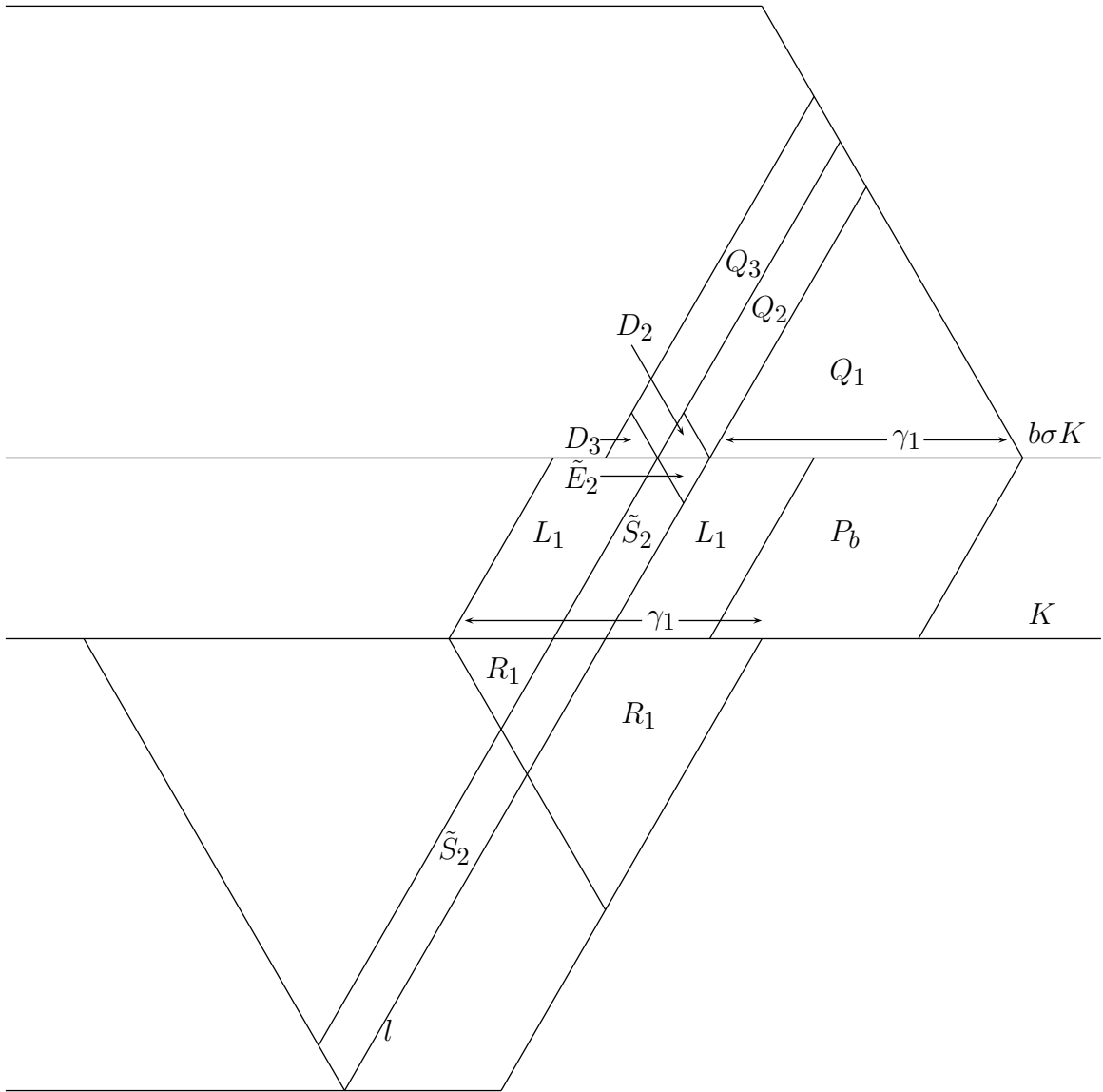


Figure 3.70: Existence of all negative values of  $\gamma_2$ , case 2 subcase 2



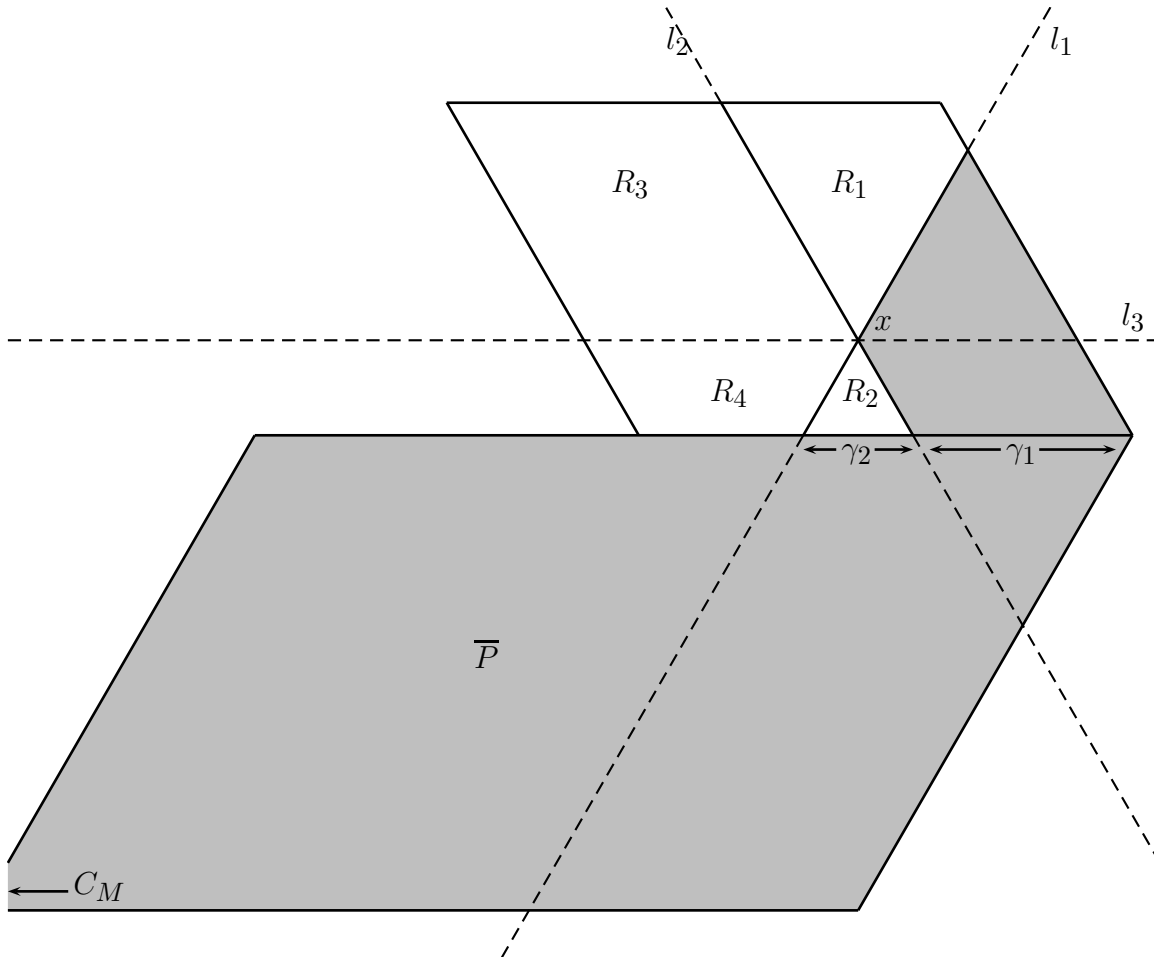


Figure 3.71:  $x^{-1}(\bar{P} \cup P_\sigma)$  for  $\gamma_2 > 0$

not send the unshaded part of the diagram to  $A_M$ . So we assume from this point forward that the shaded part of Figure 3.71 is in  $A_M$  and the unshaded part is not. It is easy to see now that  $\rho$  has the effect of reflecting the chambers in  $R_1$  across  $l_1$ , reflecting the chambers in  $R_2$  across  $l_2$ , reflecting the chambers in  $R_3$  first across  $l_1$  and then across  $l_3$ , and reflecting the chambers in  $R_4$  across  $l_2$ . So one can determine the value of  $\rho(x^{-1}b\sigma(x)C_M)$ . A specific example is given in Figure 3.72. Note that the existence of a corner at point  $x$  in the figure is necessary for the considerations that arrive at these results.

*Case 2:  $\gamma_2 \leq 0$ .* See Figure 3.73. Once again, we can arrange for the shaded part of the figure to be in  $A_M$ , and for the unshaded part to not be in  $A_M$ . According to the value of  $\gamma_2$ , we can connect  $P_\sigma$  to  $l$  using region  $\tilde{R}_1$  in Figure 3.74. Here,  $l$  is in  $\bar{P}$ , and  $\tilde{R}_1$  shares no chambers in common with  $\bar{P}$ . We can now fill in  $\tilde{R}_2$  uniquely using Lemma 3.1.6 so that it is connected above to  $P_\sigma$  and on the right to  $\tilde{R}_1$ . There now exist chambers  $\tilde{C}$  and  $\tilde{D}$  such that neither is in  $\bar{P}$ , but such that  $\tilde{C}$  is connected to

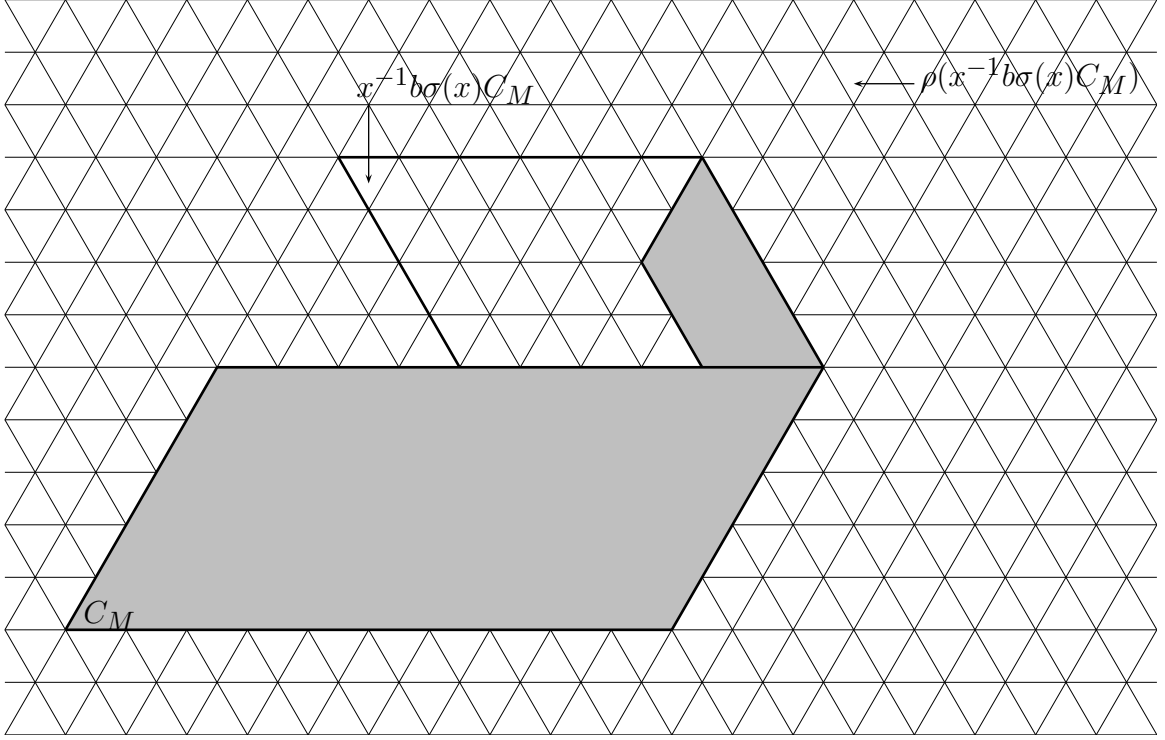


Figure 3.72: Example of how  $\gamma_1$  and  $\gamma_2$  determine  $\rho(x^{-1}b\sigma(x)C_M)$

$\tilde{R}_2$ , and  $\tilde{D}$  has its right edge in  $\overline{P}$ . Also,  $\tilde{C}$  and  $\tilde{D}$  are connected to each other. We fill in  $\tilde{R}_3$  using Lemma 3.1.6. With respect to folding, the corner labeled with an  $x$  is similar in function to the corner labeled with an  $x$  in Figure 3.71. As such, referring to Figure 3.75, chamber  $\tilde{D}$  is reflected across  $l_2$  by  $\rho$ , the chambers in region  $\tilde{B}_1$  (some of which are in  $P_\sigma$  and some of which are not in  $\overline{P} \cup P_\sigma$ ) are reflected across  $l_1$ , the chambers in  $\tilde{B}_2$  (some of which are in  $P_\sigma$  and some of which are not in  $\overline{P} \cup P_\sigma$ ) are reflected first across  $l_1$ , then across  $l_3$ , and the chambers in  $\tilde{B}_3$  are reflected across  $l_2$ . So one can determine the value of  $\rho(x^{-1}b\sigma(x)C_M)$  for any specific example.

In Section 3.1.2, we computed chambers to include in the superset  $S_1$  by computing all possible foldings of the composite gallery  $\Gamma_x$  for  $x$  giving rise to any fixed type-edge pair  $(t, e)$ . The set  $S_1$  consisted of the union of these results for all  $(t, e)$  in  $I_1 \cup I_2$ . We are now in a position to show that for all  $(t, e) \in I_1$ , the collection of possible foldings of  $\Gamma_x$  gives rise only to chambers in  $S$ . This, combined with similar results for  $I_2$  proves that  $S = S_1$  for  $b = 1$  or  $b$  with  $\alpha + 2\beta \neq 0$ .

Let  $S_{(t,e)}^f$  be the collection of chambers obtained by computing the possible foldings of  $\Gamma_x$  for  $x$  giving rise to the type-edge pair  $(t, e)$ . So

$$S_1 = \left[ \bigcup_{(t,e) \in I_1} S_{(t,e)}^f \right] \cup \left[ \bigcup_{(t,e) \in I_2} S_{(t,e)}^f \right].$$

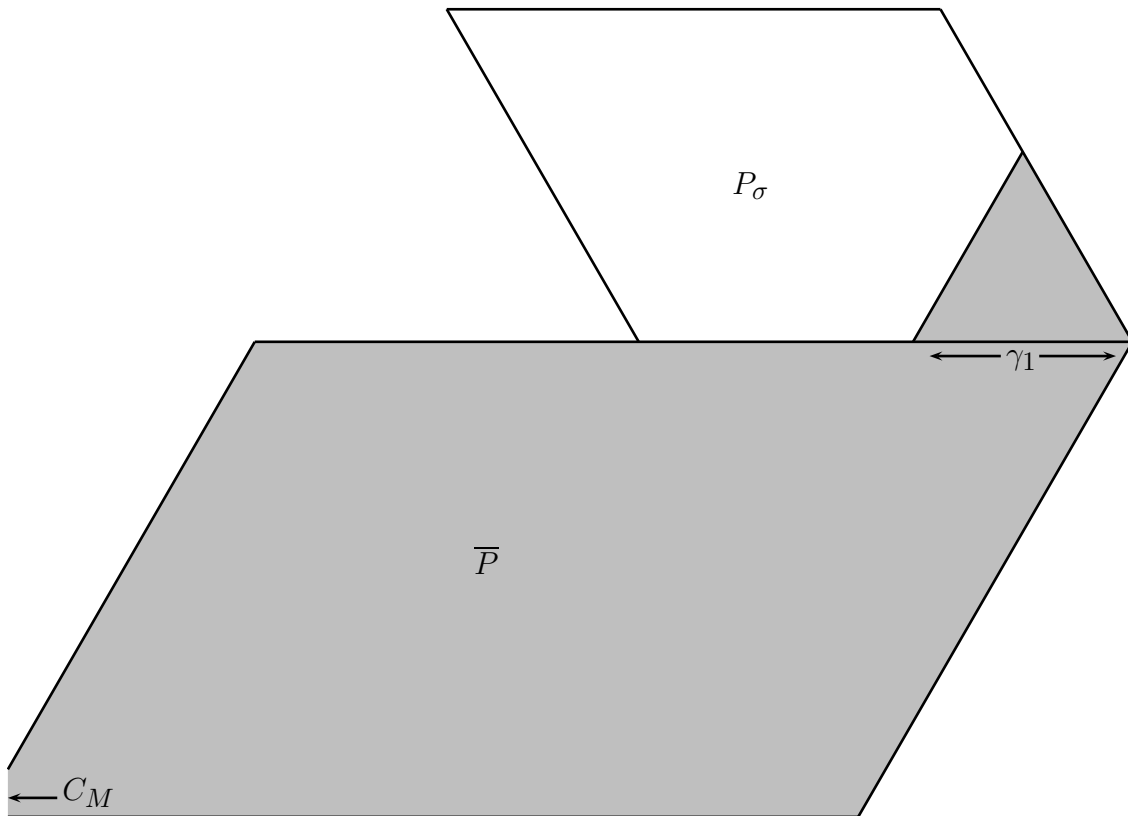


Figure 3.73:  $x^{-1}(\bar{P} \cup P_\sigma)$  for  $\gamma_2 \leq 0$

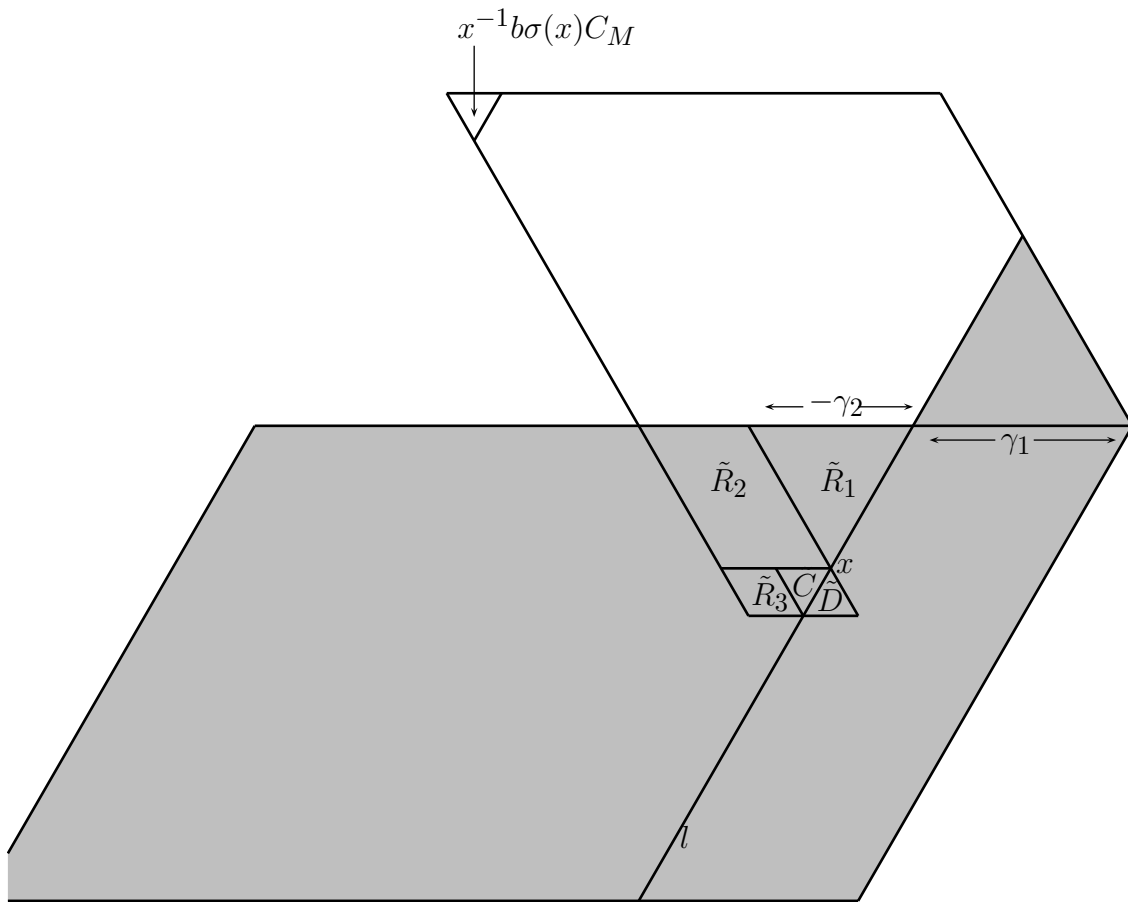


Figure 3.74:  $x^{-1}(\overline{P} \cup P_\sigma)$  for  $\gamma_2 \leq 0$ , folding explained

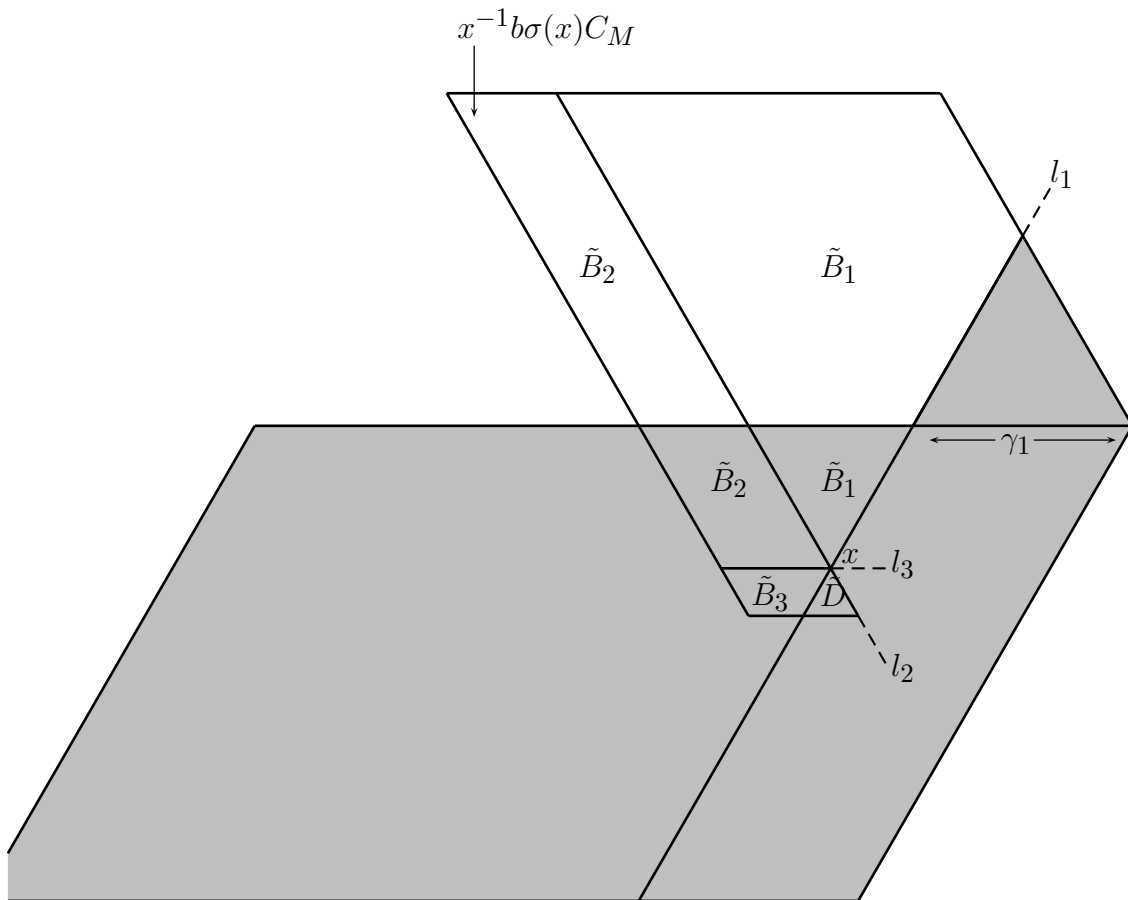


Figure 3.75:  $x^{-1}(\overline{P} \cup P_\sigma)$  for  $\gamma_2 \leq 0$ , folding explained further

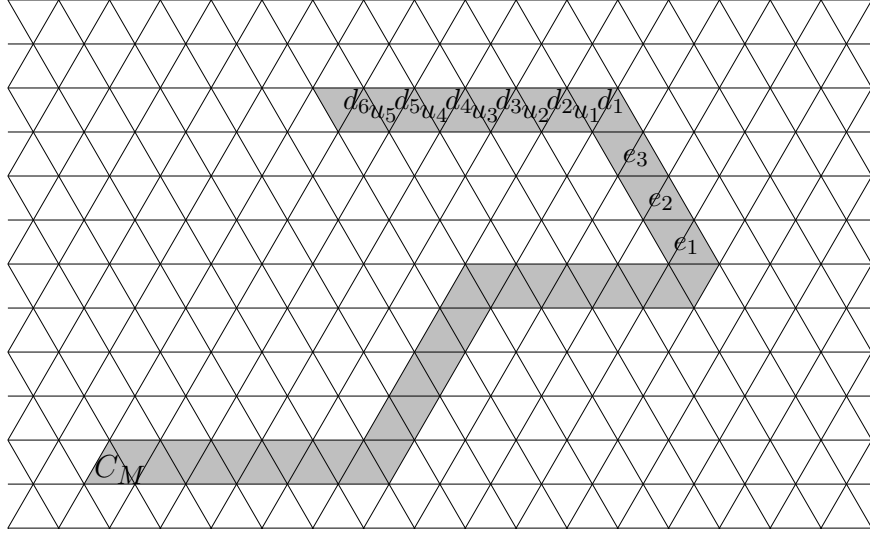


Figure 3.76: Choice Points

Let  $S_{(t,e)}^\gamma$  be the collection of the  $\rho(x^{-1}b\sigma(x)C_M)$  (which can now be computed for  $(t,e) \in I_1$  and either  $b = 1$  or  $\alpha + 2\beta \neq 0$ ) coming from  $x$  giving rise to  $(t,e)$  and any invariants  $\gamma_1$  and  $\gamma_2$  such that  $1 \leq \gamma_1 \leq \gamma_1^{\max}(t,e)$  and  $\gamma_2^{\min}(t,e,\gamma_1) \leq \gamma_2 \leq \gamma_2^{\max}(t,e,\gamma_1)$ . We will show that  $S_{(t,e)}^\gamma = S_{(t,e)}^f$  (again, only for  $(t,e) \in I_1$  and either  $b = 1$  or  $\alpha + 2\beta \neq 0$ ). To do this, we begin by dissecting  $S_{(t,e)}^f$ .

When computing the possible values of  $\rho(x^{-1}b\sigma(x)C_M)$ , one can work through the chambers of  $x^{-1}\Gamma_x$  starting with  $C_M$ , making a choice of folding direction at each choice point. At choice point  $e$  between chambers  $i$  and  $i+1$ , we define the *status quo choice* to be the one in which  $i$  and  $i+1$  go to different chambers. The *change choice* is the choice in which  $i$  and  $i+1$  go to the same chamber. Note that if a change choice is made at an edge  $e$ , then choice points subsequent to  $e$  in  $x^{-1}\Gamma_x$  may become non-choice points, and vice versa. The possible values of  $\rho(x^{-1}b\sigma(x)C_M)$  can be enumerated by exploring the binary tree described by the choice point structure of  $x^{-1}\Gamma_x$ .

It is easy to see that if one makes the status quo choice at all edges before some edge  $u_i$  in Figure 3.76, and then one makes a change choice at  $u_i$  itself, then all subsequent edges become non-choice points and  $\rho(x^{-1}b\sigma(x)C_M)$  is determined. This value for  $\rho(x^{-1}b\sigma(x)C_M)$  is in  $S_{(t,e)}^\gamma$  because we may choose  $\gamma_1 = i$  and  $\gamma_2$  maximal. The value of  $\rho(x^{-1}b\sigma(x)C_M)$  obtained by making only status quo choices is in  $S_{(t,e)}^\gamma$  because we may choose  $\gamma_1$  and  $\gamma_2$  maximal.

It is easy to see that if one makes the first change choice at some  $d_i$ , then one may make at most one subsequent change choice, and such a subsequent change choice can only be made an odd number  $s$  of edges after  $d_i$ . The resulting value

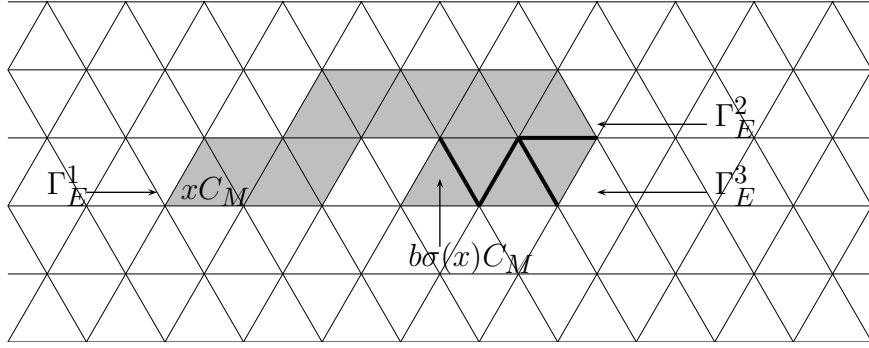


Figure 3.77: A composite gallery for  $p = 1$ ,  $\alpha = 2$ ,  $\beta = -1$

of  $\rho(x^{-1}b\sigma(x)C_M)$  is in  $S_{(t,e)}^\gamma$  because we may choose  $\gamma_1$  and  $\gamma_2$  such that  $\gamma_1 + \max\{\gamma_2, 0\} = S(P_\sigma) + i - 1$  (to ensure that the first change choice occurs at  $d_i$ ) and such that  $\gamma_1 - \min\{0, \gamma_2\} = \frac{s+1}{2}$  (to ensure that the second change choice occurs  $s$  edges after  $d_i$ ). If no second change choice is desired, then choose  $\gamma_2 = \gamma_2^{\min}(\gamma_1)$ .

If one makes the first change choice at some  $e_i$ , then only one subsequent change choice is possible. If such a change choice is made, it must be done at one of the  $u_j$ . The resulting  $\rho(x^{-1}b\sigma(x)C_M)$  is in  $S_{(t,e)}^\gamma$  because we may choose  $\gamma_1$  and  $\gamma_2$  such that  $\gamma_1 + \max\{\gamma_2, 0\} = i$  and such that  $\gamma_1 - \min\{\gamma_2, 0\} = j$ . If no second change choice is desired, choose  $\gamma_2 = \gamma_2^{\min}(\gamma_1)$ .

In essence, the choice of  $\gamma_1$  and  $\gamma_2$  above corresponds to choosing the point  $x$  in Figures 3.71 and 3.75 such that  $l_1$  passes through the first change choice and  $l_2$  passes through the second.

We now address the situation where  $(t, e) \in I_1$  still, but now  $b \neq 1$  and  $\alpha + 2\beta = 0$ . As before, let  $p$  be the number of chambers in  $\Gamma_E^3$  between the edge of departure and the turning edge. So  $p \geq 1$  is odd. We first consider the case where  $p = 1$ . So, fixing  $t, e, b$  with the specified properties, and choosing  $y \in SL_3(L)$  such that  $y$  gives rise to  $(t, e)$ , and given some possible folding of a gallery of the same type as  $y^{-1}\Gamma_y$ , we want to show that there is  $x \in SL_3(L)$  such that  $\rho(x^{-1}b\sigma(x)C_M)$  is the last chamber of this folding.

For  $p = 1$ , a sample composite gallery for  $b$  with  $\alpha = 2$ ,  $\beta = -1$  is pictured in Figure 3.77. The choice points are marked. For general  $p, b$ , we get a similar structure, with every edge in  $\Gamma_E^3$  a choice point, and the edge between  $\Gamma_E^2$  and  $\Gamma_E^3$  another choice point. Note that for  $p = 1$ , if one makes a change choice at any choice point other than the horizontal one between  $\Gamma_E^2$  and  $\Gamma_E^3$ , no subsequent choices are available. A change choice at the horizontal change point allows at most two more choices.

Let  $K$  be a wall in  $A_M$  such that  $bK = K$ . Let  $T$  be the first row of chambers in some half apartment coming out of  $K$ . Choose  $T \subseteq \mathcal{B}_1$ , so  $\sigma$  does not affect  $T$ . Then  $b\sigma(T) = T$ . Choose the first  $i$  chambers of  $\Gamma_E^3$  in  $T$ , and the rest not in

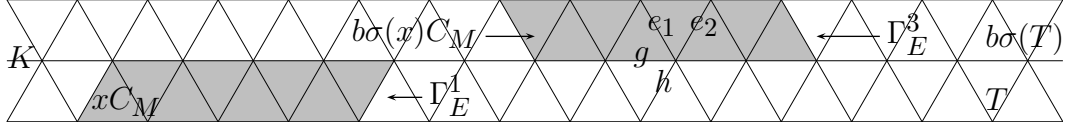


Figure 3.78: All foldings of composite galleries with  $p = 1$  occur, where  $b \neq 1$  and  $\alpha + 2\beta = 0$

$T$ . So  $\Gamma_E^1 = \sigma^{-1}b^{-1}(\Gamma_E^3)$  and  $\Gamma_E^2 \subseteq A_M$  are determined. This composite gallery construction folds in such a way that the first (and only) change choice occurs in  $\Gamma_E^3$  between the  $i$ th and  $(i + 1)$ st chambers. To arrange no change choices at all, choose  $\Gamma_E^3 \subseteq T$ .

To arrange that the edge between  $\Gamma_E^2$  and  $\Gamma_E^3$  be a change choice, take  $T \subseteq \mathcal{B}_2 \setminus \mathcal{B}_1$ . Then  $b\sigma(T) \cap T = K$ . If we want no subsequent change choice, then choose  $\Gamma_E^3 \subseteq b\sigma(T)$ . If we want the second change choice to be between the  $i$ th and  $(i + 1)$ st chambers in  $\Gamma_E^3$ , then choose the first  $i$  chambers of  $\Gamma_E^3$  in  $b\sigma(T)$ , and the rest outside of  $b\sigma(T)$ . We now have a situation for which Figure 3.78 is an example (here  $b$  has  $\alpha = 4$  and  $\beta = -2$ ). The galleries  $\Gamma_E^1$  and  $\Gamma_E^3$  are drawn as part of  $T$  and  $b\sigma(T)$ , respectively, in this diagram, even though only part of each need be.

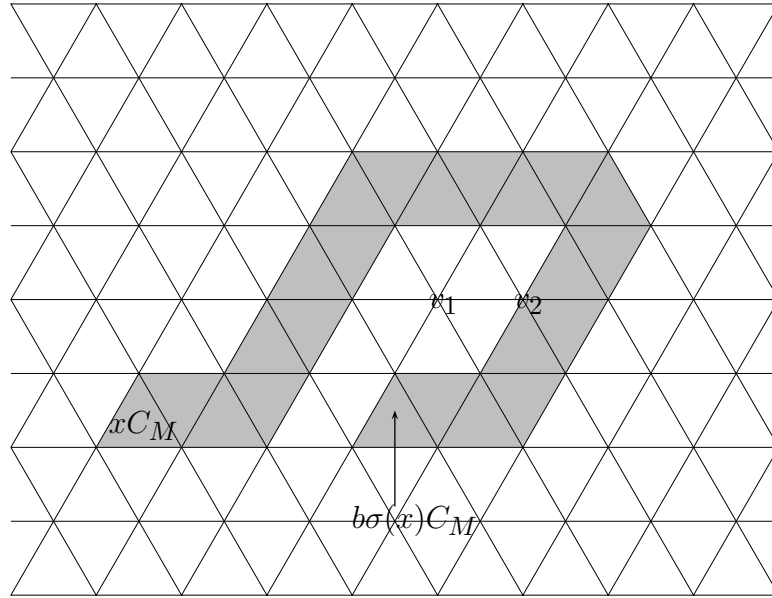
Let  $e$  be the edge in  $\Gamma_E^3$  at which the second change choice is to occur. Then the chambers of  $\Gamma_E^3$  that are part of  $b\sigma(T)$  are exactly those that occur before  $e$ . If  $e$  is an edge of the same angle as  $e_1$  in Figure 3.78, then no subsequent change choice is possible. If  $e$  is of the same angle as  $e_2$ , then  $e_1$  could be a third (and final) change choice. To arrange this, choose  $\Gamma_E^3$  in such a way that there is no chamber connecting edge  $g$  to edge  $h$ . To arrange no third change choice, choose  $\Gamma_E^3$  such that there is a chamber connecting  $g$  to  $h$ .

We have now shown for  $p = 1$  that any possible folding can occur. We now assume inductively that any possible folding can occur for  $p \leq n$ . Suppose that  $x$  gives rise to a type-edge pair  $(t, e)$  with  $p = n + 1$ , and a composite gallery  $\Gamma_x$ . We begin by defining an invariant  $\gamma_3$  of  $x$ . Consider Figure 3.79, which shows an example composite gallery for  $b$  with  $\alpha = 2$ ,  $\beta = -1$ . We use Lemma 3.1.6 to add vertices  $v_1$  and  $v_2$  to the structure. Note that  $v_2$  may or may not be part of  $\Gamma_x$ . If  $v_2$  is in  $\Gamma_x$  then we say  $\gamma_3 \geq 1$ . If  $v_2$  is not in  $\Gamma_x$ , then we say  $\gamma_3 = 0$ . Although we have only given the definition of  $\gamma_3$  for the specific example of Figure 3.79, it is clear how one would proceed in general. Note that  $\gamma_3$  does not necessarily have a specific value. We either have  $\gamma_3 = 0$  or  $\gamma_3 \geq 1$ .

In case  $\gamma_3 \geq 1$ , we can find a gallery from  $xC_M$  to  $b\sigma(x)C_M$  that is of the same shape as a composite gallery of some type-edge pair with  $p = n$ . Therefore, by induction, we need not worry about this case.

If  $\gamma_3 = 0$ , then the edge between  $\Gamma_E^2$  and  $\Gamma_E^3$  is forced to be a change choice. For instance, the gallery in Figure 3.79 becomes the gallery in Figure 3.80 upon addition of the vertex  $v_3$  (which can be done using Lemma 3.1.6). We can use techniques



Figure 3.79: Definition of  $\gamma_3$ 

similar to those used in the first part of this section to show that one can arrange for such a gallery to fold in any desired way.

To finish the proof that  $S_1 = S$ , it would be necessary to consider  $(t, e) \in I_2$ . One should consider the case  $b = 1$  and the cases  $2\alpha + \beta \neq \alpha + 2\beta$  separately from the cases in which  $b \neq 1$  but  $2\alpha + \beta = \alpha + 2\beta$ . The process is similar to what we have already done, and is omitted.

### 3.1.7 Symmetry Under a $\mathbb{Z}/3$ -action

In Section 2.1.3 we noticed from results developed in Sections 2.1.1 and 2.1.2 that for  $SL_2$ , the set of  $w$  with non-empty  $X_w(b\sigma)$  has  $\mathbb{Z}/2$ -symmetry about the center of  $C_M$ . We gave an *a priori* proof of this fact. The results developed for  $SL_3$  in the previous sections of this chapter indicate that in this case the set of  $w$  with non-empty  $X_w(b\sigma)$  has  $\mathbb{Z}/3$ -rotational symmetry about the center of  $C_M$ . We adapt the proof from Section 2.1.3 to give an *a priori* proof of the  $SL_3$  symmetry.

Let

$$q = \begin{pmatrix} 0 & 0 & \pi \\ 1 & 0 & 0 \\ 0 & 1 & 0 \end{pmatrix} \in GL_3(F).$$

This matrix acts on  $A_M$  by rotating it  $120^\circ$  counterclockwise about the center of  $C_M$ . Let

$$g = \begin{pmatrix} \pi & 0 & 0 \\ 0 & 1 & 0 \\ 0 & 0 & 1 \end{pmatrix} \in GL_3(F).$$

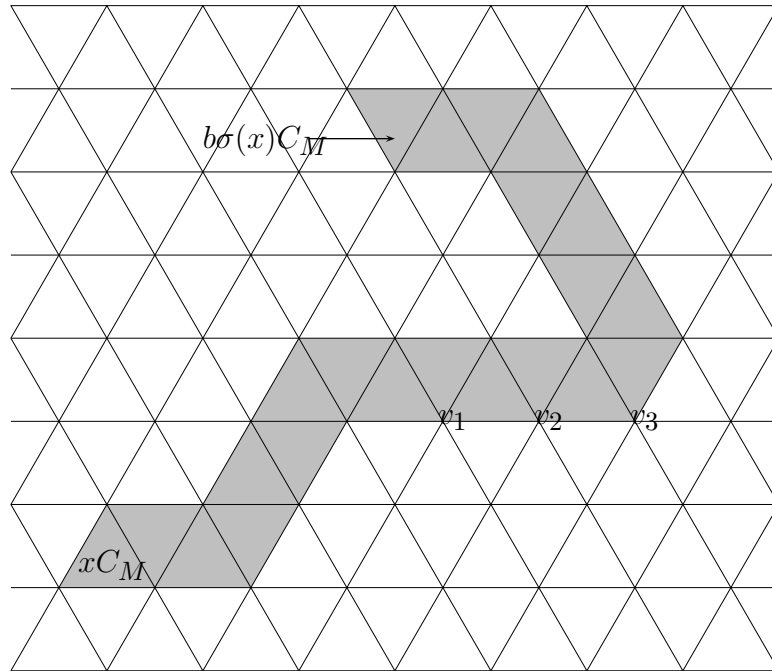


Figure 3.80: What happens to Figure 3.79 when  $\gamma_3 = 0$

**Proposition 3.1.8.**  $inv(gxC_M, b\sigma(gx)C_M) = R_{120^\circ}(inv(xC_M, b\sigma(x)C_M))$ , where  $R_{120^\circ}$  denotes rotation counterclockwise by  $120^\circ$  around the center of  $C_M$ . So  $inv(g^2xC_M, b\sigma(g^2x)C_M) = R_{240^\circ}(inv(xC_M, b\sigma(x)C_M))$ .

*Proof.* We know that  $inv(gxC_M, b\sigma(gx)C_M) = \rho(s^{-1}b\sigma(gx)C_M)$  where  $s \in SL_3(L)$  is chosen such that  $s^{-1}gxC_M = C_M$ . We may choose  $s$  such that  $s^{-1} = qx^{-1}g^{-1}$ . So  $\rho(s^{-1}b\sigma(gx)C_M) = \rho(qx^{-1}g^{-1}b\sigma(gx)C_M) = \rho(qx^{-1}b\sigma(x)C_M)$ , and this is in turn equal to  $R_{120^\circ}(\rho(x^{-1}b\sigma(x)C_M)) = R_{120^\circ}(inv(xC_M, b\sigma(x)C_M))$ .  $\square$

This is relevant because if  $y \in SL_3(L)$  is such that  $yC_M = gxC_M$ , then we have  $inv(y, b\sigma(y)) = inv(gxC_M, b\sigma(gx)C_M)$ .

One could prove an analogous result for  $SL_n$ , only it would be an invariance under a  $\mathbb{Z}/n$ -action. The proof is the same, only one replaces  $g$  and  $q$  with the analogous  $n \times n$  matrices.

### 3.2 $GL_3$ and $PGL_3$

We now have  $inv : G(L) \times G(L) \rightarrow I \backslash G(L) / I \simeq \tilde{W} \simeq W_a \rtimes M$ , where if  $G = GL_3$  then  $M = \mathbb{Z}$ , and if  $G = PGL_3$  then  $M = \mathbb{Z}/3$ . In either case,  $inv(x, y) = (\rho(x^{-1}yC_M), v(\det(x^{-1}y)))$ , but if  $G = GL_3$  then  $v(\det(x^{-1}y)) \in \mathbb{Z}$  and if  $G = PGL_3$  then  $v(\det(x^{-1}y)) \in \mathbb{Z}/3$ . The matrices  $b$  listed at the beginning of Section 3.1 as representing distinct  $\sigma$ -conjugacy classes in  $SL_3$  still represent distinct classes when

considered as elements of  $GL_3$  or  $PGL_3$ . Further, any two  $\sigma$ -conjugacy classes of  $SL_3$  remain distinct when we pass to  $\sigma$ -conjugacy classes of  $GL_3$  or  $PGL_3$ . It is also true that  $GL_3$  and  $PGL_3$  have more  $\sigma$ -conjugacy classes than  $SL_3$ , just as was the case for the analogous rank one groups. Unlike in the rank one case, we will not address these additional  $\sigma$ -conjugacy classes, since for one thing we have not even addressed all the  $\sigma$ -conjugacy classes of  $SL_3$  itself.

If  $b$  is one of the matrices listed at the beginning of Section 3.1, this time considered as an element of  $GL_3$  or  $PGL_3$ , then we ask for a description of  $\{inv(x, b\sigma(x)) : x \in G(L)\}$ , i.e., we want to describe  $\{(\rho(x^{-1}b\sigma(x)C_M), v(\det(x^{-1}b\sigma(x)))) \in W_a \times M : x \in G(L)\}$ . We note that  $v(\det(x^{-1}b\sigma(x))) = v(\det(b))$  is fixed for fixed  $b$  (and equal to 0 for the  $b$  we have chosen). So we need to examine  $\{\rho(x^{-1}b\sigma(x)C_M) \in W_a : x \in G(L)\}$ , which, *a priori*, may be bigger than  $\{\rho(x^{-1}b\sigma(x)C_M) \in W_a : x \in SL_3(L)\}$ , since  $G(L)$  acts on  $\mathcal{B}_\infty$  in ways that  $SL_3$  does not. However, if  $q$  is as defined in Section 3.1.7, and if  $y = q^{-v(\det(x))}$  then  $v(\det(xy)) = 0$ . Note that if  $G = PGL_3$ , then  $v(\det(x))$  is only determined mod 3. But since  $q^3$  is a scalar matrix, this does not cause problems with the definition of  $y$ . Now  $\det(xy) \in \mathcal{O}_L^\times$ , and since  $(\mathcal{O}_L^\times)^3 = \mathcal{O}_L^\times$ , we may further modify  $xy$  on the right by a scalar matrix of determinant  $\det(xy)^{-1}$ . Therefore we may assume without loss of generality that  $\det(xy) = 1$ , i.e.,  $xy \in SL_3(L)$ . But  $xyC_M = xC_M$ , so  $\sigma(xy)C_M = \sigma(x)C_M$ , so  $b\sigma(xy)C_M = b\sigma(x)C_M$ , so  $x^{-1}b\sigma(xy)C_M = x^{-1}b\sigma(x)C_M$ , so  $\rho(x^{-1}b\sigma(xy)C_M) = \rho(x^{-1}b\sigma(x)C_M)$ . But it is easy to see that  $\rho(y^{-1}x^{-1}b\sigma(xy)C_M)$  is just a rotation of  $\rho(x^{-1}b\sigma(xy)C_M)$  about the center of  $C_M$  by  $(120^\circ)(v(\det(x)))$  counterclockwise. Since we already proved that the set  $\{\rho(x^{-1}b\sigma(x)C_M) : x \in SL_3(L)\}$  is rotation invariant by  $120^\circ$  and  $240^\circ$ , we see that  $\{\rho(x^{-1}b\sigma(x)C_M) : x \in SL_3(L)\} = \{\rho(x^{-1}b\sigma(x)C_M) : x \in G(L)\}$ .

### 3.3 $Sp_4$

We have applied some of the methods of Section 3.1 to  $Sp_4$ . This section contains outlines of the application of these methods, and the results. The structure of the section is the same as that of Section 3.1.

The version of  $Sp_4(E)$  that we will use for  $E/F$  a field extension is the fixed points in  $GL_4(E)$  of the involution  $\Theta : GL_4(E) \rightarrow GL_4(E)$  where  $\Theta(g) = M^{-1}(g^t)^{-1}M$  for

$$M = \begin{pmatrix} 0 & 0 & 0 & 1 \\ 0 & 0 & -1 & 0 \\ 0 & 1 & 0 & 0 \\ -1 & 0 & 0 & 0 \end{pmatrix}.$$

Note that if  $T$  is the standard maximal torus in  $GL_4$ , then the fixed points  $T^\Theta$  form a split maximal torus in  $Sp_4$ , and if  $B$  is the standard Borel subgroup of  $GL_4$ , then the fixed points  $B^\Theta$  form a Borel for  $Sp_4$ .

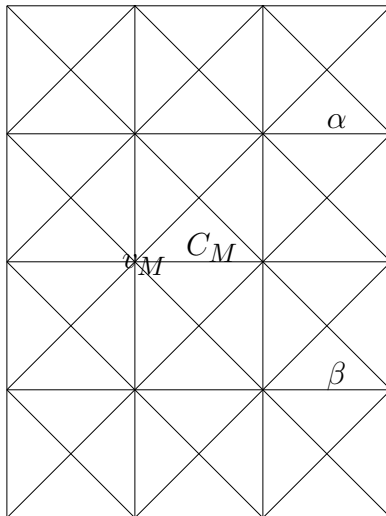


Figure 3.81: How the torus of  $Sp_4$  acts on  $A_M$

The letter  $b$  in this section will always stand for an element of  $Sp_4$  of the form

$$\begin{pmatrix} \pi^\alpha & 0 & 0 & 0 \\ 0 & \pi^\beta & 0 & 0 \\ 0 & 0 & \pi^{-\beta} & 0 \\ 0 & 0 & 0 & \pi^{-\alpha} \end{pmatrix},$$

where  $\alpha \geq \beta \geq 0$ . These represent distinct  $\sigma$ -conjugacy classes in  $Sp_4(L)$ , but they do not constitute a complete collection of  $\sigma$ -conjugacy classes. [6] [7]

To understand something about how  $Sp_4$  acts on the main apartment of its building, consider Figure 3.81. The main chamber and the main vertex are labeled in this figure, and the value of  $bC_M$  with  $\alpha = 1$  and  $\beta = 0$  is labeled with an  $\alpha$ . The value of  $bC_M$  with  $\alpha = 0$  and  $\beta = 1$  is labeled with a  $\beta$ .

### 3.3.1 Standard Minimal Galleries and Composite Galleries

We define the four *primary directions*  $D_1, D_2, D_3, D_4$  and the four *secondary directions*  $d_1, d_2, d_3, d_4$  in  $A_M$  for  $Sp_4$  as marked in Figure 3.82. Given a chamber  $E \subseteq A_M$ , we define the *standard minimal gallery* (SMG) between  $C_M$  and  $E$  as follows. If  $E$  is in one of the corridors marked  $c_1, \dots, c_8$  on Figure 3.82, then the SMG is the unique minimal gallery from  $C_M$  to  $E$ . If  $E$  is in region  $R_i$ , proceed first in direction  $D_i$ , then in direction  $d_i$ . If  $E$  is in region  $r_i$ , proceed first in direction  $D_i$ , then in direction  $d_j$ , where  $j \equiv i + 1 \pmod{4}$ .

As was the case for  $SL_3$ , one can prove that if  $E$  is now allowed to be a chamber anywhere in the building  $\mathcal{B}_\infty$  of  $Sp_4(L)$ , then there exists a unique gallery  $G_E$  between

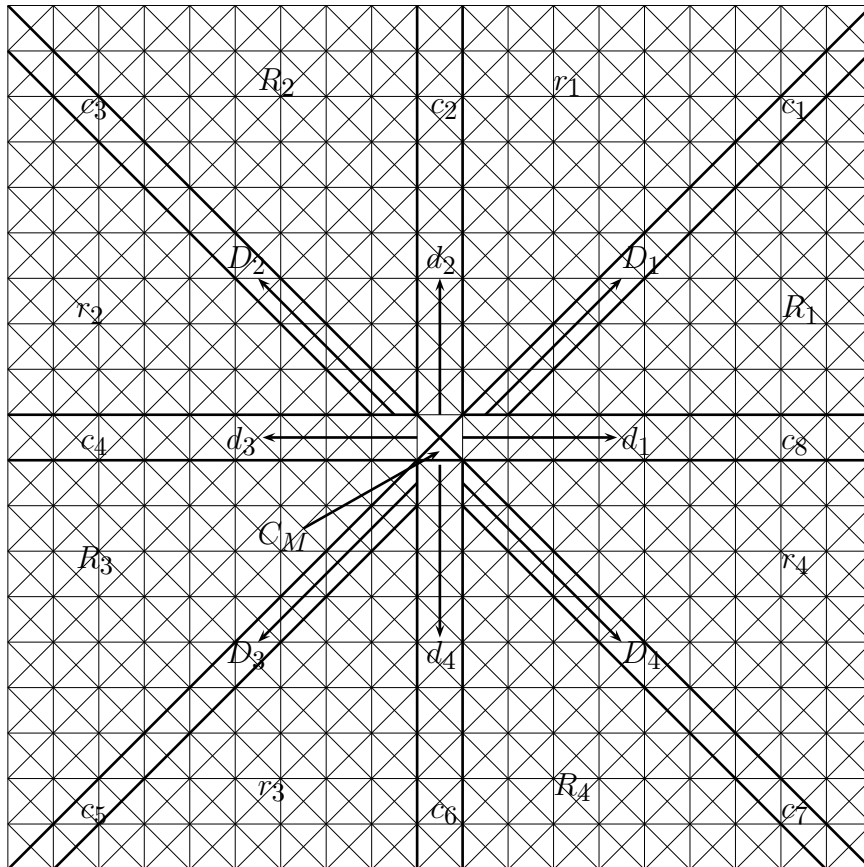


Figure 3.82: Primary and Secondary Directions in  $Sp_4$

$C_M$  and  $E$  which is minimal and such that  $\rho(G_E)$  is the SMG from  $C_M$  to  $\rho(E)$ . We define the SMG from  $C_M$  to  $E$  to be  $G_E$  in this case.

We construct the *composite gallery*  $\Gamma_E$  associated to  $E$  as in the  $SL_3$  case. We also define the *edge of departure* in the same way as for  $SL_3$

### 3.3.2 A Conjectural Superset of the Solution Set

Just as for  $SL_3$ , we can arrive at a superset  $S_1$  of the solution set  $S$  by computing  $S_1 = \cup_{(t,e)} S_{(t,e)}$ , where the union is over all type-edge pairs  $(t, e)$ , and  $S_{(t,e)}$  is the collection of final chambers of possible foldings of composite galleries arising from SMGs of type  $t$  and edge of departure  $e$ . This computation is even more prohibitively lengthy than was the case for  $SL_3$ , and has only been carried out to completion for  $b = 1$ , for which the results are in Figure 3.83.

Let  $I_1$  be the infinite class of type-edge pairs  $(t, e)$  with  $t$  the type of the SMG of some chamber in  $r_2$ , and  $e$  some horizontal departure edge. Let  $I_2$  be the infinite class of type-edge pairs  $(t, e)$  with  $t$  the type of the SMG of some chamber in  $c_4$ , and  $e$  an arbitrary departure edge. These  $I_1$  and  $I_2$  are analogous to the infinite classes of the same name for  $SL_3$ .

**Conjecture 3.3.1.**  $S_1 = \cup_{(t,e)} S_{(t,e)}$ , where the union is over all type-edge pairs in  $I_1 \cup I_2$ .

Computation of  $\cup_{(t,e)} S_{(t,e)}$  as  $(t, e)$  ranges over  $I_1 \cup I_2$  is a lengthy but reasonable computation. The details of this computation for any  $b$  are discussed in Section 3.3.3. For  $\alpha = 3$  and  $\beta = 1$ , the results are given in Figure 3.84. For  $\alpha = 6$ ,  $\beta = 3$ , the results are given in Figure 3.85, for  $\alpha = 6$ ,  $\beta = 5$  the results are given in Figure 3.86, and for  $\alpha = 7$ ,  $\beta = 1$  the results are given in Figure 3.87. The lines on these figures and on Figure 3.83 are only there to make the figures easier to look at. The chambers in Figure 3.84 that are shaded more darkly are the chambers  $w^{-1}bwC_M$  for  $w \in W$ .

The first piece of evidence supporting Conjecture 3.3.1 is that for  $\alpha = \beta = 0$ ,  $I_1$  and  $I_2$  yield Figure 3.83, which is the complete computation  $\cup_{(t,e)} S_{(t,e)}$ , as  $(t, e)$  ranges over all type-edge pairs.

The chambers marked with a  $*$  in Figures 3.84, 3.85, 3.86, and 3.87 provide evidence against Conjecture 3.3.1, as they seem to be holes in the pattern. However, it could be the case that these chambers are actually missing from the true  $S_1 = \cup_{(t,e)} S_{(t,e)}$ , where the union is over all  $(t, e)$ . Preliminary computations not presented seem to provide some evidence that this is the case, in support of Conjecture 3.3.1. However, this evidence is not a strong indication.

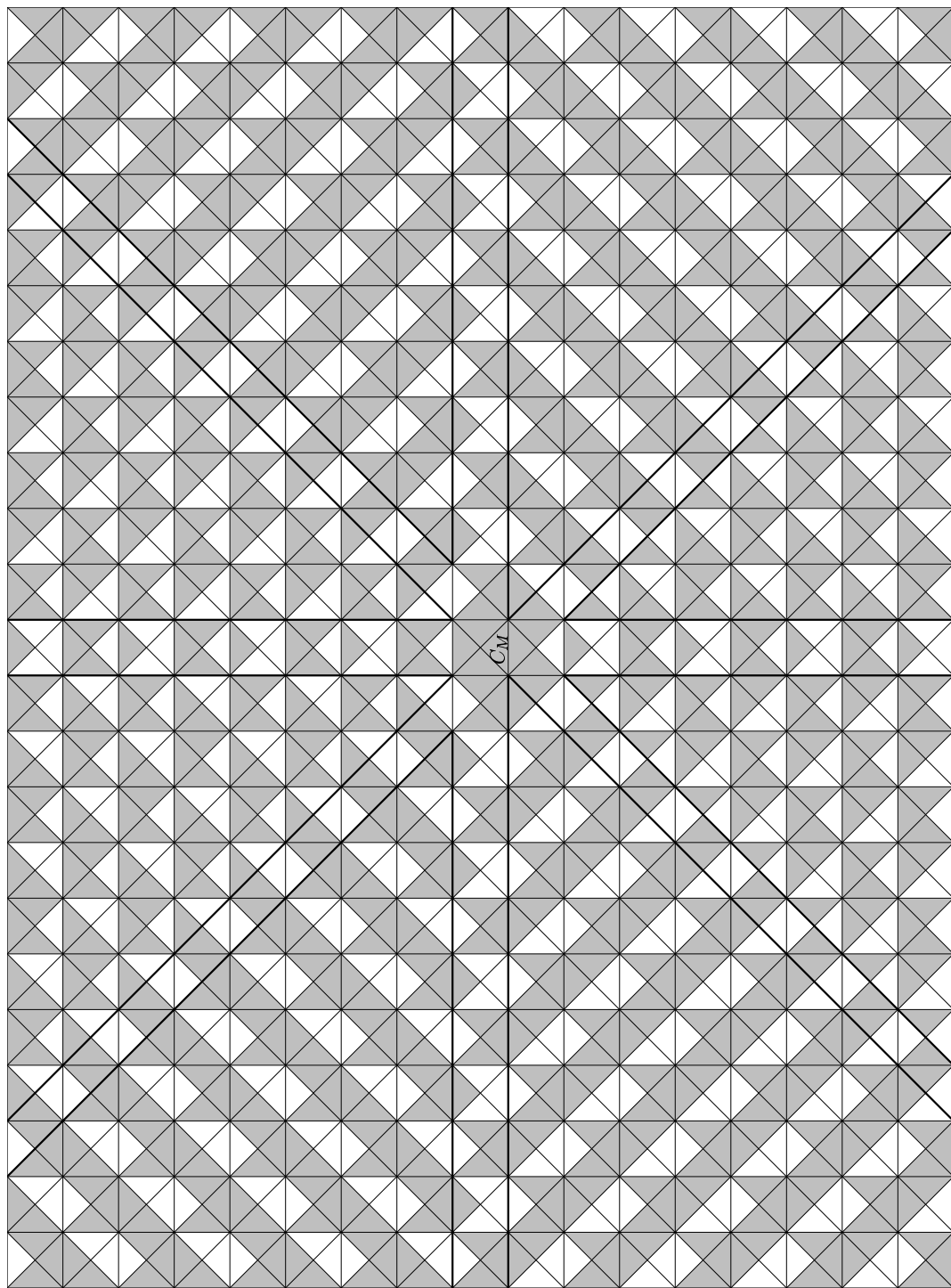


Figure 3.83: Result for  $b = 1, Sp_4$

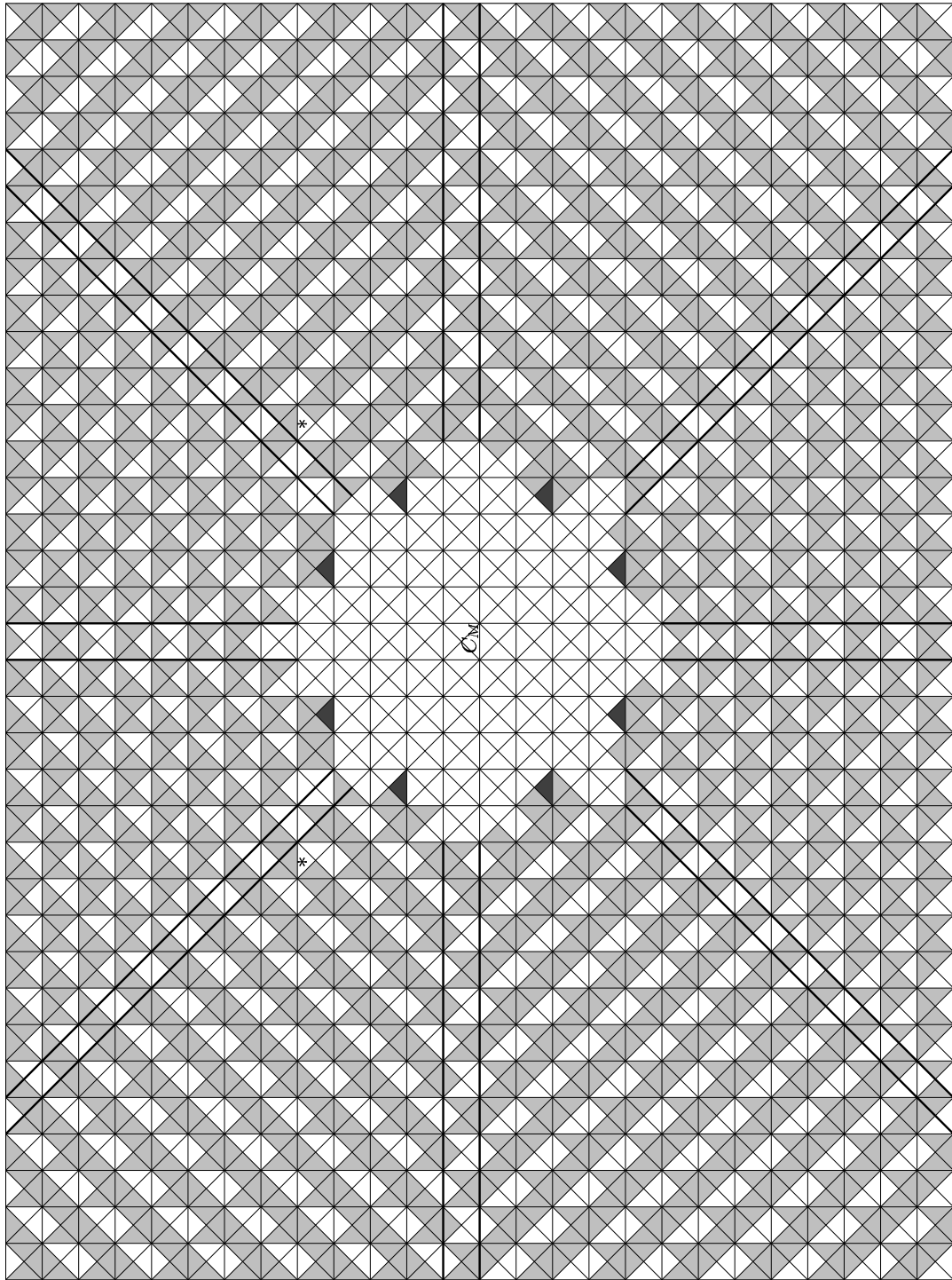


Figure 3.84: Result for  $\alpha = 3$ ,  $\beta = 1$ ,  $Sp_4$



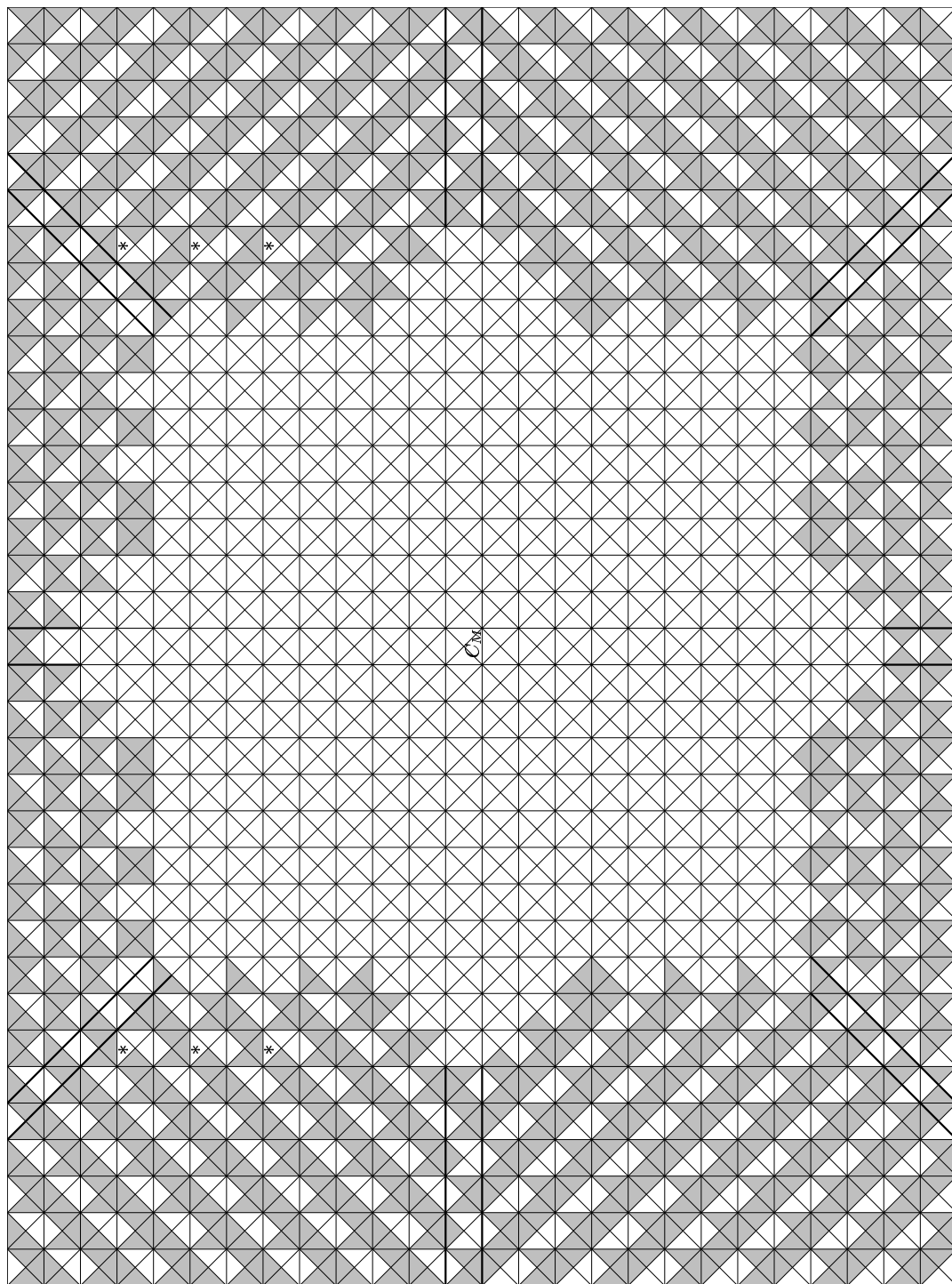


Figure 3.85: Result for  $\alpha = 6$ ,  $\beta = 3$ ,  $Sp_4$

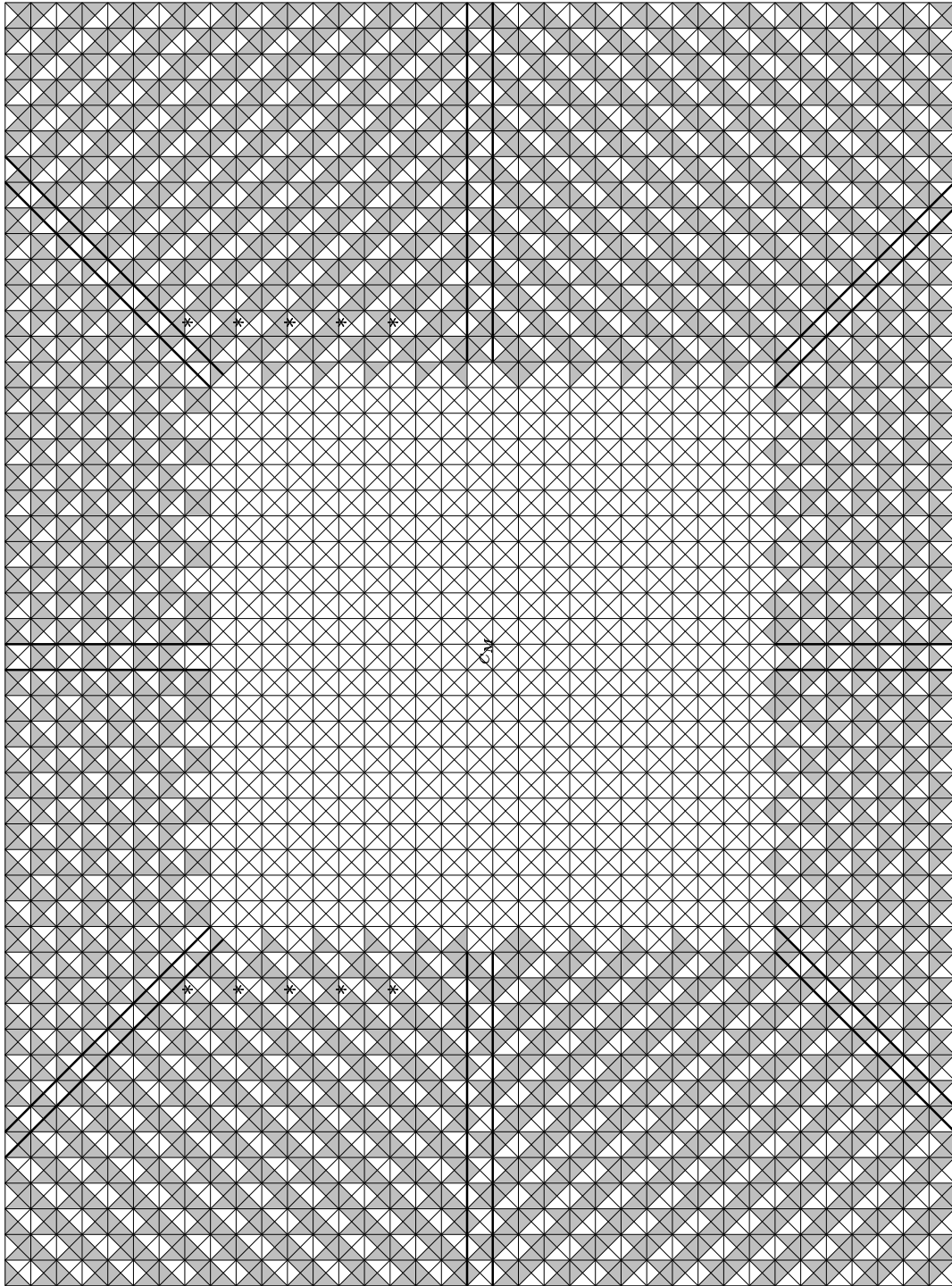


Figure 3.86: Result for  $\alpha = 6$ ,  $\beta = 5$ ,  $Sp_4$

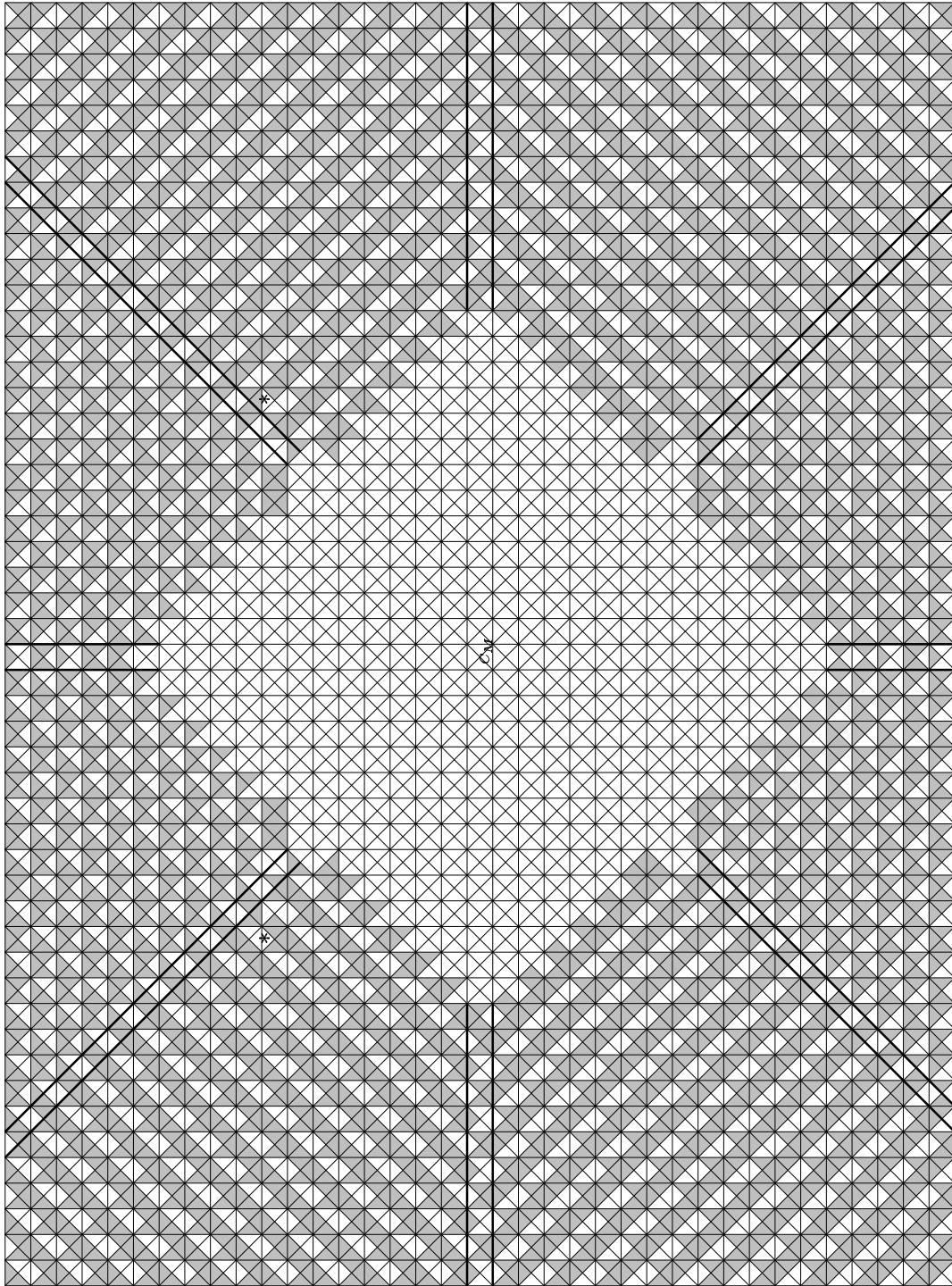


Figure 3.87: Result for  $\alpha = 7$ ,  $\beta = 1$ ,  $Sp_4$

### 3.3.3 Relationship Between $X_w(1\sigma)$ and $X_w(b\sigma)$ for $Sp_4$ , and an Efficient Way of Computing Supersets

In Section 3.1.3 we gave a more efficient method of computing the results of the folding of  $I_1 \cup I_2$ . In that case, we knew these results gave the entire superset  $S_1$  of the solution set. One can apply the methodology of Section 3.1.3 to  $Sp_4$  to produce an efficient way of computing the folding of  $I_1 \cup I_2$  for  $Sp_4$ . However, we have only conjectured that the folding of  $I_1 \cup I_2$  for  $Sp_4$  gives the entire superset  $S_1$ .

Since the methods of this section are very similar to those of Section 3.1.3, we present only results.

**Proposition 3.3.1.** For  $b$  with  $\alpha > \beta$ , computing the folding results of  $I_1 \cup I_2$  is the same as computing the folding results of some collection of half-infinite galleries analogous to those pictured in Figure 3.88, and combining those results with their own reflection across the vertical line of symmetry of  $C_M$ . For  $b$  with  $\alpha = \beta$ , computing the folding results of  $I_1 \cup I_2$  is the same as computing the folding results of some collection of half-infinite galleries analogous to those pictured in Figure 3.89, and combining these results with their reflection across the vertical line of symmetry of  $C_M$ . Although only one specific value of  $b$  is pictured in each figure, it is clear what the situation would be for arbitrary  $b$ . In other words, it is clear what the analogous collection of half-infinite galleries would be for any  $b$ .

### 3.3.4 The Method of Kottwitz and Rapoport Applied to $Sp_4$

As in the  $SL_3$  case, we produce a subset  $S_2 \subseteq S$  for  $b = 1$ . Let  $a \in Sp_4(F)$  be of the form

$$a = \begin{pmatrix} \pi^m & 0 & 0 & 0 \\ 0 & \pi^n & 0 & 0 \\ 0 & 0 & \pi^{-n} & 0 \\ 0 & 0 & 0 & \pi^{-m} \end{pmatrix}$$

where there are no conditions on  $m$  and  $n$ . Let  $w$  be one of the following matrices:

$$r = \begin{pmatrix} 0 & 0 & 1 & 0 \\ 1 & 0 & 0 & 0 \\ 0 & 0 & 0 & -1 \\ 0 & 1 & 0 & 0 \end{pmatrix} \quad ; \quad r^2 = \begin{pmatrix} 0 & 0 & 0 & -1 \\ 0 & 0 & 1 & 0 \\ 0 & -1 & 0 & 0 \\ 1 & 0 & 0 & 0 \end{pmatrix} \quad ; \quad r^3 = \begin{pmatrix} 0 & -1 & 0 & 0 \\ 0 & 0 & 0 & -1 \\ -1 & 0 & 0 & 0 \\ 0 & 0 & 1 & 0 \end{pmatrix}.$$

Note that  $r^4 = -1$ . One can check that in fact  $r \in Sp_4(F)$  by computing  $\Theta(r) = r$ . The  $r^i$  are representatives of Weyl group elements for  $Sp_4$ . In fact,  $W = D_4$ , and  $r$  is a representative of a generator of the order 4 cyclic subgroup of  $W$ .

The matrix  $aw$  belongs to a basic  $\sigma$ -conjugacy class if there is some  $l$  such that  $aw\sigma(aw)\sigma^2(aw)\cdots\sigma^{l-1}(aw)$  is central in  $Sp_4$ . Since  $Sp_4$  is simply connected,  $b = 1$  is the only basic  $\sigma$ -conjugacy class. [6] [7]

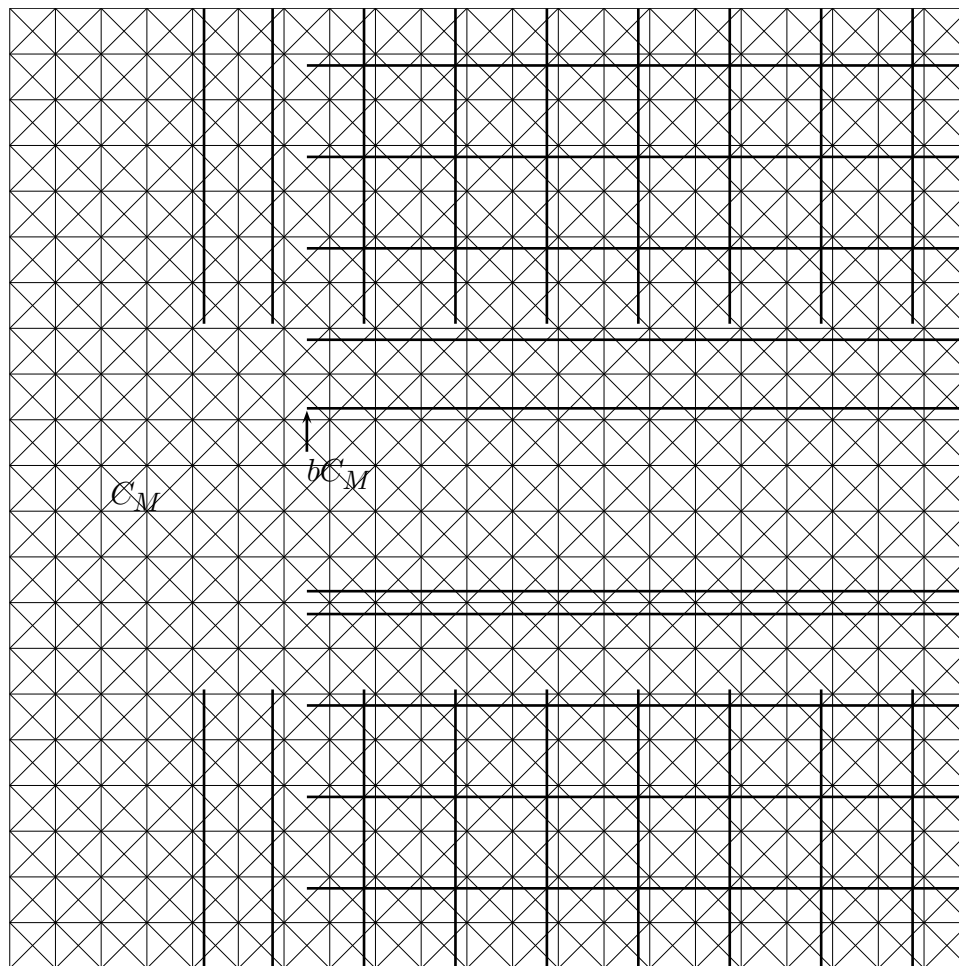


Figure 3.88: Half infinite galleries for  $Sp_4$ ,  $\alpha > \beta$  (specifically,  $\alpha = 3$ ,  $\beta = 1$ )

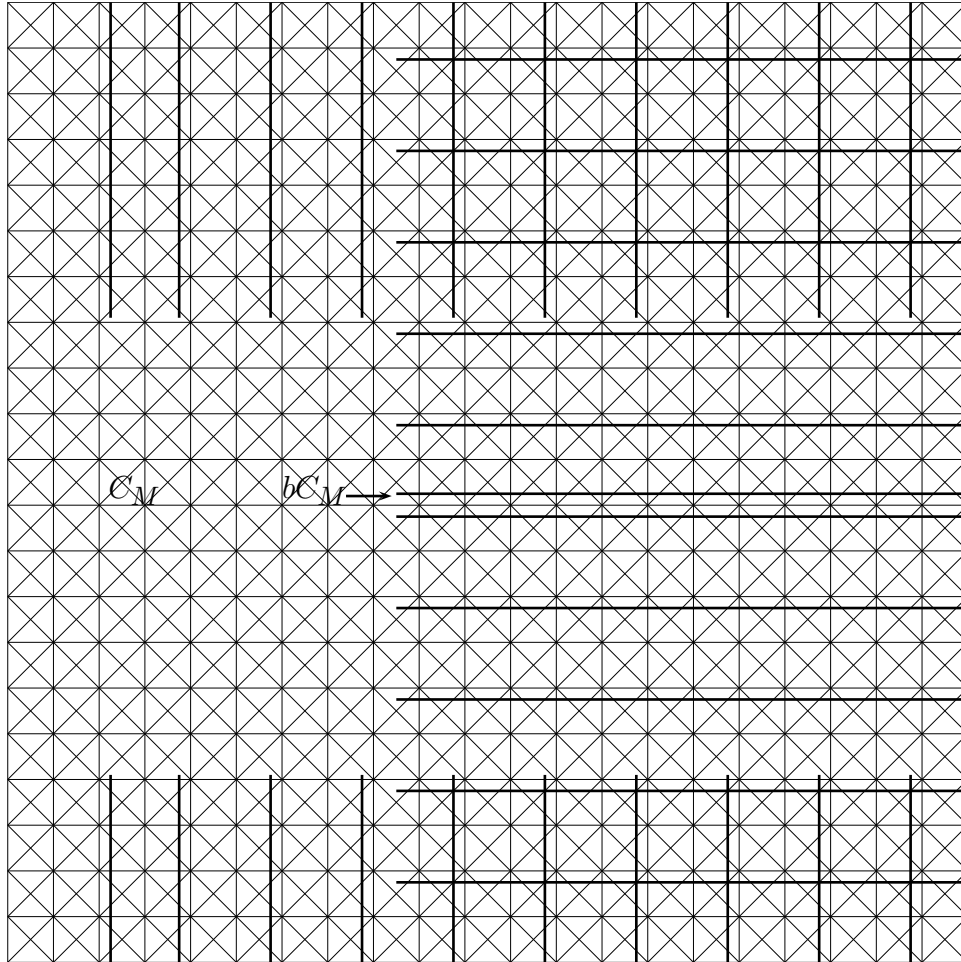


Figure 3.89: Half infinite galleries for  $Sp_4$ ,  $\alpha = \beta$  (specifically,  $\alpha = \beta = 3$ )

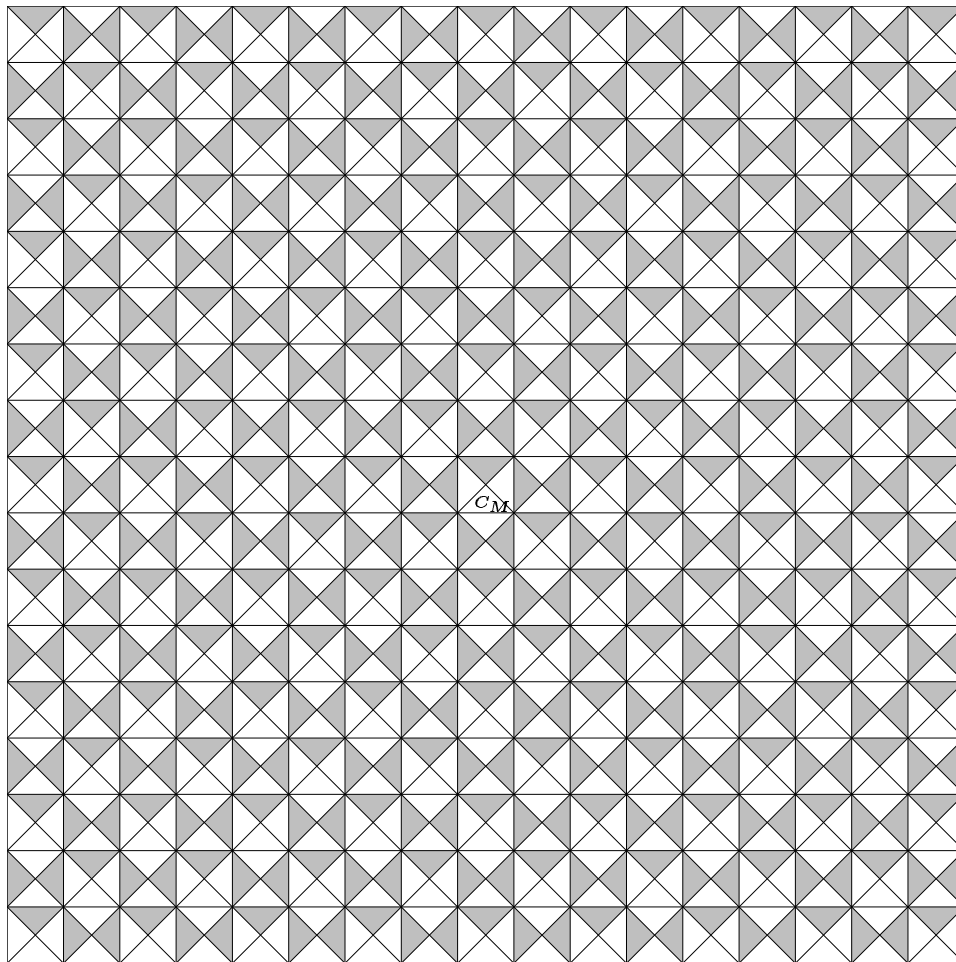


Figure 3.90: Main results of the method suggested by Rapoport and Kottwitz,  $Sp_4$

**Lemma 3.3.2.** There exists an  $l$  such that  $aw\sigma(aw)\sigma^2(aw)\cdots\sigma^{l-1}(aw)$  is central for any choice of  $m$  and  $n$ .

*Proof.* This is similar to Lemma 3.1.3. The only difference is that  $l = 4$ . □

Therefore, the double- $I$ -cosets pictured in Figure 3.90 all meet the  $\sigma$ -conjugacy class of 1 non-trivially.

If  $w$  is a representative of an element of  $W$  other than  $r^i$  for  $i = 1, 2, 3$ , and if certain conditions are placed on  $m$  and  $n$ , then it is still possible for  $(aw)^l$  to be central for some  $l$ .

**Lemma 3.3.3.** If  $a = 1$ , then for  $l = 4$ ,  $(aw)^l$  is central for any  $w \in W$ .

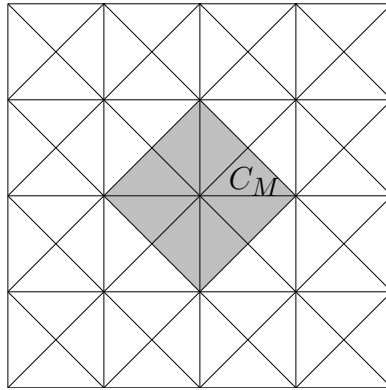


Figure 3.91: The  $a = 1$  results of the method suggested by Rapoport and Kottwitz,  $Sp_4$

This means the double- $I$ -cosets corresponding to chambers shaded in Figure 3.91 all intersect the  $\sigma$ -conjugacy class of  $b = 1$  non-trivially. Let

$$f = \begin{pmatrix} 0 & -1 & 0 & 0 \\ 1 & 0 & 0 & 0 \\ 0 & 0 & 0 & -1 \\ 0 & 0 & 1 & 0 \end{pmatrix}.$$

**Lemma 3.3.4.** If  $n = 0$  then  $aa^w a^{w^2} a^{w^3} w^4 = 1$  for  $w = rf$ . If  $m = 0$ , then  $aa^w a^{w^2} a^{w^3} w^4 = 1$  for  $w = r^3 f$ . If  $m = -n$ , then  $aa^w a^{w^2} a^{w^3} w^4 = 1$  for  $w = f$ . If  $m = n$ , then  $aa^w a^{w^2} a^{w^3} w^4 = 1$  for  $w = r^2 f$ .

*Proof.* Compute the relevant matrix products. □

The implication of this lemma is that the double- $I$ -cosets corresponding to the chambers in Figure 3.92 all intersect the  $\sigma$ -conjugacy class of 1 non-trivially.

Just as the methods of Section 3.1.4 generalize to  $SL_n$ , the results of this section generalize to  $Sp_{2n}$ .

### 3.3.5 A Subset of the Solution Set for $b = 1$ for $Sp_4$

This section is the  $Sp_4$  analogue of Section 3.1.5, and the setup is the same. In slightly different language, we choose a gallery  $G$  of length 2 or 3 starting at  $C_M$  and having only its first chamber  $C_M$  in  $A_M$ . We denote the chambers of  $G$  after  $C_M$  by  $G_1, \dots, G_i$  ( $i = 1$  or  $2$ ), and we let  $e$  be the edge by which  $G_1$  is adjacent to  $C_M$ . We let  $\Gamma^2$  be a minimal gallery from  $e$  to  $\tilde{b}e$ , where  $\tilde{b}C_M$  is one of the chambers in  $A_M$  obtained in the previous section. We form a composite gallery  $\Gamma$  from  $G_1, \dots, G_i, \Gamma^2$ , and  $\tilde{b}\sigma(G_1), \dots, \tilde{b}\sigma(G_i)$ . The collection of possible foldings of  $x^{-1}\Gamma$  gives candidates



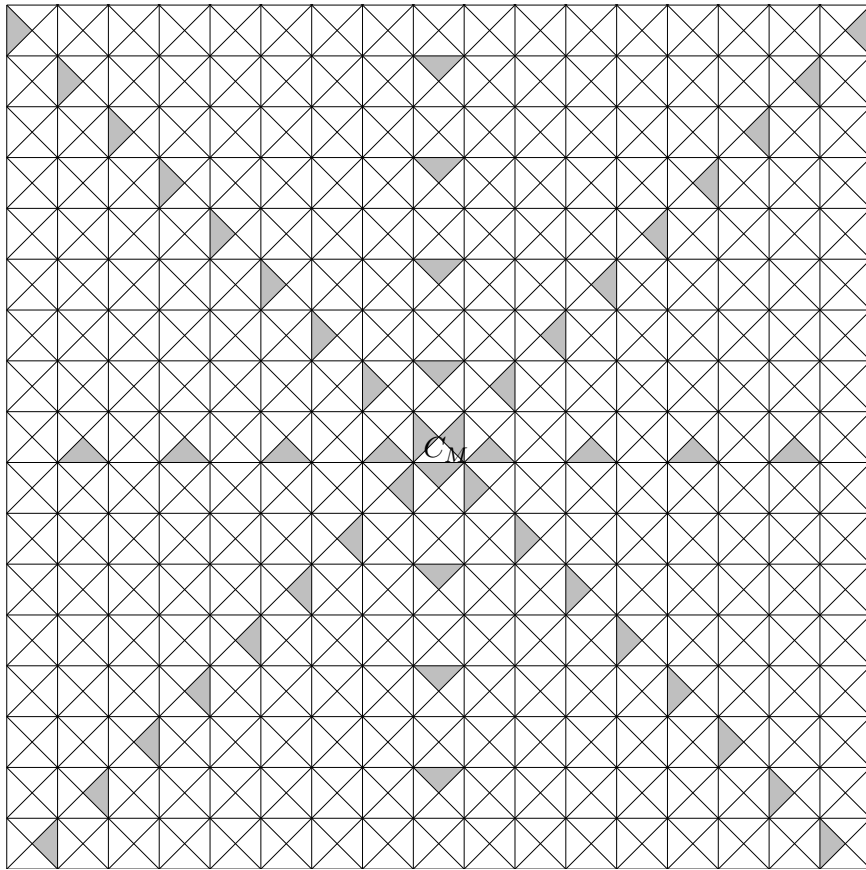


Figure 3.92: Results of the method suggested by Rapoport and Kottwitz under the circumstances of Lemma 3.3.4,  $Sp_4$

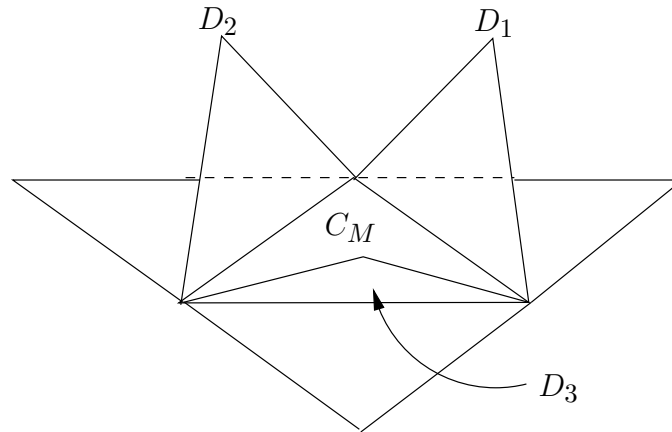


Figure 3.93: The choices  $D_1$ ,  $D_2$  and  $D_3$  of  $G_1$

for an addition to  $S_2$ . If there is only one possible folding then it gives us a new element of  $S_2$ .

Starting with  $i = 1$  and  $x C_M = G_1$  equal to one of the three chambers  $D_1$ ,  $D_2$ ,  $D_3$  pictured in Figure 3.93, we get results as pictured in Figures 3.94, 3.95, and 3.96 for  $\tilde{b} = aw$  with  $w = r$ , Figures 3.97, 3.98, and 3.99 for  $w = r^2$ , and Figures 3.94, 3.95, and 3.96 again for  $w = r^3$ . Occasionally during these computations, the composite gallery  $\Gamma$  is not minimal, and so  $\rho(x^{-1}\Gamma)$  cannot be determined (although in all such cases  $\rho(x^{-1}\Gamma)$  has one of two possible values). In these cases, neither of the possible values of  $\rho(x^{-1}\Gamma)$  is included in the result figures. So all chambers in figures 3.94 through 3.99 are actually in  $S_2$ .

Combining the results obtained so far in this section with those of the previous section gives Figure 3.83, which was already known to be the superset  $S_1 \supseteq S$ . Therefore there is no need to consider the  $i = 2$  case, and we see that  $S_2 = S_1$ , and so  $S_2 = S = S_1$ .

### 3.3.6 Subsets for Other $b$ , and Symmetry under a $\mathbb{Z}/2$ -action

So far we have established a superset  $S_1$  and a subset  $S_2$  for  $b = 1$ , and we have noted that  $S_1 = S_2$ , so  $S_2 = S = S_1$ . For  $b \neq 1$  we have produced a conjectural superset. We also know a very lengthy computation which would verify or refute the conjecture by producing the actual superset. We have not produced a subset  $S_2$  for any  $b \neq 1$ . The process of producing such an  $S_2$  for  $SL_3$  was a very lengthy and involved proof, and was done in Section 3.1.6. It seems likely that a similar process could be carried out for  $Sp_4$ . We therefore make the following conjecture.

**Conjecture 3.3.2.** The set  $\cup_{(t,e)} S_{(t,e)}$  as  $(t, e)$  ranges over all type-edge pairs is in fact equal to  $S$ . In other words,  $S_1 = S$ .

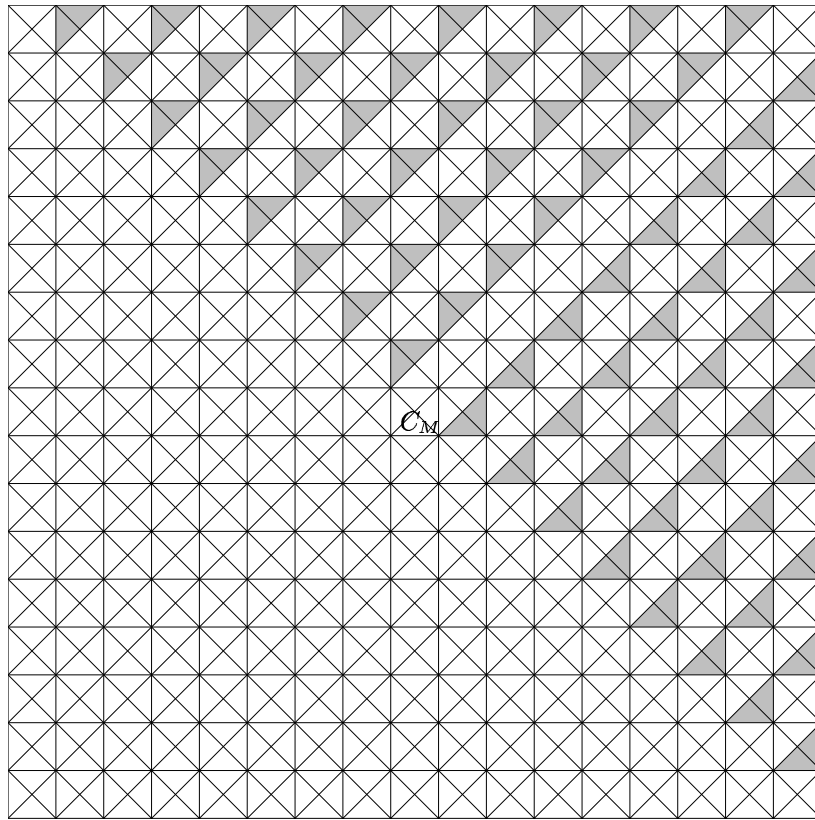


Figure 3.94: Results for  $xC_M = D_1$  and  $w = r$  or for  $xC_M = D_1$  and  $w = r^3$

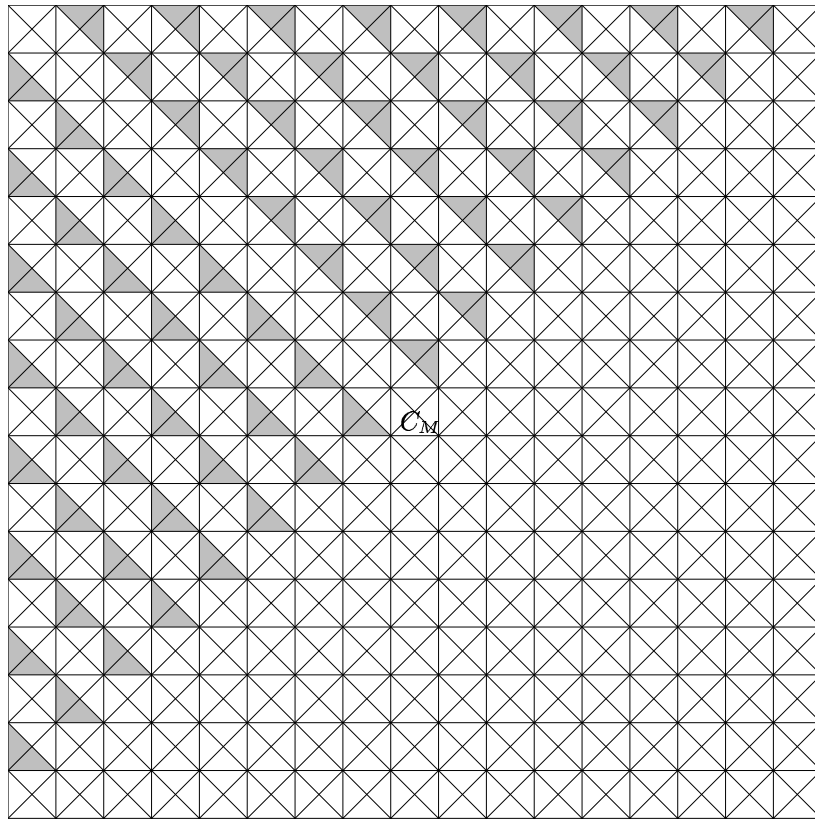


Figure 3.95: Results for  $xC_M = D_2$  and  $w = r$  or for  $xC_M = D_2$  and  $w = r^3$

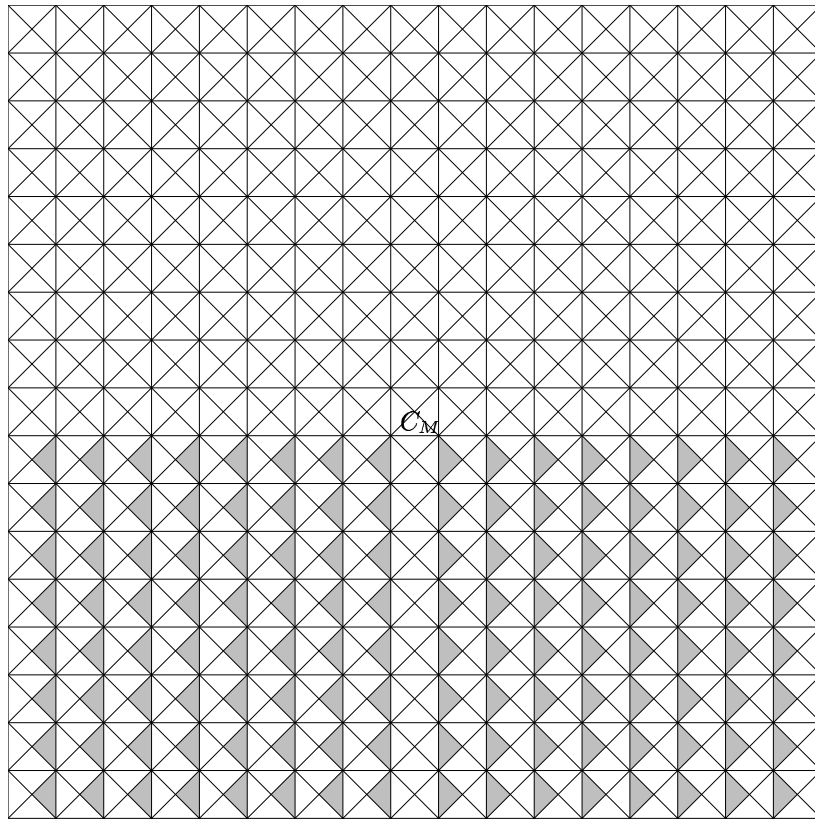


Figure 3.96: Results for  $xC_M = D_3$  and  $w = r$  or for  $xC_M = D_3$  and  $w = r^3$

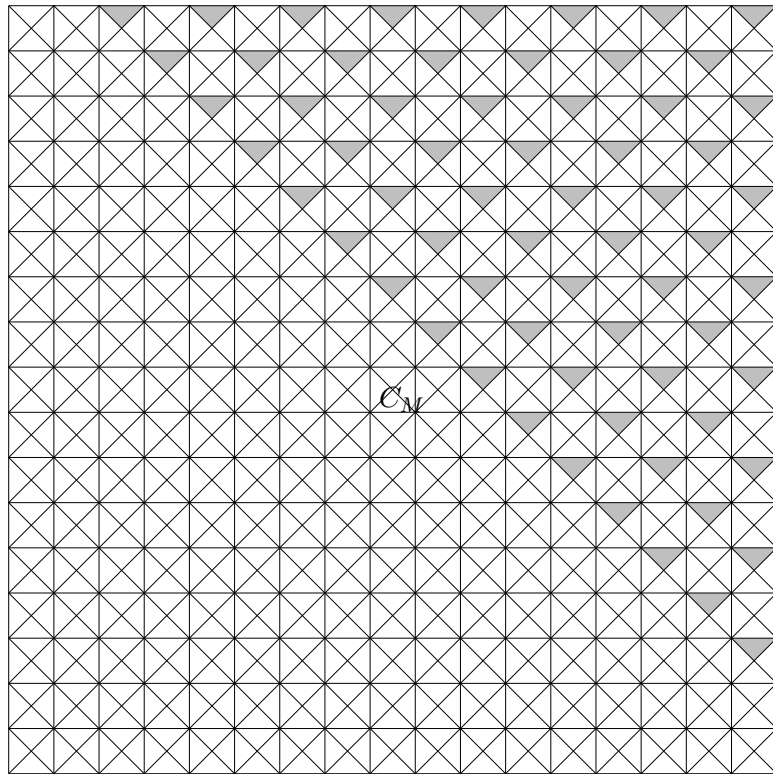


Figure 3.97: Results for  $xC_M = D_1$  and  $w = r^2$

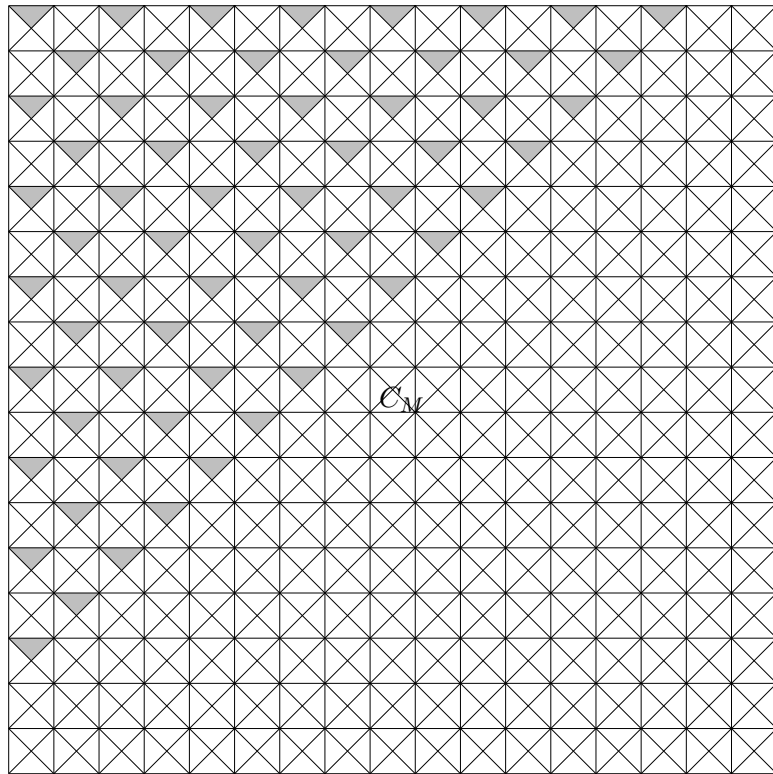


Figure 3.98: Results for  $x C_M = D_2$  and  $w = r^2$

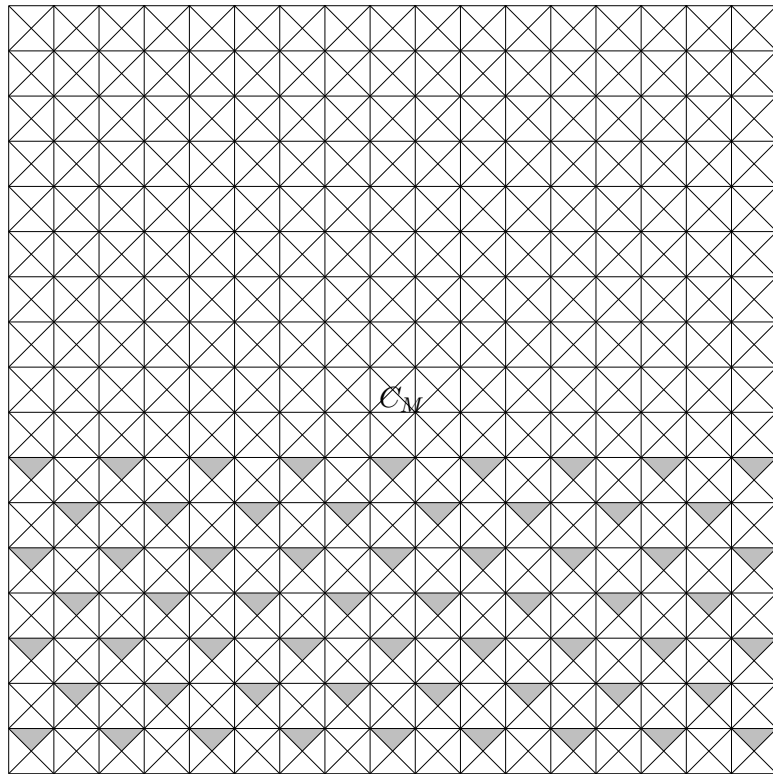


Figure 3.99: Results for  $x C_M = D_3$  and  $w = r^2$



If this conjecture and Conjecture 3.3.1 are both true, the Figures 3.84 through 3.87 represent actual solution sets for their respective  $\sigma$ -conjugacy classes.

In Section 3.1.7, we gave an *a priori* proof of  $\mathbb{Z}/3$ -rotational symmetry of the  $SL_3$  solution set  $S$ . This proof was based on the existence of a matrix  $q \in GL_3(F)$  that acted on  $A_M$  by rotating it by  $120^\circ$  around the center of  $C_M$ . We have a matrix  $q \in GSp_4(F)$  that acts on the main apartment of the building of  $Sp_4$  by flipping it across the (vertical) line of symmetry of  $C_M$ . One can prove a proposition exactly analogous to Proposition 3.1.8 in Section 3.1.7 to show that the solution set  $S$  for  $Sp_4$  will have symmetry about the vertical line through the middle of  $C_M$ . As the rotational symmetry result for  $SL_3$  generalizes easily to a  $\mathbb{Z}/n$ -symmetry result for  $SL_n$ , so this symmetry result for  $Sp_4$  generalizes to a  $\mathbb{Z}/n$ -symmetry result for  $Sp_{2n}$ .

### 3.4 Comments on $GSp_4$ , $PSp_4$ , and $G_2$

If  $G$  is  $GSp_4$  or  $PSp_4$ , we have  $inv : G(L) \times G(L) \rightarrow \tilde{W} \simeq W_a \rtimes M$ , where  $M = \mathbb{Z}$  for  $G = GSp_4$  and  $M = \mathbb{Z}/2$  for  $G = PSp_4$ . We have  $inv(x, y) = (\rho(x^{-1}yC_M), \frac{1}{2}v(\det(x^{-1}y)))$ . One can check that if  $G = GSp_4$  and  $x \in G(L)$  then  $v(\det(x)) \in 2\mathbb{Z}$ . If  $G = PSp_4$  and  $x \in G(L)$  then  $v(\det(x)) \in 2\mathbb{Z}/4\mathbb{Z} \simeq \mathbb{Z}/2\mathbb{Z}$ . The representatives  $b$  listed at the beginning of Section 3.3 still represent distinct  $\sigma$ -conjugacy classes in  $G(L)$ , but there are additional  $\sigma$ -conjugacy classes we will not consider. So if  $b$  is one of the matrices at the beginning of Section 3.3, this time considered as an element of  $G(L)$ , then we ask for a description of the set  $\{(\rho(x^{-1}b\sigma(x)C_M), \frac{1}{2}v(\det(x^{-1}b\sigma(x)))) : x \in G(L)\}$ . Using methods very similar to those of Section 3.2, we can prove that  $\{\rho(x^{-1}b\sigma(x)C_M) : x \in G(L)\} = \{\rho(x^{-1}b\sigma(x)C_M) : x \in Sp_4(L)\}$ . It is already clear that  $v(\det(x^{-1}b\sigma(x))) = v(\det(b))$  is fixed for fixed  $b$  (and equal to 0 for the  $b$  we have chosen).

We would also like to make some comments about  $G_2$ . We first note that  $W = D_6$ , the group of symmetries of a hexagon, and that  $W_a = \mathbb{Z}^2 \rtimes W$ . We ask for a description of  $\{inv(x, \sigma(x)) : x \in G_2(L)\}$ . Let  $\epsilon$  and  $\delta$  be the two standard generators of  $\mathbb{Z}^2 \subseteq \mathbb{Z}^2 \rtimes W \simeq W_a$ , where  $\epsilon$  and  $\delta$  act on  $A_M$  by translating it so that  $C_M$  goes, respectively, to the chambers marked with an  $\epsilon$  and a  $\delta$  in Figure 3.100.

Let  $r \in W$  be the element that rotates  $A_M$  counterclockwise by  $60^\circ$  around  $v_M$ , and let  $f \in W$  be the element that flips  $A_M$  about the horizontal line through  $v_M$ . We know that  $\epsilon, \delta, r$  and  $f$  generate  $W_a$ ,  $\epsilon$  and  $\delta$  commute, and  $rf = fr^5$ . One can check that  $r\epsilon = \epsilon\delta r$ ,  $r\delta = \epsilon^{-1}r$ ,  $f\epsilon = \epsilon f$ , and  $f\delta = \epsilon^{-1}\delta^{-1}f$ .

Using a similar process to that used in Sections 3.1.4 and 3.3.4, if  $a = \epsilon^s \delta^t$  and  $w \in W$ , and if  $(aw)^l = 1$  in  $W_a$  for some  $l$ , then  $aw \in \{inv(x, \sigma(x)) : x \in G_2(L)\}$ . We get:

**Lemma 3.4.1.** For any integers  $s, t$  and any  $1 \leq n \leq 5$ ,  $\epsilon^s \delta^t r^n \in \{inv(x, \sigma(x)) : x \in G_2(L)\}$ .

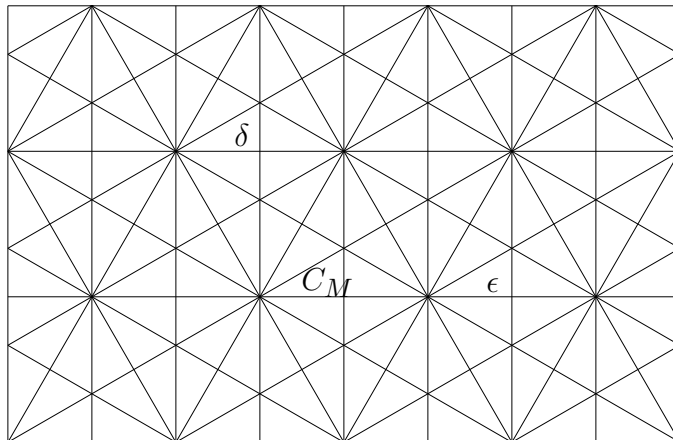


Figure 3.100: The translations  $\epsilon$  and  $\delta$  of  $A_M$  for  $G_2$

*Proof.* Just simplify  $(\epsilon^s \delta^t r^n)^6$  for each  $n = 1, 2, 3, 4, 5$  using the rules listed in the previous paragraph. For instance, if  $n = 1$ , then  $(\epsilon^s \delta^t r)^6 = (\epsilon^s \delta^t r)(\epsilon^s \delta^t r)(\epsilon^s \delta^t r)^4 = (\epsilon^s \delta^t)(\epsilon^{s-t} \delta^s r^2)(\epsilon^s \delta^t r)^4 = (\epsilon^s \delta^t)(\epsilon^{s-t} \delta^s)(\epsilon^{-t} \delta^{s-t})(\epsilon^{-s} \delta^{-t})(\epsilon^{-s+t} \delta^{-s})(\epsilon^t \delta^{-s+t}) r^6 = 1$ .  $\square$

One could also create lemmas for  $G_2$  analogous to Lemma 3.1.4 and Lemma 3.1.5 in a similar way.

These results give a starting point for the subset  $S_2$  of the solution set  $S$  for  $G_2$  with  $b = 1$ . One could enlarge  $S_2$  using methods similar to those in Section 3.1.5 and Section 3.3.5. One could produce a superset  $S_1 \supseteq S$  by folding galleries in an analogous way to Section 3.1.2 and Section 3.3.2. This has not been done, so we cannot say for sure if the resulting  $S_1$  and  $S_2$  are equal, although we guess that they would be.

We also note that  $G_2$  has no analogue to the rotational invariance developed for  $SL_3$  in Section 3.1.7, or the flip invariance developed for  $Sp_4$  in Section 3.3.6, although the general results that will be developed in Section 3.5 will hold for  $G_2$ .

### 3.5 Invariance Properties of Solution Sets

In this section we prove some results that give invariance properties of the solution set  $S$ . These results hold true if  $S$  is the solution set  $\{inv(x, b\sigma(x)) : x \in G(L)\}$  for any simply-connected group  $G$  and any  $\sigma$ -conjugacy class  $b$ . We apply the invariance results of this section to  $SL_3$ ,  $b = 1$  under the assumption that one knows whether  $X_w(1\sigma)$  is empty or non-empty only for any  $w$  in a certain subset of  $W_a = \tilde{W}$ . We will see that knowledge on whether  $X_w(b\sigma)$  is empty can be obtained on a much larger class of  $w$ .

Let  $G$  be a simple simply-connected group, let  $W_a$  be its affine Weyl group, and let  $A_M$  be the main apartment of its building. Suppose  $G$  has rank  $n$ . Let  $C_M$  be the main chamber and let  $v_M$  be the main vertex. Let  $L_1, \dots, L_n$  be the hyperplanes in  $A_M$  that contain  $v_M$  and that intersect  $C_M$  in an  $n - 1$  dimensional simplex. Let  $L_{n+1}$  be the hyperplane in  $A_M$  that intersects  $C_M$  in an  $n - 1$  dimensional simplex, but that does not contain  $v_M$ . Let  $s_i$  be reflection of  $A_M$  about  $L_i$ . Then the  $s_i$  generate  $W_a$  as a Coxeter group.

If  $D$  is a chamber in  $A_M$ , define  $p_i D$  to be the chamber obtained by reflecting  $D$  about the wall  $\tilde{L}_i$ , where  $\tilde{L}_i$  is parallel to  $L_i$ , and intersects  $D$  in an  $n - 1$  dimensional simplex. So  $p_i$  is a map from the set of chambers in  $A_M$  to itself. The elements  $s_i \in W_a$  are also maps of this kind, and as such we can state the following lemma:

**Lemma 3.5.1.** If  $i \neq j$  then  $p_i s_j = s_j p_k$  for some  $k$ . We also have  $p_i s_i = s_i p_i$ .

This can be easily checked, and is valuable because a gallery in  $A_M$  starting at  $C_M$  is just a sequence of the  $p_i$ . We can now prove:

**Lemma 3.5.2.** If  $w \in W_a$  then there is a one-to-one correspondence between Coxeter expansions of  $w$  (using the  $s_i$ ) and galleries from  $C_M$  to  $wC_M$ . A Coxeter expansion of length  $m$  corresponds to a length  $m + 1$  gallery, so minimality is preserved under the correspondence.

*Proof.* If  $w = s_{i_1} \cdots s_{i_m}$  then  $wC_M = s_{i_1} \cdots s_{i_m} C_M = s_{i_1} \cdots s_{i_{m-1}} p_{i_m} C_M = p_{k_m} s_{i_1} \cdots s_{i_{m-1}} C_M$ , where the last equality is achieved by using Lemma 3.5.1  $m - 1$  times. We then proceed:  $p_{k_m} s_{i_1} \cdots s_{i_{m-1}} C_M = p_{k_m} s_{i_1} \cdots s_{i_{m-2}} p_{i_{m-1}} C_M = p_{k_m} p_{k_{m-1}} s_{i_1} \cdots s_{i_{m-2}} C_M = \cdots = p_{k_m} p_{k_{m-1}} \cdots p_{k_1} C_M$ . Note that length is preserved, and the process is reversible.  $\square$

Let  $l(w)$  denote the length of  $w \in W_a$  as an element of the Coxeter group  $W_a$ . Then we have the following results. Note that Proposition 3.5.3 is the affine analogue of some parts of the proof of Theorem 1.6 in [3].

**Proposition 3.5.3.** If  $s = s_i$  for some  $i$  and if  $l(sws) = l(w)$  then there exists a bijective map from  $X_w(b\sigma)$  to  $X_{sws}(b\sigma)$ .

*Proof.* We define  $P$  to be the parallelogram spanned by  $C_M$  and  $wC_M$  (so it is the intersection of all apartments containing  $C_M$  and  $wC_M$ , or, alternatively, the union of all minimal galleries from  $C_M$  to  $wC_M$ ). Because of the fact that  $l(sws) = l(w)$ , one can show that exactly one of  $wsC_M$  and  $sC_M$  is in  $P$ . If  $x \in X_w(b\sigma)$ , then let  $g \in I$  be such that  $gx^{-1}b\sigma(x)C_M = wC_M$ . Consider  $xg^{-1}P$ , which contains  $xg^{-1}C_M = xC_M$  and  $xg^{-1}wC_M = b\sigma(x)C_M$ .

*Case 1:*  $sC_M \subseteq P$ . Then let  $y = xg^{-1}s$ , so  $yC_M = xg^{-1}sC_M$ . Since  $yC_M$  is adjacent to  $xC_M$ ,  $b\sigma(y)C_M$  is adjacent to  $b\sigma(x)C_M$ , and not a part of  $xg^{-1}P$ . One can now see that  $inv(y, b\sigma(y)) = swsC_M$ .

*Case 2:*  $wsC_M \subseteq P$ . Then let  $yC_M = \sigma^{-1}b^{-1}xg^{-1}wsC_M$ , so we have that  $b\sigma(y)C_M = xg^{-1}wsC_M$ . Since  $wsC_M$  is adjacent to  $wC_M$ ,  $xg^{-1}wsC_M$  is adjacent to  $b\sigma(x)C_M$ , so  $yC_M$  is adjacent to  $xC_M$  along the edge  $xg^{-1}e$ , where  $e$  is the edge of adjacency of  $C_M$  and  $sC_M$ . One can now see that  $\text{inv}(y, b\sigma(y)) = swsC_M$ .

Now let  $\Gamma_1 : X_w(b\sigma) \rightarrow X_{sws}(b\sigma)$  be defined so that  $\Gamma_1(xC_M) = yC_M$ . I claim that this is a bijection. To check this, note that the roles of  $w$  and  $sws$  in the construction of  $\Gamma_1$  were symmetric, so by replacing each with the other we get a map  $\Gamma_2 : X_{sws}(b\sigma) \rightarrow X_w(b\sigma)$ . One can check that  $\Gamma_1$  and  $\Gamma_2$  are inverses.  $\square$

**Proposition 3.5.4.** If  $s = s_i$  for some  $i$  and if  $l(w) > l(sws)$  (and so  $l(sws) = l(w) - 2$ ) then there is a surjective map from  $X_w(b\sigma)$  to  $X_{sws}(b\sigma) \cup X_{sw}(b\sigma)$ .

*Proof.* Again, let  $P$  be the parallelogram spanned by  $C_M$  and  $wC_M$ . The fact that  $l(w) > l(sws)$  means that both  $wsC_M$  and  $sC_M$  are in  $P$ . As in the previous proposition, if  $x \in X_w(b\sigma)$ , let  $g \in I$  be such that  $gx^{-1}b\sigma(x)C_M = wC_M$ . Let  $e$  be the edge of adjacency between  $wC_M$  and  $wsC_M$ , and consider  $xg^{-1}P$ . One can see that  $b\sigma(xg^{-1}s)C_M$  is adjacent to  $b\sigma(x)C_M = xg^{-1}wC_M$  via  $xg^{-1}e$ , but we may have  $b\sigma(xg^{-1}s)C_M = xg^{-1}wsC_M$  or we may have  $b\sigma(xg^{-1}s)C_M \neq xg^{-1}wsC_M$  (at least *a priori*, either the equality or the inequality could possibly hold, and it will turn out that both actually do arise).

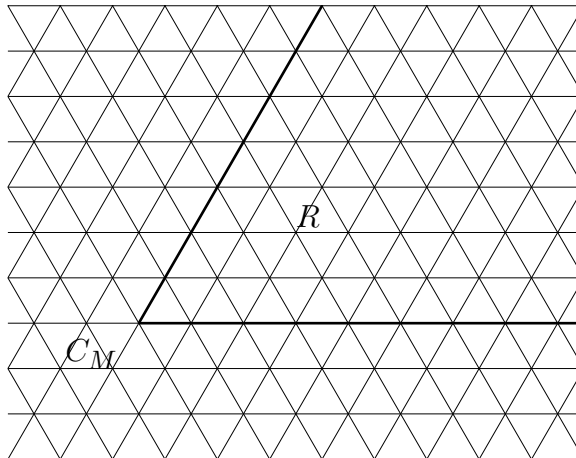
*Case 1:*  $b\sigma(xg^{-1}s)C_M = xg^{-1}wsC_M$ . Then if we let  $y = xg^{-1}s$ , we have that  $\text{inv}(y, b\sigma(y)) = \text{inv}(xg^{-1}s, xg^{-1}ws) = \text{inv}(s, ws) = \text{inv}(1, sws) = sws$ , so  $y \in X_{sws}(b\sigma)$ .

*Case 2:*  $b\sigma(xg^{-1}s)C_M \neq xg^{-1}wsC_M$ . Then if  $y = xg^{-1}s$ , we have  $\text{inv}(y, b\sigma(y)) = \text{inv}(s, w) = \text{inv}(1, sw) = sw$ , so  $y \in X_{sw}(b\sigma)$ .

So we have a map  $\Gamma : X_w(b\sigma) \rightarrow X_{sws}(b\sigma) \cup X_{sw}(b\sigma)$  where  $\Gamma(xC_M) = yC_M$ . We must show that  $\Gamma$  is surjective. Take  $z \in X_{sw}(b\sigma)$ , so  $\text{inv}(z, b\sigma(z)) = sw$ . So  $\rho_{sC_M}(sz^{-1}b\sigma(z)C_M) = wC_M$ , where  $\rho_{sC_M}$  is the retraction of  $\mathcal{B}_\infty$  onto  $A_M$  centered at  $sC_M$ . So there exists  $g \in sIs$  such that  $gsz^{-1}b\sigma(z)C_M = wC_M$ . Consider  $zsg^{-1}P$ , which contains  $zC_M$  and  $b\sigma(z)C_M = zsg^{-1}wC_M$ . Note that if  $e$  is the edge of adjacency of  $C_M$  and  $sC_M$ , then  $zC_M$  contains  $zsg^{-1}e$ . Choose a chamber  $xC_M$  containing  $e$ , but not equal to  $zC_M$ . Then  $b\sigma(x)C_M$  is adjacent to  $b\sigma(z)C_M$ . We may assume without loss of generality that  $b\sigma(x)C_M \not\subseteq zsg^{-1}P$  (we can arrange this by choosing an appropriate  $xC_M$ ). Then  $x \in X_w(b\sigma)$  and  $\Gamma(xC_M) = zC_M$ .

If  $z \in X_{sws}(b\sigma)$ , then  $\rho_{sC_M}(sz^{-1}b\sigma(z)C_M) = wsC_M$ . So there exists  $g \in sIs$  such that  $gsz^{-1}b\sigma(z)C_M = wsC_M$ . Consider  $zsg^{-1}P$ , which contains  $zC_M$  and  $b\sigma(z)C_M = zsg^{-1}wsC_M$ . Let  $e$  be the edge between  $C_M$  and  $sC_M$ . We know  $zsg^{-1}e \subseteq zC_M$ , and  $b\sigma(e) = zsg^{-1}we$ . So choose  $xC_M$  containing  $e$  and not in  $P$ . Then  $b\sigma(x)C_M$  contains  $b\sigma(e)$ . We can require without loss of generality that  $b\sigma(x)C_M \not\subseteq P$ . Then  $\Gamma(xC_M) = zC_M$ . This proves surjectivity.  $\square$

**Corollary 3.5.5.** If  $l(sws) > l(w)$  (so  $l(sws) = l(w) + 2$ ) then there is a surjective map from  $X_{sws}(b\sigma)$  to  $X_w(b\sigma) \cup X_{ws}(b\sigma)$ .

Figure 3.101: Region  $R$ 

*Proof.* Just apply the previous proposition with  $sws$  in place of  $w$ . □

**Corollary 3.5.6.** If  $l(sw) > l(w)$ ,  $l(ws) < l(w)$  and  $X_w(b\sigma) \neq \emptyset$  then  $X_{sw}(b\sigma) \neq \emptyset$ . If  $l(sw) < l(w)$ ,  $l(ws) > l(w)$ , and  $X_w(b\sigma) \neq \emptyset$ , then  $X_{ws}(b\sigma) \neq \emptyset$ .

*Proof.* This follows from the two propositions. □

Note that we used this last result repeatedly in Section 3.1.5 and Section 3.3.5 for  $SL_3$  and  $Sp_4$ .

These results are valuable because they can be used on a wide variety of groups  $G$  and  $\sigma$ -conjugacy classes  $b$  to increase partial information on the nature of the solution set  $\{inv(x, b\sigma(x)) : x \in G(L)\}$ . To illustrate the possible utility of the above propositions, we consider the hypothetical case that for  $SL_3$ ,  $b = 1$ , one knows for any  $w$  in region  $R$  on Figure 3.101 whether  $X_w(1\sigma)$  is or is not empty. So we assume that part of Figure 3.27, the solution set for  $SL_3$ ,  $b = 1$ , is given. In this case, one can repeatedly apply the results of this section, together with the rotational invariance result of Section 3.1.7, to the point where it is known whether  $X_w(b\sigma)$  is empty or non-empty for each  $w$  corresponding to a chamber shaded in Figure 3.102. We note that this represents nearly complete information about the solution set of  $SL_3$ ,  $b = 1$ , since nearly every chamber in that figure is shaded. The results of this section could be applied with the same level of effectiveness if  $b \neq 1$ , or for  $Sp_4$ . Our results could even be applied to other groups, including higher rank groups.

Also note that Sections 3.1.5 and 3.3.5 were essentially just Corollary 3.5.6 applied to the partial information of Sections 3.1.4 and 3.3.4.

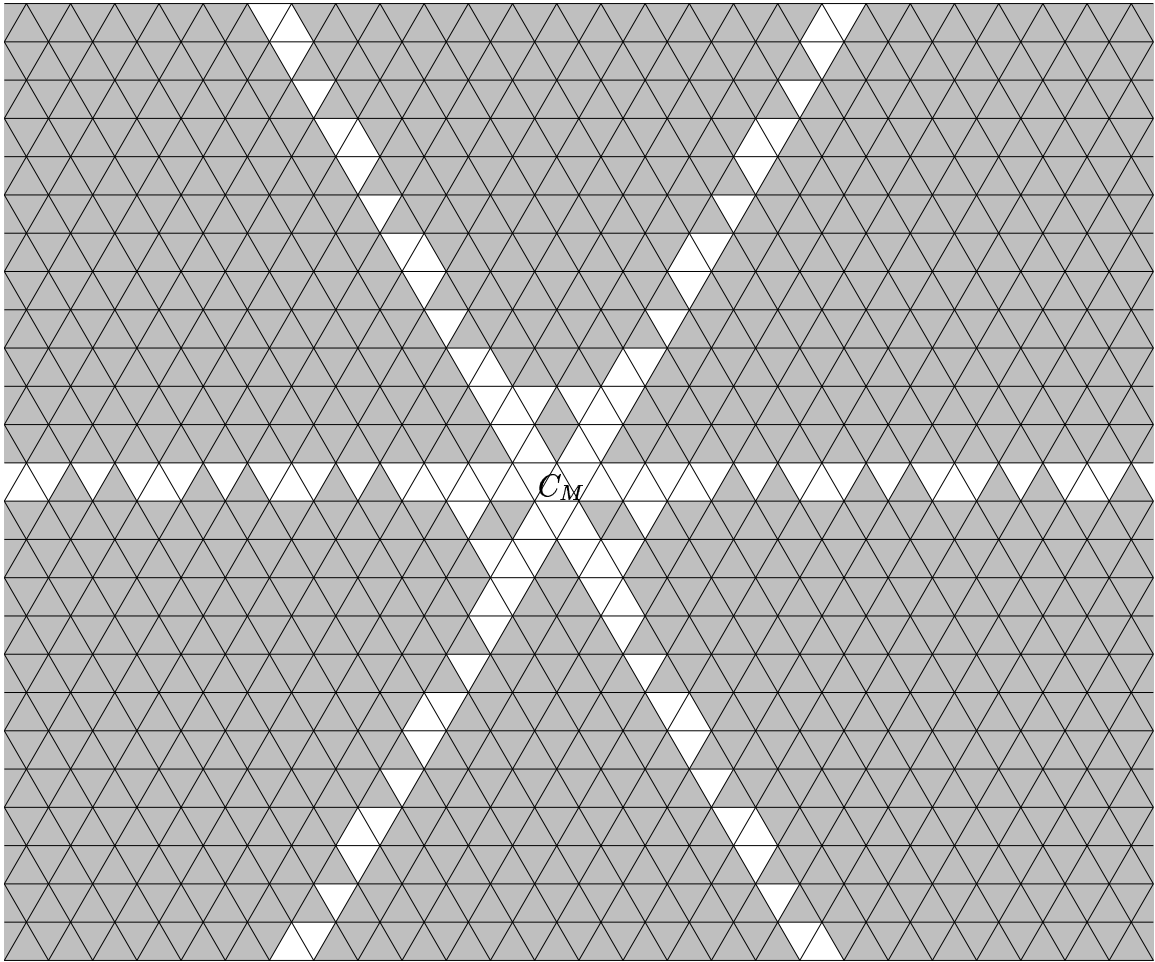


Figure 3.102: Understood region after applying invariance properties to region  $R$

## REFERENCES

- [1] Bruhat, F. and Tits, J. *Groupes reductifs sur un corps local*, Inst. Hautes Etudes Sci. Publ. Math. 41 (1972), 5–251.
- [2] Bruhat, F. and Tits, J. *Groupes reductifs sur un corps local II*, Inst. Hautes Etudes Sci. Publ. Math. 60 (1984), 197–376.
- [3] Deligne, P. and Lusztig, G. *Representations of Reductive Groups Over Finite Fields*, Annals of Mathematics 103 (1976), 103–161.
- [4] Garrett, P. *Buildings and Classical Groups*, Chapman and Hall (1997).
- [5] Kneser, M. *Chapter 10 of Algebraic Number Theory*, edited by Cassels, J.W.S., and Frohlich, A., Academic Press, (1967).
- [6] Kottwitz, R. *Isocrystals with Additional Structure*, Compositio Mathematica 56 (1985), 201–220.
- [7] Kottwitz, R. *Isocrystals with Additional Structure II*, Compositio Mathematica 109 (1997), 255–339.
- [8] Kottwitz, R. *Orbital Integrals on  $GL_3$* , American Journal of Mathematics 102 (1980), 327–384.
- [9] Kottwitz, R. and Rapoport, M. *On the Existence of  $F$ -crystals*, (2002).
- [10] Manin, Y. *The Theory of Commutative Formal Groups Over Fields of Finite Characteristic*, Russian Mathematical Survey 18 #6 (1963), 1–81.
- [11] Rapoport, M. *A Positivity Property of the Satake Isomorphism*, preprint.
- [12] Serre, J.-P. *Galois Cohomology*, Springer Verlag (1997).
- [13] Serre, J.-P. *Local Fields*, Springer Verlag (1979).